



UNIVERSIDAD DE BURGOS

DEPARTAMENTO DE BIOTECNOLOGÍA Y CIENCIA DE LOS ALIMENTOS

ÁREA DE INGENIERÍA QUÍMICA

SPAN 80: ESTUDIOS DE EXTRACCIÓN Y CARACTERIZACIÓN

TESIS DOCTORAL

Lara Roque Viadas

Burgos, 2020



UNIVERSIDAD
DE BURGOS

Memoria de investigación titulada “**Span 80: Estudios de extracción y caracterización**” realizada en el Programa de Doctorado *Avances en Ciencia y Biotecnología Alimentarias*, presentada para optar al Grado de Doctor por la Universidad de Burgos.

Lara Roque Viadas



UNIVERSIDAD
DE BURGOS

La presente Tesis Doctoral queda
registrada en el folio nº
del correspondiente Libro de Registros, con
el nº

Burgos, a de..... de 2020

El Encargado del Registro



UNIVERSIDAD DE BURGOS

FACULTAD DE CIENCIAS

DEPARTAMENTO DE BIOTECNOLOGÍA Y CIENCIA DE LOS ALIMENTOS

Dña. María Isabel Escudero Barbero y D. José Manuel Benito Moreno,
Profesores Titulares del Departamento de Biotecnología y Ciencia de los Alimentos de
la Universidad de Burgos,

INFORMAN FAVORABLEMENTE Y DECLARAN

Que la presente Tesis Doctoral, titulada «Span 80: estudios de extracción y caracterización», que presenta Dña. Lara Roque Viadas para optar al Grado de Doctor por la Universidad de Burgos, ha sido realizada bajo su dirección en el Área de Ingeniería Química del Departamento de Biotecnología y Ciencia de los Alimentos de la Universidad de Burgos.

Y para que así conste, firman el presente informe

En Burgos, a 20 de septiembre de 2020

Handwritten signature in blue ink of M.ª Isabel Escudero Barbero.

Handwritten signature in blue ink of José Manuel Benito Moreno.

Fdo. Dra. Dña. M.ª Isabel Escudero Barbero Fdo. Dr. D. José Manuel Benito Moreno



UNIVERSIDAD DE BURGOS

FACULTAD DE CIENCIAS

DEPARTAMENTO DE BIOTECNOLOGÍA Y CIENCIA DE LOS ALIMENTOS

AGRADECIMIENTOS

Son muchas las personas que han contribuido de una u otra manera en la realización de esta tesis, y a todos ellos, quiero dedicarles mis agradecimientos.

Quiero agradecer a la profesora Isabel Escudero, directora de esta tesis por ser más que una directora de tesis, por su motivación y apoyo. Gracias por su gran dedicación, por la ayuda que me has brindado en todo momento y por todo lo que he aprendido a lo largo de estos años.

Al profesor José Manuel Benito, codirector de la tesis, quien ha estado para ayudarme en cualquier momento. Gracias por tu apoyo y dedicación.

A todos los compañeros y amigos del Área de Ingeniería Química, con los que he coincidido durante mi trayectoria en el doctorado durante estos años, por su amistad y ayuda, y por hacer de esos momentos recuerdos llenos de ilusión.

En especial a Beti por su gran ayuda técnica, pero, sobre todo, porque siempre nos recibes con una gran sonrisa y por tu gran dedicación en todo momento, pudiendo contar con ella para cualquier cosa. A todas las personas con las que he coincidido y trabajado, en especial a Laura y María, decirles que ha sido un placer trabajar con ellas y que no habría podido tener mejores compañeras de trabajo, llevándome muy buenos recuerdos de estos años.

A Jorge, por estar siempre ahí, por aguantarme, por sus grandes consejos y ser quien tira de mí. Por ser esa persona que siempre me animó y me brindó su compresión.

A mis padres y mi hermana, a los que nunca podré agradecer el cariño, valores y esfuerzo que han brindado en mi vida. Sobre todo, a su gran apoyo en los momentos más difíciles.

A todos ellos, quiero dedicarles esta Tesis y darles las gracias.

Lara

ÍNDICE

1.	Prólogo	7
2.	Objetivos	13
3.	Tensioactivos o surfactantes	17
3.1.	Definición y conceptos	19
3.2.	Propiedades de los tensioactivos	20
3.3.	Clasificación de los tensioactivos	23
3.4.	Evolución del uso y consumo de los tensioactivos a nivel industrial	27
3.5.	Adsorción: propiedad de disminuir la tensión superficial.....	28
3.6.	Propiedad de agregación o asociación.....	30
3.7.	Niosomas.....	33
3.8.	Bibliografía	37
4.	Tecnología de membranas	41
4.1.	Procesos de separación con membranas.....	43
4.2.	Antecedentes y aplicaciones	47
4.3.	Procesos impulsados por una diferencia de presión transmembranal.....	49
4.4.	Eficiencia y productividad	54
4.5.	Polarización por concentración.....	55
4.6.	Ensuciamiento y limpieza de las membranas	58
4.7.	Bibliografía	60
5.	Ácido láctico	63
5.1.	Generalidades	65
5.2.	Usos y aplicaciones.....	66
5.3.	Síntesis.....	69
5.4.	Recuperación y purificación	77
5.5.	Materias primas empleadas	79
5.6.	Bibliografía	80
6.	Lactic acid recovery by microfiltration using niosomes as extraction agents.....	85
6.1.	Introduction	89

6.2. Materials and methods	90
6.2.1. Chemicals	90
6.2.2. Niosome preparation	91
6.2.3. Experimental set-up	91
6.2.3.1. Selection of the membrane pore size and working pressure	92
6.2.3.2. Membrane cleaning	92
6.2.4. Niosomal extraction procedure	92
6.2.4.1. Total recirculation mode (1 st stage)	95
6.2.4.2. Concentration mode (2 nd stage).....	96
6.2.4.3. Lactic acid back-extraction	100
6.2.4.4. Lactic acid extraction by a two-step concentration process.....	100
6.2.5. Analytical methods.....	100
6.2.5.1. Lactic acid measurement.....	100
6.2.5.2. Determination of free SDS concentration.....	101
6.2.5.3. Particle size measurement	102
6.2.5.4. Zeta potential measurement.....	102
6.2.5.5. pH measurement.....	103
6.2.5.6. Morphological analysis.....	103
6.3. Results and discussion.....	103
6.3.1. Membrane pore size and transmembrane pressure selection	103
6.3.2. Lactic acid extraction with niosomes	107
6.3.2.1. Effect of the SDS concentration in the formulation of niosomes	107
6.3.2.2. Effect of the volume of the dispersed phase	108
6.3.2.3. Effect of the lactic acid concentration in feed	109
6.3.2.4. Effect of pH.....	111
6.3.3. Effect of the feed composition on the membrane behavior during the concentration stage	114
6.3.4. Lactic acid back-extraction process.....	117
6.3.5. Lactic acid extraction in a two-step process	119
6.4. Conclusions	120

6.5. References.....	123
7. Separation of sodium lactate from Span 80 and SDS surfactants by ultrafiltration	127
7.1. Introduction	131
7.2. Materials and methods	132
7.2.1. Chemicals	132
7.2.2. Niosome formation	133
7.2.3. Experimental procedure.....	133
7.2.4. Analytical methods.....	136
7.2.5. Experimental design and statistical analysis	137
7.3. Results and discussion.....	138
7.3.1. Effect of NaOH addition on the breakup of niosomes	138
7.3.2. Experimental design.....	140
7.3.3. Optimization of operating conditions	144
7.3.4. Relationship between permeate flux and SDS rejection.....	144
7.4. Conclusions	150
7.5. References.....	151
8. Solubilization of Span 80 niosomes by sodium dodecyl sulfate.....	155
8.1. Introduction	159
8.2. Experimental section.....	161
8.3. Results and discussion.....	164
8.4. Conclusions	174
8.5. References.....	176
9. Stability and characterization studies of Span 80 niosomes modified with CTAB in the presence of NaCl	185
9.1. Introduction	189
9.2. Materials and methods	191
9.2.1. Chemicals	191
9.2.2. Solubilization experiments of Span 80 niosomes by CTAB	191
9.2.3. Mixed niosomes formulation	192
9.2.4. Analytical Techniques.....	192
9.2.4.1. Optical density.....	192

9.2.4.2.	Particle size distribution	192
9.2.4.3.	ζ -Potential	192
9.2.4.4.	Morphological analysis.....	193
9.2.4.5.	Surface tension.....	193
9.2.4.6.	Stability measurement	193
9.3.	Results and discussion.....	194
9.3.1.	Solubilization of Span 80 niosomes by CTAB	194
9.3.2.	Effect of NaCl on aggregation and surface properties	196
9.3.2.1.	Effect of NaCl on CTAB micelles	201
9.3.2.2.	Effect of NaCl on 20 mol/m ³ Span 80 niosomes.....	204
9.3.2.3.	Effect of NaCl on mixed niosomes of Span 80 (20 mol/m ³) and CTAB (4 mol/m ³)	210
9.4.	Conclusions	216
9.5.	References.....	217
10.	Conclusiones generales.....	218

1. Prólogo

En el ámbito de la Ingeniería Química, la actividad investigadora actual se centra en el avance del conocimiento orientado a la búsqueda de nuevos procesos y al uso de tecnologías emergentes con el objetivo de mejorar los procesos convencionales y encontrar alternativas que incrementen la eficacia y la selectividad de los procesos, procurando, a la vez, aumentar la sostenibilidad y la protección del medio ambiente.

En las últimas décadas hay una gran concienciación por la protección del medio ambiente, la lucha por el calentamiento global y el agotamiento de los recursos no renovables. Esto ha transcendido en la aplicación de políticas cada vez más exigentes de regulación y control de emisiones contaminantes que han incentivado la investigación, la innovación y el uso de tecnologías limpias.

En línea con esta sensibilidad, ha surgido un campo emergente de investigación denominado “Intensificación de Procesos”, que pretende combinar de forma simultánea la mejora en la productividad y la sostenibilidad medioambiental a través de la investigación y la innovación en todas las etapas y fases implicadas en los procesos de producción. Es un campo interdisciplinar que trata de aprovechar las sinergias para el desarrollo, optimización y aplicación de tecnologías más limpias, con mayor eficiencia energética, equipos más versátiles y de tamaño más reducido, tratamiento de todas las corrientes, reúso de materiales y reducción en la generación de residuos.

Las tecnologías de separación con membranas son tecnologías limpias que han demostrado numerosas aplicaciones en la Intensificación de Procesos debido principalmente a su gran versatilidad, fácil aplicabilidad y su integración en procesos híbridos. Algunas de ellas, en concreto los procesos de microfiltración y ultrafiltración, son objeto de estudio en esta Tesis.

En los últimos años, uno de los campos más activos de investigación y que ha surgido con mayor auge es la nanotecnología. Los grandes avances en nanotecnología han proporcionado nuevas herramientas para la Intensificación de los Procesos en numerosas aplicaciones. Se trata del desarrollo de nuevos materiales y técnicas de fabricación que han supuesto un avance científico y tecnológico de gran impacto en múltiples campos en sectores como la robótica, sensores, electrónica, comunicaciones, informática, nuevos materiales, medicina, biotecnología, farmacia, alimentación y automoción, entre otros.

La nanoencapsulación es una rama de la nanotecnología cuyo objetivo es el desarrollo de nanopartículas capaces de encapsular y/o atrapar compuestos. Esta tecnología ha sido empleada con gran éxito en la industria farmacéutica para la liberación controlada de fármacos,

y en la industria alimentaria para la administración de compuestos bioactivos, generalmente insolubles en medio acuoso, con el fin de mejorar su solubilidad, estabilidad y biodisponibilidad.

Los niosomas son nanopartículas que contienen una cavidad interior encerrada en una o varias bicapas formadas por agregaciones de moléculas de tensioactivos no iónicos. Estas nanopartículas pueden emplearse como sistemas de transporte, encapsulación y liberación de compuestos. Suponen una herramienta útil debido a su elevada estabilidad y su capacidad de encapsular tanto compuestos hidrofílicos como hidrofóbicos, lo que ha supuesto que sean utilizados en la encapsulación de fármacos y en la formulación de alimentos enriquecidos cuyo interés ha crecido considerablemente.

Un aspecto novedoso que se presenta en este Tesis Doctoral es la posibilidad de utilizar niosomas como agentes de extracción. Para explorar esta posibilidad se utilizó como soluto modelo el ácido láctico, dado su enorme interés en el campo alimentario y en la producción de bioplásticos.

El ácido láctico es un compuesto ampliamente utilizado en múltiples aplicaciones. En los últimos años ha aumentado enormemente su demanda debido a su empleo en la producción del ácido poliláctico, un polímero biodegradable que representa una alternativa ecológica a los plásticos derivados del petróleo.

El ácido láctico es producido generalmente mediante procesos de fermentación, donde se encuentra en muy baja concentración debido a que generalmente el proceso sufre inhibición por el producto. Los procesos tradicionales de recuperación del ácido láctico se realizan habitualmente mediante precipitación del lactato de calcio con hidróxido de calcio. Este método es costoso al constar de múltiples etapas y requerir una gran cantidad de energía y agua, suponiendo un elevado gasto económico. Además, este método es altamente perjudicial para el medio ambiente, al emplear grandes cantidades de productos químicos y generar elevadas cantidades de subproductos que deben tratarse. En la actualidad, un gran número de investigaciones se centran en la mejora de las etapas de separación y concentración del ácido láctico mediante tecnologías limpias, como las tecnologías de separación con membranas, para configurar procesos más económicos, selectivos y respetuosos con el medio ambiente.

Desde esta perspectiva, el trabajo de investigación que se presenta en esta Tesis Doctoral se desarrolla en dos partes. Una parte inicial cuyo objetivo es explorar el uso conjunto de niosomas y separación con membranas mediante microfiltración y ultrafiltración, para realizar las etapas de extracción, concentración y reextracción del ácido láctico a partir de disoluciones acuosas altamente diluidas. A esta parte se dedican los capítulos VI y VII de esta memoria.

En concreto, en el capítulo VI se estudian y se optimizan las variables de operación para realizar la etapa de extracción de ácido láctico con niosomas de monooleato de sorbitán, Span 80, modificados con dodecil sultato sódico, SDS, y la etapa de concentración con membranas de microfiltración de TiO₂. Así mismo, se determinan las condiciones del medio para realizar la etapa de reextracción, observándose, sin embargo, un fuerte ensuciamiento de la membrana en esta etapa. El capítulo VII es una continuación del anterior, en el cual se estudia el proceso de reextracción con membranas de ultrafiltración de ZrO₂ con el fin de solventar el fuerte ensuciamiento observado en el estudio anterior, y se determinan las condiciones de operación óptimas de la etapa de reextracción.

El estudio realizado en esta primera parte demostró que la optimización de este proceso de extracción – reextracción está fuertemente condicionada por la formulación de los niosomas y del medio de dispersión. Es la composición de ambas fases, continua y dispersa, la que afecta a la capacidad y la cinética de extracción, así como la que determina el tipo de membrana y las condiciones de operación.

En línea con los resultados de la primera parte, la segunda parte de la investigación que se presenta en esta memoria trata de profundizar en la caracterización y comportamiento en diferentes medios del tensioactivo no iónico Span 80, abarcando los capítulos VIII y IX. En concreto, en el capítulo VIII se estudia la interacción entre los niosomas de Span 80 y el tensioactivo aniónico SDS, y en el capítulo IX las interacciones con el tensioactivo catiónico bromuro de cetiltrimetilamonio, CTAB. Además, se estudia la estabilidad de los niosomas mixtos y las propiedades de adsorción y de agregación en agua y en presencia de diferentes concentraciones de sal.

Los tensioactivos utilizados en este trabajo (Span 80 y SDS) son biodegradables y de grado alimentario, y el CTAB posee demostradas propiedades antisépticas y antibacterianas.

Los resultados presentados en esta Tesis Doctoral son de utilidad en la optimización de formulaciones de aplicación en procesos de extracción, o en diferentes campos, incluidos la preparación de fármacos, cosméticos, y alimentos enriquecidos o funcionales.

2. Objetivos

El trabajo que se presenta en esta Tesis Doctoral se ordena en dos partes:

- Una primera parte cuyo objetivo principal es investigar y evaluar el potencial uso de los niosomas como agentes de extracción del ácido láctico y la simultánea separación y concentración mediante tecnologías de membranas.
- Una segunda parte cuyo objetivo general es buscar formulaciones de niosomas estables con baja concentración de tensioactivos. Para ello nos propusimos estudiar la estabilidad y las propiedades fisicoquímicas de diferentes formulaciones que contienen el tensioactivo no iónico monooleato de sorbitán (Span 80) y los tensioactivos iónicos dodecil sultato sódico (SDS) y bromuro de cetiltrimetilamonio (CTAB).

La consecución de estos objetivos generales abarca los siguientes objetivos concretos:

1. Estudiar el efecto de diferentes variables de formulación de la fase dispersa y de la fase continua sobre la capacidad y la cinética de extracción del ácido láctico. En concreto se estudió el efecto de las siguientes variables: concentración de SDS en la formulación de los niosomas de Span 80, volumen de fase dispersa añadida, concentración de ácido láctico y el pH de la fase continua.
2. Optimizar la formulación de las fases continua y dispersa en la etapa de extracción.
3. Seleccionar el tipo de membrana y optimizar las condiciones de operación para realizar las siguientes etapas: a) la etapa de concentración de la fase dispersa con el ácido láctico extraído en los niosomas, y b) la etapa posterior de reextracción para obtener la separación del lactato sódico en la corriente de permeado.
4. Explorar las posibilidades de trabajar con una batería de multietapas para aumentar el rendimiento de la extracción.
5. Estudiar las interacciones entre los niosomas de Span 80 y el SDS en medio acuoso. En concreto, determinar los puntos críticos de máxima adsorción de SDS y de solubilización total de los niosomas por micelización.
6. Estudiar la interacción de niosomas de Span 80 y CTAB en medio acuoso. Más concretamente, determinar los puntos críticos de máxima adsorción y solubilización total de niosomas de Span 80 con CTAB.
7. Estudiar el efecto de la presencia de diferentes concentraciones de NaCl sobre las propiedades de agregación y de superficie de niosomas de Span 80 y niosomas mixtos de Span y CTAB.

3. Tensioactivos o surfactantes

3.1. Definición y conceptos

Los tensioactivos o surfactantes son moléculas que poseen una estructura molecular característica denominada anfipática. El término surfactante se ha adaptado de la palabra inglesa “surfactant (surface active agent)”. Esta terminología es muy utilizada coloquialmente para hacer referencia a este tipo de moléculas.

Estas moléculas anfipáticas o anfílicas están constituidas por un grupo liofóbico, con poca atracción por el solvente, y un grupo liofilíco, que tiene una gran atracción por el solvente [1,2]. En la Fig. 3.1 se muestra la estructura química básica de una molécula anfipática. La parte liofóbica está formada por una cadena hidrocarbonada lineal o ramificada y en la parte liofilíca se encuentra un grupo funcional diverso [3].

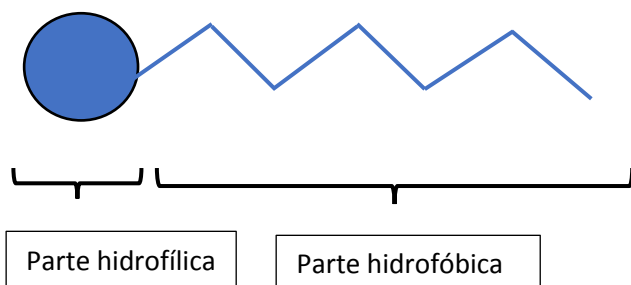


Figura 3.1. Estructura básica de una molécula anfipática.

Al poseer un grupo liofóbico y otro liofilíco en su estructura, las moléculas anfipáticas poseen propiedades físicas y químicas características. Cuando el solvente es agua, las moléculas se disponen de tal manera que las partes hidrofóbicas se orientan minimizando su contacto con el agua. En la Fig. 3.2 se muestra la disposición de las moléculas de tensioactivo en un medio acuoso.

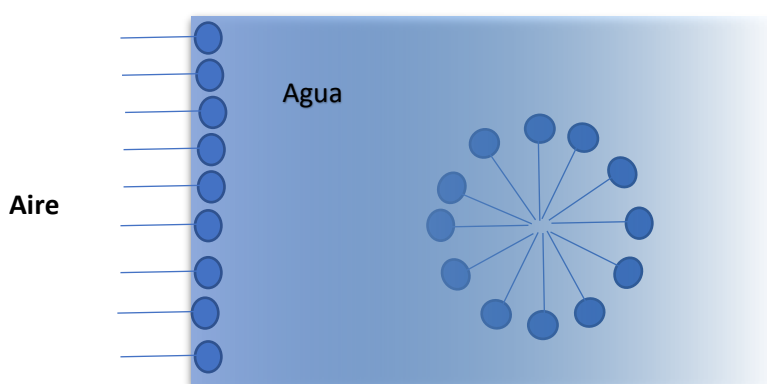


Figura 3.2. Esquema del comportamiento de las moléculas de tensioactivo en un medio acuoso.

Las moléculas anfipáticas tienden a adsorberse en la interfaz aire/agua disminuyendo la tensión superficial, o en cualquier interfaz entre fases, modificando la tensión interfacial [1].

La medida en que el carácter hidrófilo o el lipófilo dominan en un tensioactivo está representada por el balance hidrofílico – lipofílico o valor HLB (Hydrophilic-Lipophilic Balance). Un valor de HLB alto (10 a 18) indica una sustancia más hidrófila, que es adecuada para las emulsiones de aceite en agua (O/W). Las sustancias con un HLB bajo (3 a 8) son lipófilas y son adecuadas para emulsiones de agua en aceite (W/O).

3.2. Propiedades de los tensioactivos

Además de muchas otras, los tensioactivos poseen dos propiedades básicas y características [4].

Una de ellas es su capacidad de adsorberse en la superficie aire/agua y reducir la tensión superficial. La capacidad de disminuir la tensión superficial se atribuye a las fuerzas débiles de interacción de sus cadenas hidrofóbicas con las moléculas de agua y a las fuertes interacciones con los grupos hidrofílicos. El grupo hidrófilo interacciona con las moléculas de agua, quedándose localizado en la interfase aire/agua. La adsorción de las moléculas tensioactivas provoca un cambio en la interacción con las moléculas de agua, disminuyendo la energía de los enlaces y, por tanto, la tensión superficial [5].

Otra de las propiedades básicas que poseen los tensioactivos es su capacidad de agregación o asociación cuando están en solución, formando agregados denominados micelas. La fuerza impulsora para la formación de micelas (micelización) es la reducción del contacto entre las cadenas hidrofóbicas y el agua, reduciendo así la energía libre del sistema [6].

Otras propiedades que poseen los tensioactivos y que son de gran interés por su utilidad práctica, son las siguientes:

- Poder detergente: Se trata de la aplicación más conocida. Las moléculas de tensioactivos son capaces de estabilizar la grasa dentro de las micelas. Tras un proceso mecánico o de agitación, la grasa que se encuentra adherida a una superficie sólida queda liberada y puede ser atrapada por las micelas y arrastrada con el agua.
- Solubilización: Se trata de una característica muy importante, ya que los tensioactivos permiten la solubilización en un medio líquido de compuestos de diferente naturaleza, mediante interacciones de carácter polar o apolar con las diferentes partes de las estructuras agregadas de los tensioactivos presentes en dicho medio.

- Formación de emulsiones: La presencia de tensioactivos reduce la tensión interfacial entre los líquidos inmiscibles y facilita la formación y la estabilidad de pequeñas gotas de la fase dispersa en el medio continuo.
- Poder humectante: La capacidad de los tensioactivos de disminuir la tensión superficial promueve que el líquido se extienda por las superficies y las moje.
- Poder emulgente y dispersante: Se refiere a la capacidad de los tensioactivos de estabilizar las emulsiones, evitando la coalescencia de las gotas.
- Poder espumante: Es la capacidad de formar espuma. Al disminuir la tensión superficial de la interfaz aire/agua se facilita la formación de burbujas de aire.

Debido a las propiedades mencionadas, los tensioactivos poseen una gran versatilidad en cuanto a su utilidad en numerosas aplicaciones industriales [5,7].

La infinidad de aplicaciones que poseen los tensioactivos les confiere una gran relevancia en la mayoría de las industrias: detergentes, pinturas, colorantes, industria química, recubrimientos, farmacéutica, cuero, metales, petrolera, plásticos, textiles y fibras, alimentaria, celulosa, cosmética, agricultura, etc.

La aplicación más importante de los tensioactivos es su poder detergente, cuyo uso es el más empleado y genera un gran número de productos en el mercado. Mayoritariamente, se emplean los tensioactivos aniónicos para esta aplicabilidad.

La segunda aplicación de los tensioactivos más utilizada son los productos de higiene y cosmética, como los champús, perfumes, cremas, geles, etc. Al igual que la aplicación anterior, suelen emplearse los tensioactivos aniónicos. Su uso generalizado se debe a su capacidad de emulsionar todo tipo de aceites o esencias en productos cosméticos, y más recientemente por su capacidad de encapsular medicamentos y compuestos bioactivos, fundamentalmente de carácter lipófilo, en el interior de micelas y vesículas y aumentar así su solubilidad en medio acuoso [8,9]. En la Tabla 3.1 se resumen las principales aplicaciones de los tensioactivos ordenadas por el tipo de actividad industrial.

Tabla 3.1. Clasificación de las principales actividades industriales que utilizan tensioactivos.

INDUSTRIA	PROPIEDAD	PRODUCTOS
DETERGENTE	Detergente	Detergentes (polvo, líquidos)
	Estabilizadores de espuma	Jabones Productos de limpieza
HIGIENE	Detergente	Champús
	Emulsionante	Geles Productos de higiene
COSMÉTICA	Emulsionante	Aceites y cremas
	Detergente	Champús, geles, jabones, etc.
	Solubilizante	Aceites Perfumes
AGRICULTURA	Emulsionante	Plaguicidas
	Humectante	Herbicidas
FARMACIA	Agente antimicrobiano	Cremas, antisépticos
	Emulsionante	
ALIMENTARIA	Emulsionante	Mahonesa
	Dispersante	Salsas
PETRÓLEO	Humectantes	Antioxidantes
	Antiespumante	Conservantes
PINTURA	Acondicionadores	Productos de panadería y bollería
	Emulgente	Mantequilla, chocolate, etc.
PLÁSTICO	Solubilizante	
	Inhibidor de la corrosión	
	Dispersante	
CURTIDO	Emulsionante	Pintura
	Modificador de la viscosidad	Barnices
TEXTIL	Modificador de la viscosidad	Sprays
	Humectación	
TEXTIL	Desengrasante	Cuero, pintura
	Emulsionante	Detergentes
	Detergente	Jabones Productos de limpieza

3.3. Clasificación de los tensioactivos

Hay varias formas de clasificar a los tensioactivos. Una de las más comunes se basa en su aplicación, clasificándose en agentes emulsionantes, espumantes, humectantes, dispersantes, etc. Otra clasificación común es según su origen, como tensioactivos sintéticos y naturales.

Sin embargo, estas clasificaciones no proporcionan información acerca de su naturaleza química y, en muchos casos, los tensioactivos poseen varias aplicaciones [2].

Por ello, la clasificación más extendida y utilizada atiende a la estructura de la molécula, ya que ésta relacionada con sus propiedades y permite una mejor selección para sus posibles usos.

De forma generalizada, los tensioactivos se clasifican en función de la naturaleza del grupo hidrofílico en tensioactivos iónicos y no iónicos. Dentro del grupo de los tensioactivos iónicos, se clasifican a su vez según la carga que presentan en solución, como tensioactivos aniónicos, catiónicos y anfóteros. En la Tabla 3.2 se recogen las principales características de cada una de estas tipologías.

Tabla 3.2. Principales características de los tensioactivos según su tipología.

TENSIOACTIVOS CATIÓNICOS	
PARTE HIDROFÍLICA	Carga positiva
COMPUESTOS POR:	<ul style="list-style-type: none"> - Alquil aminas y sales - Aquil imidazolinas - Aminas polietoxiladas - Aminas cuaternarias
COMPATIBILIDAD	Compatibilidad: tensioactivos no iónicos y anfóteros Incompatibilidad: tensioactivos aniónicos
PROPIEDADES	<p>Adsorción a superficies con carga negativa</p> <ul style="list-style-type: none"> • Cosmética, acondicionadores, lacas y champús • Detergentes, suavizantes • Inhibidores de corrosión <p>Propiedad bactericida</p> <ul style="list-style-type: none"> • Antisépticos, esterilización y desinfectantes • Medicina, industria alimentaria y cosmética
PRODUCCIÓN	<p>Relativamente cara</p> <p>Utilizados en suavizantes, detergentes y desinfectantes</p> <p>Fines y usos específicos</p>

<u>TENSIOACTIVOS ANIÓNICOS</u>	
PARTE HIDROFÍLICA	Carga negativa
COMPUESTOS POR:	<ul style="list-style-type: none"> - Acil-aminoácidos - Sales de ésteres del ácido sulfúrico - Sales de ácidos carboxílicos - Sales de ácidos sulfónicos - Esteres del ácido fosfórico
APLICACIONES	AMPLIA VARIEDAD <ul style="list-style-type: none"> • Detergentes • Espumantes • Fungicidas • Humectantes • Emulsionantes • Solubilizantes
INDUSTRIA	Más empleados a nivel industrial Empleados mayoritariamente para detergentes

<u>TENSIOACTIVOS ANFÓTEROS</u>	
PARTE HIDROFÍLICA	Poseen grupos funcionales que pueden comportarse como aniónicos o catiónicos dependiendo de las condiciones del medio
COMPUESTOS POR:	A un pH ácido se comportan como surfactantes catiónicos y a un pH básico, como surfactantes aniónicos
COMPATIBILIDAD	Todos los grupos de tensioactivos
APLICACIONES	<p>Su fabricación supone un gran coste: aplicaciones específicas</p> <ul style="list-style-type: none"> • Inhibidores de la corrosión • Solubilizantes • Suavizantes • Espumantes • Bactericidas

<u>TENSIOACTIVOS NO IÓNICOS</u>	
PARTE HIDROFÍLICA	Neutra
COMPUESTOS POR:	<ul style="list-style-type: none"> - Alcoholes - Alcanolamidas - Óxidos de aminas - Ésteres - Éteres
	Grupo amplio y variado
PUESTO INDUSTRIA	Segundo grupo de tensioactivo más empleado
COMPATIBILIDAD	Todos los otros grupos de tensioactivos
PROPIEDADES	Baja toxicidad
APLICACIONES	<p>Actualmente ganando importancia en la industria</p> <ul style="list-style-type: none"> ● Agentes humectantes ● Espesante ● Bajo poder espumante ● Emulsionante ● Solubilizante
	Industria farmacéutica, agricultura, química, papel, textil, alimentación, cosmética, etc.

En los estudios realizados durante el desarrollo de esta Tesis Doctoral se han utilizado los siguientes tensioactivos: el tensioactivo no iónico monooleato de sorbitán (Span 80), también denominado monooleato de sorbitano, el tensioactivo aniónico dodecil sulfato sódico (SDS) y el tensioactivo catiónico bromuro de cetiltrimetilamonio (CTAB). Sus estructuras, características y principales aplicaciones industriales se recogen en la Tabla 3.3.

Tabla 3.3. Características de los tensioactivos empleados.

	MONOOLEATO DE SORBITÁN (SPAN 80)	DODECIL SULFATO SÓDICO (SDS)	BROMURO DE CETILTRIMETILAMONIO (CTAB)
TIPO SURFACTANTE	No iónico	Aniónico	Catiónico
FÓRMULA MOLECULAR	$C_{24}H_{44}O_6$	$CH_3-(CH_2)_{11}-OSO_3^- Na^+$	$(C_{16}H_{33}) N^+(CH_3)_3 Br^-$
PROPIEDADES	No tóxico Grado alimentario Fines humectantes, estabilizantes, emulsionantes	Biodegradable Bajo coste de fabricación Baja toxicidad	Antiséptico eficaz contra bacterias y hongos
ESTRUCTURA	<p>$CH_2-O-C(=O)-CH_2-(CH_2)_6-CH_2-CH=CH-CH_2-(CH_2)_6-CH_3$</p>	<p>$H_3C-(CH_2)_{11}-OSO_3^- Na^+$</p>	<p>$\text{Cetyl chain} - N(CH_3)_3^+ Br^-$</p>
USOS INDUSTRIALES	Alimentaria: chocolate, margarinas, helados, salchichas, etc. Cosmética Farmacéutica	<u>Uno de los tensioactivos más empleados en la industria</u> Detergente Productos de limpieza Cosmética Farmacéutica Alimentación (aditivo) Productos de higiene	Detergente, suavizante, acondicionador Emulsionante Antiséptico Bactericida Inhibidor de la corrosión

3.4. Evolución del uso y consumo de los tensioactivos a nivel industrial

Desde hace décadas, el consumo de tensioactivos ha ido creciendo paulatinamente, observándose un fuerte crecimiento en el último periodo analizado comprendido entre 2015 y 2018. Los tensioactivos aniónicos son el grupo de tensioactivos más importante en el mercado global [10]. Sin embargo, es de destacar que se ha producido un cambio en la tipología de los tensioactivos utilizados. Hasta el año 2016, los datos indicaban que los grupos de tensioactivos mayoritariamente utilizados eran los catiónicos y aniónicos, siendo el consumo de tensioactivos no iónicos el menor y muy por debajo de los anteriores. Sin embargo, en los últimos años el consumo de tensioactivos no iónicos ha ido aumentado hasta cifras casi equiparables a las de los tensioactivos catiónicos y aniónicos. El aumento de los tensioactivos no iónicos se debe en gran parte a sus buenas propiedades humectantes y emulsionantes, su compatibilidad con todos los tipos de tensioactivos para generar sinergias de utilidad en nuevas aplicaciones y a su baja toxicidad.

Según el Instituto Nacional de Estadística (INE) [11], en el año 2018, el consumo de tensioactivos en España (excluidos los jabones) fue de 433 millones de kilogramos, con un reparto uniforme entre los tensioactivos catiónicos, aniónicos y no iónicos, y con un valor global de 532,32 millones de euros.

En cuanto a su uso, el mayor consumo de tensioactivos se produce en la fabricación de detergentes, lo que representa aproximadamente el 50% del mercado mundial de tensioactivos [10].

La tendencia actual se dirige al uso y, por tanto, fabricación de tensioactivos más naturales y biodegradables a partir de materias primas naturales.

La búsqueda de biosurfactantes se debe a la mayor demanda de materias biodegradables debido a la creciente preocupación ambiental. Estos biosurfactantes poseen propiedades similares a las de los surfactantes convencionales y tienen a su favor una baja toxicidad. Sin embargo, los costes de su producción aún no son competitivos, lo que ha hecho que se frene su comercialización.

3.5. Adsorción: propiedad de disminuir la tensión superficial

La comprensión del fenómeno de la adsorción de las moléculas de tensioactivo en la interfaz aire/agua es de vital importancia para el conocimiento de los procesos físico-químicos que ataúnen a las propiedades de los tensioactivos, como son los procesos de emulsión, formación de espuma, humectación, detergencia, etc. [12,13].

Las fuerzas de cohesión entre las moléculas de un líquido son responsables del fenómeno conocido como tensión superficial (TS). Las moléculas que se encuentran en la superficie de un líquido no tienen el mismo número de átomos vecinos que las que se encuentran en el medio sumergido; por ello, las fuerzas de cohesión entre las moléculas de la superficie son mayores que en el interior, generándose una "película superficial" que ofrece cierta resistencia al paso de un objeto a través de ella (Fig. 3.3).

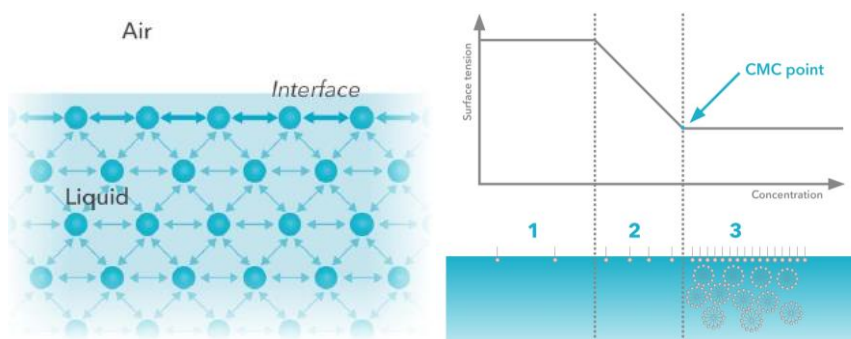


Figura 3.3. Ilustración que muestra el fenómeno de tensión superficial de un líquido (a) y su disminución en presencia de tensioactivos (b). Tomada con autorización de Biolin (2017) [14].

La presencia de tensioactivos en la superficie de un líquido interrumpe la energía de cohesión entre las moléculas del líquido y por lo tanto disminuye la tensión superficial. A medida que aumenta la concentración de tensioactivo disminuye la tensión superficial hasta alcanzar un valor mínimo, a partir del cual la tensión superficial se mantiene constante, tal como se representa en la Fig. 3.3. El valor mínimo de tensión superficial se identifica como Concentración Micelar Crítica (CMC) [15]. A partir de la CMC, cualquier cantidad de tensioactivo que se añada a la solución se incorporará en forma de agregado y no de monómero.

La CMC de un tensioactivo está relacionada con el número de átomos de carbono de su cadena hidrofóbica, de tal manera que, en un mismo tipo de tensioactivo (serie homóloga), un aumento en la longitud de la cadena hidrofóbica en un grupo $-\text{CH}_2$, produce una disminución de la CMC a la mitad. El efecto del grupo de cabeza y del contra-ión sobre la CMC es menos acusado.

La adsorción de moléculas de tensioactivo en la interfaz aire/líquido es consecuencia de su estructura anfífila. Las repulsiones entre las partes hidrofóbicas de las moléculas de tensioactivo inducen su transporte hacia fuera del seno de la solución acuosa, mientras que la parte hidrofílica del tensioactivo interactúa con las moléculas del agua mediante interacciones de carácter fuerte, quedando las moléculas solvatadas [5]. La adsorción de moléculas de tensioactivo en la superficie de un líquido se identifica como un proceso dinámico de adsorción y desorción, de tal manera que se conjuga el transporte difusional de las moléculas tensioactivas desde el seno de la disolución a la interfaz aire/agua debido a un gradiente de concentración y, a medida que la interfaz se va llenando, se produce de forma simultánea el transporte inverso de moléculas desde la región de la interfase a la región interior [16–18]. El primer proceso de transferencia molecular se denomina adsorción, mientras que el segundo proceso se denomina desorción, tal como se muestra en la Fig. 3.4.

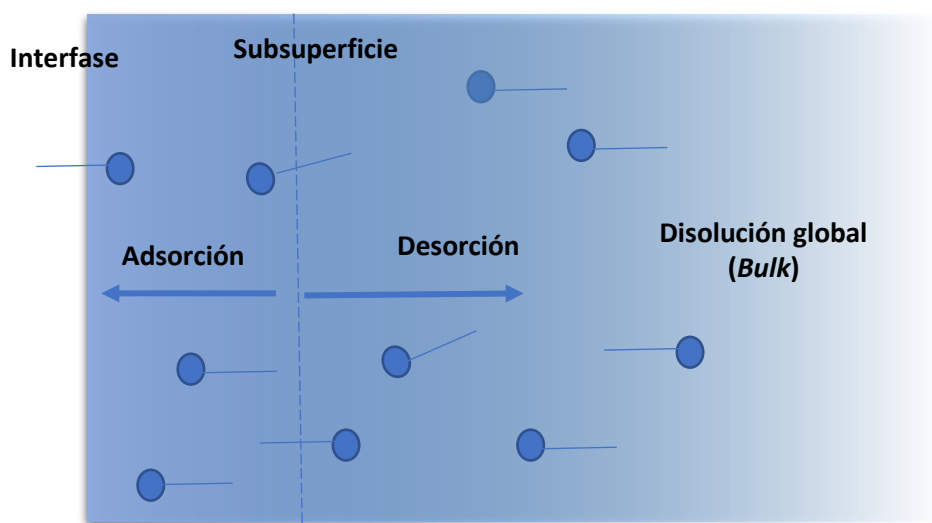


Figura 3.4. Representación de los procesos de transporte de los monómeros.

La dinámica de la adsorción depende del coeficiente de difusión del tensioactivo. Sin embargo, a medida que se va llenando la interfaz, pueden tener lugar fenómenos de impedimento a la adsorción por diferentes causas. Esos impedimentos o barreras a la adsorción pueden ser estéricos, electrostáticos, debidos a un aumento de la presión superficial o a la inexistencia de espacios libres en la superficie [19].

La adsorción de las moléculas de tensioactivo en la interfase aire/líquido provoca cambios en las fuerzas de interacción molecular en la superficie del líquido, disminuyendo la energía de los enlaces y por tanto reduciendo la tensión superficial [20].

En ausencia de gravedad, un líquido adquiere forma esférica, que es la forma con menor relación área-volumen. La reducción de la tensión superficial provoca la disminución de la superficie del líquido para un volumen dado. En este proceso interceden fuerzas intermoleculares de tipo iónico, de Van der Waals y de tipo hidrofóbico [1].

3.6. Propiedad de agregación o asociación

Como se ha mencionado anteriormente, otra de las propiedades fundamentales de los tensioactivos es su capacidad de agregación o asociación.

La autoagregación o micelización es un proceso natural y espontáneo [1]. La descripción teórica de este fenómeno es generalmente de tipo secuencial en la que se asume una primera fase de saturación de la interfase, con la formación de una monocapa adsorbida, seguida de una etapa de agregación del tensioactivo en micelas u otras estructuras de mayor tamaño. La concentración de tensioactivo a la cual se produce la formación de micelas coincide con el valor de tensión superficial mínimo y con su CMC. El valor de la CMC es característico de cada tensioactivo y varía con las condiciones del medio, fundamentalmente temperatura y composición [21–23].

Las moléculas de tensioactivo que se adicionan a partir de este punto se organizan en el seno de la disolución formando agrupaciones denominadas micelas. En un medio polar como el agua las micelas son esféricas, disponiéndose los grupos hidrófilos en contacto con la solución y las cadenas hidrofóbicas confinadas en el interior. En un líquido apolar se forman micelas invertidas, en las cuales las cadenas hidrofóbicas están en contacto con el medio, y los grupos polares confinados en el interior.

La posterior adición de moléculas de tensioactivo da como resultado la formación de mayor número de micelas y también del aumento de su tamaño, es decir, del número de agregación.

En la Fig. 3.5 se ilustra el modelo secuencial que de forma general se asume para explicar el fenómeno de agregación, una vez alcanzada la CMC. En él se representa la coexistencia de los monómeros de tensioactivo en equilibrio dinámico con las micelas y las moléculas adsorvidas en la superficie del líquido [15,24–25].

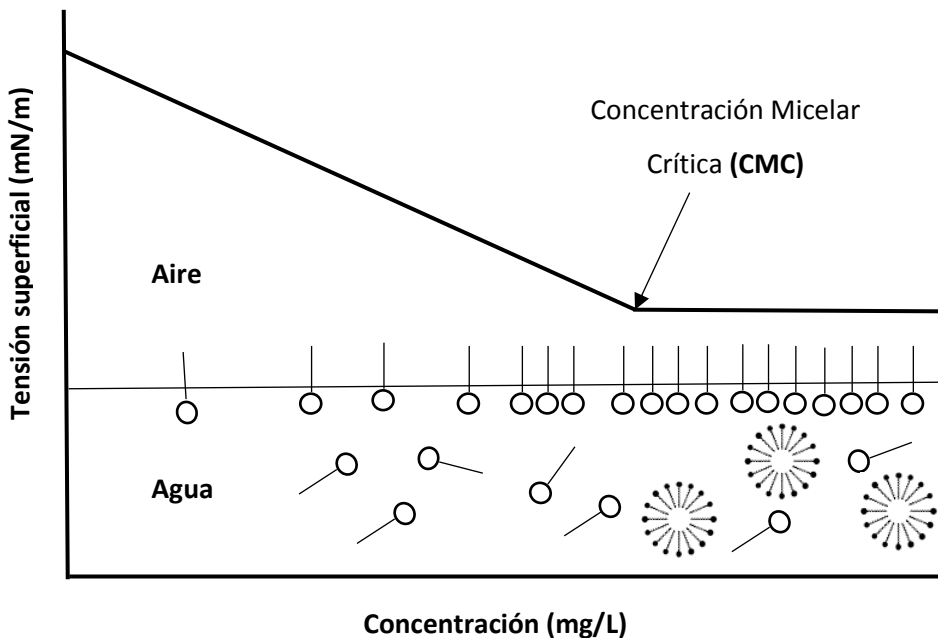


Figura 3.5. Representación del comportamiento de un tensioactivo en disolución acuosa al ir aumentando la concentración y su efecto sobre la tensión superficial.

La CMC es un valor indicativo de la tendencia a la micelización. Cuanto menor es su valor, mayor es su facilidad de agregación. Su valor depende de la intensidad de la interacción de fuerzas de carácter electrostático entre los grupos polares y de las fuerzas hidrofóbicas entre las cadenas apolares de las moléculas de tensioactivo [3].

Si las interacciones electrostáticas entre las moléculas de tensioactivo son fuertes, las moléculas no pueden acercarse lo suficiente para que tengan lugar interacciones entre las cadenas hidrófobas. Esto explica por qué los tensioactivos iónicos, que poseen cargas netas en su región hidrofílica, tienen mayor dificultad para la formación de micelas y poseen valores mayores de CMC respecto a otros tipos de tensioactivos. En cambio, los tensioactivos no iónicos poseen menos interacciones electrostáticas, favoreciendo la micelización [26].

Otros factores que afectan al valor de la CMC son el número de átomos de carbono del grupo hidrofílico, la temperatura, el pH o la presencia de otros compuestos [1,6].

Para un tensioactivo, el valor de la CMC es muy importante, ya que las moléculas tensioactivas tienen un comportamiento diferente dependiendo si se encuentran en forma de monómeros o en forma de micelas. Los monómeros pueden adsorberse en la interfaz y modificar la tensión superficial: su presencia influye sobre la capacidad del tensioactivo para la humectación y formación de espuma. La presencia de micelas no contribuye a estos efectos, pero sí afecta a otras propiedades del medio como la viscosidad, absorción de luz, conductividad, índice de refracción, etc. [25].

Algunas de estas propiedades experimentan un cambio brusco con la presencia de micelas y ese cambio de inflexión permite una determinación analítica precisa de la CMC. Algunas propiedades donde se observa este comportamiento y que se emplea para determinar la CMC de los tensioactivos son la tensión superficial, presión osmótica, turbidez, absorbancia UV-vis, solubilidad de un soluto y conductividad eléctrica, entre otras [6,15,27]. En la Fig. 3.6 se ilustra el cambio de tendencia de diferentes propiedades con la concentración de tensioactivo.

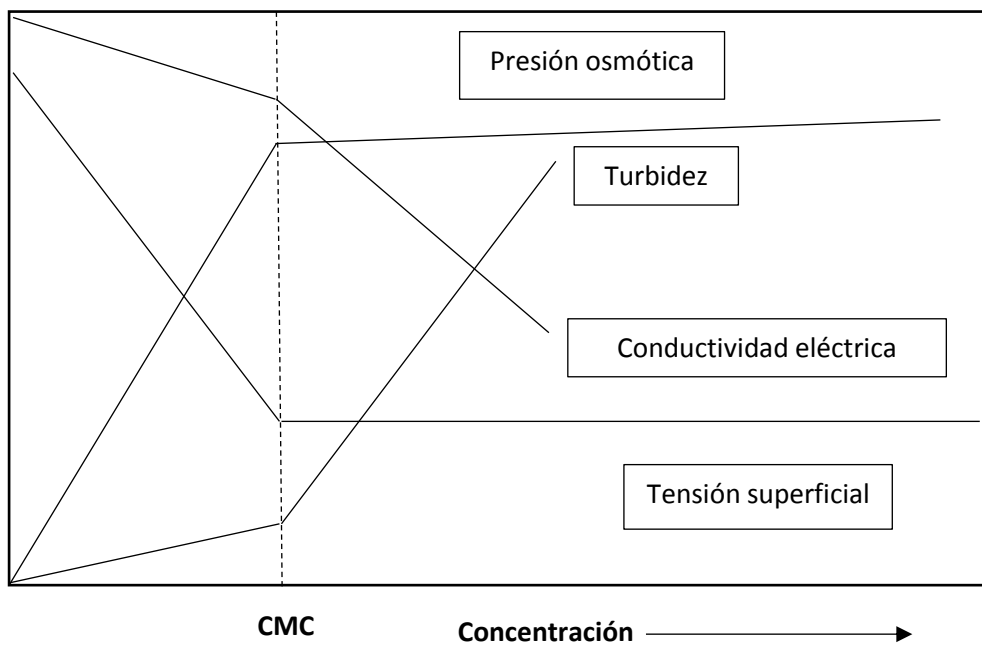


Figura 3.6. Comportamiento de diferentes propiedades de los tensioactivos con la concentración de tensioactivo.

3.7. Niosomas

Los niosomas son estructuras vesiculares formadas por una o varias bicapas de tensioactivo no iónico, que contienen en su interior una cavidad [8,9,26].

En los niosomas las moléculas de tensioactivo no iónico forman un autoensamblaje de modo que los extremos hidrofílicos se orientan hacia el exterior e interior de la vesícula, mientras que las cadenas hidrofóbicas se enfrentan dentro de la bicapa, como se muestra en la Fig. 3.7 [8,9,28–31].



Figura 3.7. Representación de la estructura de los niosomas.

Los niosomas poseen la capacidad de encapsular dentro de su estructura compuestos de carácter hidrófilo y lipófilo [32,33], disueltos en el interior acuoso o en el interior de la bicapa, respectivamente [8,9,28,34].

Aunque la estructura de los niosomas es similar a la de los liposomas, éstos se componen de agentes tensioactivos no iónicos, mientras que los liposomas están formados por fosfolípidos [35,36].

Un inconveniente que presenta el empleo de liposomas es el estar formados por fosfolípidos, ya que eso implica una estructura químicamente más inestable debido a su predisposición a la degradación oxidativa [37,38]. En cambio, los niosomas son químicamente más estables y poseen una vida útil más larga.

Además, los niosomas presentan numerosas ventajas respecto a los liposomas [33].

Las principales ventajas del uso de niosomas frente a los liposomas son las siguientes [9,30,32,36,38,39]:

- Mayor estabilidad
- Menor coste de fabricación
- Mayor control en la liberación de compuestos encapsulados
- Alta compatibilidad con sistemas biológicos
- Baja toxicidad
- Son biodegradables
- No producen reacción inmunológica
- Permiten encapsular compuestos tanto lipofílicos como hidrofílicos
- Fácil almacenamiento
- Variables de formación fácilmente controlables
- Uniformidad de tamaños
- Pueden administrarse en tratamientos médicos de diferente naturaleza (uso tópico, oral, pulmonar, ocular, parenteral, etc.)

En su inicio, los niosomas fueron empleados en la industria cosmética, fundamentalmente en cremas para mejorar la adsorción y liberación de compuestos [36,40,41]. Sin embargo, poco a poco fueron abriéndose paso en otros campos como la industria farmacéutica, alimentaria o en aplicaciones médicas [36,39,42–45].

Para la preparación de niosomas estables es necesario la aportación de energía, como puede ser agitación física o calor, a través de numerosos métodos [46]. La selección del método más apropiado depende del tipo de tensioactivo presente en la formulación, del compuesto a encapsular y de la aplicación final del producto.

Las técnicas de preparación de niosomas son muy variadas. Entre los métodos de preparación destacan los siguientes: método de hidratación de película seca, método de burbuja, método de inyección de éter, método de evaporación en fase inversa, microfluidización y sonicación, entre otros [32,36,42,47]. En la Tabla 3.4 se describen y comparan las diferentes técnicas más utilizadas.

Tabla 3.4. Principales técnicas de preparación de niosomas.

Preparación	Descripción del método	Ventaja	Desventaja	Ejemplos
Hidratación de una película delgada	Formación de una película seca de tensioactivo por evaporación del disolvente orgánico y posterior hidratación.	Técnica fácil y ampliamente utilizada	Uso de disolventes orgánicos	[28,36,48]
Inyección con éter	El tensioactivo y el compuesto se disuelven en éter dietílico o etanol y se inyectan lentamente en una fase acuosa que contiene el compuesto a encapsular, por encima del punto de ebullición del disolvente orgánico	Técnica fácil para investigación	No aplicabilidad en compuestos termosensibles	[39]
Método del gradiente de pH trans-membranal	Si el interior del niosoma tiene un valor de pH (pH ácido) inferior al externo, la sustancia a encapsular cruza la membrana del niosoma, y en el interior se ioniza en el medio ácido, siendo incapaz de abandonar el niosoma	Alta eficiencia de encapsulación	Uso de disolventes orgánicos	[39]
Inversión de fases por evaporación	Los tensioactivos se disuelven en una mezcla de éter y cloroformo y se añade una fase acuosa que contiene el compuesto. El sistema bifásico resultante se homogeneiza y la fase orgánica se evapora a baja presión	Alta eficiencia de encapsulación	Uso de disolventes orgánicos	[49]
Microfluidización	El compuesto a encapsular y el tensioactivo interactúan a una velocidad alta dentro de los microcanales del microfluidizador.	Sin disolventes orgánicos (caros, difíciles de eliminar completamente y peligrosos)	No aplicabilidad en compuestos termosensibles	[39,50]
Método de la burbuja	Se mezclan todos los componentes en un matraz a elevada temperatura (60–70 °C) utilizando un homogeneizador para obtener una buena dispersión. Posteriormente el matraz se introduce en un baño con agua y se hace burbujeante nitrógeno a través de la mezcla	Sin uso de disolventes	No aplicabilidad en compuestos termosensibles	[51]

Proniosomas	Recubrimiento soluble en agua del portador con un tensioactivo no iónico. Formulación seca en que cada partícula soluble en agua está cubierta con una fina película seca de tensioactivo	Reducción de la inestabilidad física y aumento de la eficacia de encapsulación	Proceso complejo	[52]
Método de calentamiento (HM)	Implica la hidratación de una molécula anfífila en una solución acuosa que contiene un 3% en volumen de un poliol a alta temperatura	Método de un solo paso, escalable con agentes no tóxicos	No puede aplicarse a compuestos termolábiles	[53]
Dióxido de carbono supercrítico (scCO ₂)	Proceso de formación de niosomas que utiliza CO ₂ en condiciones supercríticas	Uso de compuesto no inflamable, volátil, no tóxico, y sin disolventes orgánicos.	Largas estructuras unilaminares de gran tamaño	[35,36]
Sonicación	El tensioactivo se dispersa en la fase acuosa y esta dispersión se somete, junto con el compuesto a encapsular, a ultrasonidos utilizando una sonda de ultrasonidos de alta potencia	Método sencillo, barato y sin uso de disolventes orgánicos.	Se requiere un equipo específico para este método	[39,40]

3.8. Bibliografía

- [1] M.J. Rosen, *Surfactants and Interfacial Phenomena*, third ed., Wiley-Interscience, New York (2004).
- [2] D. Myers, *Surfaces, Interfaces, and Colloids: Principles and Applications*, second ed., Wiley, New York (1999).
- [3] M. Akram, S. Yousuf, T. Sarwar, Kabir-ud-Din, Micellization and interfacial behavior of 16-E2-16 in presence of inorganic and organic salt counterions, *Colloid Surf. A-Physicochem. Eng. Asp.* 441 (2014) 281–290.
- [4] B. Naseem, I. Arif, Effect of colloidal solutions of ionic surfactants on interactions between fertilizer and salts in saline soil at different temperatures: a thermo-acoustic study, *J. Mol. Liq.* 271 (2018) 452–471.
- [5] L. Sánchez, Influencia del contraión en las propiedades biológicas de tensioactivos aniónicos. Proyecto Fin de Carrera, Escuela Politécnica Superior de Ingeniería Industrial de Barcelona (2006).
- [6] T.F. Tadros, *Applied Surfactants: Principles and Applications*, Wiley, New York (2005).
- [7] P.K. Banipal, S. Arti, T.S. Banipal, Influence of polyhydroxy compounds on the micellization behaviour of cetyltrimethylammonium bromide: conductance and microcalorimetric, *J. Mol. Liq.* 223 (2016) 1204–1212.
- [8] I.F. Uchegbu and A.T. Florence, Non-ionic Surfactant vesicles (niosomes): physical and pharmaceutical chemistry, *Adv. Colloid Interface Sci.* 58 (1995) 1–55.
- [9] I.F. Uchegbu, S.P. Vyas, Non-ionic based vesicles (niosomes) in drug delivery, *Int. J. Pharm.* 172 (1998) 33–70.
- [10] Ceresana Research, *Market Study: Surfactants Markets Report* (2017).
- [11] Instituto Nacional de Estadística, *Encuesta Industrial Anual de Productos* (2018).
- [12] L. Suárez, M.A. Díez, R. García, F.A. Riera, Membrane technology for the recovery of detergent compounds: a review, *J. Ind. Eng. Chem.* 18 (2012) 1859–1873.
- [13] L. Junji, X. Yun, S. Hongxiu, Diffusion-controlled adsorption kinetics of surfactant at air/solution interface, *Chin. J. Chem. Eng.* 21 (2013) 953–958.
- [14] Biolin, Manual of Attension optical tensiometers. www.biolinscientific.com/service-and-support (Consultado: junio 2020).
- [15] M.L. Bhaisare, S. Pandey, M.S. Khan, A. Talib, H.F. Wu, Fluorophotometric determination of critical micelle concentration (CMC) of ionic and non-ionic surfactants with carbon dots via Stokes shift, *Talanta* 132 (2015) 572–578.

- [16] Y. He, P. Yazhgur, A. Salonen, D. Langevin, Adsorption–desorption kinetics of surfactants at liquid surfaces, *Adv. Colloid Interface Sci.* 222 (2015) 377–384.
- [17] S. Paria, K.C. Khilar, A review on experimental studies of surfactant adsorption at the hydrophilic solid-water interface, *Adv. Colloid Interface Sci.* 10 (2004) 75–95.
- [18] R. Miller, E.V. Aksenenko, V.B. Fainerman, Dynamic interfacial tension of surfactant solutions, *Adv. Colloid Interface Sci.* 247 (2017) 115–129.
- [19] J. Eastoe, J.S. Dalton, Dynamic surface tension and adsorption mechanisms of surfactants at the air-water interface, *Adv. Colloid Interface Sci.* 85 (2000) 103–144.
- [20] J.R. Fernández, P. Kalita, S. Migorski, M.C. Muñiz, C. Núñez, Variational analysis of the Langmuir-Hinshelwood dynamic mixed-kinetic adsorption model. *Nonlinear Anal. Real World Appl.* 15 (2014) 205–220.
- [21] A. Chatterjee, S.P. Moulik, S.K. Sanyal, B.K. Mishra and P.M. Puri, Thermodynamic of micelle formation of ionic surfactants: a critical assessment for sodium dodecyl sulfate, cetyl pyridinium chloride and dioctyl sulfosuccinate (Na salt) by microcalorimetric, conductometric, and tensiometric measurements, *J. Phys. Chem. B.* 105 (2001) 12823–12831.
- [22] M. Kamil, H. Siddiqui, Experimental study of surface and solution properties of gemini-conventional surfactant mixtures on solubilization of polycyclic aromatic hydrocarbon, *Model. Numer. Simul. Mater. Sci.* 3(4B) (2013) 17–25.
- [23] N. Deo, P. Somasundaran, Effects of sodium dodecyl sulfate on mixed liposome solubilization, *Langmuir* 19 (2003) 7271–7275.
- [24] Q. Xu, M. Nakajima, S. Ichikawa, N. Nakamura, P. Roy, H. Okadome, T. Shiina, Effects of surfactant and electrolyte concentrations on bubble formation and stabilization, *J. Colloid Interface Sci.* 332 (2009) 208–214.
- [25] I. Mukherjee, S.P. Moulik, A.K. Rakshit, Tensiometric determination of Gibbs surface excess and micelle point: a critical revisit, *J. Colloid Interface Sci.* 394 (2013) 329–336.
- [26] P.E. Levitz, Non-ionic surfactants adsorption: structure and thermodynamics, *C. R. Geosci.* 334 (2002) 665–673.
- [27] A. Modaressi, H. Sifaoui, M. Mielcarz, U. Domanska, M. Rogalski, CTAB aggregation in aqueous solutions of ammonium based ionic liquids; conductimetric studies, *Colloid Surf. A-Physicochem. Eng. Asp.* 296 (2007) 104–108.
- [28] V.B. Junyaprasert, V. Teeranachaideekul, T. Supaperm, Effect of charged and non-ionic membrane additives on physicochemical properties and stability of niosomes, *AAPS Pharm. Sci. Tech.* 9 (2008) 851–859.

- [29] N.O. Sahin, Niosomes as nanocarrier systems. In: M.R. Mozafari (Ed.), *Nanomaterials and Nanosystems for Biomedical Applications*, Springer, Dordrecht (2007), pp. 67–81.
- [30] L. Tavano, P. Alfano, R. Muzzalupo, B. de Cindio, Niosomes vs microemulsions: new carriers for topical delivery of capsaicin, *Colloid Surf B-Biointerfaces* 87 (2011) 333–339.
- [31] K. Hayashi, T. Shimanouchi, K. Kato, T. Miyazaki, A. Nakamura, H. Umakoshi, Span 80 vesicles have a more fluid, flexible and “wet” surface than phospholipid liposomes, *Colloid Surf B-Biointerfaces* 87 (2011) 28–35.
- [32] N.B. Mahale, P.D. Thakkar, R.G. Mali, D.R. Walunj, S.R. Chaudhari, Niosomes: novel sustained release nonionic stable vesicular systems—an overview, *Adv. Colloid Interface Sci.* 183 (2012) 46–54.
- [33] M. Carafa, E. Santucci, F. Alhaique, T. Coviello, E. Murtas, F.M. Riccieri, G. Lucania, M.R. Torrisi, Preparation and properties of new unilamellar non-ionic/ionic surfactant vesicles *Int. J. Pharm.* 160 (1998) 51–59.
- [34] G.N. Devaraj, S.R. Parakh, R. Devraj, S.S. Apte, B.R. Rao, D. Rambhau, Release studies on niosomes containing fatty alcohols as bilayer stabilizers instead of cholesterol, *J. Colloid Interface Sci.* 251 (2002) 360–365.
- [35] A. Manosroi, R. Chutoprapat, M. Abe, J. Manosroi, Characteristics of niosomes prepared by supercritical carbon dioxide (scCO₂) fluid, *Int. J. Pharm.* 352 (2008) 248–255.
- [36] C. Marianelli, L. Di Marzio, F. Rinaldi, C. Celia, D. Paolino, F. Alhaique, S. Esposito, M. Carafa, Niosomes from 80s to present: the state of the art, *Adv. Colloid Interface Sci.* 205 (2014) 187–206.
- [37] S. Gouin, Micro-encapsulation: Industrial appraisal of existing technologies and trends, *Trends Food Sci. Technol.* 15 (2004) 330–347.
- [38] A. Ritwiset, S. Krongsuk, J.R. Johns, Molecular structure and dynamical properties of niosome bilayers with and without cholesterol incorporation: a molecular dynamics simulation study, *Appl. Surf. Sci.* 380 (2016) 23–31.
- [39] R. Rajera, K. Nagpal, S.K. Singh, D.N. Mishra, Niosomes: a controlled and novel drug delivery system, *Biol. Pharm. Bull.* 34 (2011) 945–953.
- [40] D. Pando, G. Gutiérrez, J. Coca, C. Pazos, Preparation and characterization of niosomes containing resveratrol, *J. Food Eng.* 117 (2013) 227–234.
- [41] R. Muzzalupo, L. Tavano, S. Trombino, R. Cassano, N. Picci, C. La Mesa, Niosomes from α,ω -trioxyethylene-bis (sodium 2-dodecyloxy-propylenesulfonate): preparation and characterization, *Colloid Surf. B-Biointerfaces* 64 (2008) 200–207.
- [42] S. Moghassemi, A. Hadjizadeh, Nano-niosomes as nanoscale drug delivery systems: an illustrated review, *J. Control. Release* 185 (2014) 22–36.

- [43] M. Gonnet, L. Lethuaut, F. Boury, New trends in encapsulation of liposoluble vitamins, *J. Control. Release* 146 (2010) 276–290.
- [44] Z. Sezgin-Bayindir, M.N. Antep, N. Yuksel, Development and characterization of mixed niosomes for oral delivery using candesartan cilexetil as a model poorly water, *AAPS Pharm. Sci. Tech.* 16 (2014) 108–117.
- [45] P. Bhardwaj, P. Tripathi, R. Gupta, S. Pandey, Niosomes: a review on niosomal research in the last decade, *J. Drug Deliv. Sci. Technol.* 56 (2020) 101581.
- [46] L. Basiri, G. Rajabzadeh, A. Bostan, Physicochemical properties and release behavior of Span 60/Tween 60 niosomes as vehicle for α -tocopherol delivery, *LWT-Food Sci. Technol.* 84 (2017) 471–478.
- [47] S. Chen, S. Hanning, J. Falconer, M. Locke, J. Wen, Recent advances in non-ionic surfactant vesicles (niosomes): fabrication, characterization, pharmaceutical and cosmetic applications, *Eur. J. Pharm. Biopharm.* 144 (2019) 18–39.
- [48] Y.M. Hao, K. Li, Entrapment and release difference resulting from hydrogen bonding interactions in noisome, *Int. J. Pharm.* 403 (2011) 245-253.
- [49] A.S. Guinedi, N.D. Mortada, S. Mansour, R.M. Hathout, Preparation and evaluation of reverse-phase evaporation and multilamellar niosomes as ophthalmic carriers of acetazolamide, *Int. J. Pharm.* 306 (2005) 71-82.
- [50] I.F. Uchegbu and R. Duncan, Niosomes containing N-(2-hydroxypropyl)methacrylamide copolymer-doxorubicin (PK1): effect of method of preparation and choice of surfactant on niosome characteristics and a preliminary study of body distribution, *Int. J. Pharm.* 155 (1997) 7-17.
- [51] H. Talsma, M.J.V. Steenbergen, J.C.H. Borchert, D.J.A. Crommelin, A novel technique for the one-step preparation of liposomes and non-ionic surfactant vesicles without the use of organic solvents. Liposome formation in a continuous gas stream: The bubble method, *J. Pharm. Sci.* 83 (1994) 276-280.
- [52] V. R. Yasam, S. L. Jakki, J. Natarajan, and G. Kuppusamy, A review on novel vesicular drug delivery: proniosomes, *Drug Deliv.* 21 (2014) 243–249.
- [53] M. R. Mozafari, *Method and apparatus for producing carrier complexes*, UK Patent (2005) No. GB. 0404993.8, Int. Appl. No. PCT/GB05/000825.

4. Tecnología de membranas

4.1. Procesos de separación con membranas

Los procesos con membranas son procesos de separación que utilizan una membrana como barrera física de separación entre dos fases fluidas, a través de la cual se puede intercambiar materia y energía [1]. La membrana actúa permitiendo el transporte selectivo de ciertos componentes y rechazando el paso a otros [2].

La European Membrane Society definió el término membrana como una fase intermedia que separa dos fases y actúa como barrera activa o pasiva para el transporte de materia y energía entre las fases.

En la Fig. 4.1 se muestra una representación del proceso con membranas, donde se observa que el fluido denominado alimentación pasa a través de la membrana y genera dos corrientes: la corriente que pasa a través de la membrana se denomina permeado, y la corriente que no atraviesa la membrana y que contiene los solutos que son rechazados por ella se denomina retenido o concentrado [3].

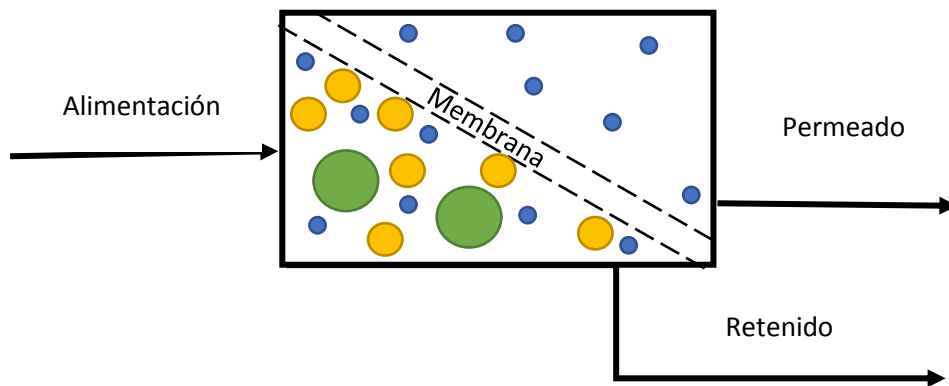


Figura 4.1. Representación genérica de un proceso con membranas.

El transporte a través de la membrana se efectúa por la acción de una fuerza impulsora capaz de provocar el paso de compuestos a través de la membrana. Esta fuerza impulsora puede ser una diferencia de concentración, potencial eléctrico, temperatura o presión, pudiendo actuar de forma única o combinadas [4,5]. Aunque hay más procesos que los indicados en la Tabla 4.1., en ella se muestran los procesos más conocidos clasificados según la naturaleza de la fuerza impulsora.

Tabla 4.1. Principales procesos de separación con membranas según la fuerza impulsora.

FUERZA IMPULSORA	PROCESOS CON MEMBRANAS
Gradiente de potencial eléctrico	Electroforesis Electrodiálisis Electrólisis
Gradiente de concentración	Diálisis Separación de gases Membranas líquidas Pervaporación
Gradiente de presión transmembranal	Microfiltración Ultrafiltración Nanofiltración Ósmosis inversa
Gradiente de temperatura	Destilación con membranas

CLASIFICACIÓN DE LAS MEMBRANAS:

Las membranas pueden clasificarse atiendo a diferentes aspectos [5]:

- Naturaleza (biológicas o sintéticas)
- Función (filtración, concentración, separación, etc.)
- Morfología (tubulares, planas, espirales, etc.)
- Composición (inorgánicas, orgánicas o mixtas)
- Porosidad (porosas, no porosas, líquidas, simétricas o asimétricas)
- Estructura (homogénea, asimétrica o compuesta)
- Estado físico (gaseosas, líquidas, sólidas o combinaciones)

En cuanto a la naturaleza de las membranas, se distingue entre membranas biológicas y sintéticas [6].

- Las membranas biológicas son aquellas que se encuentran en los seres vivos y pueden ser vivas o no vivas. Suelen emplearse en ámbitos de la medicina y la industria farmacéutica.

- Las membranas sintéticas pueden ser orgánicas o inorgánicas.

Las membranas orgánicas son de naturaleza polimérica y pueden tener una estructura porosa o densa. Debido a sus propiedades físico-químicas pueden presentar limitaciones en su resistencia mecánica y térmica, así como limitaciones en el flujo de permeado y selectividad para ciertas aplicaciones [7].

Las membranas inorgánicas poseen mayor estabilidad térmica, mecánica y química. No obstante, son más frágiles y caras. Pueden ser de naturaleza cerámica, vítreo o metálica, siendo las primeras las que hasta el momento presentan un mayor rango de aplicación.

TIPOS DE FILTRACIÓN:

Los procesos de separación con membranas permiten operar de dos modos: filtración en torta o directa y filtración tangencial o cruzada.

- Filtración en torta o directa:

En este modo de filtración, la alimentación es perpendicular a la superficie de la membrana. El flujo de permeado se ve afectado significativamente por la deposición continua de sólidos sobre la superficie de la membrana, formándose una torta que aumenta continuamente de espesor a medida que trascurre el proceso de filtración. Esto da lugar a una disminución del flujo de permeado que hace que en este modo de filtración sea necesario operar en discontinuo. Con este modo de operación, al ejercer una mayor presión no se produce un aumento el flujo.

- Filtración tangencial o cruzada:

En este modo de filtración, la alimentación circula paralelamente a la superficie de la membrana, de tal forma que los compuestos que quedan retenidos por la membrana, son arrastrados por el flujo tangencial [6]. Este modo de operar presenta la ventaja de que se minimiza la deposición de partículas sobre la membrana y disminuye el ensuciamiento, aumentando significativamente el flujo de permeado y la eficacia de la separación.

Con este modo de filtración, el flujo de permeado disminuye inicialmente hasta estabilizarse en el tiempo, alcanzándose un flujo constante durante tiempos prolongados que permiten trabajar en continuo [8]. Este es el modo de operación habitual en los procesos con membranas.

En la Figura 4.2. se ilustra de forma comparativa ambas formas de filtración.

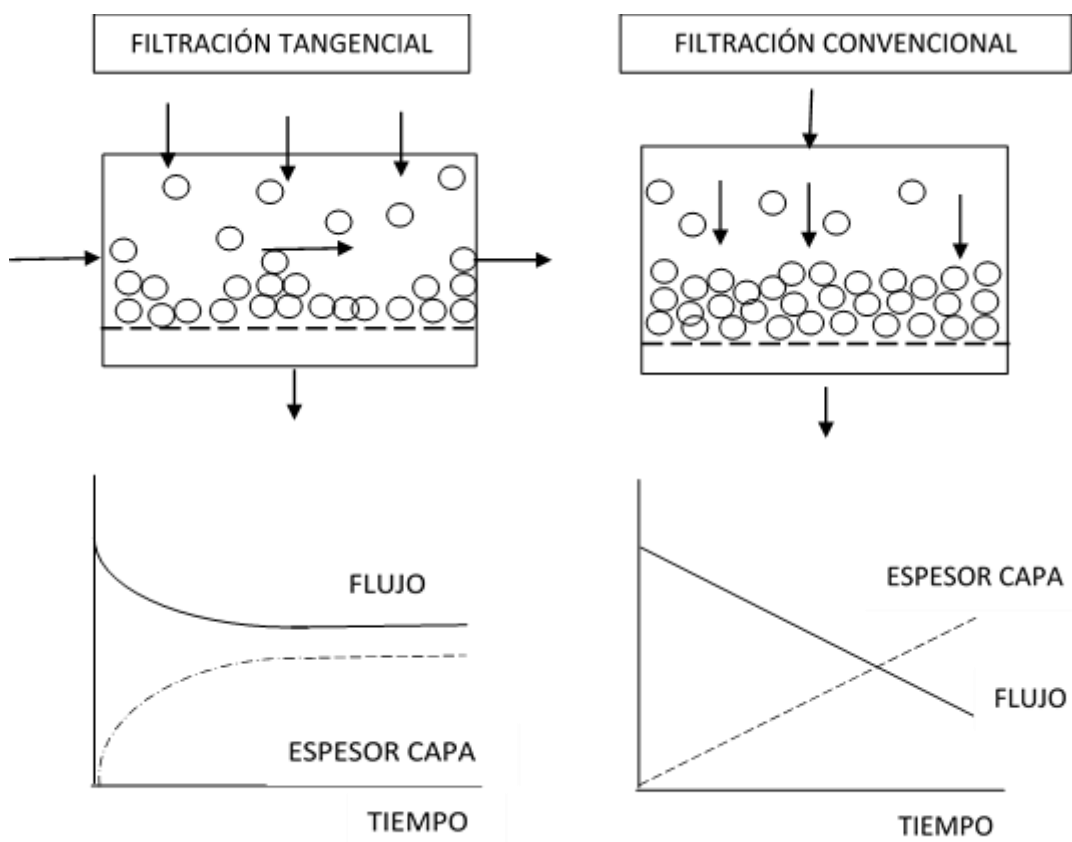


Figura 4.2. Representación de la filtración tangencial y convencional.

4.2. Antecedentes y aplicaciones

Los procesos con membranas son considerados tecnologías relativamente actuales. Los primeros estudios relacionados con las membranas tuvieron lugar en 1748 por Nollet, que estableció el término y principio básico de la ósmosis [9].

En el siglo XIX se estudiaron las propiedades de las membranas y se desarrollaron muchos de los principios, leyes y modelos teóricos de los procesos de transporte en membranas, como el transporte difusivo por la ley de Fick, la presión osmótica por la ecuación de Van't Hoff y posteriormente por Einstein, y el principio de exclusión Donnan, entre otros.

La primera membrana de uso comercial fue desarrollada en Alemania en 1920 por Sartorius, con aplicación para filtración de bacterias. Esta membrana estaba compuesta fundamentalmente de nitrato y acetato de celulosa, materiales empleados en las actuales membranas de ultrafiltración; sin embargo, fueron empleadas solamente a escala de laboratorio [9].

No fue hasta décadas posteriores cuando el uso de las membranas en procesos de filtración empezó a ser considerado viable a escala industrial. Una fecha histórica fue 1955, cuando en EEUU se emplearon las primeras membranas en un proceso de electrodialisis.

El gran avance en la aplicación tecnológica de las membranas se produjo a finales de los años 50 del pasado siglo gracias al proceso Loeb-Sourirajan para el desarrollo de membranas anisotrópicas y su aplicación en ósmosis inversa, que al proporcionar mayores flujos de permeado hicieron posible su uso práctico para la desalinización de agua de mar. Este acontecimiento permitió nuevos avances en los años posteriores. En la década de los 80 se desarrollaron los procesos de microfiltración y ultrafiltración, y posteriormente los procesos de separación de gases con membranas y la pervaporación [10].

Desde entonces, debido principalmente al desarrollo de nuevos materiales, la tecnología de membranas ha ido evolucionando y sus aplicaciones a nivel industrial han ido aumentado cada vez más. Actualmente los procesos con membranas tienen una amplia implantación a nivel industrial y se utilizan en una gran variedad de aplicaciones como la desalinización de agua de mar, recuperación y reutilización de aguas residuales e industriales, agricultura, minería, metales pesados, producción de biocombustibles [11], industria farmacéutica, química, alimentaria [12], plásticos, textil, petrolera, etc.

Las tecnologías con membranas destacan por su gran versatilidad, ya que pueden aplicarse con fines de filtración, concentración, purificación, fraccionamiento, reacción química, extracción, adsorción, destilación, etc. [11].

Las principales ventajas que presentan las tecnologías con membranas son las siguientes:

- Son procesos en continuo
- Bajo consumo energético
- Proceso fácilmente escalable a nivel industrial
- Fácilmente combinables y adaptables con otros procesos
- Equipos compactos y simples
- Posibilidad de operar en condiciones de temperatura moderada
- Fácil manejo y control del proceso
- Variedad de aplicaciones y usos
- No requiere generalmente adición de agentes externos o químicos
- Bajas pérdidas en el sobrante

Estas características que de forma genérica se atribuyen a los procesos de membranas hacen que sean consideradas “tecnologías limpias” debido al bajo impacto sobre el medio ambiente.

A pesar de las numerosas ventajas de las tecnologías con membranas, también presentan inconvenientes asociados a la limitación en el flujo de permeado causado por los fenómenos de polarización por concentración y ensuciamiento de las membranas. Para reducir estos problemas, en aquellas operaciones donde su incidencia es más acusada, como en los procesos de microfiltración y ultrafiltración, existen diferentes estrategias en las formas de operar que mejoran sustancialmente la eficiencia de los procesos y los costes de la operación [9,13]. Otros inconvenientes que presentan las tecnologías con membranas son el reducido factor de concentración que se puede alcanzar con ellas en comparación con otros procesos como la evaporación y una vida útil relativamente corta por el deterioro que provoca en las membranas el uso de disolventes orgánicos en las etapas de limpieza.

4.3. Procesos impulsados por una diferencia de presión transmembranal

Los procesos con membranas más empleados son los que utilizan como fuerza impulsora una diferencia de presión transmembranal. La presión requerida para forzar el paso de componentes a través de una membrana es proporcional al tamaño de sus poros.

Las membranas que se utilizaron en este estudio pertenecen a este grupo, empleándose un gradiente de presión como fuerza impulsora.

Los procesos con membranas impulsados por una diferencia de presión son los más conocidos e implantados a escala industrial. En función del tamaño de los poros de la membrana que utilizan, y por tanto del tamaño de partícula que rechazan, se clasifican en microfiltración (MF), ultrafiltración (UF), nanofiltración (NF) y ósmosis inversa o hiperfiltración (OI).

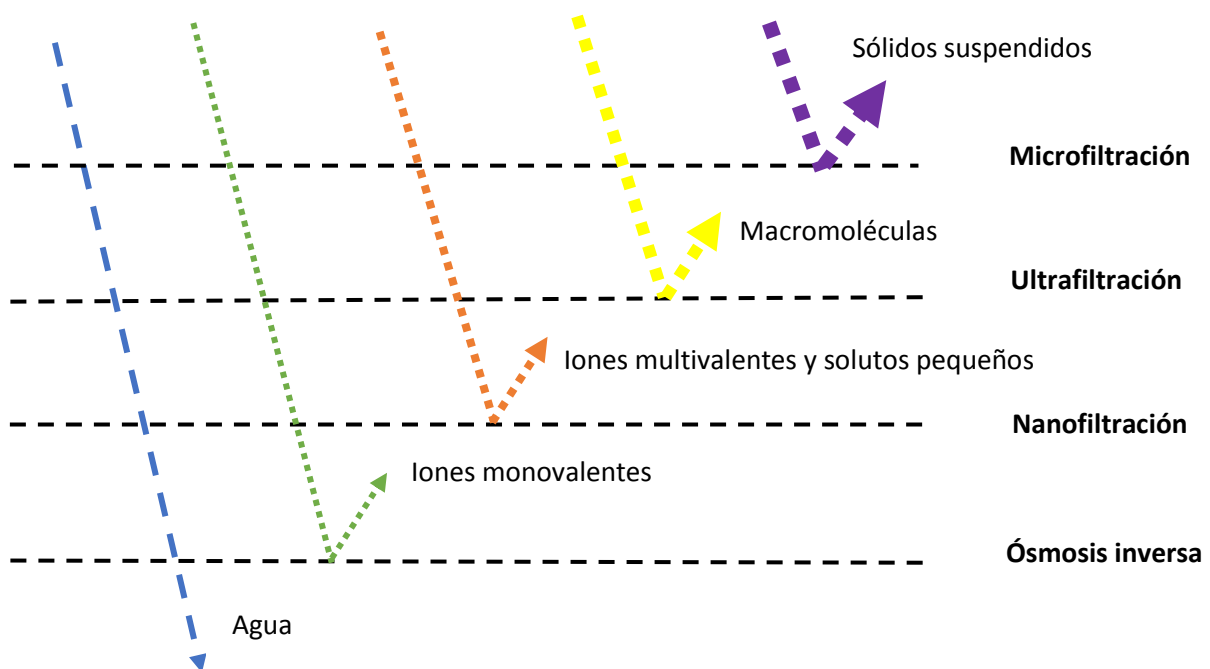


Figura 4.3. Separación de componentes en los procesos con membranas impulsados por un gradiente de presión.

Tabla 4.2. Características de los procesos con membranas impulsados por un gradiente de presión.

	TAMAÑO DE PORO	ESPECIES RETENIDAS	FUERZA IMPULSORA	PRESIONES APLICADAS (bar)	MECANISMO DE SEPARACIÓN
MICROFILTRACIÓN	0,1 -10 µm	Sólidos suspendidos y partículas finas, bacterias, etc.	Gradiente de presión	0,2-2	Tamaño de partícula
ULTRAFILTRACIÓN	1-100 nm	Coloides y macromoléculas	Gradiente de presión	1-10	Tamaño de partícula
NANOFILTRACIÓN	1 nm	Compuestos de bajo peso molecular y sales divalentes	Gradiente de presión	10-40	Tamaño de partícula y carga/Disolución-difusión
ÓSMOSIS INVERSA	< 0,5 nm	Sales monovalentes y solutos de bajo peso molecular	Gradiente de presión	10-100	Disolución-difusión

En la Fig. 4.3 y en la Tabla 4.2 se muestra una representación de la separación y las características de los procesos de separación impulsados por presión.

En las membranas de microfiltración y ultrafiltración, el mecanismo de separación de los componentes es fundamentalmente por tamizado debido al tamaño de los poros, mientras que, en las membranas densas de ósmosis inversa, la separación tiene lugar por diferencias en la solubilidad y difusividad de los componentes en el material de la membrana. La nanofiltración es una operación con características intermedias entre la ultrafiltración y la ósmosis inversa, debido al pequeñísimo tamaño de los poros.

La presión requerida para llevar a cabo los procesos de nanofiltración y ósmosis inversa es mucho mayor que la requerida para la microfiltración y ultrafiltración. Esto se debe a que, a medida que disminuye el poro de la membrana, aumenta la resistencia de la membrana al paso de la corriente de permeado, por lo que debe aplicarse mayor presión para forzar su paso a través de la membrana.

En la modelización de los procesos con membranas se debe tener en cuenta la permeabilidad y selectividad de la membrana, ambas condicionadas por las características del medio (el tamaño de las partículas, presencia de otros componentes, pH, carga de las partículas, tipo de disolvente), las interacciones de los componentes con la membrana y las condiciones de operación (temperatura, velocidad tangencial, presión aplicada, configuración del módulo, tipos de flujo y formas de operar) [4,12,14]. Debido a la diversidad de factores que intervienen en estos procesos, se debe realizar un trabajo de laboratorio previo orientado a la selección del tipo de membrana a emplear en cada contexto determinado, el tipo de módulo y las condiciones de operación y limpieza.

- **MICROFILTRACIÓN**

La microfiltración es un proceso que produce el rechazo de sólidos suspendidos o partículas en suspensión.

En general, las membranas de microfiltración tienen un tamaño de poro comprendido entre 0.1 y 2 μm y funcionan adecuadamente a presiones bajas, inferiores a 5 bar, produciendo elevados flujos de permeado [15,16]. Suelen emplearse membranas asimétricas porosas. El mecanismo de retención o rechazo se debe al efecto tamiz o cribado que ejerce el tamaño de los poros, aunque la separación está además influenciada por las interacciones entre la solución y la superficie de la membrana.

La eficiencia en estos procesos se ve afectada por la acumulación de sólidos sobre la superficie de la membrana, dando lugar a la disminución del flujo de permeado a causa a la polarización por concentración y el ensuciamiento.

Este tipo de membranas son empleadas en una amplia gama de aplicaciones y campos, destacando su uso en el tratamiento de aguas residuales y de aguas procedentes de la industria farmacéutica, química, alimentaria y electrónica [10].

Se utilizan especialmente en la industria alimentaria (eliminación de partículas, patógenos, bacterias, levaduras, clarificación de zumos, salmuera de queso, vinagre y vino y recuperación de aguas de lavado o efluentes) y farmacéutica (purificación de urea). También en el sector automovilístico para recuperación de pintura o eliminación de aceite en aguas residuales.

- **ULTRAFILTRACIÓN**

La ultrafiltración produce el rechazo de macromoléculas, virus y partículas suspendidas. Las membranas de ultrafiltración son porosas, siendo el mecanismo de retención el tamaño y forma de las partículas respecto a los poros de la membrana. Las presiones de operación requeridas son inferiores a 10 bar.

La microfiltración y ultrafiltración son tecnologías muy similares, que se diferencian en el tamaño de los poros de la membrana y en el tamaño de las partículas que quedan retenidas.

Las membranas de ultrafiltración se clasifican según su corte molecular o MWCO (molecular weight cut-off), que equivale al peso molecular del soluto de menor tamaño que queda retenido por la membrana en un 90%.

En este tipo de procesos es importante considerar la limitación del flujo de permeado por efecto de la polarización por concentración. Este fenómeno provoca la existencia de un flujo máximo, independiente de la fuerza impulsora, por lo que es un factor limitante de las condiciones de operación (presión aplicada); sin embargo, su valor depende de las formas de operación (dirección de los flujos a ambos lados de la membrana, efectos de contrapresión para la inversión cíclica del permeado, etc.) y las condiciones del medio (pH, temperatura, presencia de sales y solutos pequeños, etc.) [17].

La aplicación de las membranas de ultrafiltración abarca una gran variedad de áreas: reciclado de agua, industria química, tratamiento de aguas residuales, alimentación (zumos, láctea, almidón), medicina, biotecnología e industria farmacéutica. La ultrafiltración también suele emplearse como una barrera de desinfección para la eliminación de bacterias y virus [18].

- **NANOTRAFILTRACIÓN**

La nanofiltración es un proceso intermedio entre la ósmosis inversa y la ultrafiltración.

Las membranas de nanofiltración proporcionan un elevado grado de retención de sales inorgánicas divalentes y moléculas orgánicas de bajo peso molecular (como azúcares, aminoácidos, ácidos orgánicos, etc.). Requieren de una presión de operación en el rango de 10 a 40 bar [18]. Al igual que las membranas de ultrafiltración, estas membranas se clasifican por el peso molecular de corte o MWCO.

La diferencia con las membranas de ósmosis inversa reside fundamentalmente en el bajo rechazo por los iones monovalentes, y un mayor flujo de permeado [19].

El mecanismo de separación de las membranas de nanofiltración no solo es mediante el tamaño de partícula, sino que otro de los factores a tener en cuenta es la carga.

El rechazo de las membranas de nanofiltración se atribuye a tres mecanismos: efectos estéricos, efecto Donnan y efectos dieléctricos [20].

El mecanismo de retención de los solutos no cargados se debe fundamentalmente al efecto tamiz por su tamaño, con relación al tamaño de los poros. Sin embargo, en la retención de los solutos que presentan carga deben considerarse además las interacciones electrostáticas entre los campos eléctricos asociados al transporte de cada ion, efectos de exclusión Donnan entre los solutos y la membrana y los efectos dieléctricos [19].

El efecto Donnan influye sobre los mecanismos de transporte cuando la membrana se encuentra cargada. Se debe a un equilibrio que se establece entre las partículas cargadas que pueden atravesar la membrana y las que quedan atrapadas y que se ve afectado tanto por la carga como la concentración.

Si la membrana posee carga, los compuestos con carga opuesta son atraídos hacia la membrana y los compuestos con la misma carga son repelidos.

El mecanismo de interacción dieléctrica tiene lugar entre la carga de la superficie de la membrana y las moléculas de agua, que presentan bipolaridad. Dependiendo de la carga del compuesto, éste puede verse atraído o repelido por la membrana y el seno del fluido, favoreciendo el paso a través de los poros o su exclusión [19].

Las membranas de nanofiltración son empleadas en muchas aplicaciones: en el tratamiento y desalinización de aguas salobres y aguas residuales, en la industria farmacéutica, biotecnológica y alimentaria. Las principales aplicaciones son en la producción de agua potable (eliminación de contaminantes, metales pesados, antibióticos, hormonas, plaguicidas, etc.), pero también en el sector de la industria química (ácido acético, metanol, ácido tánico), industria alimentaria (sueros, industria láctea, bebidas, aceite y azúcar) e industria textil.

• ÓSMOSIS INVERSA

La ósmosis inversa posibilita separar las partículas de bajo peso molecular, permitiendo que las moléculas de agua pasen a través de la membrana, mientras que iones monovalentes y partículas de mayor tamaño quedan retenidas.

Las presiones de trabajo están comprendidas entre 10 y 100 bar. La ósmosis inversa es una tecnología robusta y eficiente en energía, aunque requiere bombas de alta potencia y consumo energético [21,22].

El mecanismo de separación es fundamentalmente por disolución – difusión a través de la membrana [23,24]. La separación se lleva a cabo por diferencias de solubilidad y difusividad de los componentes que atraviesan las membranas [9].

Actualmente, la ósmosis inversa es el proceso más utilizado en la tecnología de desalinización, con un 53% en la producción de agua desalinizada [25,26]. También se emplea en la generación de energía y en la industria farmacéutica [27].

4.4. Eficiencia y productividad

Los procesos de separación con membranas presentan dos parámetros importantes a tener en cuenta: la eficiencia y la productividad. La productividad está relacionada con la velocidad de permeación de los componentes a través de la membrana. La densidad de flujo de permeado referida a un componente, J_i , es la velocidad de transporte de materia de ese componente a través de la membrana, expresada por unidad de superficie de la membrana. Cuando son varios los componentes que atraviesan la membrana, la densidad de flujo total de permeado, J_T , es la suma de la de los diferentes componentes y se puede expresar de la siguiente manera:

$$J_T = \sum_i^n J_i \quad (1)$$

La eficiencia de separación está relacionada con la calidad del permeado como consecuencia del efecto de la membrana sobre cada componente. El rechazo de la membrana por un componente, R_i , se determina por el grado de reducción en la concentración de dicho componente, calculado por la Ec. (2):

$$R_i = 1 - \frac{C_{p,i}}{C_{r,i}} \quad (2)$$

donde $C_{p,i}$ y $C_{r,i}$ es la concentración del componente de interés en el permeado y en el retenido, respectivamente.

En general, ambos parámetros, J_i y R_i , están afectados por la concentración, las características del medio y por las condiciones de operación.

En los procesos impulsados por una diferencia de presión transmembranal, la relación entre la densidad de flujo volumétrico de permeado (m/s) y la fuerza impulsora (Pa) se describe mediante la siguiente ecuación:

$$J_P = \left[\frac{\Delta P - \Delta \pi}{\mu R_T} \right] \quad (3)$$

Donde ΔP es la diferencia de presión transmembranal aplicada, $\Delta\pi$ es la diferencia de presión osmótica a ambos lados de la membrana, μ es la viscosidad de la alimentación y R_T es la resistencia global del proceso al flujo de permeado, generalmente expresada como suma de resistencias en serie, entre las que se incluye la resistencia de la membrana.

La resistencia de la membrana, R_m , es constante y no depende de la composición de la alimentación, ni de la presión aplicada.

En el caso de solutos de elevado peso molecular en soluciones diluidas, la diferencia de presión osmótica a ambos lados de la membrana es despreciable.

Si el disolvente empleado es agua pura, la ecuación a utilizar es la siguiente:

$$J_w = L_p \Delta P \quad (4)$$

Donde L_p es la permeabilidad de la membrana al agua. Este valor puede obtenerse de forma experimental mediante la pendiente del flujo del agua frente a la diferencia de presión aplicada y está relacionada con la resistencia de la membrana y la viscosidad del agua mediante la siguiente ecuación, donde μ_w es la viscosidad del agua a la temperatura de operación:

$$L_p = \frac{1}{\mu_w \cdot R_m} \quad (5)$$

4.5. Polarización por concentración

La polarización por concentración es el fenómeno causado por la acumulación de solutos en la superficie de la membrana cuando se opera con flujo tangencial. Aunque es un fenómeno inherente a todos los procesos con membranas, su efecto es relevante en la electrodialisis y en los procesos impulsados por una diferencia de presión transmembranal, especialmente en microfiltración y ultrafiltración.

La polarización por concentración se produce a consecuencia de la acumulación de solutos en la superficie de la membrana como resultado de un balance entre las fuerzas paralelas a la membrana debidas al flujo tangencial a la membrana y las fuerzas perpendiculares a la membrana debidas a la permeación. El resultado de este balance es la formación de una capa límite o capa de polarización por concentración en la cara del retenido, a través de la cual se establece un gradiente de concentración. La existencia de esta capa de polarización por concentración ocasiona una resistencia a la permeación y por tanto una reducción en el flujo de permeado [20,28].

La polarización por concentración es un efecto que no puede evitarse, si bien se puede minimizar seleccionando las condiciones de operación. Se trata de un proceso reversible, ya que su efecto se anula al suprimirse la fuerza impulsora [17,29–31].

En la Fig. 4.4. se representa la formación de la capa límite que causa el proceso de polarización por concentración.

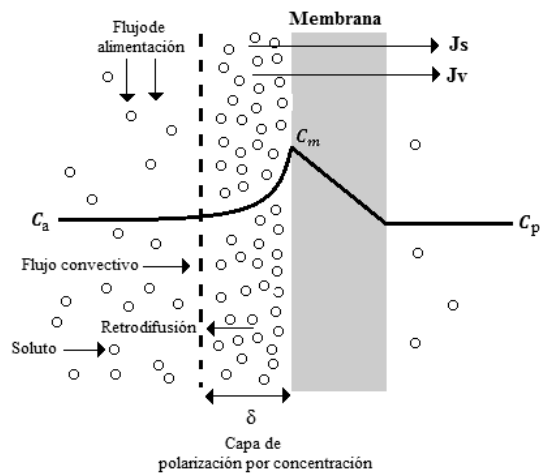


Figura 4.4. Representación del fenómeno de polarización por concentración.

En el estado estacionario el espesor de la capa estancada o capa límite y la densidad de flujo de permeado alcanza valores constantes. Esta situación se produce debido al hecho de que en la capa estancada se genera un flujo difusivo de materia hacia el seno del retenido como consecuencia de la existencia de un gradiente de concentración, expresado por la ecuación de Fick. El estado estacionario se alcanza cuando el flujo neto de un soluto hacia la membrana, es decir el flujo convectivo hacia la membrana menos el flujo difusivo en sentido opuesto, es igual al flujo de permeado de dicho componente a través de la misma. El balance de materia en la capa de polarización queda reflejado mediante la siguiente expresión:

$$J_p C + \left(D \frac{dc}{dx} \right) = J_p C_p \quad (6)$$

donde D es el coeficiente de difusión del soluto en la capa límite y J_p es la densidad de flujo de permeado [10].

La integración de esta ecuación para las condiciones de la capa límite de espesor δ , con $C=C_M$ para $x=0$, y $C=C_R$ si $x=\delta$, conduce a la siguiente ecuación:

$$J_P = k \ln \left[\frac{C_M - C_p}{C_R - C_p} \right] \quad (7)$$

Donde k es el coeficiente de transferencia de materia en la capa límite, siendo $k=D/\delta$. Esta ecuación determina que la densidad de flujo de permeado, cuando el proceso está limitado por el fenómeno de polarización por concentración, no está determinada por la presión, sino que su valor depende de las concentraciones del soluto en la superficie de membrana, permeado y retenido (C_M , C_p y C_R , respectivamente) y del coeficiente de transferencia de materia en la capa de polarización (k).

Para aumentar la densidad de flujo de permeado, como se puede ver mediante la Ec. (7), hay que aumentar el valor de k o reducir el espesor de la capa límite.

Como se ha indicado, la capa de polarización da lugar a que el rechazo real o intrínseco de la membrana sea mayor que el rechazo observado.

El rechazo real o intrínseco (R_{int}) y el rechazo observado (R_{obs}) de la membrana se expresan mediante las siguientes ecuaciones:

$$R_{int} = 1 - \left[\frac{C_p}{C_M} \right] \quad (8)$$

$$R_{obs} = 1 - \left[\frac{C_p}{C_R} \right] \quad (9)$$

La relación entre el rechazo real y el observado queda expresado mediante la siguiente ecuación:

$$R = \left\{ 1 + \left[\frac{1 - R_{obs}}{R_{obs}} \right] \exp(-Pe) \right\}^{-1} \quad (10)$$

donde Pe es el número de Peclet, que se define como $Pe = J\delta/D$ y expresa la relación entre el flujo convectivo y el flujo de retrodifusión.

En condiciones de operación de baja presión transmembranal, elevadas velocidades tangenciales sobre la membrana, y con solutos de bajo peso molecular, el efecto de la polarización por concentración es insignificante y el valor de R_{obs} es muy próximo a R_{int} .

En las situaciones contrarias, donde la polarización por concentración es significativa, el valor de R_{int} es mayor que R_{obs} .

En la Figura 4.5. se muestra el comportamiento de la densidad de flujo de permeado en función de la presión cuando existe control del proceso por efecto de la polarización por concentración, en comparación con el flujo de permeado con agua pura como alimentación.

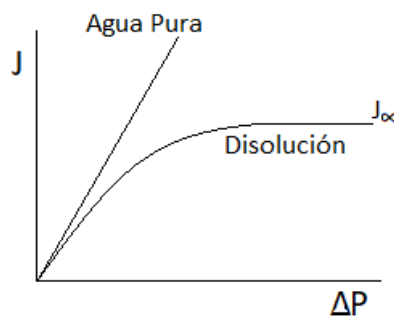


Figura 4.5. Comportamiento de la densidad de flujo de permeado en función de la presión aplicada en la filtración de agua pura y de una disolución.

La resistencia impuesta por la capa de polarización por concentración depende de las condiciones hidrodinámicas sobre la membrana, velocidad de la alimentación, temperatura, y de la concentración de solutos en la alimentación. Si la presión permanece constante y se aumenta el flujo de alimentación, y/o las turbulencias, y/o la temperatura, el flujo límite de permeado aumentará. Por el contrario, el aumento de la concentración de solutos en la alimentación disminuirá el flujo límite de permeado.

4.6. Ensuciamiento y limpieza de las membranas

El ensuciamiento es un conjunto de fenómenos que modifican las propiedades de filtración de las membranas y producen la disminución continua del flujo de permeado. Algunas de las causas del ensuciamiento más habituales en los procesos con membranas impulsados por un gradiente de presión son: el bloqueo de los poros de la membrana (total o parcial), adsorción de solutos sobre la superficie, precipitación de compuestos en la superficie formando una torta, o la interacción entre los solutos y la membrana [32]. Muchas veces estos fenómenos tienen lugar de forma simultánea, sin que puedan describirse mecanismos secuenciales de actuación.

El ensuciamiento de la membrana puede ser un fenómeno reversible o irreversible. Cuando se trata de un fenómeno reversible, su efecto puede eliminarse mediante la cesión de la presión transmembranal o mediante un aclarado.

Pero el fenómeno de ensuciamiento de la membrana, a diferencia de la polarización por concentración, puede ser irreversible, pudiendo eliminarse mediante un lavado de la membrana o requerir del uso de detergentes o compuestos químicos, generalmente ácidos, bases, biocidas u otros, según el tipo de ensuciamiento.

El ensuciamiento y la posterior limpieza de las membranas pueden ocasionar, tras un uso continuado, la pérdida de permeabilidad y reducción de la vida útil de las membranas [17,19,29].

El diseño y la optimización de los procesos de separación con membranas debe contemplar la inclusión de ciclos de limpieza programados y también del equipamiento necesario para la limpieza de las membranas, que afectan al rendimiento y los costes de la operación.

La limpieza de las membranas puede ser química, física o biológica.

En la limpieza física suele emplearse aire, agua a presión en contrasentido (retrolavado) o aplicación de ondas ultrasónicas [33].

En la limpieza química se hace pasar agentes químicos (ácidos o bases) a través de la membrana. Es el tipo de limpieza más frecuentemente empleado. Suele producir a largo plazo un deterioro de las membranas y la reducción de su vida útil [34]. Los agentes químicos reaccionan con los compuestos que se encuentran depositados sobre la membrana o incrustaciones produciendo su separación de la membrana.

En la limpieza biológica se utilizan enzimas para regenerar la membrana.

El objetivo de la limpieza de las membranas es restaurar el flujo de permeado inicial de la membrana, generalmente por encima del 90%, por lo que su tipología, es decir el agente de limpieza a utilizar y la forma de operar, así como la frecuencia de aplicación, dependerá del tipo de ensuciamiento y del material de la membrana.

4.7. Bibliografía

- [1] R.J. Petersen, Composite reverse osmosis and nanofiltration membranes, *J. Membr. Sci.* 83 (1993) 81–150.
- [2] M. Ulbricht, Advanced functional polymer membranes, *Polymer* 47 (2006) 2217–2262.
- [3] A. Maher, M. Sadeghi, A. Moheb, Heavy metal elimination from drinking water using nanofiltration membrane technology and process optimization using response surface methodology, *Desalination* 352 (2014) 166–173.
- [4] K.S. Scott, R. Hughes, *Industrial Membrane Separation Technology*, Blackie Academic & Professional, Glasgow (1996).
- [5] M. Issaoui, L. Limousy, Low-cost ceramic membranes: synthesis, classifications, and applications, *C. R. Chim.* 22 (2019) 175–187.
- [6] M. Raventós Santamaría, *Industria Alimentaria. Tecnologías Emergentes*, Edicions UPC, Barcelona (2005).
- [7] C. Guizard, A. Bac, M. Barboiu, Hybrid organic–inorganic membranes with specific transport properties: applications in separation and sensors technologies, *Sep. Purif. Technol.* 25 (2001) 167–180.
- [8] S. Ripperger, J. Altmann, Crossflow microfiltration—state of the art, *Sep. Purif. Technol.* 26 (2002) 19–31.
- [9] M. Mulder, *Basic Principles of Membrane Technology*, second ed., Kluwer Academic Publishers, Dordrecht (1996).
- [10] R.W. Baker, *Membrane Technology and Applications*, second ed., John Wiley & Sons Ltd., Chichester (2004).
- [11] N.L. Le, S.P. Nunes, Materials and membrane technologies for water and energy sustainability, *Sustain. Mater. Technol.* 7 (2016) 1–28.
- [12] R. Castro-Muñoz, G. Boczkaj, E. Gontarek, A. Cassano, V. Fíla, Membrane technologies assisting plant-based and agro-food by-products processing: a comprehensive review, *Trends Food Sci. Technol.* 95 (2020) 219–232.
- [13] H. Strathmann, *Introduction to Membrane Science and Technology*, Wiley-VCH, Weinheim (2011).
- [14] D.L. Oatley, B. Cassey, P. Jones, W.R. Bowen, Modelling the performance of membrane nanofiltration—recovery of a high-value product from a process waste stream, *Chem. Eng. Sci.* 60 (2005) 1953–1964.

- [15] M.R. Wiesner, P. Aptel, Mass transport and permeate flux and fouling in pressure-driven processes. In: AWWA Research Foundation, *Water Treatment: Membrane Processes*, McGraw-Hill, New York (1996).
- [16] J.W. Chew, J. Kilduff, G. Belford, The behavior of suspensions and macromolecular solutions in crossflow microfiltration: an update, *J. Membr. Sci.* 601 (2020) 117865.
- [17] X. Shi, G. Talb, N.P. Hankins, V. Gitisb, Fouling and cleaning of ultrafiltration membranes: a review, *J. Water Process Eng.* 1 (2014) 121–138.
- [18] F.J. Benítez, J.L. Acero, A.I. Leal, M. González, The use of ultrafiltration and nanofiltration membranes for the purification of cork processing wastewater, *J. Hazard. Mater.* 162 (2009) 1438–1445.
- [19] A.W. Mohammad, Y.H. Teow, W.L. Ang, Y.T. Chung, D.L. Oatley-Radcliffe, N. Hilal, Nanofiltration membranes review: recent advances and future prospects, *Desalination* 356 (2015) 226–254.
- [20] S. Bouranene, P. Fivet, A. Szymczyk, M. E. Hadi Samar, A. Vidonne, Influence of operating conditions on the rejection of cobalt and lead ion in aqueous solutions by a nanofiltration polyamide membrane, *J. Membr. Sci.* 325 (2008) 150–157.
- [21] S. Jiang, Y. Li, B.P. Ladewig, A review of reverse osmosis membrane fouling and control strategies, *Sci. Total Environ.* 595 (2017) 567–583.
- [22] G.R. Xu, J.-N. Wang, C.L. Li, Strategies for improving the performance of the polyamide thin film composite (PA-TFC) reverse osmosis (RO) membranes: surface modifications and nanoparticles incorporation, *Desalination* 328 (2013) 83–100.
- [23] D.R. Paul, Reformulation of the solution-diffusion theory of reverse osmosis, *J. Membr. Sci.* 241 (2004) 371–386.
- [24] S.F. Anis, B.S. Lalia, R. Hashaike, Controlling swelling behavior of poly (vinyl) alcohol via networked cellulose and its application as a reverse osmosis membrane, *Desalination* 336 (2014) 138–145.
- [25] B. Al-Najar, C.D. Peters, H. Albuflas, N.P. Hankins, Pressure and osmotically driven membrane processes: a review of the benefits and production of nano-enhanced membranes for desalination, *Desalination* 479 (2020) 114323.
- [26] T. Mezher, H. Fath, Z. Abbas, A. Khaled, Evaluación tecno-económica asesment and environmental impacts of desalination technologies, *Desalination* 266 (2011) 263–273.
- [27] S. Zhao, L. Zou, C.Y. Tang, D. Mulcahy, Recent developments in forward osmosis: opportunities and challenges, *J. Membr. Sci.* 396 (2012) 1–21.
- [28] S.S. Sablani, M.F.A. Goosen, R. Al-Belushi, M. Wilf, Concentration polarization in ultrafiltration and reverse osmosis: a critical review, *Desalination* 141 (2001) 269–289.

- [29] S. Judd, B. Jefferson, *Membranes for Industrial Wastewater Recovery and Re-use*, Elsevier Science Ltd., Oxford (2003).
- [30] K.-V. Peinemann, S.P. Nunes, *Membranes for Water Treatment*, Wiley-VCH, Weinheim (2010).
- [31] J.R. McCutcheon, M. Elimelech, Influence of concentrative and dilutive internal concentration polarization on flux behavior in forward osmosis, *J. Membr. Sci.* 284 (2006) 237–247.
- [32] L. Wang, L. Song, Flux decline in crossflow microfiltration and ultrafiltration: experimental verification of fouling dynamics, *J. Membr. Sci.* 160 (1999) 41–50.
- [33] A.I. Schäfer, N. Andritsos, A.J. Karabelas, E.M.V. Hoek, R. Schneider, M. Nyström, Fouling in nanofiltration. In: A.G. Fane, A. Schäfer, T.D. Waite (Eds.), *Nanofiltration. Principles and Applications*, Elsevier Science Ltd., Oxford (2004).
- [34] A. Al-Amoudi, R.W. Lovitt, Fouling strategies and the cleaning system of NF membranes and factors affecting cleaning efficiency, *J. Membr. Sci.* 303 (2007) 4–28.

5. Ácido láctico

5.1. Generalidades

El ácido láctico fue descubierto en 1780 por el químico sueco Scheele, quien inicialmente consideró que era un componente lácteo [1]. En 1789 fue aislado por Lavoisier en la leche agria y lo denominó con el nombre que posee actualmente. Pero no fue hasta 1857 cuando Pasteur descubrió que no se trataba de un componente lácteo como se planteó inicialmente, sino de un producto de la fermentación generado por microorganismos.

El ácido láctico fue el primer ácido orgánico en ser producido a escala industrial en el año 1880. En 1881 fue producido comercialmente por Avery [2], y desde entonces su producción ha aumentado de forma progresiva con el tiempo.

El ácido láctico o ácido 2-hidroxipropanoico ($C_3H_6O_3$) tiene una estructura química como la que se muestra en la Fig. 5.1. El carbono asimétrico le confiere a la molécula dos formas isoméricas ópticamente activas, las formas D (-) y L (+) del ácido láctico; mientras que su forma racémica está formada por una mezcla equimolar de ambas [3–5].

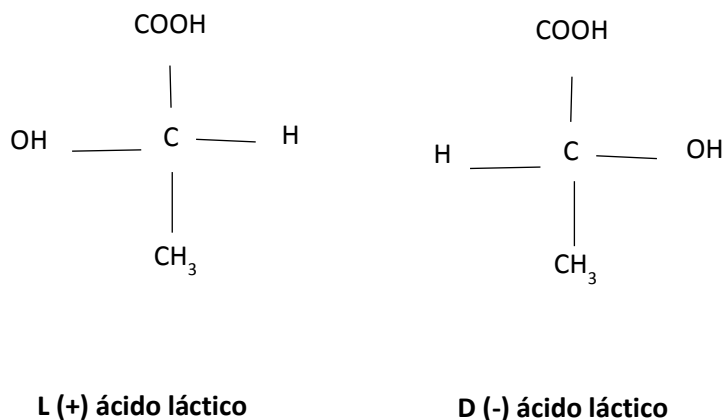


Figura 5.1. Estructuras químicas del L (+) y D (-) ácido láctico.

Cada forma isomérica del ácido láctico tiene diferentes propiedades debido a su configuración espacial, como se puede apreciar en la Tabla 5.1 que se muestra a continuación.

Tabla 5.1. Propiedades del ácido láctico [6,7].

PROPIEDADES	VALOR	FORMAS ISÓMERO
Peso molecular	90,08 g/mol	D, L, DL
Punto de fusión	52,8 °C	D, L, DL
	53 °C	L
	16,8 °C	DL
Punto de ebullición	103 °C	D
	122 °C	DL
Constante de disociación	$1,90 \times 10^{-4}$	D
Ka a 25 °C	$1,38 \times 10^{-4}$	DL
pKa (25 °C)	3,83	D
	3,79	L
	3,73	DL

El isómero D (-) ácido láctico es tóxico en humanos en dosis elevadas [3,7]. En cambio, la configuración L (+) ácido láctico es metabolizada por el organismo humano, por lo que se emplea esta forma para su uso en industria alimentaria y farmacéutica.

El ácido L (+) láctico es clasificado por la FDA como una sustancia GRAS, es decir, que puede emplearse como aditivo alimentario y reconocido como sustancia segura [7].

5.2. Usos y aplicaciones

En los últimos años la producción de ácido láctico ha aumentado [8], debido principalmente a su empleo como materia prima en la producción del ácido poliláctico, un plástico biodegradable con un amplio espectro de aplicaciones en fabricación de envases, biomedicina, industrias agrícola y textil, y otros tipos de industrias [9–11].

Las previsiones para el año 2020 indican que el mercado mundial del ácido láctico alcanzará los 3820 millones de dólares (frente a los 2650 millones en 2017), lo que corresponde a un crecimiento anual del 18,6% [12].

En los próximos años, los pronósticos estiman que el mercado mundial del ácido láctico seguirá aumentando en un 18% o superior entre 2019-2025 [13,14]. Este crecimiento se debe a la creación de nuevas aplicaciones del ácido láctico que han surgido debido a nuevos retos, o en la búsqueda de nuevos materiales o aplicaciones debido a las exigencias medioambientales.

El ácido láctico tiene numerosas aplicaciones, pero es empleado principalmente en cuatro sectores: la industria alimentaria, cosmética, farmacéutica y química.

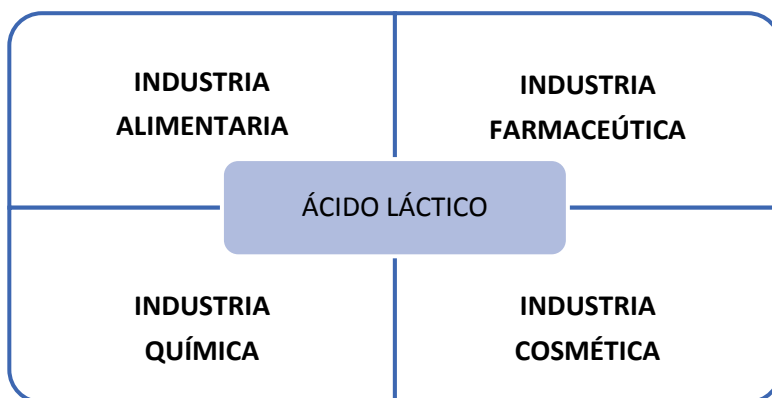


Figura 5.2. Representación usos comerciales y aplicaciones del ácido láctico.

- **INDUSTRIA ALIMENTARIA**

El principal uso del ácido láctico es en la industria alimentaria [7,15] debido a sus propiedades como:

- Preservante antimicrobiano y desinfectante
- Intensificador del aroma (saborizante y aromatizante)
- Regulador del pH (acidulante)
- Fortificación de minerales
- Antioxidante (conservante)
- Emulsionante

Todas estas propiedades hacen que sea empleado como aditivo alimentario en una amplia gama de productos: dulces, pan, productos de panadería, bebidas, sopas, carnes, productos lácteos, cerveza, mermeladas, jaleas, mayonesa, aceitunas, etc.

En la industria alimentaria se emplea la forma isomérica L (+), ya que, como se ha mencionado, es la forma asimilable por el cuerpo humano [16].

- **INDUSTRIA FARMACEÚTICA Y MÉDICA**

En la industria farmacéutica es empleado fundamentalmente en la producción de cosméticos, cremas, lociones, y preparaciones anti-acné. En el campo médico se destaca fundamentalmente su aplicación en el desarrollo de nuevas prótesis y suturas quirúrgicas.

Algunas de las aplicaciones en estas industrias se indican a continuación:

- Agente anti-acné
- Humectante y emulsionante
- Regulador pH
- Solución diálisis
- Preparaciones minerales
- Prótesis
- Suturas quirúrgicas
- Sistemas controladores de liberación de fármacos

Al igual que en la industria alimentaria, se emplea el L (+) ácido láctico debido a su compatibilidad con el cuerpo humano, y a la tendencia creciente al uso de productos naturales y biodegradables.

- **INDUSTRIA QUÍMICA**

En la industria química el ácido láctico es empleado mayoritariamente como:

- Regulador del pH, neutralizador, solvente, agente limpiador
- Producción de otros productos químicos: acetaldehído, ácido acrílico, ácido propanoico, 2-3-pantanodiona, etil lactato, ácido poliláctico (PLA), etc.

El ácido láctico es empleado como materia prima en la producción de muchos productos químicos, pero el más representativo e importante es el ácido poliláctico (PLA), un polímero biodegradable derivado del ácido láctico que presenta un gran potencial hacia nuevas aplicaciones o como sustituto de otros materiales.

El PLA surge como una alternativa frente a los plásticos tradicionales derivados del petróleo, al tratarse de un polímero biodegradable y que puede ser sintetizado mediante fuentes renovables [17].

El PLA presenta propiedades de barrera, biocompatibilidad, elasticidad y alta resistencia química y térmica. Esto ha hecho que sea empleado en numerosas aplicaciones y en un amplio rango de productos, como en la fabricación de fibras, utensilios, envases, etc. [18].

En el sector de la medicina es empleado como hilo de sutura, en implantes, liberación de fármacos y prótesis.

La forma óptica del ácido láctico es un factor vital para las propiedades físicas del PLA, requiriendo las formas ópticas puras. Por ello, el ácido láctico empleado para producir PLA se obtiene mayoritariamente por la ruta de fermentación, ya que por la vía química se genera la mezcla racémica y confiere diferentes propiedades al PLA [19,20].

El PLA presenta dos formas puras: el poli (L-lactida) (PLLA) y poli (D-lactida) (PDLA). La mezcla racémica (PLLA y PDLA) presenta la característica de poseer una temperatura de fusión más alta que las formas puras [21,22].

El PLA es sintetizado a partir del ácido láctico por polimerización mediante diferentes procesos, como policondensación, polimerización por apertura de anillo y por métodos directos como deshidratación azeotrópica y polimerización enzimática [17,23].

Las técnicas más empleadas para la producción de PLA a nivel industrial son mediante la polimerización directa y polimerización por apertura de anillo [6].

El inicio del PLA tuvo lugar en 1932, cuando Carothers sintetizó PLA de bajo peso molecular y posteriormente se fue incrementando el peso molecular. Pero su producción a nivel industrial se inició en 1954, cuando la empresa DuPont patentó un PLA de alto peso molecular y, desde entonces, se empezó su comercialización [24].

Sin embargo, no ha sido hasta hace unos años cuando se ha retomado su interés por el empleo de plásticos más respetuosos con el medio ambiente.

5.3. Síntesis

El ácido láctico puede ser producido mediante la ruta química o biotecnológica (fermentación). Actualmente, el ácido láctico proviene mayoritariamente de la ruta de producción fermentativa, con alrededor del 90% de la producción mundial [25,26].

La ruta biotecnológica para la producción de ácido láctico es la preponderante, debido a que se considera medioambientalmente más favorable, utiliza bajas temperaturas en su producción, bajos requerimientos de energía, es un sistema de producción de alto rendimiento, más rápido y se consigue una alta pureza [9,11,27–29].

- **RUTA QUÍMICA**

La reacción fue descubierta en 1863 por Wislicenus mediante la hidrólisis de cianohidrinas.

La producción química se lleva a cabo mediante la reacción de acetaldehído con ácido cianhídrico (HCN) dando como producto el lactonitrilo, el cual puede ser hidrolizado a ácido láctico. Posteriormente, se realiza una purificación mediante esterificación con alcohol metílico, dando lugar al producto lactato de metilo, que es purificado por evaporación o destilación; y como último paso, se hidroliza con un ácido fuerte como catalizador [10].

Como se ha mencionado, esta ruta química no es muy utilizada debido a que es más cara y compleja que la vía biotecnológica, ya que la materia prima base es el petróleo, suponiendo un alto coste económico y medioambiental.

Otro de los inconvenientes que presenta la producción de ácido láctico mediante la ruta química, es que se obtiene una mezcla de D (-) y L (+) ácido láctico, mientras que la vía fermentativa conduce a la obtención de una u otra forma isomérica, dependiendo del tipo de microorganismo empleado en el proceso [5,16,19].

En la tabla 5.2 y en la Fig. 5.3 se muestra un resumen de las características y diagrama de etapas de la producción del ácido láctico mediante la ruta química o biotecnológica.

Tabla 5.2. Características de las dos vías de producción del ácido láctico.

	PRODUCCIÓN QUÍMICA	PRODUCCIÓN BIOTECNOLÓGICA
MATERIA PRIMA	Petróleo y derivados	Sustratos naturales ricos en carbohidratos
PRODUCCIÓN	Escasa	Mayoritaria
RUTAS	Reacción química	Fermentación homofermentativa o heterofermentativa
ACCIÓN	Productos químicos	Microorganismos: bacterias y hongos
COSTE	Cara	Etapas de separación y purificación suponen alto coste
RENDIMIENTO	Alto	Productos secundarios Bajas concentraciones
CARACTERÍSTICAS	Alto coste Mezcla racémica: D y L ácido láctico	Una de las formas puras del ácido láctico Contaminación por microorganismo Inhibición por sustrato o producto

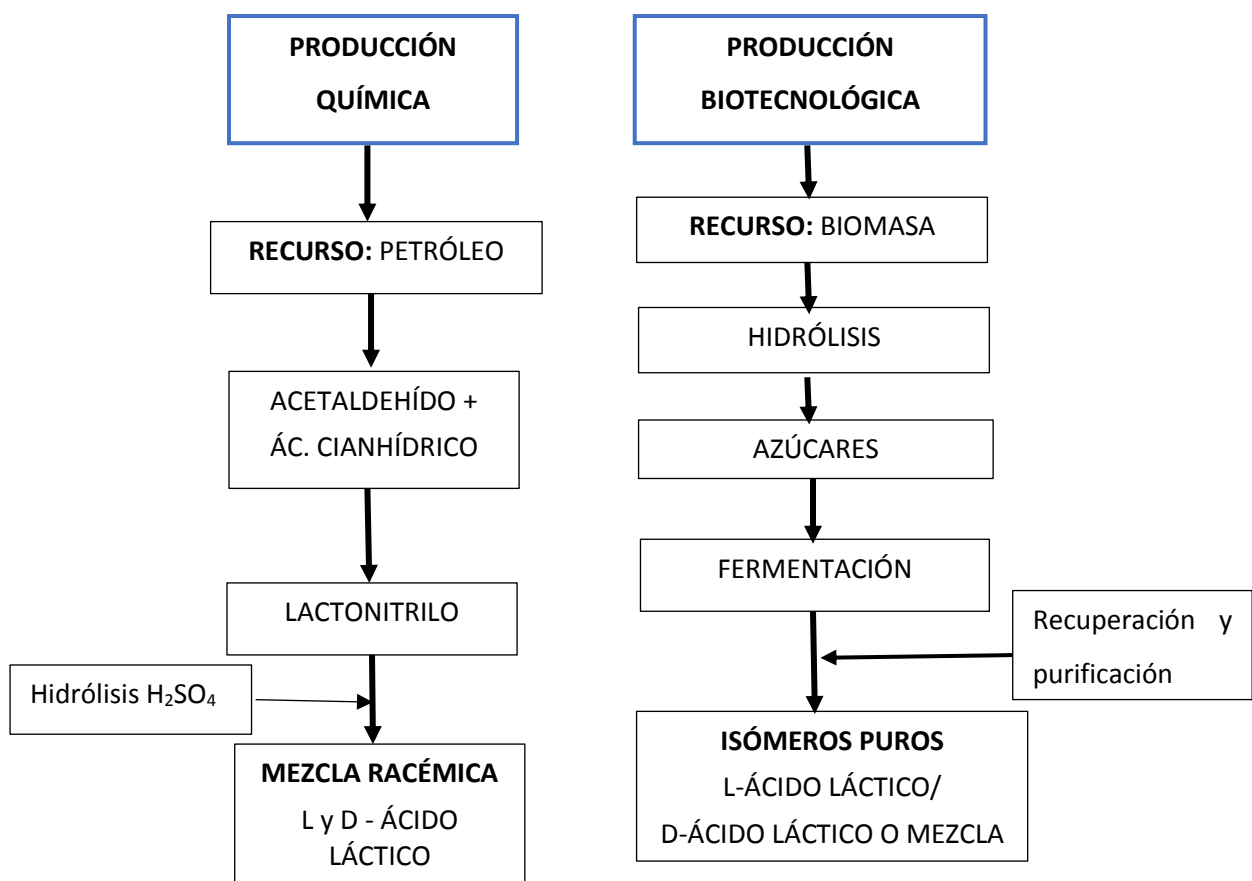


Figura 5.3. Diagrama etapas de las vías de obtención de ácido láctico.

- **RUTA BIOTECNOLÓGICA**

Se basa en la fermentación de sustratos naturales ricos en carbohidratos empleando bacterias u hongos [30].

❖ BACTERIAS

Las bacterias que suelen emplearse para la producción de ácido láctico son las bacterias ácido lácticas (LAB). Éstas son un grupo de bacterias relacionadas que producen ácido láctico como producto metabólico principal.

Las LAB constituyen un grupo muy amplio de microorganismos que se caracterizan generalmente por ser Gram positivas, anaerobios facultativos, no esporulados, inmóviles y catalasa negativa, pertenecientes a los géneros *Lactobacillus* (*Lb*), *Carnobacterium*, *Leuconostoc* (*Leu*), *Pediococcus* (*Pd*), *Streptococcus* (*Str*), *Tetragenococcus*, *Lactococcus* (*Lc*), *Vagococcus*, *Enterococcus* (*Ent*), *Aerococcus* y *Weissella* [3,28,31].

Otros géneros empleados en la producción de ácido láctico son el género *Bacillus*, *Escherichia coli* y *Clostridium glutamicum*, estas últimas modificadas genéticamente.

El microorganismo más empleado en la fermentación del ácido láctico a nivel industrial es *Lactobacillus delbrueckii* (LAB) debido a que solo produce isómeros L (+), con alta eficiencia en el consumo de glucosa, y posee baja temperatura óptima de crecimiento. Esto reduce los costes de enfriamiento y esterilización y no se requiere de procesos posteriores de concentración y purificación.

Hay dos rutas principales para la fermentación mediante LAB dependiendo de los productos obtenidos en la fermentación de los hidratos de carbono: fermentación homofermentativa o homoláctica y heterofermentativa o heteroláctica.

Fermentación homofermentativa

Las bacterias ácido lácticas mediante fermentación homofermentativa producen como producto final ácido láctico a partir de glucosa por la vía de Embden-Meyerhof-Parnas (EMP) o glucólisis. A partir de un mol de glucosa se obtiene dos moles de ácido láctico [32].

Los microorganismos que emplean solo esta ruta se denominan homofermentativos obligatorios [33]. En esta ruta solo se puede fermentar glucosa y no pueden fermentarse pentosas o compuestos relacionados [34].

Si se dan situaciones de limitación de glucosa, pH o temperaturas excesivas, algunos microorganismos pueden consumir otros sustratos como fuente de carbono y producir ácido fórmico por fermentación mixta [18,32].

Sólo las LAB homofermentativas están disponibles para la producción comercial de ácido láctico [31]. Esto se debe a que el crecimiento de las bacterias mediante esta vía es más rápido, y conducen a un producto final de alta pureza con rendimientos altos.

Fermentación heterofermentativa

Las LAB mediante fermentación heterofermentativa producen, además de ácido láctico, varios productos como etanol, ácido acético y dióxido de carbono como productos finales mediante la vía 6-fosfogluconato / fosfocetolasa/ pentosa fosfato [16]. Mediante esta ruta, por cada mol de glucosa se obtiene 1 mol de ácido láctico más otros productos como etanol o dióxido de carbono. Las LAB que emplean solo esta vía metabólica para la fermentación de glucosa se denominan heterofermentativas obligatorias [28].

A diferencia de éstas, las LAB heterofermentativas facultativas fermentan hexosas por la vía homoláctica (vía Embden-Meyerhoff) y pentosas y otras sustancias por la heteroláctica (vía fosfocetolasa) [33].

Tabla 5.3. Características de diferentes rutas de las bacterias ácido lácticas [35].

TIPO DE FERMENTACIÓN	HOMOFERMENTATIVA	HETEROFERMENTATIVA FACULTATIVA	HETEROFERMENTATIVA
RUTA	Hexosas: Embden-Meyerhof	Hexosas: Ruta Embden-Meyerhof Pentosas: Ruta fosfoacetolasa	Pentosas: Ruta fosfocetolasa
PRODUCTOS	Ácido láctico	Ácido láctico, etanol, ácido acético y dióxido de carbono	Ácido láctico, etanol, ácido acético y dióxido de carbono
RENDIMIENTO (A partir de 1 mol glucosa)	2 moles ácido láctico	2 moles ácido láctico/ 1 mol ácido láctico + otros productos	1 mol ácido láctico + otros productos (etanol, ácido acético y dióxido de carbono)
MICROORGANISMOS	<i>Lactobacillus sp.</i>	<i>Enterococcus/ Lactococcus, Lactovum, Streptococcus, Pedicoccus, Lactobacillus sp.</i>	<i>Leuconostoc, Oenococcus y Lactobacillus sp.</i>
ESCALA INDUSTRIAL	Viable comercialmente debido a su alta selectividad	No viable debido a su alta producción de otros productos	No viable debido a su alta producción de otros productos

La clasificación de las LAB como homofermentativas y heterofermentativas se rige por la presencia o ausencia de las enzimas fructosa-1,6-bifosfato aldolasa o la fosfocetolasa, dos enzimas clave en la glucólisis y la vía de la fosfocetolasa, respectivamente.

Los microorganismos homofermentativos estrictos solo pueden fermentar los azúcares por glucólisis debido a que poseen la enzima aldolasa pero no la fosfocetolasa, por lo que no pueden metabolizar otros azúcares que no sean hexosas.

Los microorganismos heterofermentativos obligados sólo pueden metabolizar hexosas y pentosas mediante la vía de fosfocetolasa, ya que presentan la enzima fosfocetolasa, pero carecen de la enzima aldolasa, por lo que utilizan la vía de las pentosas fosfato.

En cambio, las heterofermentativas facultativas poseen enzimas aldolasa y fosfocetolasa, comportándose generalmente como homofermentativos frente a las hexosas y heterofermentativos con las pentosas. Las circunstancias externas como estrés, fuente de carbono, ósmosis o temperatura, afecta a estas bacterias hacia un comportamiento homofermentativo o heterofermentativo [16].

Las LAB tienen la cualidad de poder producir una única forma pura D (-) y L (+) del ácido láctico o también su mezcla racémica. Esta cualidad depende de la presencia de la enzima lactato deshidrogenasa (LDH) y de la forma isomérica que presente esta enzima [32–34]. Algunas bacterias poseen solo un tipo de enzima, produciendo solo una forma D (-) y L (+) del ácido láctico, y otras poseen ambas y producen la mezcla racémica.

A pesar de las ventajas que presenta la producción de ácido láctico mediante la ruta biotecnológica, también tiene algunos inconvenientes o limitaciones. Algunos de los inconvenientes son el riesgo de contaminación por otros microorganismos, la inhibición del crecimiento por el producto o el sustrato, posible estrés y requerimientos nutricionales [27].

La mayoría de las LAB demandan algunos nutrientes específicos (aminoácidos, vitaminas, minerales, etc.) para su crecimiento, puesto que carecen de muchas capacidades biosintéticas. Esto hace que sea más compleja la recuperación del ácido láctico desde el medio de fermentación y aumenten los costos de producción [3,30,32].

También puede darse inhibición por parte del sustrato o producto reduciendo el crecimiento y, por tanto, la productividad. En el caso más generalizado de inhibición por producto, la acidez del medio debido a la concentración de ácido láctico produce la inhibición de la fermentación; por ello, se estudia el empleo de cepas tolerantes a los medios más ácidos [26].

Por tanto, la elección de la cepa, del tipo de sustrato y la composición del medio son factores primordiales para optimizar el rendimiento de la fermentación [33].

❖ HONGOS

Otro de los microorganismos que pueden emplearse en la producción de ácido láctico mediante la vía biotecnológica son los hongos.

Los hongos utilizados en la producción de ácido láctico son mohos y levaduras que pertenecen a los géneros *Rhizopus*, *Zymomonas* y *Saccharomyces*.

El principal hongo empleado para la producción de ácido láctico es la especie *Rhizopus* (*R. oryzae* y *R. arrhizus*), que ha mostrado grandes ventajas frente a las LAB [19]. Este hongo tiene la ventaja de producir también un único isómero de ácido láctico como producto final, pero sin requerir condiciones de fermentación tan estrictas como en el caso de las LAB [36,37].

Al igual que la fermentación con bacterias, la producción dirigida hacia una forma de ácido láctico específica (L (+) o D (-)) depende de la cepa fúngica escogida para la fermentación.

Uno de los principales problemas que presenta la fermentación mediante el empleo de hongos es el tamaño y tipo de micelios. Los micelios en forma filamentosa provocan un aumento de la viscosidad, reduciendo la transferencia de masa, problemas con la homogeneidad, bloqueo de sistemas de aireación, etc. Los micelios en forma granular solventan parcialmente estos problemas, pero desencadenan otros como restringir la transferencia de masa reduciendo la velocidad de producción [5]. Esto provoca un aumento en los tiempos de fermentación, aumentan los subproductos formados, y disminuyen los rendimientos en conversión del sustrato.

La selección de los procesos de fermentación es vital para la producción de ácido láctico y dependerá del tipo de sustrato y microorganismo empleado [35].

FORMAS DE OPERACIÓN

Podemos encontrar procesos con fermentaciones discontinuas y continuas. La fermentación discontinua o en lotes es el método más simple y tradicional empleado en la producción de ácido láctico [32].

Se trata de un sistema cerrado donde se agregan todos los componentes inicialmente y se trabaja en estado no estacionario durante el tiempo que dura la fermentación. Con este sistema de operación se obtienen altas concentraciones de producto, pero presenta el inconveniente del daño de los microorganismos debido a la acumulación de sustrato e inhibición por producto y/o sustrato. Esto supone tiempos de fermentación más largos y la necesidad de trabajar con bajas concentraciones celulares, que se reflejan en baja productividad [9].

Como alternativa, y para solucionar el efecto de la inhibición por sustrato, se ha trabajado con fermentadores discontinuos alimentados. Esta modalidad implica ciclos repetidos mediante la inoculación de una parte o la totalidad de la carga microbiana en cada uno, de tal forma que se mejora la productividad debido al aumento de la concentración de células por la re-inoculación en cada lote, a la vez que el reactor se alimenta secuencialmente en cada etapa con sustrato, resultando la dilución del medio y resolviendo la inhibición por sustrato y por producto.

Presenta además las ventajas de aumentar los rendimientos, ahorro de tiempo y alta concentración celular [35].

Otra modalidad es operar de modo continuo, con la cual se consigue mayor productividad y se solventa también el problema de la inhibición por sustrato y producto [32].

En la tabla 5.4 se muestra las ventajas e inconvenientes que poseen cada modo de fermentación.

Tabla 5.4. Propiedades de los diferentes procesos de fermentación [35].

MODO FERMENTACIÓN	VENTAJAS	INCONVENIENTES
Fermentación discontinua o por lotes	<ul style="list-style-type: none"> • Simple • Alta concentración de producto • Menor riesgo por contaminación 	<ul style="list-style-type: none"> • Baja productividad • Inhibición por sustrato y producto
Fermentación por lotes alimentados	<ul style="list-style-type: none"> • No hay problema de inhibición por sustrato • Alta concentración de producto 	<ul style="list-style-type: none"> • Inhibición por producto
Fermentación repetida	<ul style="list-style-type: none"> • Ahorro de tiempo • Alta productividad • Alta tasa de crecimiento 	<ul style="list-style-type: none"> • Dispositivos especiales
Fermentación continua	<ul style="list-style-type: none"> • Alta productividad • Control tasa de crecimiento 	<ul style="list-style-type: none"> • No se utiliza totalmente la fuente de carbono • Baja concentración de producto

El ácido láctico es un ácido orgánico muy valorado por su amplio campo de aplicación en la industria y su potencial como materia prima para la producción de polímeros biodegradables.

En las últimas décadas, las investigaciones están dirigidas a optimizar la producción de ácido láctico con la premisa de lograr mayor productividad, rendimientos y bajos costes.

En la producción de ácido láctico existen fundamentalmente dos grandes problemas. Uno de ellos consiste en el coste de los métodos de separación y purificación y el otro es el coste de los sustratos empleados como fuente de carbono.

Todos los esfuerzos de investigación se han centrado en disminuir esos costes mediante la búsqueda de nuevos sustratos, nuevas tecnologías y nuevos microorganismos.

5.4. Recuperación y purificación

Tras la producción de ácido láctico mediante fermentación, se debe realizar la separación, purificación y concentración del ácido láctico obtenido. La purificación del ácido láctico supone uno de los pasos más costosos del proceso de producción [9,16].

Además, los procesos de recuperación y purificación del ácido láctico son complejos a causa de la alta afinidad del ácido láctico por el agua y a su baja volatilidad [38,39].

En el proceso tradicional de recuperación, el ácido láctico es precipitado como lactato de calcio como resultado de la neutralización del pH [9]. Esto se debe a que durante la formación de ácido láctico se produce una bajada del pH, y es necesario añadir un agente base (hidróxido sódico, hidróxido de amonio o carbonato de calcio) que produce la formación de lactato [40]. El lactato de calcio es separado mediante filtración y posteriormente se procede a la acidificación con ácido sulfúrico para producir ácido láctico, produciendo a su vez sulfato de calcio insoluble (yeso) como subproducto [10,38]. El empleo de grandes cantidades de productos químicos como agentes neutralizantes, el uso de diversos procesos de separación y purificación secuenciales, así como la generación de desechos, supone que la producción de ácido láctico tenga un elevado coste económico y medioambiental [16].

La recuperación y purificación del ácido láctico es objeto de investigación desde hace décadas con el objetivo de mejorar la concentración y la pureza de ácido láctico en el producto final, así como mejorar la economía y la sostenibilidad de los procesos de separación a aplicar.

Por ello, se han estudiado una gran variedad de procesos de separación y purificación del ácido láctico, destacando los que se relacionan en la Tabla 5.5, si bien el empleo de uno u otro método depende del grado de pureza deseado, el rendimiento y el coste económico.

Tabla 5.5. Procesos alternativos para la separación y purificación del ácido láctico.

PROCESO	VENTAJAS	INCONVENIENTES	REFERENCIAS
PRECIPITACIÓN	Proceso sencillo	Alto consumo de productos químicos Generación de subproducto (yeso) Baja pureza del producto final Problemas ambientales	[41]
EXTRACCIÓN CON SOLVENTES	Proceso rápido Altas concentraciones	Toxicidad de células por los disolventes orgánicos Bajos rendimientos Coeficientes de distribución bajos Regeneración de resinas	[41]
ADSORCIÓN	Combinable con fermentación	Baja vida útil Baja capacidad	[39,42]
DESTILACIÓN MOLECULAR	Alta pureza del producto final No empleo de solventes orgánicos	Difícil escalado industrial Condiciones altas de vacío	[43]
DESTILACIÓN DIRECTA	Alto coeficiente de distribución	Alto requerimiento energético Polimerización del ácido láctico	[41,42]
DESTILACIÓN REACTIVA	Alta pureza del producto Bajo consumo de energía	Proceso complejo Aplicaciones limitadas: velocidad de reacción alta Problemas de corrosión y separación de catalizadores	[41]
MEMBRANAS (UF, NF y OI)	Alta selectividad Alta pureza del producto final Bajo coste energético Integración con otros procesos (procesos híbridos)	Costoso Polarización por concentración y ensuciamiento de las membranas Requiere limpieza de las membranas	[10,39,44]
CROMATOGRAFÍA / INTERCAMBIO IÓNICO	Selectivo Gran capacidad Proceso rápido	Muestras desalinizadas	[44]
ELECTRODIÁLISIS	Eliminación continua Menor coste que las resinas de intercambio iónico	Baja selectividad (impurezas) Ensuciamiento de las membranas	[39,42,45]

De todos estos procesos de separación alternativos, los procesos con membranas han despertado interés debido a su selectividad, su flexibilidad en escala de producción, combinación con otros procesos y reducido coste de inversión del equipo [10].

Además, los procesos con membranas no requieren altas temperaturas ni cambios de fase.

Los estudios realizados durante el desarrollo de esta Tesis Doctoral se centraron en el empleo de procesos de separación alternativos mediante procesos con membranas.

5.5. Materias primas empleadas

En la producción biotecnológica de ácido láctico se utilizan generalmente sustratos puros, como glucosa, sacarosa (azúcar de caña y remolacha azucarera), lactosa (lactosuero) y dextrosa (almidón), siendo los dos primeros sustratos los más empleados [37,39].

El empleo de estas materias primas como sustrato para la producción de ácido láctico constituye el 40-70% del coste total de producción, lo cual supone un gran gasto económico [18,46].

Para abaratar estos costes de producción y emplear otro tipo de sustratos que no compitan con suministros alimentarios, se ha estudiado el empleo de sustratos alternativos.

Una de las opciones estudiadas es el empleo de sustratos procedentes de fuentes renovables, como la biomasa procedente de la agricultura o industria alimentaria.

Otra de las alternativas estudiadas es el empleo de otro tipo de sustratos: residuos de madera, melazas, vinazas, trigo, microalgas, cebada, glicerol, productos lácteos, materiales lignocelulósicos, etc. [32,35].

Los materiales lignocelulósicos proceden de fuentes agrícolas, forestales e industriales, y lo integran un grupo numeroso de materiales como bagazo, papel, hierbas, paja, tallos, hojas, cáscaras, etc., constituyendo un sustrato potencial para la producción de ácido láctico debido a su alto contenido en polisacáridos. Son materiales renovables, abundantes en la naturaleza, formados por subproductos y desechos cuyo interés reside en su bajo coste económico y la reutilización dentro de una cultura de sostenibilidad [9].

No obstante, presentan un inconveniente importante, que consiste en que los azúcares no se encuentran fácilmente accesibles para su conversión a ácido láctico. Esto se debe a que la celulosa y la hemicelulosa de la lignocelulosa se encuentran asociados con la lignina, y los microorganismos que suelen emplearse en la fermentación presentan falta de enzimas hidrolíticas necesarias para su conversión [16]. El empleo de estas nuevas fuentes de hidratos de carbono requiere de un pretratamiento de hidrólisis de los sustratos hasta azúcares que puedan ser fermentables, lo que supone un gasto adicional [46].

Una alternativa que se está estudiando es el empleo de microalgas como precursores del ácido láctico. Se pretende así reducir significativamente los costes de la materia prima, ya que presentan varias ventajas: su producción es fácil, los tiempos de cosecha son cortos, no requieren de sacrificio al no contener lignina y presentan un alto contenido de azúcares fermentables [4].

5.6. Bibliografía

- [1] H. Benninga, *A History of Lactic Acid Making*, Kluwer Academic Publishers, Dordrecht (1990).
- [2] T.B. Vickroy, Lactic acid. In: M. Moo-Young (Ed.), *Comprehensive Biotechnology*, Vol. 3, Pergamon Press, Oxford (1985), pp. 761–776.
- [3] G. Reddy, Md. Altaf, B.J. Naveeba, M. Venkayeshwar, E.V. Kumar, Amylolytic bacterial lactic acid fermentation-a review, *Biotechnol. Adv.* 26 (2008) 22–34.
- [4] C.M. Nguyen, G.J. Choi, Y.H. Choi, K.S. Jang, J.-C. Kim, D- and L- lactic acid production from fresh sweet potato through simultaneous saccharification and fermentation, *Biochem. Eng. J.* 81 (2013) 40–46.
- [5] Z.Y. Zhang, B. Jin, J.M. Kelly, Production of lactic acid from renewable materials by *Rhizopus* fungi, *Biochem Eng. J.* 35 (2007) 251–263.
- [6] R. Auras, L.T. Lim, S.E.M. Selke, H. Tsuji, *Poly (Lactic Acid): Synthesis, Structures, Properties, Processing, and Application*, Wiley, Hoboken (2010).
- [7] R. Datta, S.P. Tsai, P. Bonsignore, S.H. Moon, J.R. Frank, Technological and economic potential of poly (lactic acid) and lactic acid derivatives, *FEMS Microbiol. Rev.* 16 (1995) 221–231.
- [8] Research and Markets, Lactic Acid-Global Market Outlook (2017-2026).
<https://www.researchandmarkets.com/reports/4655800/lactic-acid-global-market-outlook-2017-2026#rela0-5003273> (Consultado: abril 2020).
- [9] M.A. Abdel-Rahman, Y. Tashiro, K. Sonomoto, Lactic acid production from lignocellulose-derived sugars using lactic acid bacteria: overview and limits, *J. Biotechnol.* 156 (2011) 286–301.
- [10] P. Pal, J. Sikder, S. Roy, L. Giorno, Process intensification in lactic acid production: a review of membrane based processes, *Chem. Eng. Process.* 48 (2009) 1549–1559.
- [11] Y.J. Wee, J.N. Kim, H.W. Ryu, Biotechnological production of lactic acid and its recent applications, *Food Technol. Biotechnol.* 44 (2006) 63–72.
- [12] Markets and Markets research report, Lactic acid market by application (biodegradable polymer, food & beverage, personal care & pharmaceutical) & polylactic acid market by application (packaging, agriculture, automobile, electronics, textile), & by geography – Global trends & forecast to 2020 (2017). <https://www.marketsandmarkets.com/Market-Reports/polylacticacid-387.html> (Consultado: febrero 2020)

- [13] Grand View Research Inc., Lactic acid market size worth \$8.77 billion by 2025 | CAGR: 18.7%. <http://www.grandviewresearch.com/press-release/global-lactic-acid-and-poly-lactic-acid-market> (Consultado: febrero 2020).
- [14] Research and Markets, Lactic acid market report: trends, forecast and competitive analysis. <https://www.researchandmarkets.com/reports/5003273/lactic-acid-market-report-trends-forecast-and#pos-0> (Consultado: febrero 2020).
- [15] C.A. Batt, M.-L. Tortorello, *Encyclopedia of Food Microbiology*, second ed., Academic Press, San Diego (2014).
- [16] R. Alves de Oliveira, A. Komesu, C.E. Vaz Rossell, R. Maciel Filho, Challenges and opportunities in lactic acid bioprocess design—from economic to production aspects, *Biochem. Eng. J.* 133 (2018) 219–239.
- [17] A.J. Lasprilla, G.A. Martinez, B.H. Lunelli, A.L. Jardini, R.M. Filho, Poly-lactic acid synthesis for application in biomedical devices — a review, *Biotechnol. Adv.* 30 (2012) 321–328.
- [18] R. Mazzoli, F. Bosco, I. Mizrahi, E.A. Bayer, E. Pessione, Towards lactic acid bacteria-based biorefineries, *Biotechnol. Adv.* 32 (2014) 1216–1236.
- [19] G. Juodeikiene, D. Vidmantiene, L. Basinskiene, D. Cernauskas, E. Bartkiene, D. Cizeikien, Green metrics for sustainability of biobased lactic acid from starchy biomass vs chemical synthesis, *Catal. Today* 239 (2015) 11–16.
- [20] B.P. Upadhyaya, L.C. DeVeaux, L.P. Christopher, Metabolic engineering as a tool for enhanced lactic acid production, *Trends Biotechnol.* 32 (2014) 637–644.
- [21] J. Wu, Y. Hu, J. Zhou, W. Qian, X. Lin, Y. Chen, X. Chen, J. Xie, J. Bai, H. Ying, Separation of D-lactic acid from aqueous solutions based on the adsorption technology, *Colloid Surf. A-Physicochem. Eng. Asp.* 407 (2012) 29–37.
- [22] H.R. Kricheldorf, Syntheses and application of polylactides, *Chemosphere* 43 (2001) 49–54.
- [23] S. Pivsa-Art, T. Tong-ngok, S. Junngam, R. Wongpajan, W. Pivsa-Art, Synthesis of poly (D-lactic acid) using a 2-steps direct polycondensation process, *Energy Procedia* 34 (2013) 604–609.
- [24] K.M. Nampoothiri, N.R. Nair, R.P. John, An overview of the recent developments in polylactide (PLA) research, *Bioresour. Technol.* 101 (2010) 8493–8501.
- [25] S.R. Kadam, S.S. Patil, K.B. Bastawde, J.M. Khire, D.V. Gokhale, Strain improvement of *Lactobacillus delbrueckii* NCIM 2365 for lactic acid production, *Process Biochem.* 41 (2006) 120–126.
- [26] K. Hetényi, Á. Németh, B. Sevella, Role of pH-regulation in lactic acid fermentation: second steps in a process improvement, *Chem. Eng. Process.* 50 (2011) 293–299.

- [27] Y. Wang, Y. Tashiro, K. Sonomoto, Fermentative production of lactic acid from renewable materials: recent achievements, prospects, and limits, *J. Biosci. Bioeng.* 1 (2015) 10–18.
- [28] L. Axelsson, Lactic acid bacteria: classification and physiology. In: S. Salminen, A. von Wright, A.C. Ouwehand (Eds.), *Lactic Acid Bacteria: Microbiological and Functional Aspects*, third ed., Marcel Dekker, New York (2004).
- [29] C. Gao, C. Ma, P. Xu, Biotechnological routes based on lactic acid production from biomass, *Biotechnol. Adv.* 29 (2011) 930–939.
- [30] J.H. Litchfield, Microbiological production of lactic acid, *Adv. Appl. Microbiol.* 42 (1996) 45–95.
- [31] J.S. Yun, Y.J. Wee, H.W. Ryu, Production of optically pure L-(+)-lactic acid from various carbohydrates by batch fermentation of *Enterococcus faecalis* RKY1, *Enzyme Microb. Technol.* 33 (2003) 416–423.
- [32] K. Hofvendahl, B. Hahn-Hägerdal, Factors affecting the fermentative lactic acid production from renewable resources, *Enzyme Microb. Technol.* 26 (2000) 87–107.
- [33] F.A. Castillo Martínez, E.M. Balciunas, J.M. Salgado, J.M. Domínguez González, A. Converti, R.P. de Souza Oliveira, Lactic acid properties, applications and production: a review, *Trends Food Sci. Technol.* 30 (2013) 70–83.
- [34] P.S. Panesar, J.F. Kennedy, D.N. Gandhi, K. Bunko, Bioutilisation of whey for lactic acid production, *Food Chem.* 105 (2007) 1–14.
- [35] M.A. Abdel-Rahman, Y. Tashiro, K. Sonomoto, Recent advances in lactic acid production by microbial fermentation processes, *Biotechnol. Adv.* 31 (2013) 877–902.
- [36] Y. Zhou, J.M. Domínguez, N. Cao, J. Du, G.T. Tsao, Optimization of L-lactic acid production from glucose by *Rhizopus oryzae* ATCC 52311, *Appl. Biochem. Biotechnol.* 78 (1999) 401–407.
- [37] S. Bulut, M. Elibol, D. Ozer, Effect of different carbon sources on L-(+)-lactic acid production by *Rhizopus oryzae*, *Biochem. Eng. J.* 21 (2004) 33–37.
- [38] X. Sun, Q. Wang, W. Zhao, H. Ma, K. Sakata, Extraction and purification of lactic acid from fermentation broth by esterification and hydrolysis method, *Sep. Purif. Technol.* 49 (2006) 43–48.
- [39] H.G. Joglekar, I. Rahman, S. Babu, B.D. Kulkarni, A. Josh, Comparative assessment of downstream processing options for lactic acid, *Sep. Purif. Technol.* 52 (2006) 1–17.
- [40] C. Åkerberg, G. Zacchi, An economic evaluation of the fermentative production of lactic acid from wheat flour, *Bioresour. Technol.* 75 (2000) 119–126.

- [41] Q.H. Wang, G.S. Cheng, X.H. Sun, B. Jin, Recovery of lactic acid from kitchen garbage fermentation broth by four-compartment configuration electrodialyzer, *Process Biochem.* 41 (2006) 152–158.
- [42] E.G. Lee, S.-H. Moon, Y.K. Chang, I.-K. Yoo, H.N. Chang, Lactic acid recovery using two-stage electrodialysis and its modelling, *J. Membr. Sci.* 145 (1998) 53–66.
- [43] R.A. de Oliveira, A. Komesu, C.E. Vaz Rossell, M.R. Wolf Maciel, R. Maciel Filho, A study of the residual fermentation sugar influence on alternative downstream process for first and second-generation lactic acid, *Sustain. Chem. Pharm.* 15 (2020) 100206.
- [44] T. Ghaffar, M. Irshad, Z. Anwar, T. Aquil, Z. Zulifqar, A. Tariq, M. Kamran, N. Ehsan, S. Mehmood, Recent trends in lactic acid biotechnology: a brief review on production to purification, *J. Rad. Res. Appl. Sci.* 7 (2014) 222–229.
- [45] P. Boontawan, S. Kanchanathawee, Extractive fermentation of L-(+)-lactic acid by *Pediococcus pentosaceus* using electrodeionization (EDI) technique, *Biochem. Eng. J.* 54 (2011) 192–199.
- [46] M.A. Abdel-Rahman, K. Sonomoto, Opportunities to overcome the current limitations and challenges for efficient microbial production of optically pure lactic acid, *J. Biotechnol.* 236 (2016) 176–192.

6. Lactic acid recovery by microfiltration using niosomes as extraction agents

En este primer trabajo se estudia la recuperación del ácido láctico de soluciones acuosas diluidas mediante membranas de microfiltración empleando niosomas como agente de extracción. Los niosomas se formaron mediante la aplicación de ultrasonidos a dispersiones acuosas del tensioactivo no iónico monooleato de sorbitán (Span 80) en presencia de pequeñas cantidades del tensioactivo aniónico dodecil sulfato de sodio (SDS).

El trabajo examina el efecto de las variables asociadas a la composición del medio (concentración de ácido láctico, pH, volumen de fase dispersa y contenido de SDS en los niosomas) sobre la velocidad de extracción y el grado de extracción alcanzado en el equilibrio. Simultáneamente, se analiza el efecto de estas variables sobre el comportamiento de la membrana durante la etapa de concentración. Los resultados mostraron que los principales factores que afectan al grado de extracción del ácido láctico son el pH de la dispersión, la concentración del tensioactivo SDS en la formulación de los niosomas, y la relación molar entre el SDS y el ácido láctico. Las condiciones óptimas de extracción se alcanzaron con niosomas formulados con 20 mol/m³ de Span 80 y 4 mol/m³ de SDS, una relación molar de SDS y ácido láctico de 0,01, y un pH menor que el pKa del ácido láctico. Bajo estas condiciones, el porcentaje de ácido láctico extraído en los niosomas fue del 33%.

La concentración de la fase dispersa se realizó utilizando membranas cerámicas de microfiltración, en concreto se utilizaron discos planos de TiO₂ con un tamaño de poro de 0,2 µm y se aplicó una presión transmembranal de 0,3 bar. Bajo estas condiciones, el rechazo de la membrana a los niosomas fue total y la densidad de flujo de permeado fue 26 L/m² h, valor que se mantuvo constante durante la etapa de concentración hasta un factor de concentración en volumen de 2,5.

Se comprobó experimentalmente que una extracción en dos etapas, en el que el permeado de la primera etapa sirve de alimentación a la segunda etapa, aumentaba considerablemente, hasta un 43%, el grado de extracción. Este hecho permite inferir la conveniencia de realizar el proceso de extracción en multietapas, manteniendo las condiciones óptimas del medio de dispersión en cada una de ellas.

La reextracción del ácido láctico se realizó mediante adición de NaOH hasta un pH > 12. Bajo estas condiciones, se produce la ruptura de los niosomas, liberándose el ácido láctico y alcanzándose su recuperación como lactato, libre de tensioactivos, en el permeado de microfiltración.

Span 80: Estudios de extracción y caracterización

Este trabajo ha sido presentado en el “IX Ibero-American Congress on Membrane Science and Technology”, Santander (2014) y publicado en la revista *Separation and Purification Technology* 151 (2015) 1–13. <https://doi.org/10.1016/j.seppur.2015.07.018>

6.1. Introduction

Several plant effluents from pharmaceutical, pulp and paper, and petrochemical industries contain organic acids of low molecular weight, whose recovery may be highly profitable notwithstanding their low concentration. Among them, lactic acid has a paramount importance in biotechnology and food industry, where is used as a food preservative, acidulant, flavoring agent and pH buffer [1,2], and also as a substitute for glycerin in the cosmetics sector. Further fields of applications, such as the production of biodegradable polymers derivatives of polylactic acid (PLA), 'green' solvents from lactate esters, and fine chemical commodity [3,4] reveal the potential of lactic acid and its importance on the chemical market. It is usually obtained by biotechnological fermentation using lactic acid bacteria [5–7] and its recovery from fermentation broths is mainly made by precipitation with calcium hydroxide or by solvent extraction [8,9]. Continuous lactic acid removal by membrane-based processes has been shown to effectively increase lactic acid productivity [10]. Although several organic solvents containing the tertiary amine alamine 336 [11], the secondary amine Amberlite LA-2 [12], tri-n-octylamine or tributylphosphate [13,14] have been studied for efficient lactic acid reactive extraction, an economical method for lactic acid recovery from the fermentation broth is still needed.

Micellar-enhanced ultrafiltration (MEUF) is an alternative process that can be used for organic acids recovery. The surfactant forms large amphiphilic aggregate micelles when added to aqueous streams at a concentration higher than its critical micellar concentration (CMC). The solutes can be retained after being trapped by the micelles, whereas the untrapped species readily pass through the UF membranes. In previous works we studied the recovery of several biocompounds including lactic acid and citric acid with SDS (sodium dodecyl sulphate) by MEUF [15,16]. These processes are considered to be clean technologies as they have the advantages of large-scale continuous separation without phase change, avoiding the use of organic solvents.

In this work we explore the use of niosomes as lactic acid extraction agents, a new technology that so far, to our knowledge, has not been explored. Niosomes or non-ionic surfactant vesicles are formed by one or more surfactant bilayers enclosing an aqueous inside cavity: both hydrophilic and hydrophobic compounds can be encapsulated inside their core and in the bilayer, respectively. Niosomes are preferred to liposomes because of their greater chemical stability, high purity, low cost, content uniformity, and their easy handling and storage [17,18]. Moreover, their large-scale production without using unacceptable solvents is uncomplicated, so they are widely used in pharmaceutical, cosmetic and, to a lesser extent, food applications [19–23]. Another advantage for industrial production of these vesicles is the large number of

non-toxic and relatively low-cost non-ionic surfactants available for niosome formulation [24]. Encapsulation efficiency depends mainly on niosome structure, the nature and size of the hydrophilic head and the length of the hydrophobic group of surfactants forming the bilayer, pH and composition of the formulation medium, and the nature of the solute [25–27]. Several additives can be added to the formulation in order to stabilize the niosomes. Cholesterol is the most used among them, because of its ability to modify the mechanical strength of the bilayers and their permeability to water [28,29].

In a recent previous work [30] the effect of different formulations containing Span 80 (sorbitan monooleate) as the encapsulating surfactant, cholesterol and SDS as membrane modifiers, and lactic acid as loaded solute has been investigated. Results revealed that SDS acts as a niosome stabilizer that can be used as a substitute of cholesterol because it increased the zeta potential absolute value while decreased the particle size. Additionally, SDS also increased the lactic acid entrapment efficiency, which indicates that Span 80 niosomes modified with SDS can be used as selective extraction agents for the lactic acid recovery when it is in aqueous solutions at low concentration. Based in previous results, this work aims to investigate the potential use of niosomes formulated with Span 80 and SDS as extraction agents of lactic acid in aqueous solution, and the simultaneous separation and concentration of dispersions using flat-disc ceramic microfiltration (MF) membranes. Kinetics and equilibrium capacities of niosomes for lactic acid extraction under different medium conditions are investigated in this work, in order to achieve acceptable levels of lactic acid extraction from dilute aqueous solutions.

6.2. Materials and methods

6.2.1. Chemicals

DL-Lactic acid (>90% purity, Fluka) was used as solute. The non-ionic surfactant sorbitan monooleate (Span 80, Sigma-Aldrich), with a hydrophilic–lipophilic balance value (HLB) of 4.3 [23], and the anionic surfactant sodium dodecyl sulphate (SDS, 99%, Sigma-Aldrich), with CMC value of 8.3 mol/m³ [15,16], were used in the formulation of niosomes. Other chemicals such as methanol (HPLC grade, HiPerSolv Chromanorm), maleic acid (>99%, Fluka), phosphoric acid (>85%, Sigma-Aldrich), disodium hydrogen phosphate dodecahydrate (>98%, Panreac), potassium dihydrogen phosphate (>99.5%, Merck), sodium hydroxide (analysis grade, Scharlau), and phenolphthalein (99%, Panreac) were used throughout the experiments. For the determination of SDS the following chemicals were used: ethyl violet (99%, Sigma-Aldrich), glacial acetic acid of analysis quality (Panreac), sodium acetate for analysis (Merck), anhydrous

sodium sulphate for analysis (Scharlau), toluene (>99.5%, AnalarNormapur VWR Chemicals) and ethylenediaminetetraacetic acid (EDTA, >99%, Sigma-Aldrich).

Ultrapure deionized Milli-Q water (Millipore, USA) was used for the preparation of all solutions.

6.2.2. *Niosome preparation*

Aqueous solutions of single surfactants of Span 80 and SDS were prepared 24 h before their use, in order to hydrate and relax the carbonated chains of their molecular structures, weighing out the exact amounts of surfactant on an analytical balance (Sartorius, accurate to ± 0.0001 g), and deionized water addition up to a final volume of 100 cm^3 . Niosomes were prepared by direct ultrasonication of 10 cm^3 aqueous solutions of Span 80 (20 mol/m^3) and SDS ($0, 2$, and 4 mol/m^3), formulated by mixing appropriate volumes of the single surfactant solutions, in round-based polystyrene tubes, 115 mm in height and 29 mm in diameter, supplied by Labbox (Spain). These concentrations were chosen on the basis of the previous results obtained in our laboratory where synergism for lactic acid entrapment was obtained for formulations of Span 80 and SDS with SDS molar fraction lower than 0.4 [30].

The application of ultrasounds was carried out over a 5-min effective time, with pulses every 5 s (5 s on and 5 s off, 60 cycles; 30% amplitude, 500 W), to avoid overheating of the sample, using a high-intensity ultrasonic processor (Vibra-Cell VCX 500, Sonics & Materials Inc., USA) equipped with a 3 mm-diameter titanium alloy bicylindrical probe. The 1 cm skirt at the base of polystyrene tubes assisted homogeneous probe positioning in all samples. Throughout the ultrasonication process, the samples were immersed in an ice bath to prevent chemical degradation. Temperature of the process was lower than $70\text{ }^\circ\text{C}$, well above the gel–liquid phase transition temperature. Subsequently, the samples were centrifuged (Eppendorf 5804 centrifuge) in 15 cm^3 polystyrene centrifuge tubes for 45 min at 9000 rpm, in order to remove traces of metal detached from the probe.

6.2.3. *Experimental set-up*

Tangential MF experiments were carried out in a Spirlab filtration cell (TAMI Industries, France) using flat-disc ceramic membranes (INSIDE DisRAM, TAMI Industries, France), with an active layer of TiO_2 supported on titania, 90 mm of diameter, and 56.3 cm^2 of effective area. The system is equipped with a jacketed feed tank (1 L) where the feed solutions are kept at constant temperature ($20\text{ }^\circ\text{C}$) and stirred at 375 rpm. Feed solution is fed to the filtration cell by a

peristaltic pump (Masterflex I/s economy drive Cole Parmer, CRS rotor EW-07518-00) at a prefixed flow rate and pressure. Adjustment of transmembrane pressure (TMP) is achieved by a needle valve located in the retentate stream. The system is also equipped with a rotameter and a pressure gauge, both placed at the inlet of the filtration cell [30].

Preliminary tests with Milli-Q water were made to determine the flows obtained at different positions of the pump rotor. A fixed position of the rotor that provides a water flow rate of 20 L/h was maintained throughout the experiments.

6.2.3.1. Selection of the membrane pore size and working pressure

Three MF membranes of TiO_2 supported on titanium with 0.14, 0.20 and 0.45 μm pore size were tested. Experiments were carried out with 400 cm^3 of deionized water to which were added 10 cm^3 of the dispersed phase containing niosomes formulated with Span 80 (20 mol/m³) and SDS (4 mol/m³). The system worked in concentration mode, after a period of 30 min in which the membrane worked in total recirculation mode and membrane fouling was achieved. The TMP was 0.3 bar. The permeate flux was determined throughout the concentration process.

In order to select the working pressure, experiments with different TMP (0, 0.3, 0.5, 0.65, and 0.8 bar) were performed with the selected membrane of 0.20 μm pore size, using the same feed. The permeate flux was measured for each TMP after a period of at least 15 minutes to allow steady state conditions were achieved.

6.2.3.2. Membrane cleaning

Membrane cleaning was accomplished by rinsing with deionized water, followed by washing with 0.1 N sodium hydroxide solution for 30 min, and then with 0.17 wt% phosphoric acid solution for 30 minutes. A final rinsing step with deionized water until neutrality was sufficient to restore the initial water flux of the membrane.

6.2.4. *Niosomal extraction procedure*

All experiments were carried out using the filtration cell with the selected membrane (0.20 μm) at 20 °C and 375 rpm stirring speed in the feed tank. The TMP was kept at 0.3 bar. The feed was a 400 cm^3 solution of lactic acid to which was added a certain volume of the dispersed phase

containing niosomes formulated with Span 80 (20 mol/m³) and different SDS concentrations, as it was described in section 6.2.2. The factors to be studied were the feed lactic acid concentration (5, 10 and 20 mol/m³), feed pH (natural and modified by addition of 0.1 N HCl or 0.1 N NaOH up to a set point pH between 2 and 12), volume of the dispersed phase (10, 30, and 60 cm³) added to the aqueous feed, and SDS concentration in the niosome formulation (0, 2, and 4 mol/m³). Table 6.1 summarizes the feed conditions of the experiments.

The microfiltration experiments were performed in two consecutive stages as follows.

Table 6.1. Summary of the feed dispersion compositions. $V^0_{(W)}$ and $C_A^0_{(W)}$ are the volume and lactic acid concentration of the continuous phase, whereas $V^0_{(d)}$ and $C_{SDS}^0_{(d)}$ are the volume and the total SDS concentration of the dispersed phase containing niosomes formulated with Span 80 (20 mol/m³) and the indicated SDS concentration. Size (medium diameter), PDI (polydispersity index) and zeta potential of formulated niosomes are also indicated.

Experiment	$V^0_{(W)} \pm 2$ (cm ³)	$C_A^0_{(W)}$ (mol/m ³)	pH ⁰ _(W) ± 0.01	$V^0_{(d)}$ (cm ³)	$C_{SDS}^0_{(d)}$ (mol/m ³)	Size _(d) (nm)	PDI _(d)	Z-pot _(d) (mV)
<i>Experiments at natural pH</i>								
1	400	10.65 ± 0.17	2.88	0	0	-	-	-
2	400	10.19 ± 0.29	2.91	10 ± 0.1	4.0 ± 0.1	-	-	-
3 A	400	10.34 ± 0.24	2.80	10 ± 0.1	4.0 ± 0.1	184.50 ± 10.01	0.24 ± 0.03	-44.80 ± 1.43
3 B	400	10.08 ± 0.56	2.82	30 ± 0.2	4.0 ± 0.1	200.10 ± 07.90	0.21 ± 0.01	-45.10 ± 2.02
3 C	400	10.78 ± 0.37	2.81	60 ± 0.3	4.0 ± 0.1	188.50 ± 06.35	0.29 ± 0.01	-45.30 ± 3.26
4 A	400	10.98 ± 0.55	2.80	10 ± 0.1	2.0 ± 0.1	219.83 ± 12.26	0.21 ± 0.01	-44.75 ± 3.29
4 B	400	10.84 ± 0.58	2.82	30 ± 0.2	2.0 ± 0.1	148.13 ± 07.97	0.21 ± 0.01	-45.40 ± 2.02
5 A	400	10.51 ± 0.47	2.83	10 ± 0.1	0	158.60 ± 05.84	0.23 ± 0.01	-37.60 ± 1.21
5 B	400	10.36 ± 0.38	2.84	30 ± 0.2	0	154.97 ± 03.31	0.14 ± 0.00	-40.92 ± 1.19
6 A	400	5.37 ± 0.59	2.83	10 ± 0.1	4.0 ± 0.1	183.15 ± 03.19	0.20 ± 0.04	-38.51 ± 5.16
6 B	400	5.28 ± 0.46	2.82	30 ± 0.3	4.0 ± 0.1	213.61 ± 05.12	0.21 ± 0.03	-34.62 ± 3.94
7 A	400	20.11 ± 0.56	2.84	10 ± 0.2	4.0 ± 0.1	212.30 ± 10.06	0.15 ± 0.02	-34.91 ± 1.23
7 B	400	20.31 ± 0.36	2.81	30 ± 0.2	4.0 ± 0.1	207.51 ± 07.91	0.20 ± 0.05	-36.89 ± 1.54
<i>Experiments with pH modification</i>								
8 A	400	10.25 ± 0.05	2.08	10 ± 0.1	4.0 ± 0.1	200.20 ± 03.88	0.30 ± 0.05	-39.70 ± 4.32
8 B	400	10.09 ± 0.04	2.08	30 ± 0.2	4.0 ± 0.1	198.90 ± 02.95	0.21 ± 0.02	-38.73 ± 1.97
9 A	400	10.52 ± 0.37	4.05	10 ± 0.1	4.0 ± 0.1	195.23 ± 02.86	0.10 ± 0.01	-39.07 ± 3.98
9 B	400	10.71 ± 0.55	4.06	30 ± 0.3	4.0 ± 0.1	210.23 ± 10.36	0.23 ± 0.10	-42.07 ± 3.96
10 A	400	10.31 ± 0.21	6.07	10 ± 0.2	4.0 ± 0.1	202.20 ± 05.79	0.25 ± 0.10	-44.55 ± 2.13
10 B	400	10.62 ± 0.67	6.06	30 ± 0.2	4.0 ± 0.1	206.53 ± 08.05	0.27 ± 0.04	-35.16 ± 1.06
11 A	400	10.24 ± 0.07	7.95	10 ± 0.1	4.0 ± 0.1	212.93 ± 04.42	0.21 ± 0.09	-38.41 ± 1.99
11 B	400	10.54 ± 0.50	7.91	30 ± 0.3	4.0 ± 0.1	217.57 ± 03.57	0.29 ± 0.09	-37.61 ± 1.17
12 A	400	10.55 ± 0.30	9.63	10 ± 0.3	4.0 ± 0.1	167.20 ± 02.31	0.21 ± 0.07	-39.60 ± 6.08
12 B	400	10.37 ± 0.50	9.67	30 ± 0.2	4.0 ± 0.1	171.79 ± 03.15	0.20 ± 0.10	-44.15 ± 2.34
13 A	400	10.06 ± 0.03	12.19	10 ± 0.1	4.0 ± 0.1	208.04 ± 06.96	0.20 ± 0.05	-44.15 ± 3.15
13 B	400	10.07 ± 0.08	12.22	30 ± 0.2	4.0 ± 0.1	213.83 ± 14.36	0.31 ± 0.04	-39.22 ± 1.59

6.2.4.1. Total recirculation mode (1st stage)

The objective of this stage was the study of the lactic acid extraction kinetics and the determination of the niosomes extraction efficiency at the equilibrium conditions. Experiments were conducted in constant concentration mode, with total recirculation of permeate and retentate to the feed tank, starting the operation time with the addition of the dispersed phase. Permeate samples were collected over time and their lactic acid concentrations were determined by titration with NaOH, or by HPLC in experiments where the pH was modified.

Results were evaluated in terms of the extraction degree estimated as the molar ratio between the lactic acid extracted in the niosomes and its total amount present in the initial dispersion. It was calculated by the mass balance shown in Eq. (1), assuming a two-phases model in which the total lactic acid concentration in the feed dispersion volume, $V_{(F)}$, is the sum of the fraction extracted by the niosomes, $C_{A(NS)}$, and the remained free in the continuous phase that pass through the MF membrane to the permeate stream, $C_{A(p)}$. The equilibrium distribution coefficient, P_A , expressed as the molar ratio between the lactic acid extracted in the niosomes and the lactic acid in the continuous phase at the equilibrium time, was determined by Eq. (2).

$$EE_{A,t} = \frac{C_{A(NS)t}V_{(F)t}}{C_{A(w)}^0 V_{(w)}} = \frac{C_{A(w)}^0 V_{(w)}^0 - \sum_{t-1} C_{A(p)i} V_{(p)i} - C_{A(p)t} V_{(F)t-1}}{C_{A(w)}^0 V_{(w)}^0} \quad (1)$$

$$P_A = \frac{C_{A(w)}^0 V_{(w)}^0 EE_{A,eq}}{C_{A(p)eq} V_{(F)eq}} \quad (2)$$

where $C_{A(w)}^0$ and $V_{(w)}^0$ are the lactic acid molar concentration and volume of the continuous phase at time zero, before the niosomes addition, $C_{A(p)t}$ is the lactic acid concentration in the permeate sample collected at time t , $V_{(F)t-1}$ is the volume of the feed dispersion before collecting the permeate sample at time t , and the summation represents the total moles of lactic acid that have been removed in the permeate samples before the time t , being $V_{(p)i}$ the volume of each permeate sample collected for analysis whose lactic acid concentration is $C_{A(p)i}$, and $EE_{A,eq}$, $C_{A(p)eq}$ and $V_{(F)eq}$ are the lactic acid extraction degree, lactic acid concentration in permeate, and dispersion volume at the equilibrium time, respectively.

6.2.4.2. Concentration mode (2nd stage)

The second stage aims to evaluate the behavior of the MF membrane during the lactic acid-loaded niosomes concentration process. Once the equilibrium was reached in the previous stage, the system continued working in concentration mode, removing continuously the permeate stream and recirculating the retentate to the feed tank up to a volume concentration ratio (VCR) around 2.5.

The permeate flux (J_p) was calculated throughout the process time by the following equation:

$$J_p = \frac{V_p}{t \text{ Area}} \quad (3)$$

where V_p is the permeate volume collected, t is the process time needed for collecting the permeate volume, and Area is the membrane effective area.

Assuming a total retention of niosomes by the 0.20 μm membrane (experimentally observed, as explained in section 6.3.1), the degree of lactic acid extracted by the niosomes with respect to the total amount present in the final retentate ($X_{A(NS)}$) were calculated assuming the aforementioned two-phases model, as follows:

$$X_{A(NS)} = \frac{C_{A(NS)} VCR}{C_{A(NS)} VCR + C_{A(p)}} \quad (4)$$

where $C_{A(NS)}$ is the lactic acid extracted in niosomes in the dispersion before starting the concentration stage, calculated by Eq. (1), VCR is the volume concentration ratio, and $C_{A(p)}$ is the lactic acid concentration in the final permeate.

The SDS concentration, zeta potential, and particle size were also measured in the dispersions before concentration stage (data not shown) and in the final permeates and retentates after concentration (data shown in Tables 6.2 and 6.3), following the procedures described in section 6.2.5.

Table 6.2. Results of MF experiments made at natural pH 0.20 μm flat-disc TiO_2 membrane. SDS/A is the SDS to lactic acid molar ratio in the feed dispersion, $C_{A,\text{eq}}$ is the lactic acid concentration in the continuous phase (permeate) at the equilibrium conditions, P_A is the lactic acid equilibrium distribution coefficient (Eq. (2)), $EE_{A,\text{eq}}$ is the lactic acid equilibrium extraction degree (Eq. (1)), K_a is the overall volumetric mass-transfer coefficient (Eq. (7)), and R^2 the coefficient of determination. $SDS_{(\text{NS})}$ and $SDS_{(\text{m})}$ are the degree of SDS linked to the niosomes and the membrane, respectively, with respect to the initial SDS content in the feed. VCR is the volume concentration ratio, J_p the permeate flux, $C_{A(p)}$ and $C_{SDS(p)}$ are the lactic acid and SDS monomer concentrations in the final permeate, $X_{A(\text{NS})}$ and $X_{SDS(\text{NS})}$ are the molar ratio of lactic acid (Eq. (4)) and SDS, respectively, that remain linked to the niosomes with respect to the total amount present in the retentate after the concentration stage. Size, PDI and zeta potential are the properties of the niosomes in the final retentate.

1 st stage (total recirculation mode)									
Exp.	SDS/A	$C_{A,\text{eq}}$ (mol/m ³)	P_A	$EE_{A,\text{eq}}$ (%)	K_a (min ⁻¹)	R^2	$C_{SDS,\text{eq}} \times 10^2$ (mol/m ³)	$SDS_{(\text{NS})}$ (%)	$SDS_{(\text{m})}$ (%)
<i>Niosomes of Span 80 (20 mol/m³) + SDS (4 mol/m³)</i>									
3 A	0.010	5.92 ± 0.13	0.59	33.01	0.092	0.98	0.32 ± 0.05	94.94	1.82
3 B	0.030	6.27 ± 0.07	0.38	25.00	0.084	0.98	0.73 ± 0.05	95.12	2.28
3 C	0.060	6.78 ± 0.05	0.12	9.58	0.083	0.99	1.07 ± 0.01	94.71	3.23
6 A	0.020	3.64 ± 0.11	0.24	18.20	0.121	0.98	0.25 ± 0.01	94.34	2.09
6 B	0.060	3.80 ± 0.03	0.13	10.50	0.198	0.96	0.72 ± 0.01	95.19	2.22
7 A	0.005	14.60 ± 0.09	0.12	9.52	0.155	0.99	0.22 ± 0.01	95.87	2.28
7 B	0.015	14.23 ± 0.12	0.09	7.23	0.092	0.99	0.86 ± 0.03	94.50	2.42
<i>Niosomes of Span 80 (20 mol/m³) + SDS (2 mol/m³)</i>									
4 A	0.010	8.26 ± 0.08	0.10	8.25	0.108	0.99	0.20 ± 0.01	95.19	1.22
4 B	0.020	8.04 ± 0.07	0.07	5.85	0.096	0.99	0.32 ± 0.02	97.44	1.52
<i>Niosomes of Span 80 (20 mol/m³)</i>									
5 A	0	8.24 ± 0.04	0.12	9.31	0.133	0.99	-	-	-
5 B	0	8.30 ± 0.08	0.06	4.72	0.115	0.99	-	-	-

2nd stage (concentration mode)

Exp.	VCR	J _p (L/m ² h)	C _{A(p)} (mol/m ³)	X _{A(NS)} (%)	C _{SDS(p)} × 10 ² (mol/m ³)	X _{SDS(NS)} (%)	Size _(r) (nm)	PDI _(r)	Z-pot _(r) (mV)
<i>Niosomes of Span 80 (20 mol/m³) + SDS (4 mol/m³)</i>									
3 A	2.31	26.00 ± 3.13	5.96 ± 0.07	54.33	0.27 ± 0.03	99.41	200.80 ± 3.58	0.27 ± 0.01	-32.31 ± 2.13
3 B	2.58	24.07 ± 6.54	6.31 ± 0.06	47.11	0.83 ± 0.05	99.32	263.41 ± 13.21	0.27 ± 0.02	-34.62 ± 1.84
3 C	2.24	18.22 ± 4.61	6.43 ± 0.02	17.22	1.05 ± 0.04	99.39	195.70 ± 12.41	0.22 ± 0.03	-41.95 ± 1.61
6 A	2.21	27.71 ± 6.87	3.65 ± 0.11	33.75	0.26 ± 0.08	99.63	195.14 ± 7.12	0.30 ± 0.01	-28.40 ± 5.69
6 B	1.92	25.58 ± 7.25	3.80 ± 0.05	18.75	0.82 ± 0.06	99.74	226.63 ± 9.17	0.15 ± 0.07	-30.91 ± 3.05
7 A	2.76	25.05 ± 7.87	16.11 ± 0.03	21.25	0.14 ± 0.07	99.55	287.50 ± 5.88	0.21 ± 0.05	-26.31 ± 2.87
7 B	1.92	22.37 ± 6.74	16.16 ± 0.07	11.52	0.74 ± 0.09	99.37	249.40 ± 12.26	0.25 ± 0.02	-30.16 ± 0.87
<i>Niosomes of Span 80 (20 mol/m³) + SDS (2 mol/m³)</i>									
4 A	2.85	28.77 ± 7.71	8.61 ± 0.04	19.81	0.14 ± 0.05	99.47	231.14 ± 4.27	0.34 ± 0.02	-35.72 ± 2.21
4 B	2.04	22.92 ± 5.41	8.67 ± 0.09	10.57	0.32 ± 0.08	98.94	216.40 ± 11.04	0.23 ± 0.01	-33.30 ± 4.12
<i>Niosomes of Span 80 (20 mol/m³)</i>									
5 A	1.85	25.04 ± 5.13	8.28 ± 0.02	16.11	-	-	179.14 ± 6.35	0.16 ± 0.04	-26.45 ± 4.59
5 B	1.95	23.45 ± 2.64	8.36 ± 0.04	9.05	-	-	189.41 ± 3.79	0.21 ± 0.02	-29.65 ± 1.36

Table 6.3. Results of MF experiments made with pH modification using a 0.20 μm flat-disc TiO_2 membrane. The parameters are the same than those explained in Table 6.2 caption.

1st stage (total recirculation mode)

Exp	SDS/A	$C_{A\text{ eq}}$ (mol/m ³)	P_A	$EE_{A\text{ eq}}$ (%)	K_a (min ⁻¹)	R^2	$C_{\text{SDS eq}} \times 10^2$ (mol/m ³)	$SDS_{(\text{NS})}$ (%)	$SDS_{(\text{m})}$ (%)
8 A	0.010	7.34 ± 0.13	0.51	31.43	0.1085	0.99	0.29 ± 0.01	96.01	1.01
8 B	0.010	7.38 ± 0.14	0.41	27.80	0.1048	0.99	0.40 ± 0.03	95.61	1.13
9 A	0.010	7.90 ± 0.01	0.42	27.56	0.0984	0.98	0.14 ± 0.01	96.64	3.19
9 B	0.010	8.18 ± 0.08	0.27	18.81	0.0732	0.98	0.28 ± 0.02	95.35	3.40
10 A	0.010	7.90 ± 0.05	0.38	25.07	0.0866	0.99	0.15 ± 0.01	95.58	3.96
10 B	0.010	7.94 ± 0.05	0.28	20.47	0.1018	0.99	0.28 ± 0.01	94.53	4.10
11 A	0.010	8.74 ± 0.05	0.24	18.09	0.1057	0.98	0.14 ± 0.01	94.89	4.52
11 B	0.010	8.75 ± 0.03	0.18	14.68	0.1059	0.98	0.29 ± 0.01	94.01	5.11
12 A	0.010	9.21 ± 0.03	0.17	13.61	0.1022	0.98	0.15 ± 0.02	93.84	5.48
12 B	0.010	9.22 ± 0.07	0.11	9.37	0.0962	0.99	0.29 ± 0.02	92.97	5.87
13 A	0.010	9.87 ± 0.08	-	0.00	-	-	1.46 ± 0.12	-	58.11
13 B	0.010	9.88 ± 0.07	-	0.00	-	-	2.17 ± 0.09	-	61.08

2nd stage (concentration mode)

Exp	VCR	J_p (L/h m ²)	$C_{A(p)}$ (mol/m ³)	$X_{A(\text{NS})}$ (%)	$C_{\text{SDS}(p)} \times 10^2$ (mol/m ³)	$X_{\text{SDS}(\text{NS})}$ (%)	$\text{Size}_{(r)}$ (nm)	$\text{PDI}_{(r)}$	$Z\text{-pot}_{(r)}$ (mV)
8 A	3.04	26.65 ± 7.13	7.17 ± 0.03	57.92	0.27 ± 0.02	99.43	348.83 ± 12.58	0.59 ± 0.07	-27.72 ± 1.94
8 B	2.24	23.45 ± 6.64	7.37 ± 0.03	44.77	0.99 ± 0.06	99.18	237.77 ± 11.98	0.29 ± 0.06	-27.70 ± 2.48
9 A	1.89	23.33 ± 2.69	7.95 ± 0.05	42.20	0.14 ± 0.07	99.65	251.57 ± 06.14	0.37 ± 0.03	-28.70 ± 3.33
9 B	2.24	22.30 ± 1.47	8.09 ± 0.03	35.94	0.30 ± 0.02	99.75	295.60 ± 10.76	0.27 ± 0.06	-39.60 ± 2.46
10 A	1.93	22.88 ± 2.85	7.95 ± 0.05	39.11	0.14 ± 0.01	99.66	322.20 ± 04.94	0.45 ± 0.05	-29.70 ± 6.13
10 B	2.27	21.31 ± 2.85	7.92 ± 0.05	37.52	0.32 ± 0.02	99.73	316.8 ± 09.39	0.45 ± 0.05	-23.70 ± 1.67
11 A	2.25	21.31 ± 5.52	8.74 ± 0.09	31.96	0.14 ± 0.04	99.66	259.67 ± 12.58	0.20 ± 0.13	-25.80 ± 7.60
11 B	1.92	22.38 ± 3.18	8.67 ± 0.02	24.34	0.14 ± 0.07	99.88	289.33 ± 07.57	0.29 ± 0.01	-24.25 ± 5.63
12 A	1.63	19.19 ± 4.29	9.20 ± 0.02	20.21	0.30 ± 0.03	99.32	217.57 ± 03.67	0.29 ± 0.09	-31.20 ± 1.59
12 B	1.64	18.12 ± 5.08	9.21 ± 0.03	14.48	0.16 ± 0.02	99.61	225.83 ± 01.50	0.36 ± 0.09	-39.61 ± 6.08
13 A	1.72	19.19 ± 3.77	9.89 ± 0.03	-	1.92 ± 0.12	-	-	-	-8.23 ± 3.04
13 B	1.65	17.05 ± 1.57	9.90 ± 0.04	-	2.47 ± 0.34	-	-	-	-8.40 ± 2.10

6.2.4.3. Lactic acid back-extraction

This experiment was designed to study the release rate of the lactic acid extracted in the niosomes. First, the extraction of lactic acid was carried out. The feed consisted of a 400 cm^3 aqueous solution containing 10 mol/m^3 of lactic acid to which were added 10 cm^3 of dispersed phase formulated with Span 80 (20 mol/m^3) and SDS (4 mol/m^3). The system was kept under stirring for 60 minutes at 20°C to reach the equilibrium. Subsequently, the dispersion was fed to the membrane at $\text{TMP} = 0.3\text{ bar}$ for 15 min working in total recirculation mode before sodium hydroxide was added to the feed tank until reaching a pH of 12.2. From that moment, membrane worked in total recirculation mode and permeate samples were collected during 3 h for lactic acid concentration determination. The particle size and zeta potential were measured in permeates and retentates at both pH, under the extraction and stripping equilibrium conditions.

6.2.4.4. Lactic acid extraction by a two-step concentration process

In order to increase the lactic acid extraction process efficiency, a two-step extraction experiment was conducted using the permeate of the first step as the feed of the second step. The first step was carried out following the same procedure as previously described, that is the feed containing 400 cm^3 of 10 mol/m^3 lactic acid solution to which 10 cm^3 of dispersed phase was added, was firstly kept under stirring for 60 min at 20°C to achieve the equilibrium, and then it was concentrated up to a VCR about 2. Subsequently, the permeate was contacted with a fresh dispersed phase keeping the same volume proportion (about the half of the dispersed phase volume used in the first step), maintained for 60 min until equilibrium and then concentrated 3.75 times. The niosomal formulation added was Span 80 (20 mol/m^3) and SDS (4 mol/m^3). Lactic acid concentration was measured throughout the process.

6.2.5. *Analytical methods*

6.2.5.1. Lactic acid measurement

Lactic acid concentration was measured in the initial aqueous solutions and permeates, both without niosomes. In experiments performed at natural pH (about 2.8), the lactic acid concentration was analyzed by acid-base titration with NaOH. In experiments with pH modification (experiment series 8-13, in Table 6.1), lactic acid concentration was determined by high performance liquid chromatography using a HPLC Shimadzu with a SCL-10A VP controller, LC-10AD VP pump, and SPD-M20A diode array. A reverse phase column ACE 5C18 (ACE HPLC

columns) and a UV-vis detector at 216 nm were used. The mobile phase was a pH 2 aqueous solution of 0.2 vol% phosphoric acid and 0.16 wt% potassium dihydrogen phosphate with a flow rate of 1.2 mL/min. Samples were prepared using 1.5 cm³ of sample and 30 µL of a 500 mg/L maleic acid solution which was used as internal standard.; they were measured by triplicate and the analytical error was lower than ± 0.001 mol/m³. Calibration was performed using lactic acid standards with concentrations between 1 and 16 mol/m³. The detection limit of the method was 0.005 mol/m³. Cleaning of the column was carried out by washing with deionized water for 30 min, and subsequently with a methanol-water solution (85/15 vol%) for 30 minutes.

6.2.5.2. Determination of free SDS concentration

SDS monomer concentration was determined by spectrophotometry at 615 nm with a Hitachi U-2000 spectrophotometer, according to the ethyl violet method [31]. The samples were measured in triplicate in the case of standards, and twice in the case of experimental samples. SDS concentration was measured in the final permeate and retentate after the concentration process (2nd stage). SDS was also measured in the dispersed phases. For this, a replica of the dispersed phase used in each experiment was properly diluted with water and measured, yielding more than 98% of SDS is linked to the niosomes in all formulations used in this work. In the same way, all dispersions were replicated twice in a thermostated tank to which were allowed to reach equilibrium, without membrane for one of the two replicas, and with membrane for the other one, operating in total recycle mode and the same conditions than that used in the experiments. Samples of the two equilibrium dispersions were collected and SDS monomer concentrations were measured.

The degree of SDS linked to niosomes ($SDS_{(NS)}$) and SDS adsorbed in the membrane ($SDS_{(m)}$) were calculated by the following mass balances:

$$SDS_{(NS)} = \frac{C_{SDS(d)}^0 V_{(d)}^0 - C_{SDS(F,bis)}(V_{(d)}^0 + V_{(w)}^0)}{C_{SDS(d)}^0 V_{(d)}^0} \quad (5)$$

$$SDS_{(m)} = \frac{C_{SDS(d)}^0 V_{(d)}^0 - C_{SDS(F)}(V_{(d)}^0 + V_{(w)}^0)}{C_{SDS(d)}^0 V_{(d)}^0} - SDS_{(NS)} = \frac{(C_{SDS(F,bis)} - C_{SDS(F)})(V_{(d)}^0 + V_{(w)}^0)}{C_{SDS(d)}^0 V_{(d)}^0} \quad (6)$$

where $C_{SDS(d)}^0$ and $V_{(d)}^0$ are the total SDS concentration and volume, respectively, of the dispersed phase added, $V_{(w)}^0$ is the initial continuous phase volume, $C_{SDS(F,bis)}$ and $C_{SDS(F)}$ are the equilibrium SDS monomer concentrations in the feed dispersions without membrane, and with membrane, respectively.

The degree of SDS that remained linked to the niosomes after the concentration stage with respect to the total amount present in the final retentate ($X_{\text{SDS(NS)}}$) was calculated using the same mass balance of Eq. (4) where $C_{\text{SDS(NS)}}$, calculated by mass balance from Eq. (5), and the experimental value of SDS concentration in permeate, $C_{\text{SDS(p)}}$, must be used instead $C_{\text{A(NS)}}$ and $C_{\text{A(p)}}$, respectively.

6.2.5.3. Particle size measurement

The particle size distribution, the mean hydrodynamic diameter and the polydispersity index (PDI) of the samples were measured by dynamic light scattering (DLS) using a Zetasizer Nano ZS apparatus (Malvern Instruments Ltd., UK). The apparatus was equipped with a He-Ne laser emitting at 633 nm and with a 4.0 mW power source. It was set for backscattering detection at a scattering angle of 173°. Samples (2 cm³) were diluted 1:100 to avoid multiple scattering effects and filtered with 0.45 µm Minisart RC 15 filters. Measurements were performed in DTS0012 square disposable polystyrene cells at 20 °C.

Three replicates, each of 20 runs, were performed for each sample. The values shown in the tables are the average value of the 3 replicates with the relative measurement error. The PDI is a dimensionless measure of the width of the size distribution ranging from 0 to 1, a higher value being indicative of a broader distribution of particle size [32].

6.2.5.4. Zeta potential measurement

Zeta potential measurements were conducted with the aforementioned Zetasizer Nano ZS apparatus, using the Laser Doppler Velocimetry technique. They were performed on the same sample previously prepared to measure the particle size, but using the appropriate DTS1061 disposable folded capillary cell equipped with electrodes to allow the passage of electric current and the movement of the particles according to their charge. Zeta potential is calculated using Henry's equation and the Smoluchowski approximation, which considers that the double layer thickness is much smaller than the particle size [33]. Six replicates of 11 measurements were performed for each sample at 20 °C. Figures and tables show average values of the 6 runs with the relative measurement error.

6.2.5.5. pH measurement

The pH was measured at 20 °C using a Crison GLP 22 pH-meter fitted with a Crison 52-02 glass pH electrode, with an error of ± 0.01 pH units.

6.2.5.6. Morphological analysis

Morphological analysis of niosomes was performed by negative staining transmission electron microscopy (NS-TEM), using a JEOL-2000 EX-II TEM operating at 160–180 kV, with an image resolution of 1 nm, located at the University of Oviedo (Spain). A drop of the selected niosome formulation was placed on a carbon-coated copper grid, and the sample excess was removed using a piece of filter paper. Then, a drop of phosphotungstic acid solution (2% w/v) was applied to the carbon grid and left for 2 min. Once the excess of staining agent was removed by absorbing with the filter paper, the sample was air-dried and the thin film of stained niosomes was observed by TEM.

6.3. Results and discussion

6.3.1. Membrane pore size and transmembrane pressure selection

Fig. 6.1 depicts the permeate flux obtained in the microfiltration tests of niosomes in water dispersions, using the three 0.14, 0.20 and 0.45 μm pore size membranes, under the conditions described in section 6.2.3.1. Niosomes were formulated with Span 80 (20 mol/m³) and SDS (4 mol/m³). The results reveal an initial permeate flux decrease, followed by a constant permeate flux for the 0.14 and 0.20 μm pore size membranes which is associated with concentration polarization; however, a greater flux was obtained with the 0.20 μm membrane, as a consequence of small differences in membrane permeabilities. Concentration polarization is caused by the accumulation of retained solutes such as surfactant monomers, micelles, and niosomes, on the membrane surface. Differently, 0.45 μm pore size membrane shows a progressive decline of permeate flux indicating fouling, maybe due to adsorption processes of surfactants inside its larger pores.

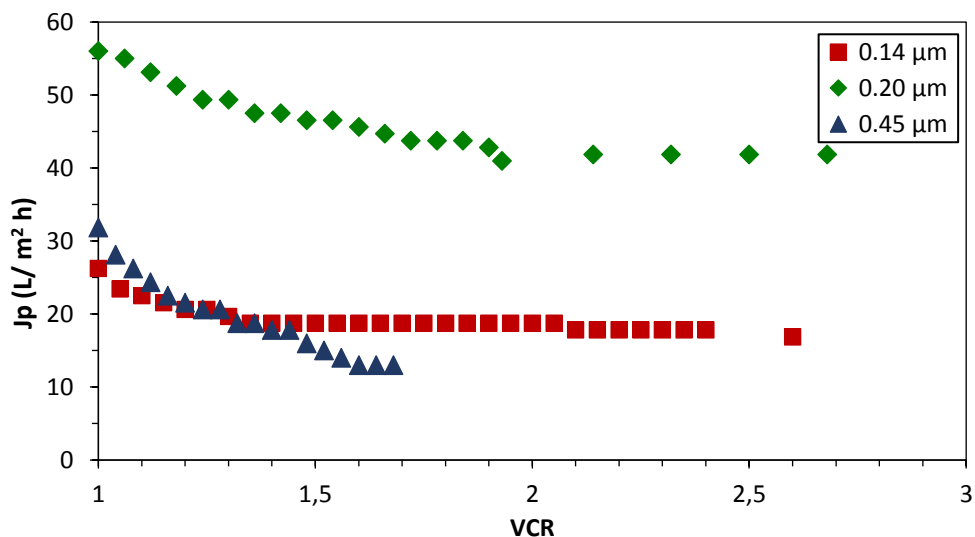


Figure 6.1. Variation of permeate flux with the volume concentration ratio (VCR) for microfiltration of niosomes in water dispersions using flat-disc ceramic membranes with different pore size. TMP = 0.3 bar, T = 20 °C, $V_d/V_w = 10/400$. Niosomes formulation: Span 80 (20 mol/m³) and SDS (4 mol/m³).

Particle size measurements in the water dispersions shown in Table 6.1 reveal the presence of niosomes with sizes ranging from 170 to 220 nm and PDI lower than 0.31 that were consistent with those obtained in a previous work [30]. Niosomes formation in the dispersed phase and morphology were confirmed by TEM measurements. Fig. 6.2 shows two negative stain micrographs for niosomes obtained by 5 min of ultrasounds on formulations of Span 80 (20 mol/m³) and SDS (4 mol/m³) in deionized water. Dark structures shown in these micrographs correspond to spherical niosomes, with diameters ranging from 160 to 200 nm, which agrees with sizes measured by DLS shown in Table 6.1. Size values obtained in permeates indicated the absence of particles in them.

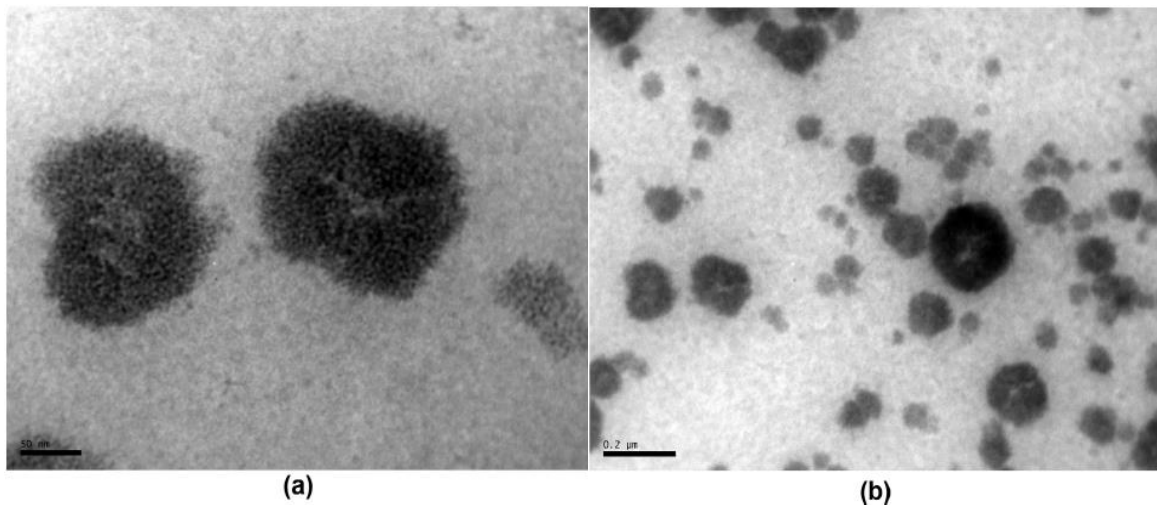


Figure 6.2. TEM micrographs of niosomes obtained by ultrasonication (5 min) of Span 80 (20 mol/m³) and SDS (4 mol/m³) in aqueous solution. Scale bars: (a) 50 nm, and (b) 0.2 lm.

Zeta potentials of dispersions shown in Table 6.1 are between -45 mV and -35 mV indicating the presence of negatively charged particles. Zeta potential values of permeates (not shown) were similar to those obtained for water ($\approx 0 \pm 6$ mV) corroborating the absence of particles in permeates. The pH of the niosomes in water dispersions was slightly higher than 6, superior to the isoelectric point (IEP) of the membrane which is about 6.4.1 in demineralized water [34], therefore the membrane surface is negatively charged and the electrostatic repulsions with the niosomes also negatively charged may explain the results of 100% niosome rejections obtained with the three membranes. However, the higher flux obtained with the 0.20 μ m pore size membrane, as shown in Fig. 6.1, was the reason to select this membrane for the following experiments.

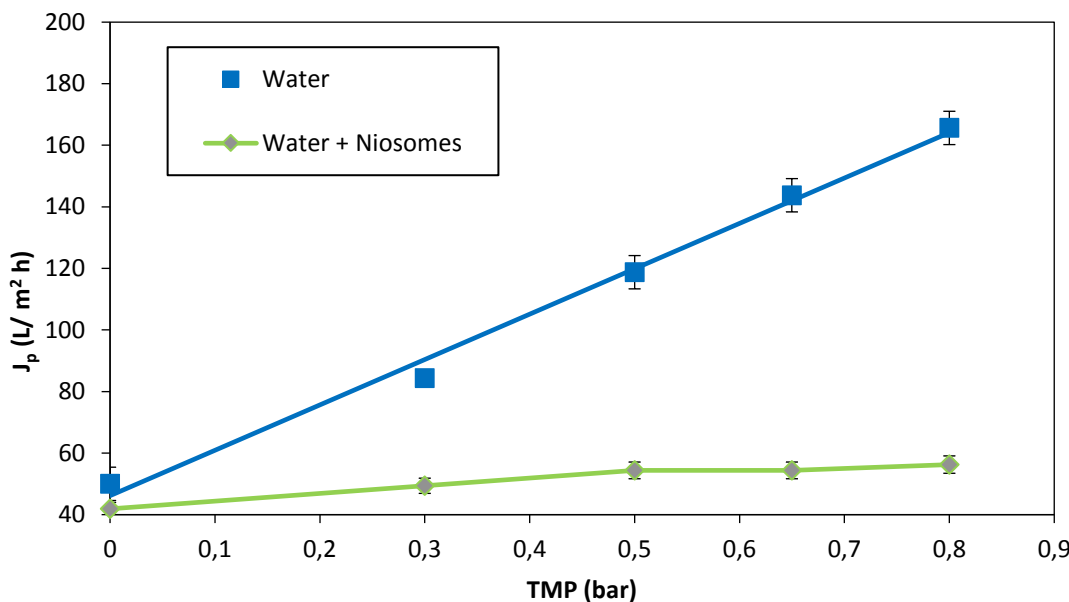


Figure 6.3. Permeate flux variation with the TMP for niosomes in water dispersions using the $0.20 \mu\text{m}$ pore size membrane. $T = 20^\circ\text{C}$, $V_d/V_w = 10/400$. Niosomes formulation: Span 80 (20 mol/m³) and SDS (4 mol/m³).

Fig. 6.3 shows the permeate flux values versus the TMP for pure water and niosomes in water dispersion using the $0.20 \mu\text{m}$ membrane. The experimental conditions are described in section 6.2.3.1. A lower increase in permeate flux was observed as TMP increased for MF of the niosomes in water dispersion, due to the formation of a concentration polarization layer, mainly consisting of free surfactant monomers that can reach micellization conditions. The applied pressure increases the concentration of species on the membrane surface, and also the resistance to the permeation. A pressure increase causes the compression of the species deposited layer and the flux-pressure relationship becomes non-linear [35], which indicates the occurrence of concentration polarization phenomenon. A pronounced curvature is observed in Fig. 6.3, achieving a plateau when the pressure is around 0.5 bar. A TMP of 0.3 bar, which provides values close to the limiting flux, was selected for the following experiments. The accumulation of the micelles on the membrane can continue until a gel layer (with C_g concentration) is formed yielding a zero permeate flux. For the anionic surfactant SDS, C_g has been reported to be 737 and 708 mol/m³ for ultrafiltration using 1 and 5 kDa cellulose acetate membranes, respectively [36]. The low SDS concentration used in this work made it unlikely that gelation conditions were met. Furthermore, taking into account the CMC value of SDS [15,16] and the low HLB of Span 80 [23,37], it is highly unlikely the presence of Span 80 monomers in the dispersion, but not of SDS monomers that may bind to the membrane surface and pore walls through its polar head increasing the membrane hydrophobicity and reducing the permeate flux.

6.3.2. Lactic acid extraction with niosomes

6.3.2.1. Effect of the SDS concentration in the formulation of niosomes

Fig. 6.4 compares the lactic acid extraction kinetic curves in experiments with 400 cm³ of aqueous solutions with 10 mol/m³ of lactic acid at its natural pH, to which 10 cm³ of a dispersed phase containing niosomes formulated with Span 80 (20 mol/m³) and different SDS concentration (0, 2 and 4 mol/m³) (experiments 3A, 4A and 5A in Table 6.1) were added. Experiments were performed as described in section 6.2.4.1. Extraction degrees over time were calculated by Eq. (1). For comparison, lactic acid extraction degrees in absence of niosomes (experiments 1 and 2 in Table 6.1) are also depicted in Fig. 6.4 showing, as it was expected, that no extraction occurred in the absence of niosomes. Fig. 6.4 also shows that equilibrium was achieved after 30-40 minutes, but significant differences between the systems studied were observed. The highest extraction degree was achieved with the niosomal formulation of 4 mol/m³ SDS, being much better than the other formulations. As it was observed in a previous work [30], the SDS is associated with Span 80 in the bilayer of niosomes through links of hydrophobic character and acts as a modifier of the niosomal bilayer affecting in greater or lesser extent the entrapment of the lactic acid by these structures. The lactic acid presence in these experiments leads to pHs around 2.80, that is lower than its pKa (pKa = 3.86 for lactic acid [38]) and therefore the protonated form of the lactic acid is the main species. Under these conditions, the increased lactic acid extraction of 4 mol/m³ SDS niosomal formulation may occur due to the complex formation at the external interface of niosomes by hydrogen bonds between the SDS adsorbed in the niosome bilayer and the lactic acid protonated species [30]. This extraction mechanism could explain the lower extraction obtained by niosomes formulated with 2 mol/m³ of SDS, due to the lower capacity to complex formation with the lactic acid. Besides, a similar equilibrium extraction degree of lactic acid for system containing niosomes without SDS and with 2 mol/m³ SDS was obtained. Results of Fig. 6.4 reveal that the synergistic effect of the lactic acid extraction depends on the niosomal formulation.

Kinetic data were fitted to the following mass transfer equation:

$$-\frac{dC_{A(p)t}}{dt} = K_a \left(C_{A(p)t} - C_{A(p)eq} \right) \quad (7)$$

where K_a is the overall volumetric mass-transfer coefficient referred to the aqueous phase, and $C_{A(p)eq}$ represents the lactic acid concentration of the continuous phase in equilibrium with the dispersed phase. Integration of Eq. (7) between the initial ($C_{A(p)t=0}$) and equilibrium conditions

Lactic acid recovery by microfiltration using niosomes as extraction agents

$(C_{A(p)eq})$ allows to obtain K_a values as the slope of the linear equation $\ln((C_{A(p)t} - C_{A(p)eq})/(C_{A(p)t=0} - C_{A(p)eq}))$ versus time for each system. Values of K_a , along with the coefficient of determination (R^2) are shown in Table 6.2. Kinetic curves calculated with the K_a coefficients are shown in Fig. 6.4 where good agreement between the calculated (lines) and experimental (symbols) values is observed.

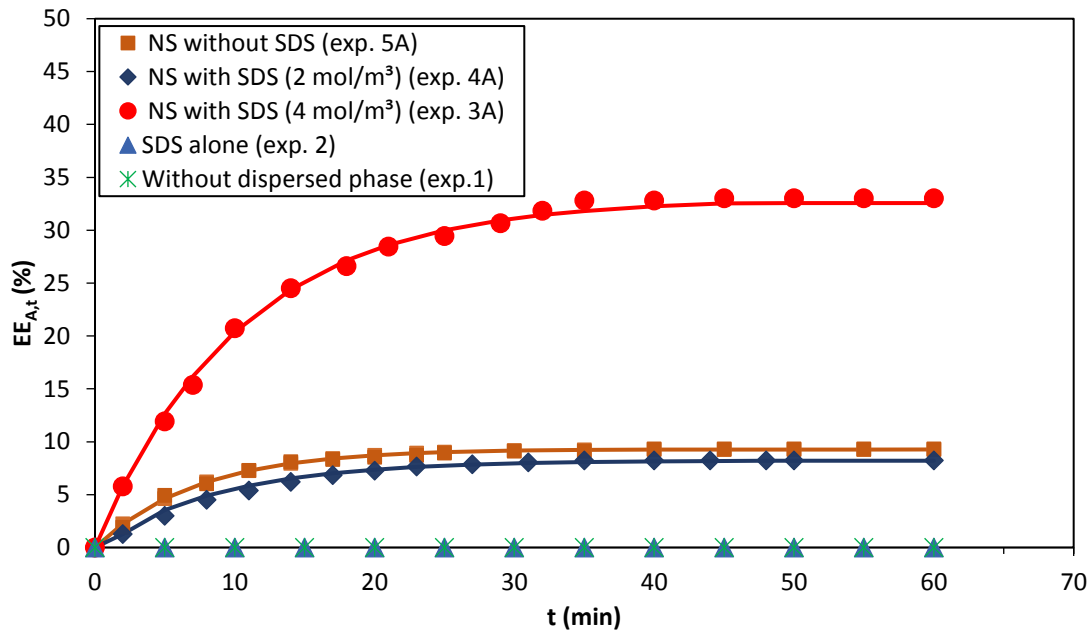


Figure 6.4. Effect of niosomes formulation: Span 80 (20 mol/m³) and SDS (0, 2, and 4 mol/m³) on the lactic acid extraction kinetics. Symbols: experimental values. Lines: calculated values.

$TMP = 0.3$ bar, $T = 20$ °C, 10 mol/m³ initial lactic acid concentration, $V_d/V_w = 10/400$.

6.3.2.2. Effect of the volume of the dispersed phase

Fig. 6.5 depicts the kinetic curves obtained in experiment series 3, 4 and 5 of Table 6.1, where different volumes of the dispersed phase formulated with Span 80 (20 mol/m³) and SDS (0, 2 and 4 mol/m³) were added to 400 cm³ of aqueous solution with 10 mol/m³ of lactic acid. It is observed for all formulations a significant decrease in the lactic acid extraction degree as the volume of dispersed phase increases. Equilibrium extraction degrees of lactic acid ($EE_{A,eq}$), and equilibrium distribution coefficients (P_A) are shown in Table 6.2, where the greatest value corresponds to the experiment with 10 cm³ of dispersed phase. Kinetic curves calculated by Eq. (7) and K_a values shown in Table 6.2 are also depicted in Fig. 6.5, where good agreement is observed.

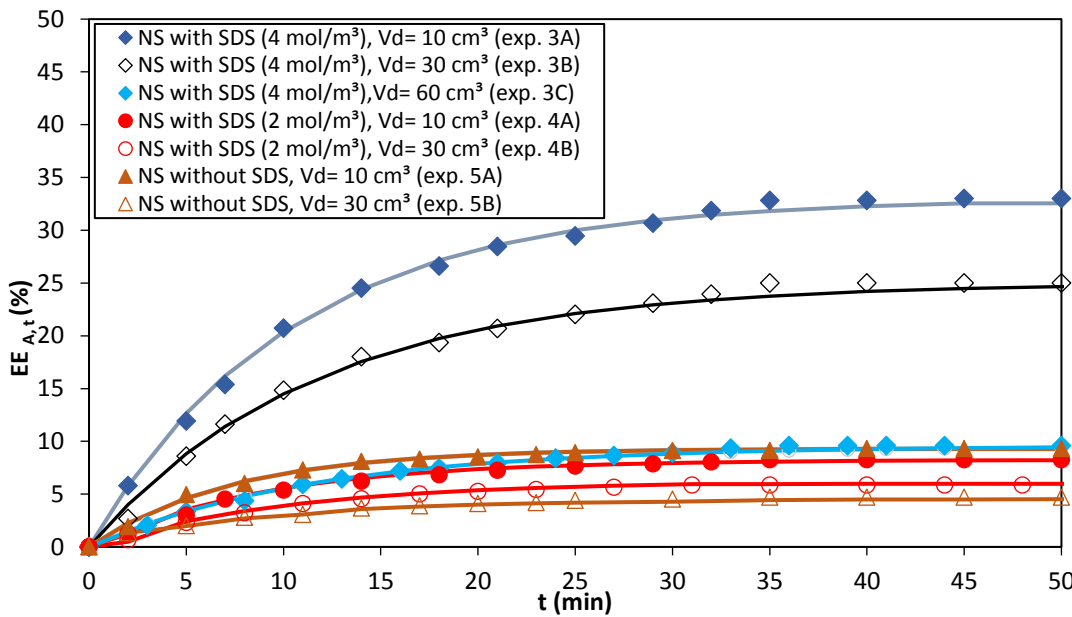


Figure 6.5. Effect of the dispersed phase volume (V_d) added to the feed on the lactic acid extraction kinetics. Symbols: experimental values. Lines: calculated values. TMP = 0.3 bar, $T = 20\text{ }^\circ\text{C}$, 10 mol/m³ initial lactic acid concentration.

Taking into account that the dispersion pHs are slightly higher than the acidic dissociation constant of SDS (pKa is around 2.3 for SDS [39]), the $\text{EE}_{\text{A},\text{eq}}$ decrease as increasing the volume of dispersed phase added to the feed solution can be explained as a consequence of the competition between the sodium counterions of the SDS dissociated form and lactic acid protonated species, resulting that the excess of sodium counterions is unfavorable for the lactic acid extraction by hydrogen bonds.

6.3.2.3. Effect of the lactic acid concentration in feed

The effect of the lactic acid concentration in the continuous phase is also relevant on the extraction kinetics and the extraction capacity of niosomes. Fig. 6.6 compares systems with 5, 10 and 20 mol/m³ of lactic acid in the continuous phase and two dispersed phase volumes (10 and 30 cm³) of identical formulation: Span 80 (20 mol/m³) and SDS (4 mol/m³) (experiments A and B in series 3, 6 and 7 in Table 6.1).

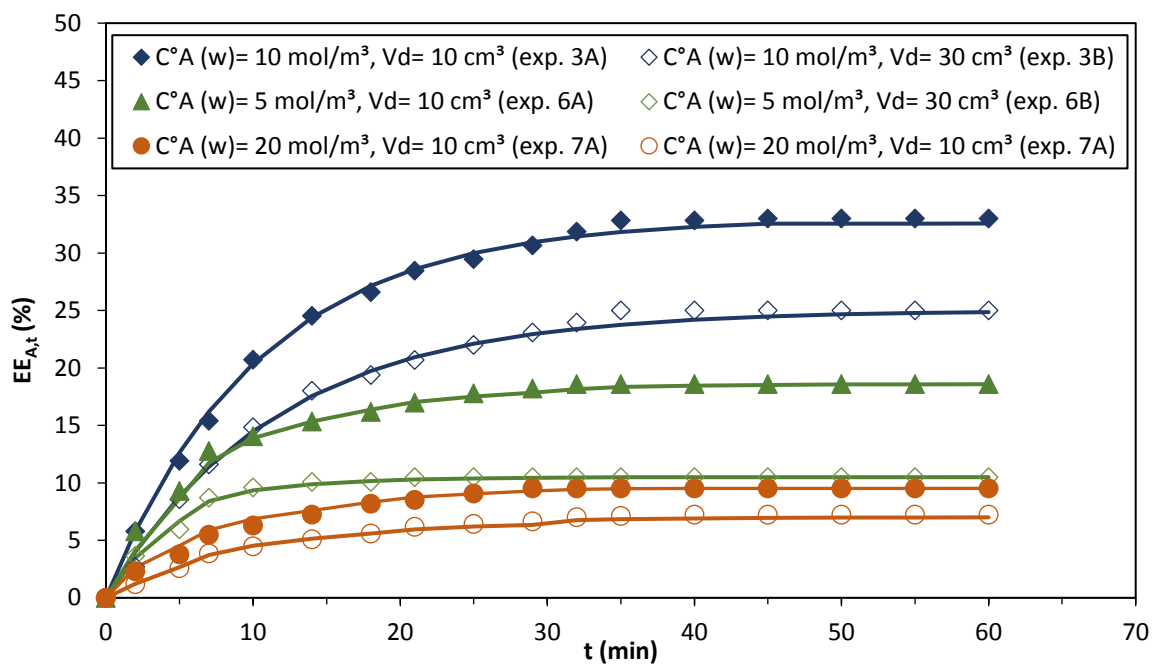


Figure 6.6. Effect of initial lactic acid concentration in the feed tank on the lactic acid extraction kinetics. Symbols: experimental values. Lines: calculated values. TMP = 0.3 bar, T = 20 °C.

It is observed that the greatest extraction degree was obtained for the system of 10 mol/m³ of lactic acid concentration (experiment 3A). Conversely, systems with 5 and 20 mol/m³ of lactic acid reached significantly lower extraction degrees. These results reveal that there is an optimum SDS to lactic acid molar ratio (SDS/A). In our case, into the range of SDS and lactic acid concentrations studied, such optimum corresponds to a SDS/A ratio of 0.010.

Table 6.2 shows the equilibrium (P_A and $EE_{A,eq}$) and kinetic (K_a) parameters for systems made at natural pH. It is observed in Table 6.2 that P_A and $EE_{A,eq}$ are lower for SDS/A ratio values far from 0.010. Several authors [40–42] studied the recovery of metals by micellar-enhanced ultrafiltration (MEUF) using SDS as surfactant. They reported that the surfactant concentration and the surfactant to metal molar ratio (SDS/M) are the two important control parameters for metal removal efficiency. At their regard, the surfactant concentration has to be higher than the CMC of the surfactant, and SDS/M ratio has to be higher than 5. Such conditions are very different from those required in the niosomal extraction of lactic acid made in this work, disclosing that the SDS concentration used in this work is much lower than its CMC, and the optimum SDS/A ratio is also much lower than 5.

Very different results were also obtained in a previous work [16] for the recovery of lactic acid and citric acid from aqueous solutions by MEUF using SDS. In that work, the acid retention depended upon the SDS concentration, however it was unaffected by the initial acid concentration or the presence of another acid. The best results were obtained with 80 mol/m³ of SDS in the feed solution at natural pH, greater than approximately 150 times the SDS concentration used in this study, with lactic acid extraction degrees of 48% by MEUF, and 33% in experiment 3A of this work.

6.3.2.4. Effect of pH

The effect of pH was studied in experiment series 8–13 of Table 6.1 where kinetic studies were carried out as described in section 6.2.4.1. Niosome formulation was Span 80 (20 mol/m³) and SDS (4 mol/m³), the concentration of lactic acid in the continuous phase was 10 mol/m³ for all experiments, and the volume of the dispersed phase was 10 and 30 cm³. The pH was modified by the addition of HCl 0.1N (experiment series 8) or NaOH 0.1 N (experiment series 9–13). The extraction kinetic curves are shown in Fig. 6.7 where good agreement between the experimental (symbols) and calculated (lines) values is observed.

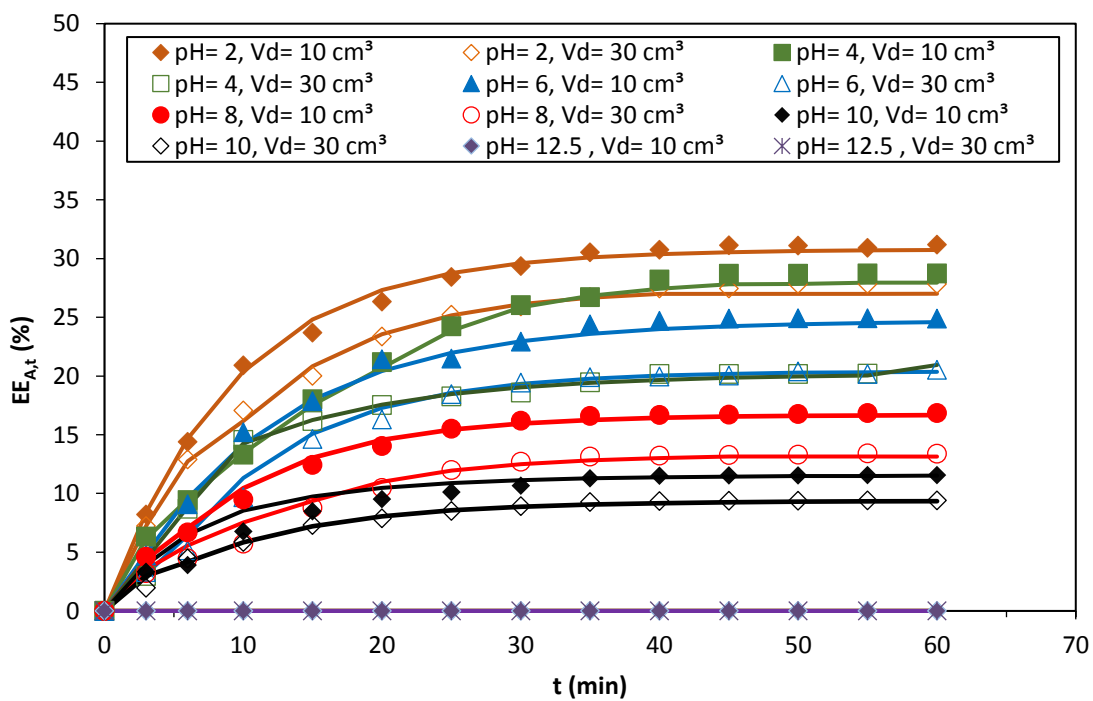


Figure 6.7. Effect of the feed pH on the lactic acid extraction kinetics. Symbols: experimental values. Lines: calculated values. TMP = 0.3 bar, T = 20 °C, 10 mol/m³ initial lactic acid concentration.

Kinetic and equilibrium parameters are shown in Table 6.3. A decrease in the equilibrium data of $EE_{A,eq}$ and P_A was obtained as pH increased. As it was previously observed, lower extraction degrees were obtained with 30 cm^3 of the dispersed phase. Systems at pH 12.2 (experiments 13A and 13B) showed absence of lactic acid extraction.

Besides, as depicted in Table 6.3, experiments at pH 12.2 showed error in the particle size determination due to the very few particles counted by the equipment. Equilibrium dispersions of these experiments at pH 12.2 showed very low zeta potential absolute values, indicating the breakup of the niosomes. This fact suggests that these conditions can be used in back-extraction process for the recovery of lactic acid entrapped in niosomes, studied in section 6.3.4 of this work.

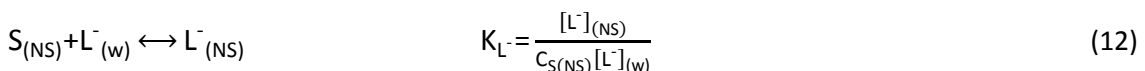
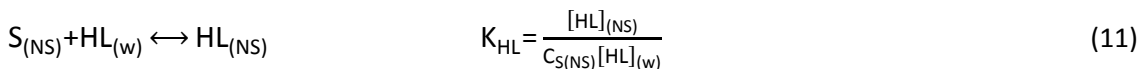
As the lactic acid has a pH-dependent dissociation in aqueous phase, the concentration of protonated ($[HL]$) and anionic ($[L^-]$) species of lactic acid were calculated by Eqs. (8-10). Lactic acid concentrations in the continuous phase and pH, both at the equilibrium conditions, are reported in Table 6.4.

$$C_{A(w)} = [L^-]_{(w)} + [HL]_{(w)} \quad (8)$$

$$[HL]_{(w)} = \frac{C_{A(w)}}{1+10^{(pH-pka)}} \quad (9)$$

$$[L^-]_{(w)} = \frac{C_{A(w)}}{1+10^{(pka-pH)}} \quad (10)$$

The affinity of the niosomes by the different lactic acid species can be represented by the following equilibrium equations [15,43]:



where the subscripts (NS) and (w) refer to the niosomal and continuous phases at equilibrium conditions, respectively, and $C_{S(NS)}$ is the total surfactant (Span 80 and SDS) concentration in the feed dispersion (0.5856 and 1.6741 mol/m^3 for 10 and 30 cm^3 of the dispersed phase added, respectively).

Taking into account that the total concentration of lactic acid in the dispersed phase is the sum of the concentration of both species, $[HL]_{(NS)}$ and $[L^-]_{(NS)}$, the replacement of Eqs. (11) and (12) into Eq. (1) leads to the following expression:

$$\frac{EE_{A,eq}}{C_{S(NS)}V_{(F)eq}} = K_{HL} [HL]_{(w)} + K_{L^-} [L^-]_{(w)} \quad (13)$$

The equilibrium coefficients K_{HL} and K_{L^-} were determined by fitting of the experimental data (shown in Table 6.4) to the Eq. (13) using the Marquardt algorithm and the MicroMath Research Scientist software. K_{HL} and K_{L^-} values are shown in Table 6.4, along with the coefficient of determination (R^2).

Table 6.4. Equilibrium values of pH and lactic acid concentration $C_{A(w) eq}$ in the continuous phase (permeate), being $[HL]_{(w) eq}$ and $[L^-]_{(w) eq}$ the relative concentrations of each species in the aqueous phase at the equilibrium conditions. K_{HL} and K_{L^-} are the equilibrium coefficients of each species calculated by Eq. (13), and R^2 the coefficient of determination.

Exp.	pH _{eq}	$C_{A(w) eq}$ (mol/m ³)	$[HL]_{(w) eq}$ (%)	$[L^-]_{(w) eq}$ (%)	K_{HL} (mol/m ³) ⁻¹	K_{L^-} (mol/m ³) ⁻¹	R^2	K_{HL}/K_{L^-}
<i>Volume of dispersed phase = 10 cm³</i>								
8A	2.09	7.34	98.34	1.66	0.91 ± 0.10	0.41 ± 0.01	0.98	2.22
9A	4.04	7.90	39.97	60.03				
10A	6.15	7.90	0.51	99.49				
11A	7.95	8.75	0.01	99.99				
12A	9.63	9.20	0.00	100				
<i>Volume of dispersed phase = 30 cm³</i>								
8B	2.08	7.38	98.38	1.62	0.24 ± 0.02	0.11 ± 0.01	0.99	2.18
9B	4.05	8.18	39.05	60.95				
10B	6.11	7.94	0.56	99.44				
11B	7.91	8.75	0.01	99.99				
12B	9.68	9.21	0.00	100				

It can be observed that K_{HL} and K_{L^-} values depend on the dispersed phase volume, being significantly higher in the case of lower concentration of niosomes (10 cm³ of dispersed phase); however, the K_{HL}/K_{L^-} ratio is slightly higher than 2 in both cases, indicating that the affinity of the SDS-modified niosomes to extract the lactic acid protonated species (HL) is at least twice than their affinity for the anionic species (L^-).

The results of Fig. 6.7 can be explained by considering that at $\text{pH} > \text{pKa}$ of lactic acid, the lactic acid extraction efficiency decreases as a consequence of the lower concentration of lactic acid protonated species that are able to bind to the niosomes by hydrogen bonds with the SDS adsorbed in them. Besides, a decreasing degree of SDS linked to niosomes ($\text{SDS}_{(\text{NS})}$) as the pH increases is observed in Table 6.3, indicating some SDS desorption. Conversely, at pH 2 (experiment 8A) an excess of hydrogen cations are present in the medium and formation of hydrogen bonds between the SDS adsorbed in niosome surface and lactic acid protonated species is favored. In this regard, comparison of kinetic and equilibrium parameters shown in Tables 6.2 and 6.3 between the experiment 3A (at natural pH 2.8) and 8A (at pH about 2.1 modified with HCl addition) hardly show differences. These results justify that the extraction process with niosomes must be done at a feed pH lower than the pKa of lactic acid.

6.3.3. Effect of the feed composition on the membrane behavior during the concentration stage

In the 2nd stage described in section 6.2.4.2, the MF experiments were performed in concentration mode, after the equilibrium between the continuous and dispersed phases was reached, and the permeate flux was measured over time until a certain VCR was obtained. Fig. 6.8 shows the permeate flux in experiments made at natural pH with 10 cm³ of dispersed phase. No differences between deionized water flux and permeate flux for lactic acid aqueous solution without dispersed phase (experiment 1 in Table 6.1) is observed.

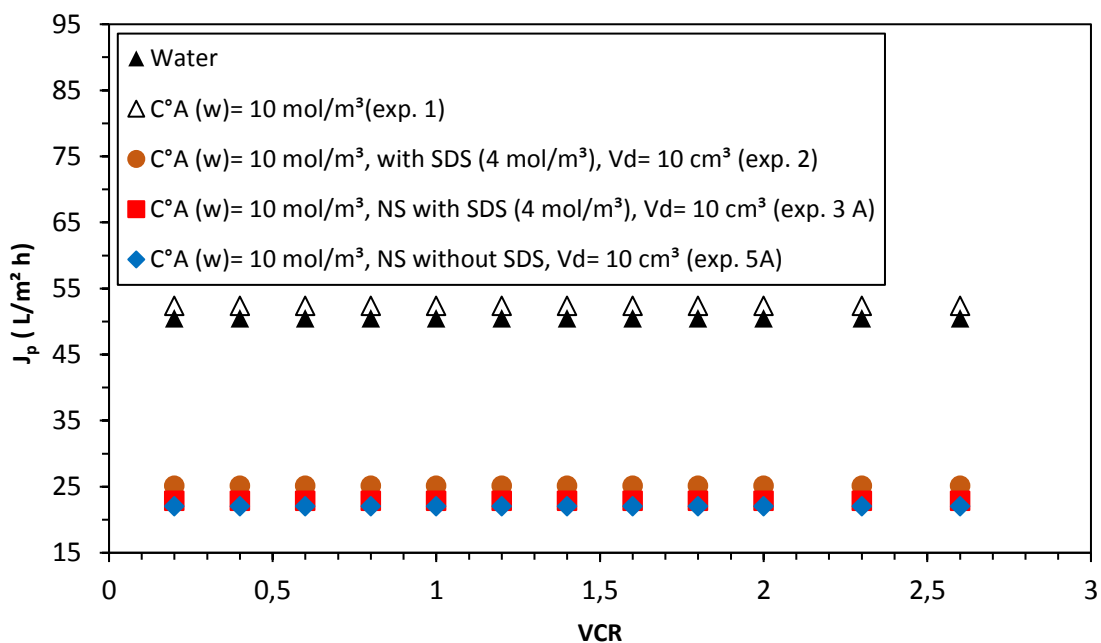


Figure 6.8. Permeate flux vs. volume concentration ratio (VCR) during the concentration stage in experiments at natural pH. TMP = 0.3 bar, T = 20 °C.

For all systems with dispersed phase it is observed that the permeate flux remains constant indicating no membrane fouling; however, permeate flux values lower than that of water were obtained due to concentration polarization phenomena. The pH of these experiments was about 2.8 (Table 6.1), and electrostatic interactions between the negatively charged niosomes, as indicate the negative zeta potential values reported in Table 6.2, and the positively charged membrane surface occur. The pH is slightly higher than the pKa of the SDS, and interactions between the SDS monomer anionic species and the membrane are also favored. As shown in Fig. 6.8, the permeate flux in experiment 2, where only SDS surfactant was used as dispersed phase, was slightly higher than the obtained in experiments 5A and 3A, where niosomes without and with SDS were used, indicating that both SDS monomers and niosomes contribute to the concentration polarization layer. The permeate flux decrease when the dispersed phase volume increased, as shown in Table 6.2, reveals a more severe concentration polarization that can be attributed to the increased concentration of both species, niosomes and SDS monomers, in the stagnant layer. Values of the SDS fraction linked to the niosomes ($SDS_{(NS)}$), and SDS adsorbed on the membrane ($SDS_{(m)}$), calculated as described in section 6.2.5.2., are shown in Table 6.2. It is observed that 94-96% of the SDS added in the dispersed phase is linked to niosomes at the equilibrium conditions, and 2-3% was adsorbed in the membrane or in the concentration polarization layer, being partially responsible of flux decline. The mass balance error, considering the SDS fraction linked to the niosomes, the SDS monomers fraction collected in permeate

samples during the first stage, and the SDS fraction analyzed in both, the final permeate (shown in Table 6.2) and final retentate (same value than the final permeate) after the concentration stage, was lower than 1.5%.

Particle size values in the equilibrium dispersion (not shown) were practically identical to those obtained in the final retentate after concentration (shown in Table 6.2), indicating that the size of the niosomes is maintained throughout the concentration process. This fact suggests that the load of lactic acid extracted in the niosomes was kept during the concentration stage, and consequently also the amount of SDS linked to the niosomes, which justifies the validity of Eq. (4) and $X_{A(NS)}$ and $X_{SDS(NS)}$ values provided in Table 6.2. The best result was obtained for systems at pH 2 and SDS/A ratio of 0.010 (experiment 3A), where $X_{A(NS)} = 54.33\%$ and $X_{SDS(NS)} = 99.41\%$ for a VCR = 2.31 was obtained, with a constant permeate flux of 26 L/m² h.

Zeta potentials in permeates were very low (about -8 mV) corroborating the absence of niosomes in permeates, which indicate that 100% niosomes rejection was kept through the concentration stage. However, zeta potentials in the final retentates (shown in Table 6.2) were somewhat lower than those in the equilibrium feed, before the concentration stage (not shown), indicating a slightly increased instability due to the greater concentration of particles in suspension.

Fig. 6.9 depicts the permeate flux obtained during the concentration stage for systems with pH modification and 10 cm³ added of an identical dispersed phase. It is observed a lowering flux as the pH increases, which indicates a more severe concentration polarization. In this regard, it must be considered that the sodium cations addition to increase the dispersion pH partially neutralizes the negative charge of the membrane when the pH is higher than 4.1 (the IEP of the membrane), facilitating the accumulation of species on the membrane surface. Furthermore, the increased $SDS_{(m)}$ values shown in Table 6.3 as the pH increases indicate that SDS monomers that remain free in dispersion (not linked to the niosomes) are the main responsible for the permeate flux decline above the isoelectric point of the membrane.

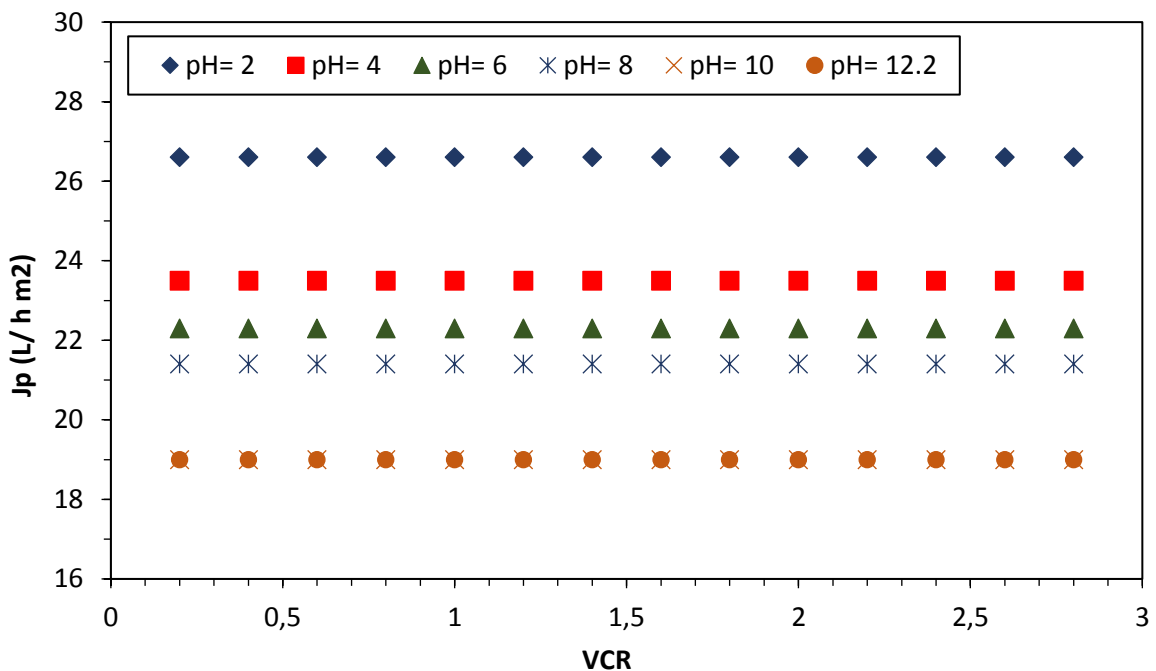


Figure 6.9. Permeate flux vs. volume concentration ratio (VCR) during the concentration stage in experiments with feed pH modification. TMP = 0.3 bar, T = 20 °C, 10 mol/m³ initial lactic acid concentration, $V_d/V_w = 10/400$.

At pH 12.2 (experiments 13A and 13B) permeates and retentates yielded erroneous particle size measurement values (due to a very few particles counting), which indicates the absence of niosomes. The low zeta potential absolute values of these retentates corroborate the breakup of the niosomes at pH > 12. This fact is consistent with the absence of lactic acid extraction shown in Fig. 6.7 for systems at pH 12.2. Besides, the high fractions of SDS monomers associated to the membrane ($SDS_{(m)}$ of 58% and 61% in Table 6.3) are consistent with the lowest fluxes obtained during the concentration stage. As the breaking of niosomes was tested, the mass balance of Eq. (5) applied to systems 13A and 13B yielded that a 27% and 31%, respectively, of SDS was forming SDS–Span 80 mixed micelles, instead of niosomes, dispersed in solution.

6.3.4. Lactic acid back-extraction process

Based on the results obtained at pH 12.2, the lactic acid back-extraction kinetic was studied at this pH. After the equilibrium with the dispersed phase at natural pH was reached, the pH was modified by addition of NaOH up to pH 12.2 following the procedure described in section 6.2.4.3.

Lactic acid recovery by microfiltration using niosomes as extraction agents

The kinetic data for the back-extraction process were fitted to the following mass transfer equation:

$$\frac{dC_{A(p)t}}{dt} = K_a b \left(C_{A(p)eq} - C_{A(p)t} \right) \quad (14)$$

where $K_a b$ is the overall volumetric mass-transfer coefficient of the back-extraction process referred to the aqueous phase. Integration of Eq. (14) between the initial ($C_{A(p)t=0}$) and equilibrium ($C_{A(p)eq}$) conditions allows to obtain the $K_a b$ value as the slope of the linear equation $\ln((C_{A(p)eq} - C_{A(p)t=0})/(C_{A(p)eq} - C_{A(p)t}))$ versus time.

Results of the $EE_{A(t)}$ throughout process time are depicted in Fig. 6.10. It is observed that after 20 min, the lactic acid extraction degree is zero, indicating that all the lactic acid extracted in niosomes has been released as sodium lactate. A $K_a b$ of 0.128 min^{-1} ($R^2 = 0.98$) allowed calculating the kinetic curve with a good agreement, as shown in Fig. 6.10.

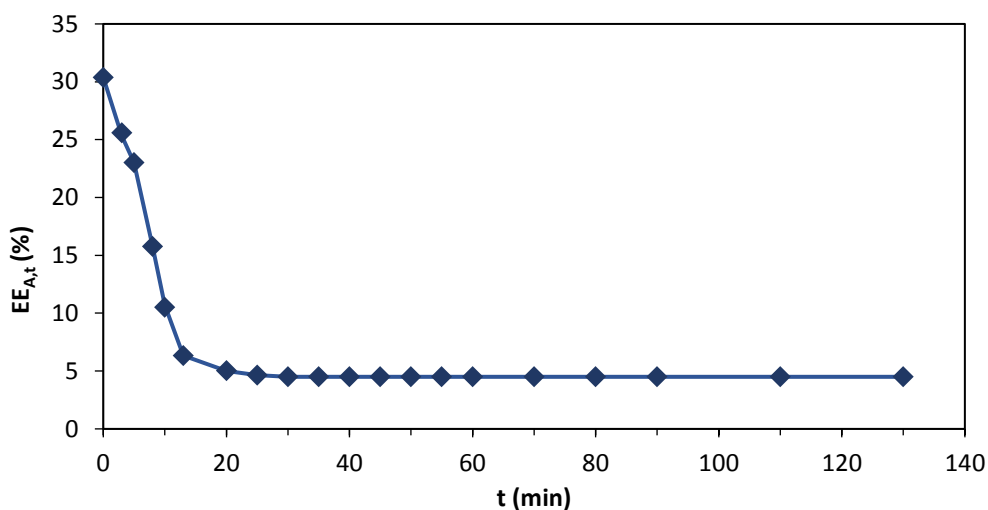


Figure 6.10. Kinetics of lactic acid back-extraction at $pH = 12.2$. Symbols: experimental values.

Lines: calculated values. $TMP = 0.3 \text{ bar}$, $T = 20 \text{ }^\circ\text{C}$.

Fig. 6.11 shows the zeta potentials of permeates and retentates before (pH 2.94) and after the back-extraction process (pH 12.35). As expected, significant differences in the retentates indicate the breaking of niosomes at $pH > 12$.

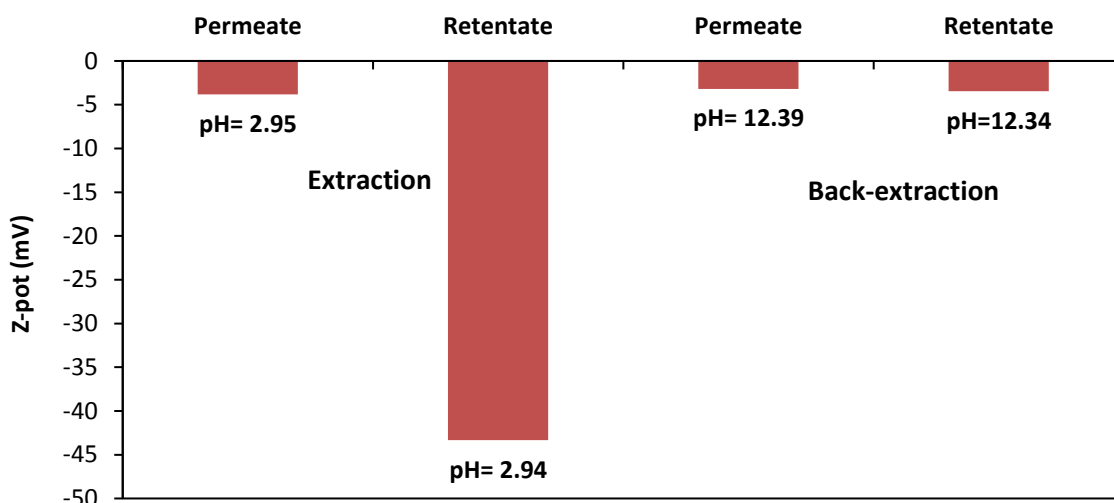


Figure 6.11. Zeta potential values in the extraction and back-extraction stages.

6.3.5. Lactic acid extraction in a two-step process

Due to the moderate lactic acid extraction degree obtained for the best conditions (33% for experiment 3A, as shown in Table 6.2), it was considered adequate the study of a two-step process to check the increased efficiency of the lactic acid extraction. The study was conducted by two consecutive steps where the permeate obtained in the first step was used as the feed of the second one, as described in section 6.2.4.4. The lactic acid concentration in the 400 cm³ of the initial aqueous phase was 12.66 mol/m³; 10 cm³ of dispersed phase was added and the SDS/A molar ratio was 0.008, reaching a EE_{A,eq} of 32.86%. Then, the dispersion was microfiltrated until VCR = 2 with a constant permeate flux of 25.8 L/m² h. The permeate obtained in the first step, with a lactic acid concentration of 8.20 mol/m³, was contacted again with 5 cm³ of a fresh dispersed phase yielding a SDS/A molar ratio of 0.012 and reaching a EE_{A,eq} of 29.60%. Results yielded a global lactic acid extraction degree of 42.77% for the two-step process, with respect to the initial lactic acid concentration in the feed tank.

These results support the feasibility of a multiple-step process in which the optimum operating conditions (pH < pKa, niosomes formulated with Span 80 (20 mol/m³) and SDS (4 mol/m³), and a SDS/A molar ratio of 0.010) should be sought in each step in order to conveniently perform the lactic acid extraction.

6.4. Conclusions

This work examines the influence of several factors related to dispersion composition and operation conditions of a membrane hybrid process using Span 80 niosomes modified with SDS as lactic acid extraction agents. Niosome formulation was performed by 5 min direct ultrasonication of aqueous solutions of 20 mol/m³ Span 80 and different SDS concentrations, following the results obtained in a previous work [30].

Experiments were performed at 20 °C, 350 rpm of feed stirring, using a 0.20 µm pore size flat-disc TiO₂ membrane and 0.3 bar of transmembrane pressure, as they provide a total rejection of the niosomes and high permeate flux that were kept constant during the concentration stage until a volume concentration ratio (VCR) around 2.5.

The lactic acid extraction degree is affected by the SDS concentration in the niosome formulation, the volume of dispersed phase added, pH and concentration of lactic acid in the aqueous solution. SDS concentration used in niosome formulation, pH, and SDS to lactic acid molar ratio (SDS/A) were the three important control parameters for the lactic acid extraction efficiency, for the range of feed compositions studied. Such optimal parameters were pH around 2, 4 mol/m³ of SDS in the niosomal formulation, and a SDS/A molar ratio of 0.010. The highest lactic acid extraction degree (33%) was obtained under the mentioned conditions, which corresponds to the addition of 10 cm³ of dispersed phase containing niosomes formulated with Span 80 (20 mol/m³) and SDS (4 mol/m³), to 400 cm³ of aqueous solution with 10 mol/m³ of lactic acid.

The greater affinity of the niosomes by the non-dissociated species of lactic acid justifies the process optimization when working at pH < pKa of lactic acid (3.4). As pH increases, the lactic acid extraction efficiency decreases as a consequence of the lower concentration of lactic acid protonated species that are able to bind to the niosomes by hydrogen bonds with the SDS adsorbed in the niosomes.

The increased concentration of SDS monomers that remained free in dispersion (not linked to the niosomes) as the pH increases above the isoelectric point of the membrane (about 4.1) was the main responsible for the permeate flux decline. At pH > 12 the breaking of niosomes took place and consequently there was no lactic acid extraction, and a significant permeate flux decline was observed during the concentration stage. A lactic acid recovery efficiency of 100% was obtained in the back-extraction process by addition of sodium hydroxide until pH > 12.

From this work, it is inferred that the lactic acid extraction could be performed in a multiple-step process using the permeate obtained in each step as the feed of the following step, and keeping the optimum operating conditions ($\text{pH} < \text{pKa}$, niosomes formulated with Span 80 (20 mol/m³) and SDS (4 mol/m³), and a SDS/A molar ratio of 0.010) in each step in order to increase significantly the lactic acid extraction efficiency of the process. Furthermore, SDS and Span 80 are non-toxic surfactants with low market price, compared to other surfactants, improving the attractiveness for their use on a large scale or industrial scale.

Nomenclature

C	concentration of species (mol/m ³)
EE _A	lactic acid extraction efficiency (Eq. (1))
HL	lactic acid protonated species
J _p	permeate flux (L/m ² h) (Eq. (3))
K _a	forward overall volumetric mass-transfer coefficient referred to the aqueous phase (Eq. (7))
K _{a_b}	backward overall volumetric mass-transfer coefficient referred to the aqueous phase (Eq. (14))
K _{HL}	equilibrium coefficient for the extraction reaction of the lactic acid protonated species (Eq. (11))
K _{L-}	equilibrium coefficient for the extraction reaction of the anion lactate (Eq. (12))
L ⁻	lactate anion
P _A	equilibrium distribution coefficient for the lactic acid (Eq. (2))
SDS _(NS)	molar ratio between the SDS bind to niosomes and the initial added as dispersed phase (Eq. (5))
SDS _(m)	molar ratio between the SDS adsorbed in the membrane and the initial added as dispersed phase (Eq. (6))
SDS/A	molar ratio between the SDS added in the dispersed phase and the lactic acid content in the initial aqueous phase
t	time (min)
V	volume (cm ³)
VCR	volume concentration ratio (relationship between the feed volume and the retentate volume)

Lactic acid recovery by microfiltration using niosomes as extraction agents

$X_{A(NS)}$ molar ratio between the lactic acid extracted in niosomes and the total amount present in the final retentate after the concentration stage (Eq. (4))

$X_{SDS(NS)}$ molar ratio between the SDS linked to the niosomes and the total amount present in the retentate (Eq. (4))

Subscripts

A	lactic acid
d	dispersed phase
eq	equilibrium conditions
F	feed dispersion
m	membrane
NS	niosomes
p	permeate
r	retentate
S	total surfactant (Span 80 and SDS)
SDS	sodium dodecyl sulphate
w	aqueous phase

Superscripts

0	initial conditions
---	--------------------

Acknowledgments

Financial support from the Ministerio de Economía y Competitividad (MINECO, Spain) through project CTQ2011-25239 is gratefully acknowledged. The authors would like to thank Dr. Carlos Álvarez (Scientific Technical Services, University of Oviedo, Spain) for his valuable help and assistance with TEM measurements.

6.5. References

- [1] M.I. González, S. Álvarez, F.A. Rivera, R. Álvarez, Lactic acid recovery from whey ultrafiltrate fermentation broths and artificial solutions nanofiltration, *Desalination* 228 (2008) 84–96.
- [2] M.C. Duke, A. Lim, S.C. da Luz, L. Nielsen, Lactic acid enrichment with inorganic nanofiltration and molecular sieving membranes by pervaporation, *Food Bioprod. Process.* 86 (2008) 290–295.
- [3] R. Datta, M. Henry, Lactic acid: recent advances in products, processes and technologies – a review, *J. Chem. Technol. Biotechnol.* 81 (2006) 1119–1129.
- [4] G. Dreschke, M. Probst, A. Walter, T. Pümpel, J. Walde, H. Insam, Lactic acid and methane: improved exploitation of biowaste potential, *Bioresour. Technol.* 176 (2015) 47–55.
- [5] K.M. Nampoothiri, N.R. Nair, R.P. John, An overview of the recent developments in polylactide (PLA) research, *Bioresour. Technol.* 101 (2010) 8493–8501.
- [6] M.A. Abdel-Rahman, Y. Tashiro, K. Sonomoto, Lactic acid production from lignocellulose-derived sugars using lactic acid bacteria: overview and limits, *J. Biotechnol.* 156 (2011) 286–301.
- [7] S. Taskila, H. Ojamo, The current status and future expectations in industrial production of lactic acid by lactic acid bacteria. In: J. Marcelino Kongo (Ed.), *Lactic Acid Bacteria – R & D for Food, Health and Livestock Purposes*, IntechOpen, London (2013).
- [8] K.L. Wasewar, A.A. Yawalkar, J.A. Moulijn, V.G. Pangarkar, Fermentation of glucose to lactic acid coupled with reactive extraction: a review, *Ind. Eng. Chem. Res.* 43 (2004) 5969–5982.
- [9] D. Yankov, J. Molinier, J. Albet, G. Malmary, G. Kyuchoukov, Lactic acid extraction from aqueous solutions with tri-n-octylamine dissolved in decanol and dodecane, *Biochem. Eng. J.* 21 (2004) 63–71.
- [10] P. Pal, J. Sikder, S. Roy, L. Giorno, Process intensification in lactic acid production: a review of membrane based processes, *Chem. Eng. Process.* 48 (2009) 1549–1559.
- [11] H. Huang, S.-T. Yang, D.E. Ramey, A hollow-fiber membrane extraction process for recovery and separation of lactic acid from aqueous solution, *Appl. Biochem. Biotechnol.* 114 (2004) 671–688.
- [12] M. Rodríguez, M.J. González-Muñoz, S. Luque, J.R. Álvarez, J. Coca, Extractive ultrafiltration for the removal of carboxylic acids, *J. Membr. Sci.* 274 (2006) 209–218.

- [13] R.-S. Juang, J.-D. Chen, H.-C. Huan, Dispersion-free membrane extraction: case studies of metal ion and organic acid extraction, *J. Membr. Sci.* 165 (2000) 59–73.
- [14] M. Matsumoto, T. Nakaso, K. Kondo, Application of microcapsules containing extractants to the extractive fermentation of lactic acid, *Solvent Extr. Res. Dev. Japan* 8 (2001) 113–119.
- [15] M.O. Ruiz, J.M. Benito, B. Barriuso, J.L. Cabezas, I. Escudero, Equilibrium distribution model of betaine between surfactant micelles and water: application to a micellar-enhanced ultrafiltration process, *Ind. Eng. Chem. Res.* 49 (2010) 6578–6586.
- [16] R.M. Geanta, M.O. Ruiz, I. Escudero, Micellar-enhanced ultrafiltration for the recovery of lactic acid and citric acid from beet molasses with sodium dodecyl sulphate, *J. Membr. Sci.* 430 (2013) 11–23.
- [17] M.J. Choi, H.I. Maibach, Liposomes and niosomes as topical drug delivery systems, *Skin Pharmacol. Physiol.* 18 (2005) 209–219.
- [18] C. Marianelli, L. Di Marzio, F. Rinaldi, C. Celia, D. Paolino, F. Alhaique, S. Esposito, M. Carafa, Niosomes from 80s to present: the state of the art, *Adv. Colloid Interface Sci.* 205 (2014) 187–206.
- [19] E. Acosta, Bioavailability of nanoparticles in nutrient and nutraceutical delivery, *Curr. Opin. Colloid Interface Sci.* 14 (2009) 3–15.
- [20] S. Gouin, Microencapsulation: industrial appraisal of existing technologies and trends, *Trends Food Sci. Technol.* 15 (2004) 330–347.
- [21] D.J. McClements, E.A. Decker, Y. Park, J. Weiss, Structural design principles for delivery of bioactive components in nutraceuticals and functional foods, *Crit. Rev. Food Sci. Nutr.* 49 (2009) 577–606.
- [22] Y.-M. Hao, K. Li, Entrapment and release difference resulting from hydrogen bonding interactions in niosome, *Int. J. Pharm.* 403 (2011) 245–253.
- [23] A.Y. Waddad, S. Abbad, F. Yu, W.L.L. Munyendo, J. Wang, H. Lv, J. Zhou, Formulation, characterization and pharmacokinetics of Morin hydrate niosomes prepared from various non-ionic surfactants, *Int. J. Pharm.* 456 (2013) 446–458.
- [24] Z. Sezgin-Bayindir, N. Yuksel, Investigation of formulation variables and excipient interaction on the production of niosomes, *AAPS Pharm. Sci. Tech.* 13 (2012) 826–835.
- [25] I.F. Uchegbu, A.T. Florence, Non-ionic surfactant vesicles (niosomes): physical and pharmaceutical chemistry, *Adv. Colloid Interface Sci.* 58 (1995) 1–55.
- [26] R. Nagarajan, Molecular packing parameter and surfactant self-assembly: the neglected role of the surfactant tail, *Langmuir* 18 (2002) 31–38.

- [27] I. Escudero, R.M. Geanta, M.O. Ruiz, J.M. Benito, Formulation and characterization of Tween 80/cholesterol niosomes modified with tri-n-octylmethylammonium chloride (TOMAC) for carboxylic acids entrapment, *Colloid Surf. A-Physicochem. Eng. Asp.* 461 (2014) 167–177.
- [28] B. Nasser, Effect of cholesterol and temperature on the elastic properties of niosomal membranes, *Int. J. Pharm.* 300 (2005) 95–101.
- [29] D. Pozzi, R. Caminiti, C. Marianelli, M. Carafa, E. Santucci, S.C. De Sanctis, G. Caracciolo, Effect of cholesterol on the formation and hydration behavior of solid-supported niosomal membranes, *Langmuir* 26 (2010) 2268–2273.
- [30] R. Fraile, R.M. Geanta, I. Escudero, J.M. Benito, M.O. Ruiz, Formulation of Span 80 niosomes modified with SDS for lactic acid entrapment, *Desalin. Water Treat.* 56 (2015) 3463–3475.
- [31] B.A. Uzoukwu, L.M.L. Nollet, Analysis of surfactants. In: L.M.L. Nollet (Ed.), *Handbook of Water Analysis*, Marcel Dekker, New York (2000), pp. 767–784.
- [32] S.Y. Tang, S. Manickam, T.K. Wei, B. Nashiru, Formulation development and optimization of a novel Cremophore EL-based nanoemulsion using ultrasound cavitation, *Ultrason. Sonochem.* 19 (2012) 330–345.
- [33] M. Kaszuba, J. Corbett, F.M. Watson, A. Jones, High-concentration zeta potential measurements using light-scattering techniques, *Philos. Trans. R. Soc. A-Math. Phys. Eng. Sci.* 368 (2010) 4439–4451.
- [34] E. Chevereau, N. Zouaoui, L. Limousy, P. Dutournié, S. Déon, P. Bourseau, Surface properties of ceramic ultrafiltration TiO₂ membranes: effects of surface equilibria on salt retention, *Desalination* 255 (2010) 1–8.
- [35] K. Xu, G.-M. Zeng, J.-H. Huang, J.-Y. Wu, Y.-Y. Fang, G. Huang, J. Li, B. Xi, H. Liu, Removal of Cd²⁺ from synthetic wastewater using micellar-enhanced ultrafiltration with hollow fiber membrane, *Colloid Surf. A-Physicochem. Eng. Asp.* 294 (2007) 140–146.
- [36] J.F. Scamehorn, S.D. Christian, D.A. El-Sayed, H. Uchiyama, S.S. Younis, Removal of divalent metal cations and their mixtures from aqueous streams using micellar-enhanced ultrafiltration, *Sep. Sci. Technol.* 29 (1994) 809–830.
- [37] L.J. Peltonen, J. Yliruusi, Surface pressure, hysteresis, interfacial tension, and CMC of four sorbitan monoesters at water–air, water–hexane, and hexane–air Interfaces, *J. Colloid Interface Sci.* 227 (2000) 1–6.
- [38] R.E. Kirk, D.F. Othmer, *Encyclopedia of Chemical Technology*, Wiley, New York (1991).

- [39] S.-O. Ko, M.A. Schlautman, E.R. Carraway, Partitioning of hydrophobic organic compounds to sorbed surfactants. 1. Experimental studies, *Environ. Sci. Technol.* 32 (1998) 2769–2775.
- [40] Y.-C. Huang, B. Batchelor, S.S. Koseoglu, Crossflow surfactant-based ultrafiltration of heavy metals from waste streams, *Sep. Sci. Technol.* 29 (1994) 1979–1998.
- [41] J. Landaburu-Aguirre, V. García, E. Pongrácz, R.L. Keiski, The removal of zinc from synthetic wastewaters by micellar-enhanced ultrafiltration: statistical design of experiments, *Desalination* 240 (2009) 262–269.
- [42] C-K. Liu, C.-W. Li, Simultaneous recovery of copper and surfactant by an electrolytic process from synthetic solution prepared to simulate a concentrate waste stream of a micellar-enhanced ultrafiltration process, *Desalination* 169 (2004) 185–192.
- [43] J. Sabaté, M. Pujolà, E. Centelles, M. Galán, J. Llorens, Determination of equilibrium distribution constants of phenol between surfactant micelles and water using ultrafiltering centrifuge tubes, *Colloid Surf. A-Physicochem. Eng. Asp.* 150 (1999) 229–245.

**7. Separation of sodium lactate from Span 80 and SDS surfactants by
ultrafiltration**

El estudio de investigación que se presenta en este capítulo surge de la necesidad de solventar el fuerte ensuciamiento de la membrana de microfiltración utilizada en el estudio anterior y presentado en el capítulo 6. Por ello, en este trabajo, que representa una continuación del anterior, se utilizarán membranas de ultrafiltración planas de ZrO₂ y se tratará de optimizar el proceso de separación de lactato sódico en la etapa de reextracción.

El estudio se llevó a cabo mediante un diseño de experimentos del tipo compuesto central y metodología de superficie de respuesta. Los factores experimentales fueron el límite de peso molecular nominal de la membrana (NMWL), la presión transmembranal (TMP), y la concentración inicial de ácido láctico (C_A), y las variables respuestas la densidad de flujo de permeado (J_p) y los rechazos observados del lactato sódico (R_A) y del tensioactivo SDS (R_S).

Las experiencias se realizaron a 25 °C en cuatro etapas: una primera etapa de extracción del ácido láctico mediante niosomas formulados con monoleato de sorbitán (Span 80, 20 mol/m³) y dodecil sulfato de sodio (SDS, 4 mol/m³), una segunda etapa de reextracción realizada por adición de NaOH hasta un pH superior a 12 donde se produce la ruptura de los niosomas y la liberación del lactato de sodio, y una tercera y cuarta etapas de ultrafiltración, a concentración constante y subsiguientemente en modo de concentración, con el fin de separar los iones de lactato de los tensioactivos empleados.

Las condiciones óptimas de operación se obtuvieron empleando membranas de 15 kDa y trabajando a una presión transmembranal de 2 bar. En estas condiciones, se obtuvieron valores máximos de flujo de permeado (42,63 L/m²h) y de rechazo a los tensioactivos Span 80 (100%) y SDS (87,3%), mientras que el rechazo de la membrana al ion lactato fue muy bajo (4,31%).

Asimismo, se observó un efecto adverso en la retención de SDS a medida que aumenta el flujo de permeado. Este fenómeno es explicado considerando los fenómenos que pueden ocurrir en la capa de polarización en presencia de elevadas cantidades de sal.

Este trabajo ha sido publicado en la revista *Separation and Purification Technology* 180 (2017), 90–98. <https://doi.org/10.1016/j.seppur.2017.02.048>

7.1. Introduction

Lactic acid is of paramount importance in pharmaceutical and food industries due to its properties as a preservative, acidulant, pH regulator, and flavoring. Its use has considerably increased in the last years because of the increased production of polylactic acid (PLA) biodegradable thermoplastic [1–4].

In lactic acid bioproduction, unsustainable and high energy consumption conventional separation techniques, such as precipitation with calcium hydroxide or solvent extraction, are usually used for the lactic acid separation from fermentation broths [5,6]. Membrane-based separation techniques [7] have proven to be effective because they can avoid accumulation of lactic acid in the fermentation broths, preventing product inhibition and increasing productivity of the fermentation process. In this way, hollow-fiber contactors using organic solvents [8–10] and micellar enhanced ultrafiltration (MEUF) using surfactants have been studied [11–14]. More recently, the use of niosomes as lactic acid extraction agents has also been studied [15].

Niosomes are vesicles formed by one or more bilayers of non-ionic surfactants enclosing an aqueous inside cavity. Niosomes are widely used in medical and pharmacological applications for their ability to microencapsulate compounds of different nature [16–20]. However, the use of niosomes as extraction agents of solutes from very low concentration aqueous solutions is a new application in the field of sustainable processes that has barely been explored.

Fraile et al. [21] observed that the addition of suitable amounts of the anionic surfactant sodium dodecyl sulfate (SDS) to non-ionic surfactant Span 80 (sorbitan monooleate) formulations yields a stabilizing effect on the niosome bilayer, improving lactic acid entrapment efficiency. However, the addition of ionic surfactants to the niosome dispersions can lead to the complete solubilization of vesicles. The solubilization process of Span 80 niosomes by addition of SDS has been recently studied [22]. It was identified as a three-stage micellization process: SDS adsorption until saturation, intensification of the bilayer solubilization by mixed micelles formation, and complete bilayer solubilization by micellization. The critical points corresponding to SDS concentration for niosome saturation and total solubilization were identified for several Span 80 niosome concentrations, being 12 and 16 mol/m³ of SDS, respectively, for the 20 mol/m³ Span 80 formulation.

The membrane hybrid process of lactic acid extraction by niosomes formulated with Span 80 and SDS in pre-saturation concentrations, using a 0.20 µm pore size flat-disc TiO₂ microfiltration membrane and 0.3 bar of transmembrane pressure, has been studied in a previous work [15].

Best results showed a 33% lactic acid extraction degree after 30 min equilibrium time, using niosomes of Span 80 (20 mol/m³) and SDS (4 mol/m³) as extraction agents, pH < pKa of lactic acid (pKa = 3.4), and a SDS/lactic acid molar ratio of 0.01. Back-extraction of lactate ion was conducted by addition of NaOH until pH > 12 where breaking of niosomes was observed. However, a significant permeate flux decline with respect to water flux ($J_p/J_w = 0.38$) was obtained during the separation of components due to fouling by mixed micelles and SDS monomers in the polarization layer and within the large pores of the microfiltration membrane. These results have led to the present work focused on the use of ultrafiltration (UF) membranes in order to reduce fouling and to improve the permeate flux during the back-extraction stage at pH > 12.

This work is a continuation of the previous one [15] and aims to model and optimize the removal of lactate ion from back-extraction aqueous solutions at pH > 12 containing Span 80 and SDS surfactants in the stated concentrations, using ultrafiltration membranes. A Central Composite Design (CCD) and Response Surface Methodology (RSM) were used to study the effect of the factors (lactate ion concentration, transmembrane pressure, and membrane nominal molecular weight limit), on the permeate flux and rejection of components. RSM approach was also used to gain an understanding of the concentration polarization phenomenon. The optimization of the process conditions was conducted in order to achieve maximum permeate flux and surfactants rejection, and minimum lactate ion rejection.

7.2. Materials and methods

7.2.1. Chemicals

DL-Lactic acid (>90% purity, Fluka) was used as solute. The non-ionic surfactant sorbitan monooleate (Span 80, >95% purity, Sigma-Aldrich) and the anionic surfactant sodium dodecyl sulfate (SDS, 99%, Sigma-Aldrich) were used in the formulation of niosomes. Other chemicals such as methanol (HPLC grade, HiPerSolvChromanorm), maleic acid (>99%, Fluka), phosphoric acid (>85%, Sigma-Aldrich), disodium hydrogen phosphate dodecahydrate (>98%, Panreac), potassium dihydrogen phosphate (>99.5%, Merck), sodium hydroxide (analysis grade, Scharlau), and phenolphthalein (99%, Panreac) were used throughout the experiments. For the determination of SDS concentration the following chemicals were used: ethyl violet (99%, Sigma-Aldrich), glacial acetic acid of analysis quality (Panreac), sodium acetate for analysis (Merck), anhydrous sodium sulfate for analysis (Scharlau), toluene (>99.5%, AnalarNormapur VWR Chemicals) and ethylenediaminetetraacetic acid (EDTA, >99%, Sigma-Aldrich). Ultrapure

deionized Milli-Q water (Millipore, USA), with a conductivity of 0.1 $\mu\text{S}/\text{cm}$, was used for the preparation of all solutions.

7.2.2. Niosome formation

Niosomes were prepared by ultrasonication of 10 cm^3 aqueous solutions of Span 80 (20 mol/ m^3) and SDS (4 mol/ m^3). These concentrations were chosen on the basis of previous works [15,21]. The application of ultrasounds was carried out over a 5-min effective time, by pulses every 5 s (5 s on and 5 s off, 60 cycles; 30% amplitude, 500 W), to avoid overheating of the sample, using a high-intensity ultrasonic processor (Vibra-Cell VCX 500, Sonics & Materials Inc., USA) equipped with a 3 mm-diameter titanium alloy bicylindrical probe. Following, samples were centrifuged (Eppendorf 5804 centrifuge) for 15 min at 9000 rpm, in order to remove any trace of metal detached from the probe.

7.2.3. Experimental procedure

UF experiments were carried out using a Spirlab filtration cell (TAMI Industries, France) with 90 mm diameter flat-disc ceramic membranes (INSIDE DisRAM, TAMI Industries, France), made of a ZrO_2 active layer supported on TiO_2 , with 56.3 cm^2 of effective area. The nominal molecular weight limits (NMWL) of the membranes were 3, 8 and 15 kDa.

All experiments were conducted using the following four-stage protocol:

1. Extraction stage: it was carried out by mixing 400 cm^3 of aqueous solution containing lactic acid ($C_A = 5, 10$ and $15 \text{ mol}/\text{m}^3$), named as F_o , and 10 cm^3 of dispersed phase containing niosomes, named as F_d . The mixture was continuously stirred at 375 rpm and 20 °C for 30 min to reach equilibrium.
2. Back-extraction stage: this stage was performed by addition of a required volume of NaOH (1 N) aqueous solution to the above mentioned dispersion until pH about 12.2 ± 0.2 . It was allowed 45-50 min to reach equilibrium and then a 60 cm^3 sample was withdrawn for analysis. The sample and remaining dispersion were identified as F_{bis} .
3. UF stage in constant concentration mode. The feed solution (F_{bis}) was fed to the ultrafiltration cell by a peristaltic pump (Masterflex I/s economy drive Cole Parmer, CRS rotor EW-07518-00) at a prefixed flow rate and pressure. Permeate and retentate streams were recirculated to the 1 L jacketed feed tank, where the feed solution was kept at constant temperature (20 °C) and stirred at 375 rpm. Adjustment of

transmembrane pressure (TMP) was achieved by a needle valve located in the retentate stream. The system is also equipped with a flowmeter and a pressure gauge, both placed at the inlet of the filtration cell. Experiments were run for 30 min under specific TMP (1, 1.5 or 2 bar) in order to achieve stable conditions in the polarization layer and membrane. Subsequently, a 60 cm³ sample was withdrawn for analysis and the sample and remaining dispersion were identified as F.

4. UF stage in concentration mode. Once the equilibrium with the membrane was reached, the feed solution F was ultrafiltrated in concentration mode, removing continuously the permeate stream and recirculating the retentate to the feed tank up to a volume concentration ratio (VCR, the quotient between initial feed volume and retentate volume) around 2. The permeate flux was calculated by measuring the time needed for collecting 10 cm³ permeate samples. Finally, permeate and retentate were separated for analysis and named as P and R, respectively.

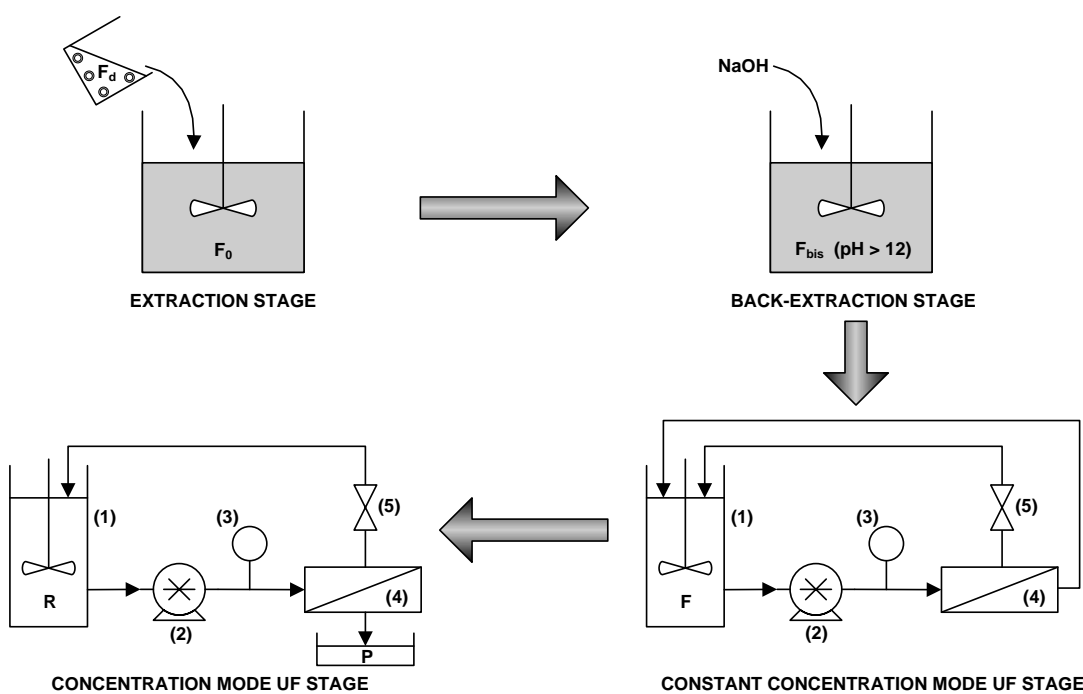


Figure 7.1. Schematic diagram of the four-stage experimental procedure. F_d : dispersed phase, F_o : continuous phase, F_{bis} : dispersion at pH > 12 without membrane contact, F : feed dispersion at pH > 12 in contact with the membrane under UF conditions at constant concentration, P and R : permeate and retentate after UF in concentration mode, 1: feed tank, 2: peristaltic pump, 3: pressure gauge, 4: membrane module, 5: needle valve.

Fig. 7.1 shows a scheme of the four-stage procedure and the set-up of the UF experimental equipment. Table 7.1 summarizes the analytical measurements made to different samples through the experimental process.

Membrane cleaning was accomplished afterwards by rinsing with deionized water to remove the foam, followed by washing with 0.1 N sodium hydroxide solution for 30 min, and then with 0.17 wt.% phosphoric acid solution for 30 min. A final rinsing step with deionized water until neutrality was sufficient to restore the initial water flux of the membrane.

Table 7.1. Summary of analytical measurements made to samples through the experimental procedure.

Sample	Description	Analytical measurements
F_o	Lactic acid aqueous solution (initial continuous phase)	Lactic acid concentration and pH
F_d	Aqueous dispersion of niosomes (initial dispersed phase)	Size, PDI, zeta potential, and pH
F_{bis}	Equilibrium dispersion at pH > 12 (without membrane)	Lactate ion concentration, SDS monomers concentration, size, PDI, zeta potential, and pH
F	Bulk dispersion at pH > 12 under steady-state UF conditions in constant concentration mode	Lactate ion concentration, SDS monomers concentration, size, PDI, zeta potential, and pH
P	Final permeate after UF in concentration mode ($VCR = 2$)	Lactate ion concentration, SDS monomers concentration, size, PDI, zeta potential, and pH
R	Final retentate after UF in concentration mode ($VCR = 2$)	Lactate ion concentration, SDS monomers concentration, size, PDI, zeta potential, and pH

7.2.4. Analytical methods

Lactate ion concentration was determined by high performance liquid chromatography using a HPLC Shimadzu. A reverse phase column ACE 5C18 (ACE HPLC columns) and a UV-vis detector at 216 nm were used. Detailed conditions of the analytical method can be found elsewhere [15]. Samples were measured in triplicate and the analytical error was lower than $\pm 0.001 \text{ mol/m}^3$.

SDS monomer concentration was determined by spectrophotometry at 615 nm with a Hitachi U-2000 equipment, using the ethyl violet method [23]. Samples were measured in triplicate and the analytical error was lower than $\pm 0.002 \text{ mol/m}^3$.

The particle size distribution, the mean hydrodynamic diameter and the polydispersity index (PDI) of the samples were carried out by dynamic light scattering (DLS) using a Zetasizer Nano ZS apparatus (Malvern Instruments Ltd., UK). The PDI is a dimensionless measure of the width of the size distribution ranging from 0 to 1, a higher value being indicative of a broader distribution of particle size. The average value and the relative error of the 3 replicates, each of 5 measurements at 20°C, was considered for each sample.

Zeta potential measurements were conducted with the aforementioned Zetasizer Nano ZS apparatus, using the Laser Doppler Velocimetry technique. They were performed on the same sample previously prepared to measure the particle size, but using the appropriate DTS1061 disposable folded capillary cell equipped with electrodes to allow the passage of electric current and the movement of the particles according to their charge [24]. Six replicates of 11 measurements were performed for each sample at 20 °C.

The pH measurement was performed at 20 °C using a Crison GLP 22 pH-meter fitted with a Crison 52-02 glass pH electrode (Crison, Spain), with an error of $\pm 0.01 \text{ pH}$ units.

Morphological analysis of niosomes was performed by negative staining transmission electron microscopy (NS-TEM), using a JEOL-2000 EX-II TEM operating at 160–180 kV, with an image resolution of 1 nm, located at the University of Oviedo (Spain). A droplet of the selected sample was placed on a carbon-coated copper grid, and the sample excess was removed using a piece of filter paper. Then, a drop of phosphotungstic acid solution (2% w/v) was applied to the carbon grid and left for 2 min. Once the excess of staining agent was removed by absorbing with the filter paper, the sample was air-dried and the thin film of stained niosomes was observed by TEM.

7.2.5. Experimental design and statistical analysis

Response Surface Methodology (RSM) and Central Composite Design (CCD) with three levels of each independent variable were used to study the effect of NMWL (X_1 : 3–15 kDa), TMP (X_2 : 1–2 bar) and lactic acid initial concentration (X_3 : 5–15 mol/m³) on the permeate flux (J_p), lactate ion observable rejection (R_A), and SDS observable rejection (R_s). The factors and levels studied are summarized in Table 7.2. Based on the selected high and low levels, the NMWL ideal central point should be 9 kDa. However, 8 kDa membrane was used at the central points in this study, assuming that this change does not significantly influence the experimental design.

Table 7.2. Factors and levels studied.

Factors	Levels		
	Low (-1)	Centre (0)	High (+1)
X_1 : NMWL (kDa)	3	8	15
X_2 : TMP (bar)	1	1.5	2
X_3 : C _A (mol/m ³)	5	10	15

The response variables were calculated using the following equations:

$$J_p = \frac{V}{t \times A} \quad (1)$$

$$R_i = 1 - \frac{C_{i(p)}}{C_{i(F_{bis})}} \quad (2)$$

where V is the volume of the permeate sample collected, t is the time needed for collecting the permeate sample, A is the membrane effective area (56.3 cm²), and C_{i(p)} and C_{i(F_{bis})} are the total concentration of lactate ion or SDS in the final permeate and dispersion at pH > 12 (F_{bis} dispersion), respectively.

The CCD model generated 17 experimental runs with three replicates at the central point which highlight the reproducibility of the experiments. A second-order degree polynomial equation was used to express each predicted response (Y) as a function of the independent variables under study (X_1 , X_2 and X_3). The model equation is as follows:

$$Y = a_0 + a_1 X_1 + a_2 X_2 + a_3 X_3 + a_{11} X_1^2 + a_{22} X_2^2 + a_{33} X_3^2 + a_{12} X_1 X_2 + a_{13} X_1 X_3 + a_{23} X_2 X_3 \quad (3)$$

where Y represents the response variable (J_p , R_A , and R_S , in this case), a_0 is a constant, and a_i , a_{ii} , a_{ij} are the linear, quadratic, and interactive coefficients, respectively. Analysis of variance (ANOVA) and least significant difference (LSD) test were applied to detect the effect of the factors and statistically significant differences among values, respectively. The model was fitted by multiple linear regressions (MLR). The validity of the empirical model was tested with ANOVA. The significance of each estimated regression coefficient was assessed through values of the statistic parameters F and p (probability) with a 95% confidence level. The experimental design and data analysis were performed using STATGRAPHICS Centurion XVI (Statpoint Technologies, Inc., Warrenton, VA, USA).

Optimal conditions were determined with the help of the STATGRAPHICS Centurion XVI software, in order to reach the maximum permeate flux and SDS rejection, and the minimum lactate ion rejection, according with the work objectives.

7.3. Results and discussion

7.3.1. Effect of NaOH addition on the breakup of niosomes

Particle size measurement in the dispersed phase (F_d) reveals niosomes of 200 nm average diameter and a PDI value of 0.27, which indicates a homogeneous population (Fig. 7.2a). Otherwise, detailed analysis of DLS intensity data of dispersions at pH > 12 revealed that the main peak observed in F_d , which is attributed to niosomes, disappears in these samples indicating niosome destruction by the addition of NaOH until pH > 12. However, peaks associated with mixed micelles of 78–80 nm in size and Span 80 aggregates larger than 1000 nm were observed in any of the F_{bis} , F and R dispersions. Results corresponding to a R dispersion are also depicted in Fig. 7.2a. They are according with previous works [15,21]. As expected, zeta potential values between –45 and –38.5 mV were obtained in the F_d samples used in different experiments (–40.8 mV for F_d sample shown in Fig. 7.2b), which indicate the presence of negatively charged niosomes due to the SDS adsorbed in their surface. Besides, as shown in Fig. 7.2b, two particle populations are observed in the R dispersion, with zeta potential values of –8 and –20 mV, indicating weakly negatively charged particles. Similar results were obtained for any of F_{bis} and F dispersions (not shown), which corroborate the breakup of the niosomes at pH > 12. No particles were found in permeates, regardless of the membrane NMWL.

The presence and morphology of niosomes in the dispersed phase (F_d) have been confirmed by TEM measurements. Fig. 7.3 shows two photomicrographs of formulations of 20 mol/m^3 of Span 80 and 4 mol/m^3 of SDS, where the white areas correspond to the grid. Fig. 7.3a shows the presence of spherical niosomes of about 200 nm in F_d , whose sizes agree with those measured by DLS. Fig. 7.3b shows absence of niosomes in the dispersion at $\text{pH} > 12$ (F_{bis}). Fig. 7.3b could correspond to large structures of Span 80, as its concentration (20 mol/m^3) is well above its CMC ($\approx 0.1 \text{ mol/m}^3$ in water [25]), and they would be in accordance with the large particles shown in Fig. 7.2a.

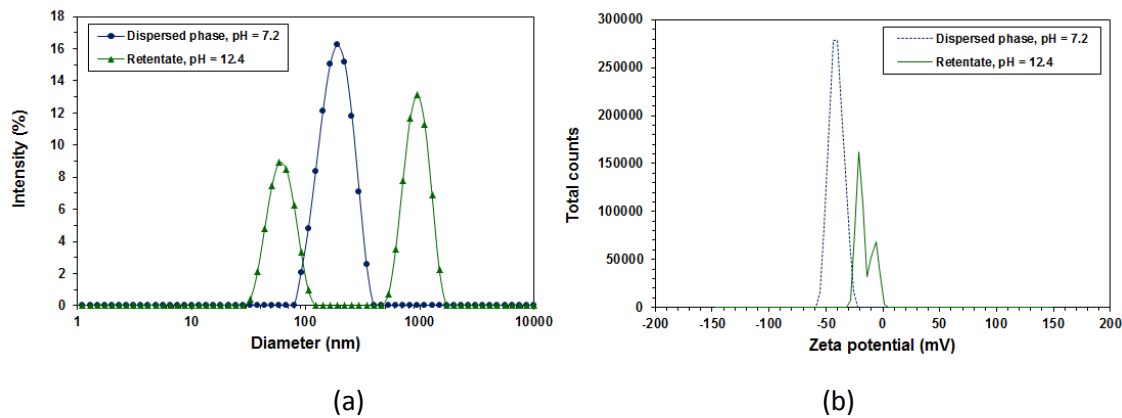


Figure 7.2. (a) Particle size distributions corresponding to dispersed phase, F_d , and retentate, R , and (b) Zeta potential of F_d and R dispersions, as described in Table 7.1.

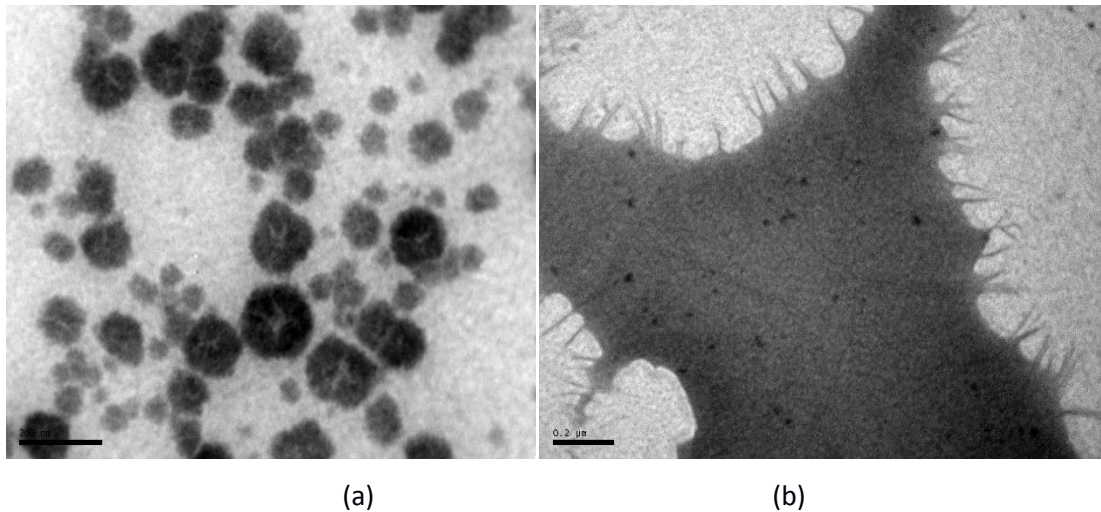


Figure 7.3. TEM micrographs. (a) Niosomes of Span 80 ($20 \text{ mol}/\text{m}^3$) and SDS ($4 \text{ mol}/\text{m}^3$) in the dispersed phase (F_d). (b) Formulation of Span 80 ($20 \text{ mol}/\text{m}^3$) and SDS ($4 \text{ mol}/\text{m}^3$) in aqueous solution at $\text{pH} > 12$ (F_{bis}). Scale bars: $0.2 \mu\text{m}$.

It is well documented that addition of low concentration of cations to anionic surfactant (SDS) solutions decreases the repulsive forces between head groups of SDS monomers due to the electrostatic shielding effect, resulting in the formation of micelles at lower concentration than its CMC ($8.1 \text{ mol}/\text{m}^3$ in water [11,26–32]). However, beyond a critical concentration, the sodium ions start disrupting the micellar packing, resulting in less stable micelles [29,30].

In light of the results, it can be assumed that the presence of Span 80 monomers is highly improbable in dispersions at $\text{pH} > 12$ due to its hydrophobic character ($\text{HLB} = 4.3$ [20]), whereas the coexistence of large Span 80 aggregates with mixed micelles and SDS surfactant monomers is highly probable.

7.3.2. Experimental design

The matrix of the CCD and experimental values of the response variables are given in Table 7.3.

Table 7.3. Matrix of the central composite design (CCD) and experimental values of the response variables: permeate flux (J_p), lactate ion observable rejection (R_A), and SDS observable rejection (R_S).

Experiment	Factors				Responses	
	NMWL (kDa)	TMP (bar)	C _A (mol/m ³)	J _p (L/m ² h)	R _A	R _S
1	15	1	5	15,99 ^{abc}	0,0191 ^a	0,897 ^a
2	8	1,5	10	24,51 ^{cd}	0,0182 ^a	0,864 ^a
3	3	1	15	8,53 ^a	0,0115 ^a	0,888 ^a
4	8	1,5	5	26,64 ^{cd}	0,0160 ^a	0,865 ^a
5	3	1,5	10	12,79 ^{ab}	0,0056 ^a	0,881 ^a
6	15	1,5	10	34,10 ^{de}	0,0315 ^a	0,880 ^a
7	8	1,5	15	19,18 ^{cd}	0,0171 ^a	0,891 ^a
8	8	1	10	14,92 ^{abc}	0,0117 ^a	0,881 ^a
9	8	1,5	10	22,38 ^{cd}	0,0208 ^a	0,866 ^a
10	15	1	15	17,05 ^{abcd}	0,0193 ^a	0,887 ^a
11	3	1	5	9,06 ^a	0,0025 ^a	0,902 ^a
12	3	2	5	20,25 ^{bcd}	0,0313 ^a	0,889 ^a
13	15	2	5	42,63 ^f	0,0431 ^a	0,873 ^a
14	15	2	15	40,50 ^f	0,0448 ^a	0,870 ^a
15	8	1,5	10	23,45 ^{cd}	0,0077 ^a	0,871 ^a
16	8	2	10	27,71 ^{de}	0,0055 ^a	0,869 ^a
17	3	2	15	17,05 ^{abcd}	0,0313 ^a	0,890 ^a

Values with different letters in each column are significantly different (LSD test, $p < 0.05$)

Table 7.3 shows that J_p values present large variation, between 8 and 43 L/m²h. However, R_A and R_S values were lower than 4.5% and higher than 86%, respectively, with very similar values among them for all experiments. LSD test was applied for each response variable, revealing that R_A and R_S values were no significantly different ($p > 0.05$). However, J_p values identified in Table 7.3 that do not share a same letter were considered statistically different among them ($p < 0.05$).

ANOVA of the fitted model for the J_p response shows that the model was statistically significant (p -value = 0.001). Table 7.4 shows that NMWL, TMP and their interaction are statistically significant ($p < 0.05$) on J_p . F values indicate that, for the range of factors studied, NMWL and TMP factors have the stronger influence on J_p , and also that interaction between NMWL and TMP has synergistic effect on J_p . Otherwise, C_A factor was not significant on J_p , indicating that it does not contribute on the J_p response, in the range of concentrations tested.

Table 7.4. Analysis of variance (ANOVA) for the model. Response: permeate flux (J_p).

Factors	SS	DF	MS	F-value	p-value
X ₁ : NMWL	682.111	1	682.111	131.17	0.0017
X ₂ : TMP	702.524	1	702.524	135.09	0.0016
X ₃ : C _A	14.6575	1	14.6575	2.82	0.0694
X ₁ ²	3.45166	1	3.45166	0.66	0.2232
X ₁ X ₂	119.472	1	119.472	22.97	0.0094
X ₁ X ₃	1.51815	1	1.51815	0.29	0.3668
X ₂ ²	9.59837	1	9.59837	1.85	0.1006
X ₂ X ₃	4.29245	1	4.29245	0.83	0.1911
X ₃ ²	0.237523	1	0.237523	0.05	0.6921
Lack of fit	34.1339	5	6.82679	6.02	0.1486
Pure error	2.26847	2	1.13423		

SS (sum of squares), DF (degrees of freedom), MS (mean of squares)

Considering the significance of the factors, expressed by p-values, the empirical model was simplified, and experimental data were fitted to Eq. (4), which was able to correctly predict the permeate flux. Fig. 7.4 depicts the closeness between the observed and predicted values of the permeate flux.

$$J_p = -17.0207 - 0.109287 \times \text{NMWL} + 30.8566 \times \text{TMP} + 1.28459 \times \text{NMWL} \times \text{TMP} \quad (4)$$

The model obtained (Eq. (4)) was robust and showed no lack of fit ($p > 0.05$, Table 7.4), with high value of the coefficient of determination ($R^2 = 0.942$), high adjusted statistical coefficient ($R^2_{\text{adj}} = 0.923$) and a normal distribution of the residuals.

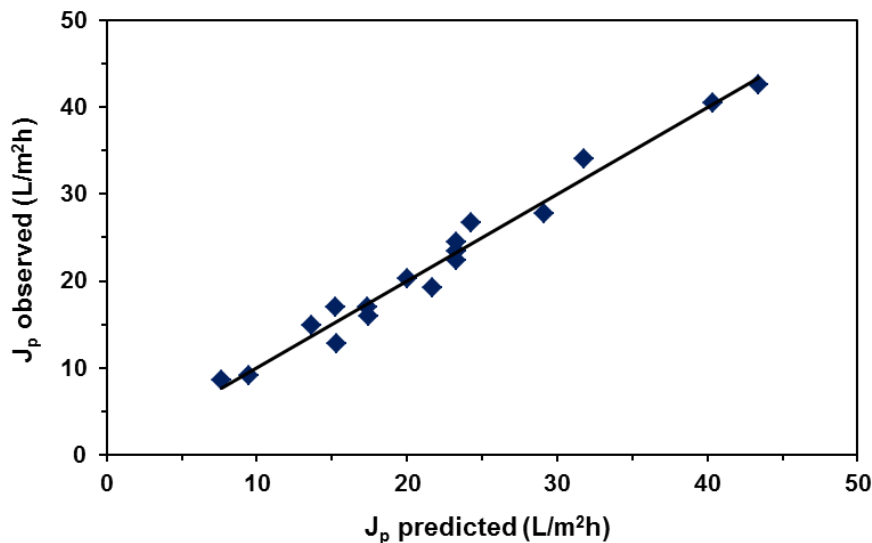


Figure 7.4. Observed vs. predicted values for permeate flux.

In order to study the effect of the independent variables on J_p , surface response and contour plots of the model were generated by varying two of the independent variables within the experimental range while holding the third one constant at the central point. Fig. 7.5 shows that NMWL and TMP factors, and their interaction, have a statistically significant positive effect on the permeate flux. A TMP increase causes a positive effect on J_p increase, being more appreciable as NMWL increases. This behavior can also be seen later in Fig. 7.6.

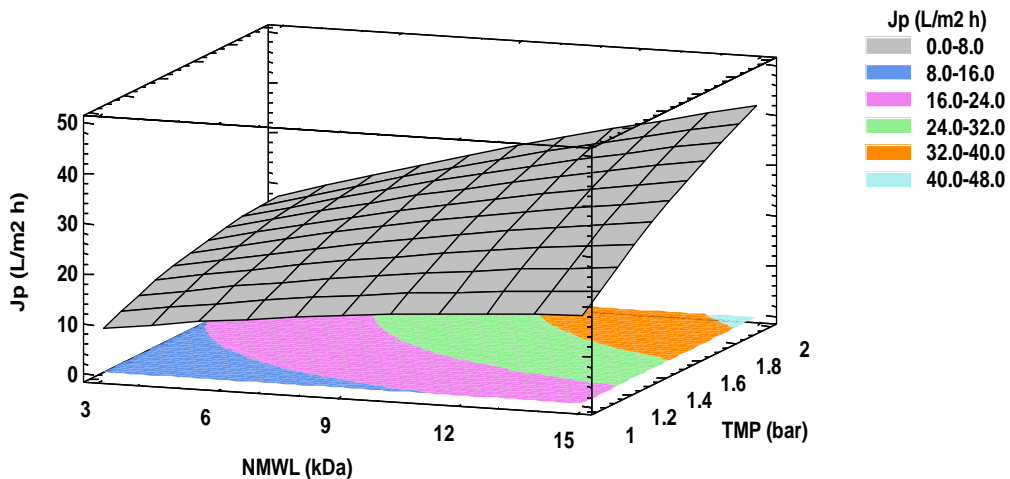


Figure 7.5. Response surface and contour plots of J_p vs. NMWL and TMP for $C_A = 10 \text{ mol/m}^3$.

7.3.3. Optimization of operating conditions

Optimal conditions were established by maximizing the permeate flux. Rejections of lactate ion and SDS were not optimized because they are no statistically different between them (LSD test, $p > 0.05$), in the range of concentrations tested. Table 7.5 shows that best results can be obtained using the 15 kDa NMWL ultrafiltration membrane, and 2 bar TMP. Under these conditions, corresponding to experiment 13 of Table 7.3, predicted values of J_p , R_s , and R_A were 43.35 L/m²h, 87.05%, and 1.6%, respectively.

Table 7.5. Optimal operating conditions for the ultrafiltration process, and predicted and experimental values of the response variables J_p , R_A , and R_s .

Response	Optimization	Prediction	Lower limit (95.0%)	Upper limit (95.0%)	Factor	Optimal conditions
J_p	Yes	43.3483	38.5473	48.1493	NMWL	15.0
R_A		0.0159915	-0.0134268	0.0454098	TMP	2.0
R_s		0.870568	0.852023	0.889112	C _A	5.0

7.3.4. Relationship between permeate flux and SDS rejection.

Fig. 7.6 shows that J_p linearly increases with TMP, a fact that is more significant for the 15 kDa membrane. Similar results were obtained in several works [31–33]. The linear behavior of J_p with TMP shown in Fig. 7.6 means that the process is mainly controlled by convection; however, accumulation of species near the membrane takes place and concentration polarization layer contributes, to some extent, as a resistance to permeation. Variation of J_p with TMP during the concentration process for the 15 kDa membrane is depicted in Fig. 7.7: J_p was kept constant during the concentration process by ultrafiltration, indicating stable conditions of the membrane surface and polarization layer during this stage.

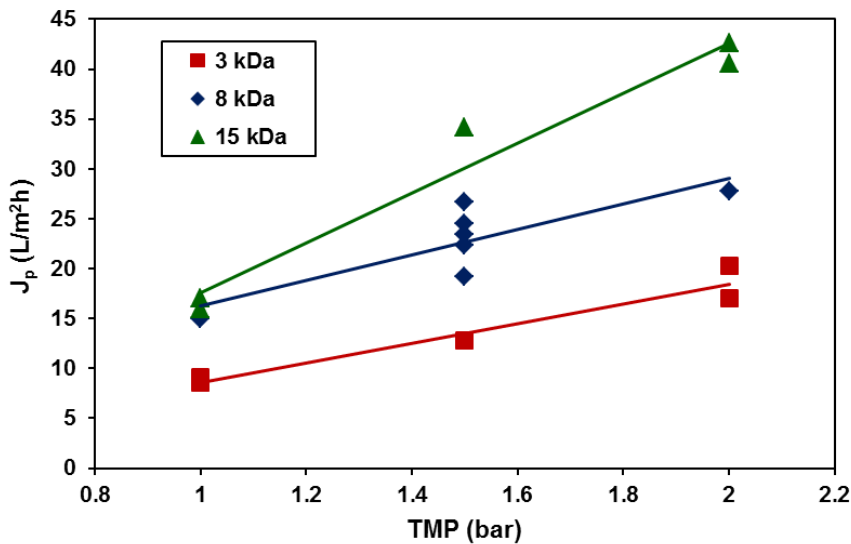


Figure 7.6. Permeate flux variation with TMP using different NMWL ceramic membranes (3, 8 and 15 kDa). Symbols: experimental data. Lines: behavior trends.

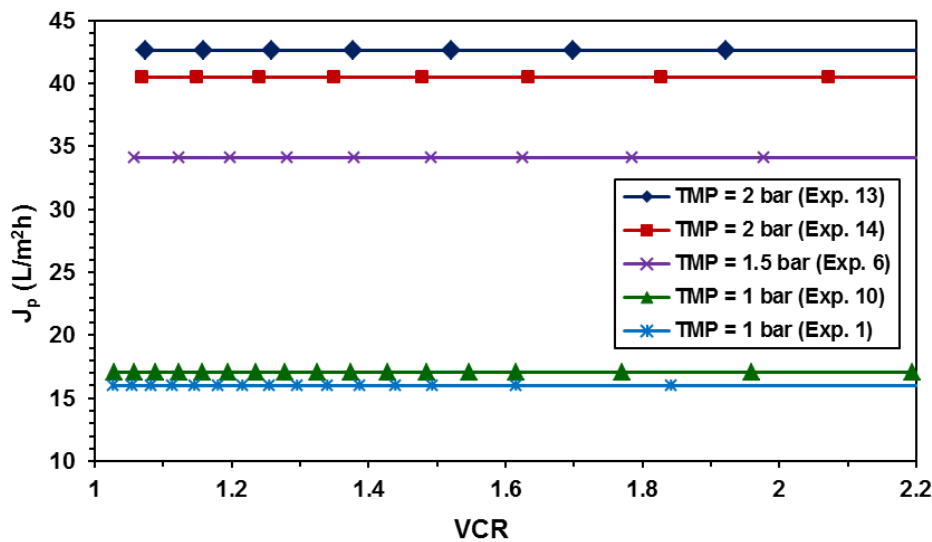


Figure 7.7. Experimental values of the permeate flux during the concentration process by ultrafiltration under different TMP using the 15 kDa membrane. Symbols: experimental data. Lines: behavior trends.

As it stated above, niosomes are broken at pH > 12 and large Span 80 aggregates and mixed micelles of Span 80 and SDS coexist in equilibrium with SDS monomers in the dispersion (F_{bis}). During the UF process, retention of large aggregates and micelles take place by sieving effect of the UF membranes, as the pore size is assumed to be lower than the size of these structures.

It has been documented that the mean pore radius of several 5 to 30 kDa UF polymeric membranes was in the range from 0.8 to 11 nm [31], whereas the SDS micelle radius is about 2.5 nm, with an average molecular weight of 14 kDa [29,31]. Furthermore, the excess of Na^+ cations drives micellar systems towards larger micelles [33–35] and also affect their shape [36]. However, besides sieving, other phenomena such as the effect of membrane charge, adsorption and concentration polarization, can affect the retention of surfactants.

Surfactants have tendency to adsorb at interfaces, so under UF conditions (dispersion F), part of SDS monomers can be adsorbed on the membrane surface and pore walls. Many researchers have demonstrated that for a strongly hydrophilic membrane as the ones used in this work, adsorption is unlikely unless the solute and the membrane have opposite charges [33,37]. However, in this case at $\text{pH} > 12$ the membrane negative charge is partially shielded by the excess of Na^+ ions and adsorption of SDS monomers could take place to some extent [26,38]. SDS monomers can also accumulate in the polarization layer under pressure conditions and form micelles although the SDS concentration in the bulk is lower than the CMC value. The mixed micelles are negatively charged and, although they are unlikely to be associated with the membrane, their presence in the polarization layer is admissible.

SDS monomers concentration has been measured throughout the experimental process, as indicated in Table 7.1. The fraction of SDS forming mixed micelles ($\text{SDS}_{(\text{mx})}$), SDS monomers ($\text{SDS}_{(\text{m})}$), and SDS adsorbed on the membrane and accumulated in the polarization layer ($\text{SDS}_{(\text{M-PL})}$), under UF conditions (dispersion F), were calculated by the following mass balances, where identical fraction of mixed micelles in F and F_{bis} has been assumed:

$$\text{SDS}_{(\text{mx})} = \frac{\text{C}_{\text{S}}(\text{F}_{\text{d}})\text{V}_{(\text{Fd})} - \text{C}_{\text{S}}(\text{F}_{\text{bis}})\text{V}_{(\text{F}_{\text{bis}})}}{\text{C}_{\text{S}}(\text{F}_{\text{d}})\text{V}_{(\text{Fd})}} \quad (5)$$

$$\text{SDS}_{(\text{m})} = \frac{\text{C}_{\text{S}}(\text{F})\text{V}_{(\text{F})}}{\text{C}_{\text{S}}(\text{F}_{\text{d}})\text{V}_{(\text{Fd})}} \quad (6)$$

$$\text{SDS}_{(\text{M-PL})} = 1 - \text{SDS}_{(\text{mx})} - \text{SDS}_{(\text{m})} \quad (7)$$

where C_{S} is the SDS concentration and V is the volume of the dispersion, respectively.

Table 7.6 shows the distribution of the total SDS amount in the dispersion F. Under ultrafiltration conditions, most of the SDS is adsorbed on the membrane or accumulated in the polarization layer ($\text{SDS}_{(\text{M-PL})}$), being this fact the mainly responsible of the permeate flux decrease.

Being a process mainly controlled by convection, the increase of the driving force as TMP increases leads to the SDS monomers accumulated in the boundary layer to pass through the membrane whose charge is shielded by Na^+ ions. It should be taken into account that the excess of Na^+ ions cause micelles destabilization, resulting in a less compact micellar layer which facilitates permeation of the SDS monomers [29,33,39]. This fact is observed in Fig. 7.8a, where the amount of SDS monomers, that freely pass through the membrane, increases as TMP increases, thereby decreasing the membrane rejection to SDS, as shown in Fig. 7.8b. These results show the existence of an antagonistic behavior between J_p and R_s , to the extent that R_s decreases as J_p increases, as depicted in Fig. 7.9. A similar behavior of permeate flux increase, as well as surfactant concentration in permeates, with TMP can be found elsewhere [29,32,40].

Table 7.6. Distribution of total SDS amount in dispersion F under ultrafiltration conditions: mixed micelles, $\text{SDS}_{(mx)}$, free monomers, $\text{SDS}_{(m)}$, and adsorbed on the membrane and accumulated in the polarization layer, $\text{SDS}_{(M-PL)}$.

Experiment	$\text{SDS}_{(mx)}$ (wt.%)	$\text{SDS}_{(m)}$ (wt.%)	$\text{SDS}_{(M-PL)}$ (wt.%)
1	38.40	8.64	52.96
2	34.77	10.92	54.31
3	37.31	8.64	54.05
4	33.75	9.41	56.84
5	37.49	9.12	53.39
6	41.81	10.48	47.71
7	35.08	9.40	55.53
8	33.26	9.29	57.45
9	33.87	10.67	55.46
10	34.07	11.18	54.75
11	35.62	8.47	55.91
12	36.39	9.58	54.02
13	36.53	11.12	52.35
14	34.07	11.18	54.75
15	35.19	10.74	54.07
16	32.84	11.70	55.46
17	33.75	9.41	56.84

Separation of sodium lactate from Span 80 and SDS surfactants by ultrafiltration

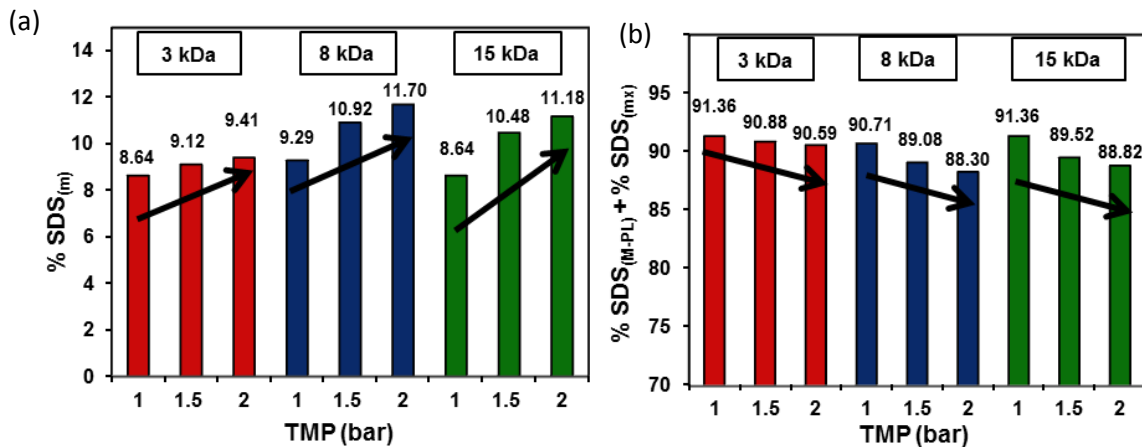


Figure 7.8. Variation of SDS amount (wt.%) with TMP in the dispersion F: (a) SDS monomers, (b) SDS in mixed micelles plus adsorbed on the membrane and accumulated in the polarization layer.

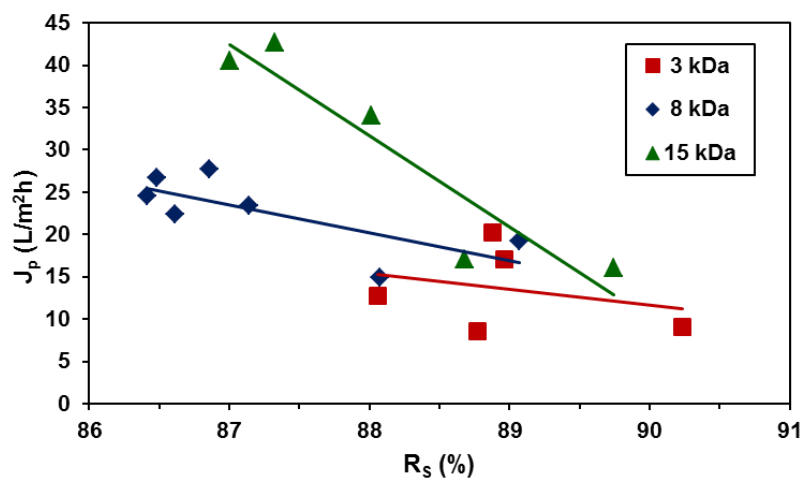


Figure 7.9. Relationships between the permeate flux and SDS rejection under ultrafiltration conditions. Symbols: experimental data. Lines: behavior trends.

The effects of TMP and Na⁺ ions presence on J_p have also been tested for single surfactant dispersions using the 15 kDa membrane and the results have been compared with those of the surfactant mixtures. Fig. 7.10 shows that permeate flux increases with TMP for all systems but it also depends on the medium composition.

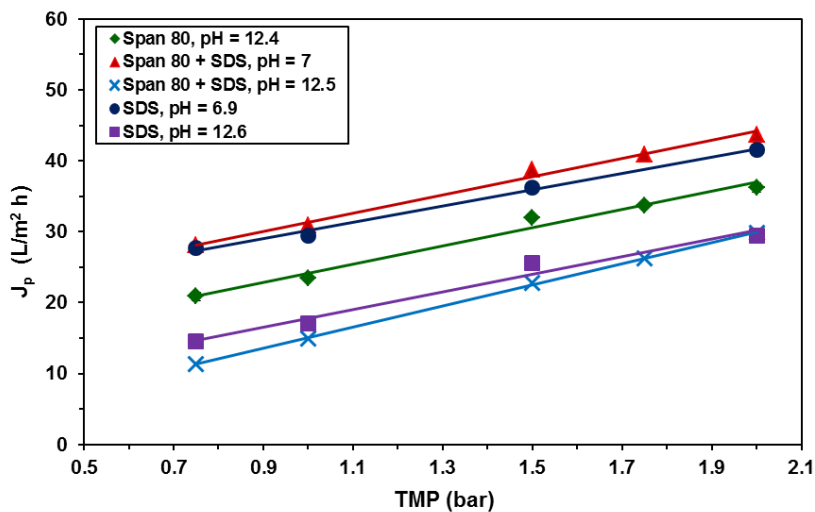


Figure 7.10. Relationships between the permeate flux and TMP for different medium compositions. Symbols: experimental data. Lines: behavior trends.

The higher fluxes were obtained for Span 80 (20 mol/m³) + SDS (4 mol/m³) niosome dispersions at natural pH (≈ 7). For this system both niosomes and membrane have negative charge and electrostatic repulsions favor the solvent permeation. The lower flux observed for the dispersion with niosomes formulated only with Span 80 (20 mol/m³) at pH > 12 can be attributed to accumulation of the negatively charged Span 80 large aggregates in the polarization layer, because of the membrane charge shielding by Na⁺ ions. Zeta potential of Span 80 aggregates at pH > 12 was -20 mV, probably due to the adsorption of hydroxyl ions; in addition, the presence of Na⁺ decreases the electrostatic repulsion between particles, which increases their tendency to accumulate in the polarization layer. A much lower J_p was obtained for the system with formulation identical to the first one (Span 80 + SDS) but at pH > 12, with J_p values similar to those achieved for a single SDS dispersion at pH > 12, indicating that the presence of SDS monomers is the main cause of this permeate flux reduction. Comparison of the single SDS systems at pH > 12 and natural pH (≈ 6.9) shows a significant J_p decrease in the former. This result confirms that the Na⁺ ions shield the negatively charged membrane surface and also decrease the electrostatic repulsions between SDS monomers, yielding to their accumulation in the polarization layer.

7.4. Conclusions

ZrO₂ ceramic ultrafiltration membranes can be successfully used for the separation of ion lactate from the surfactants Span 80 and SDS in aqueous solutions at pH > 12. Process optimization by RSM showed that, in the range of conditions studied (TMP: 1–2 bar, NMWL: 3–15 kDa, and C_A: 5–15 mol/m³), best results were obtained for the 15 kDa membrane and a transmembrane pressure of 2 bar. Under these conditions the permeate flux (J_p) was 42.63 L/m²h and SDS rejection (R_s) was 87.3%. Ion lactate concentration effect was not statistically significant on J_p and its rejection was lower than 4.5%. Span 80 rejection was 100% in all range of experimental conditions tested, as it forms large aggregates that are retained by membranes.

Although the differences between R_s values were not statistically significant with 95% significance level, an antagonistic behavior between R_s and J_p has been experimentally tested. It was observed that UF process was mainly controlled by convection and J_p increased as TMP increases, being this effect more appreciable for membranes with higher NMWL. Besides, as J_p increases part of SDS molecules adsorbed on the membrane or accumulated in the polarization layer pass through the membrane decreasing the SDS monomers rejection. The retention of surfactants at pH > 12 are influenced by three predominant effects: the membrane sieving that yields retention of mixed micelles and large aggregates of Span 80, the de-compaction of the polarization layer due to the micelles destabilization caused by the excess of Na⁺ ions, and the shielding of the negatively charged membrane surface by Na⁺ ions which improves the permeation of SDS monomers as J_p increases.

This study complements a previously one performed with a 0.20 µm TiO₂ microfiltration membrane and 0.3 bar TMP [15] where a significant permeate flux decline was obtained during the separation of components due to SDS monomers accumulated in the polarization layer and adsorbed within the large pores of the microfiltration membrane. A comparison between both studies shows that J_p obtained with the 15 kDa ultrafiltration membrane ($J_p = 42.63 \text{ L/m}^2\text{h}$ at TMP = 2 bar) was higher than the obtained with the 0.20 µm microfiltration membrane ($J_p = 19.19 \text{ L/m}^2\text{h}$ at TMP = 0.3 bar). Besides, smaller decrease of J_p with relation to pure water flux (J_w) was obtained with the UF membrane ($J_p/J_w = 0.61$) than with the microfiltration one ($J_p/J_w = 0.38$). These results indicate an improvement in the extraction-backextraction process of lactic acid with Span 80 and SDS niosomes using ultrafiltration membranes.

Acknowledgments

Financial support from the Ministerio de Economía y Competitividad (MINECO, Spain) through project CTQ2011-25239, and from Junta de Castilla y León through project BU055U16 cofinanced by the European Regional Development Fund (ERDF-FEDER) is gratefully acknowledged. The authors would like to thank Dr. Carlos Álvarez (Scientific Technical Services, University of Oviedo, Spain) for his valuable help and assistance with TEM measurements.

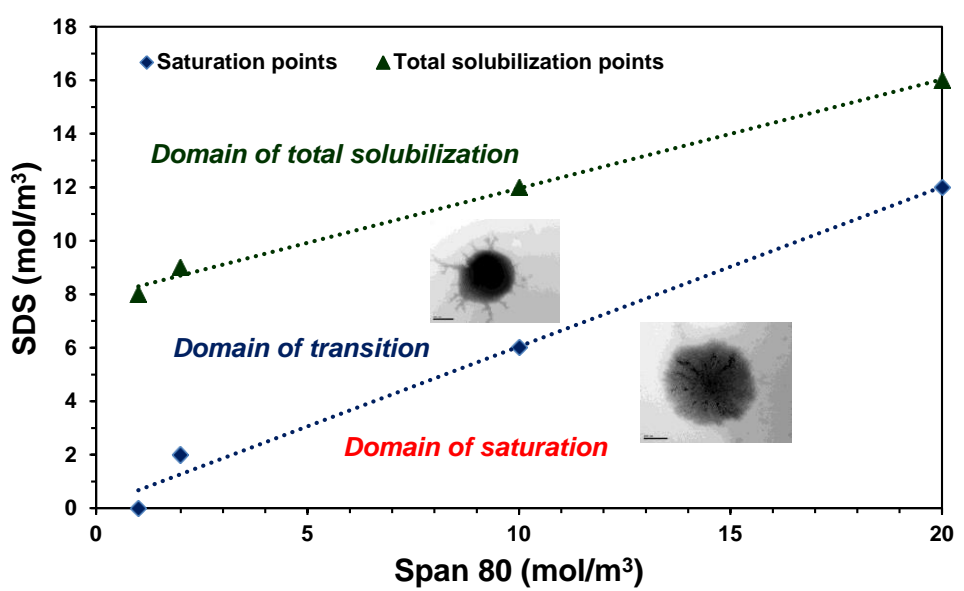
7.5. References

- [1] M.A. Abdel-Rahman, Y. Tashiro, K. Sonomoto, Lactic acid production from lignocellulose-derived sugars using lactic acid bacteria: overview and limits, *J. Biotechnol.* 156 (2011) 286–301.
- [2] R. Datta, S.-P. Tsai, P. Bonsignore, S.-H. Moon, J.R. Frank, Technological and economic potential of poly (lactic acid) and lactic acid derivatives, *FEMS Microbiol. Rev.* 16 (1995) 221–231.
- [3] K.M. Nampoothiri, N.R. Nair, R.P. John, An overview of the recent developments in polylactide (PLA) research, *Bioresour. Technol.* 101 (2010) 8493–8501.
- [4] S. Taskila, H. Ojamo, The current status and future expectations in industrial production of lactic acid by lactic acid bacteria. In: J. Marcelino Kongo (Ed.), *Lactic Acid Bacteria – R&D for Food, Health and Livestock Purposes*, IntechOpen, London (2013).
- [5] K.L. Wasewar, A.A. Yawalkar, J.A. Moulijn, V.G. Pangarkar, Fermentation of glucose to lactic acid coupled with reactive extraction: a review, *Ind. Eng. Chem. Res.* 43 (2004) 5969–5982.
- [6] D. Yankov, J. Molinier, J. Albet, G. Malmary, G. Kyuchoukov, Lactic acid extraction from aqueous solutions with tri-n-octylamine dissolved in decanol and dodecane, *Biochem. Eng. J.* 21 (2004) 63–71.
- [7] P. Pal, J. Sikder, S. Roy, L. Giorno, Process intensification in lactic acid production: a review of membrane based processes, *Chem. Eng. Process.* 48 (2009) 1549–1559.
- [8] H. Huang, S.T. Yang, D.E. Ramey, A hollow-fiber membrane extraction process for recovery and separation of lactic acid from aqueous solution, *Appl. Biochem. Biotechnol.* 114 (2004) 671–688.
- [9] R.-S. Juang, J.-D. Chen, H.-C. Huan, Dispersion-free membrane extraction: case studies of metal ion and organic acid extraction, *J. Membr. Sci.* 165 (2000) 59–73.
- [10] M. Rodríguez, M.J. González-Muñoz, S. Luque, J.R. Álvarez, J. Coca, Extractive ultrafiltration for the removal of carboxylic acids, *J. Membr. Sci.* 274 (2006) 209–218.

- [11] R.M. Geanta, M.O. Ruiz, I. Escudero, Micellar-enhanced ultrafiltration for the recovery of lactic acid and citric acid from beet molasses with sodium dodecyl sulphate, *J. Membr. Sci.* 430 (2013) 11–23.
- [12] J. Landaburu-Aguirre, E. Pongrácz, R.L. Keiski, Separation of cadmium and copper from phosphorous rich synthetic waters by micellar-enhanced ultrafiltration, *Sep. Purif. Technol.* 81 (2011) 41–48.
- [13] J. Landaburu-Aguirre, E. Pongrácz, A. Sarpola, R.L. Keiski, Simultaneous removal of heavy metals from phosphorous rich real wastewaters by micellar-enhanced ultrafiltration, *Sep. Purif. Technol.* 88 (2012) 130–137.
- [14] M.O. Ruiz, J.M. Benito, B. Barriuso, J.L. Cabezas, I. Escudero, Equilibrium distribution model of betaine between surfactant micelles and water: application to a micellar-enhanced ultrafiltration process, *Ind. Eng. Chem. Res.* 49 (2010) 6578–6586.
- [15] L. Roque, I. Escudero, J.M. Benito, Lactic acid recovery by microfiltration using niosomes as extraction agents, *Sep. Purif. Technol.* 151 (2015) 1–13.
- [16] E. Acosta, Bioavailability of nanoparticles in nutrient and nutraceutical delivery, *Curr. Op. Colloid Interface Sci.* 14 (2009) 3–15.
- [17] Y.-M. Hao, K. Li, Entrapment and release difference resulting from hydrogen bonding interactions in niosome, *Int. J. Pharm.* 403 (2011) 245–253.
- [18] C. Marianelli, L. Di Marzio, F. Rinaldi, C. Celia, D. Paolino, F. Alhaique, S. Esposito, M. Carafa, Niosomes from 80s to present: the state of the art, *Adv. Colloid Interface Sci.* 205 (2014) 187–206.
- [19] D.J. McClements, E.A. Decker, Y. Park, J. Weiss, Structural design principles for delivery of bioactive components in nutraceuticals and functional foods, *Crit. Rev. Food Sci. Nutr.* 49 (2009) 577–606.
- [20] A.Y. Waddad, S. Abbad, F. Yu, W.L.L. Munyendo, J. Wang, H. Lv, J. Zhou, Formulation, characterization and pharmacokinetics of Morin hydrate niosomes prepared from various non-ionic surfactants, *Int. J. Pharm.* 456 (2013) 446–458.
- [21] R. Fraile, R.M. Geanta, I. Escudero, J.M. Benito, M.O. Ruiz, Formulation of Span 80 niosomes modified with SDS for lactic acid entrapment, *Desalin. Water Treat.* 56 (2015) 3463–3475.
- [22] L. Alonso, L. Roque, I. Escudero, J.M. Benito, M.T. Sanz, S. Beltrán, Solubilization of Span 80 niosomes by sodium dodecyl sulfate, *ACS Sustain. Chem. Eng.* 4 (2016) 1862–1869.
- [23] B.A. Uzoukwu, L.M.L. Nollet, Analysis of surfactants. In: L.M.L. Nollet (Ed.), *Handbook of Water Analysis*, Marcel Dekker, New York (2000), pp. 767–784.

- [24] M. Kaszuba, J. Corbett, F.M. Watson, A. Jones, High-concentration zeta potential measurements using light-scattering techniques, *Philos. Trans. R. Soc. A-Math. Phys. Eng. Sci.* 368 (2010) 4439–4451.
- [25] J. Wei, Q. Xue, Effects of surfactants on the tribological properties of a Cr₂O₃ coating, *Wear* 162–164 (1993) 229–233.
- [26] E. Samper, M. Rodríguez, M.A. De la Rubia, D. Prats, Removal of metal ions at low concentration by micellar-enhanced ultrafiltration (MEUF) using sodium dodecyl sulfate (SDS) and linear alkylbenzene sulfonate (LAS), *Sep. Purif. Technol.* 65 (2009) 337–342.
- [27] K. Xu, G.-M. Zeng, J.-H. Huang, J.-Y. Wu, Y.-Y. Fang, G. Huang, J. Li, B. Xi, H. Liu, Removal of Cd²⁺ from synthetic wastewater using micellar-enhanced ultrafiltration with hollow fiber membrane, *Colloid Surf. A-Physicochem. Eng. Asp.* 294 (2007) 140–146.
- [28] J.-S. Yang, K. Baek, J.-W. Yang, Crossflow ultrafiltration of surfactant solutions, *Desalination* 184 (2005) 385–394.
- [29] I. Kowalska, M. Kabsch-Korbutowicz, K. Majewska-Nowak, T. Winnicki, Separation of anionic surfactants on ultrafiltration membranes, *Desalination* 162 (2004) 33–40.
- [30] A. Patist, P.D.T. Huibers, B. Deneka, D.O. Shah, Effect of tetraalkylammonium chlorides on foaming properties of sodium dodecyl sulfate solutions, *Langmuir* 14 (1998) 4471–4474.
- [31] K. Majewska-Nowak, I. Kowalska, M. Kabsch-Korbutowicz, Ultrafiltration of SDS solutions using polymeric membranes, *Desalination* 184 (2005) 415–422.
- [32] E. Fernández, J.M. Benito, C. Pazos, J. Coca, Ceramic membrane ultrafiltration of anionic and nonionic surfactant solutions, *J. Membr. Sci.* 246 (2005) 1–6.
- [33] L. Suárez, M.A. Diez, F.A. Riera, Transport mechanisms of detergent ingredients through ultrafiltration membranes, *Sep. Purif. Technol.* 136 (2014) 115–122.
- [34] F.H. Quina, P.M. Nassar, J.B.S. Bonilha, B.L. Bales, Growth of sodium dodecyl sulfate micelles with detergent concentration, *J. Phys. Chem.* 99 (1995) 17028–17031.
- [35] M. Sammalkorpi, M. Karttunen, M. Haataja, Ionic surfactant aggregates in saline solutions: sodium dodecyl sulfate (SDS) in the presence of excess sodium chloride (NaCl) or calcium chloride (CaCl₂), *J. Phys. Chem. B* 113 (2009) 5863–5870.
- [36] C.S. Gangabadage, A. Najda, D. Bogdan, S.S. Wijmenga, M. Tessari, Dependence of the size of a protein-SDS complex on detergent and Na⁺ concentrations, *J. Phys. Chem. B.* 112 (2008) 4242–4245.
- [37] A.-S. Jönsson, B. Jönsson, The influence of nonionic and ionic surfactants on hydrophobic and hydrophilic ultrafiltration membranes, *J. Membr. Sci.* 56 (1991) 49–76.
- [38] L. Villafaña-López, M. Ávila-Rodríguez, M.P. González-Muñoz, Study of the zeta potential and streaming current of ultrafiltration membranes in contact with an anionic surfactant,

- Desalin. Water Treat.* 56 (2015), 3456–3462.
- [39] I. Kowalska, Surfactant removal from water solutions by means of ultrafiltration and ion-exchange, *Desalination* 221 (2008) 351–357.
- [40] I. Kowalska, K. Majewska-Nowak, M. Kabsch-Korbutowicz, Influence of temperature on anionic surface active agent removal from water solution by ultrafiltration, *Desalination* 198 (2006) 124–131.



8. Solubilization of Span 80 niosomes by sodium dodecyl sulfate

En este capítulo se aborda el estudio del proceso de solubilización de los niosomas formulados con el tensioactivo monooleato de sorbitán (Span 80) con la adición del tensioactivo aniónico dodecil sulfato de sodio (SDS). Para la preparación de los niosomas se empleó el método de sonicación.

La densidad óptica (longitud de onda a 350 nm), la distribución del tamaño de partícula, el potencial zeta y la concentración de monómeros de SDS de las dispersiones fueron los principales parámetros estudiados en este trabajo.

Los resultados permitieron distinguir las diferentes etapas del proceso de solubilización, permitiendo determinar los puntos críticos de saturación del SDS adsorbido en la bicapa niosomal y la solubilización total de los niosomas. En el diagrama de equilibrio de pseudo-fases, se observó que los puntos de saturación y solubilización total siguen un comportamiento lineal.

Los puntos críticos de solubilización total fueron corroborados mediante la medición de la concentración de monómeros de SDS. Así mismo, se confirmó que la cantidad de SDS añadida a la dispersión por encima de los valores críticos de solubilización total se agrega formando micelas mixtas, las cuales aumentan su concentración, mientras que la concentración de SDS monomérica se mantiene constante. Estos resultados verifican que la solubilización de los niosomas se lleva a cabo mediante un proceso de micelización.

Los resultados de este trabajo pueden ayudar en la formulación de niosomas estables para aplicaciones que requieran del uso de estos sistemas mixtos biodegradables.

Este trabajo ha sido publicado en la revista *ACS Sustainable Chemistry & Engineering*, 4 (2016) 1862–1869. <https://doi.org/10.1021/acssuschemeng.6b00148>

8.1. Introduction

Niosomes are non-ionic surfactant vesicles formed by one or more surfactant bilayers enclosing an aqueous inside cavity [1,2]. Similarly to liposomes, both hydrophilic and hydrophobic compounds can be encapsulated inside their core and in the niosome bilayer, respectively [3]. Niosomes are preferred to liposomes because of their greater chemical stability, high purity, low cost, content uniformity, and easy handling and storage [4]. The large number of non-toxic and relatively low-cost non-ionic surfactants available for niosomes formulation [5,6] provide their large-scale production in pharmaceutical, cosmetic and, to a lesser extent, food applications [7–11].

The use of niosomes as extraction agents of solutes at very low concentration in aqueous solutions is a new application in the field of green and sustainable processes that has barely been explored. The encapsulation efficiency of lactic acid by niosomes of Span 80 (sorbitan monooleate) and SDS (sodium dodecyl sulfate) was investigated in a previous work [12]. Results revealed that SDS acts as a niosome bilayer stabilizer, also providing a synergistic effect on lactic acid encapsulation in formulations with a SDS molar fraction lower than 0.4. Kinetics and equilibrium capacities of niosomes for lactic acid extraction under different medium conditions were investigated in a recent work [13], in order to attain acceptable levels of lactic acid extraction from dilute aqueous solutions. The best conditions were achieved with niosomes formulated with 20 mol/m³ Span 80 and 4 mol/m³ SDS, a SDS to lactic acid molar ratio of 0.01, and pH lower than the pKa of lactic acid, yielding a 33% of lactic acid extraction degree after 40 min contact time, when the equilibrium conditions were reached.

This work aims to study the Span 80 niosome solubilization by interactions with increasing amounts of the anionic surfactant SDS. A similar process has been studied in the liposome solubilization by SDS and described as a three-stage model [14–17]: liposome saturation, progressive transformation of the mixed bilayer into lipid-rich mixed micelles, and finally, complete solubilization of liposomes as mixed micelles.

To our knowledge, the solubilization process of niosomes by ionic surfactants has not been studied yet, but a similar solubilization mechanism can be *a priori* accepted. In the initial stage, the gradual incorporation of the SDS monomers to the vesicles until saturation occurs, yielding to coexisting vesicles and SDS monomers in the dispersion medium, while the presence of monomers of non-ionic surfactant is highly unlikely because of its extremely low water solubility. Some authors [15–17] have verified the formation of mixed micelles during the adsorption step,

so that the void produced by the expulsion of the mixed micelles in the bilayer is filled by new surfactant adsorbed in it. In the second stage, at higher concentrations of SDS, the vesicles solubilization begins or intensifies yielding the mixed micelles formation, so that vesicles, mixed micelles and SDS monomers coexist in solution. In the last stage, the complete solubilization of vesicles is reached and the mixed micelles coexist in equilibrium with the SDS monomers. Complete solubilization of vesicles leads to modification of the medium properties, and represents a critical point in the behavior of some parameters such as light absorption, conductivity or refractive index. The SDS added above this critical point is aggregated in mixed micelles, keeping constant the concentration of monomeric SDS in solution. The SDS concentration that produces the complete solubilization of vesicles by micellization is the critical micellar concentration of total solubilization of vesicles (CMC of total solubilization) and depends on the formulation of the vesicles and the properties of the dispersion medium. The CMC of total solubilization is named in the literature as CMC [18,19], and its interpretation can be misleading.

The CMC of SDS in water is 8.3 mol/m^3 [20–22]. This value represents the concentration above which the SDS surfactant molecules aggregate to form micelles which remain in equilibrium with their monomers at a constant concentration equal to the CMC. The SDS concentration needed to achieve the total solubilization of vesicles is well above the CMC of SDS, and this fact is explained in the literature as an increase of the CMC value by the presence of vesicles in the suspensions. However, it should be noted that, above the CMC of total solubilization, the concentration of SDS monomers that remain in equilibrium with the mixed micelles is much lower than the value of the CMC of the SDS surfactant alone, as it will be further discussed in this study.

The increasing use of niosomes as encapsulating agents in several applications has resulted in the continuous development of vesicular systems whose efficiency should be tested. Solubility and stability are the most important key aspects of any successful formulation. However, formulations with biodegradable or food-grade surfactants, as those used in this work, should be used in order to ensure their chemical and environmental sustainability. The results of this study shed light on the stages of the solubilization process of Span 80 niosomes by the SDS presence and allow the construction of the pseudo-phase equilibrium diagram. Its knowledge is of paramount interest in formulations of these mixed systems regarding their possible use in multiple applications.

8.2. Experimental section

Materials. The non-ionic surfactant sorbitan monooleate (Span 80, Sigma-Aldrich) and the anionic surfactant sodium dodecyl sulfate (SDS, 99%, Sigma-Aldrich) were used as supplied throughout the experiments. For the determination of SDS concentration the following chemicals were used: ethyl violet (99%, Sigma-Aldrich), glacial acetic acid of analysis quality (Panreac), sodium acetate for analysis (Merck), anhydrous sodium sulfate for analysis (Scharlau), toluene (>99.5%, AnalarNormapur VWR Chemicals) and ethylenediaminetetraacetic acid (EDTA, >99%, Sigma-Aldrich). Ultrapure deionized Milli-Q water (Millipore, USA), with a conductivity of 0.1 $\mu\text{S}/\text{cm}$, was used for the preparation of all solutions.

Niosome preparation. Single surfactant aqueous solutions of 1, 2, 10 and 20 mol/m^3 Span 80 were prepared 24 h before their use, in order to hydrate and relax the carbonated chains of its molecular structure, weighing out the exact amounts of surfactant on an analytical balance (Sartorius, accurate to ± 0.0001 g), and with deionized water addition up to a final volume of 100 cm^3 . Niosomes were prepared by direct ultrasonication of 10 cm^3 Span 80 aqueous solutions in round-based polystyrene tubes, 115 mm in height and 29 mm in diameter, supplied by Labbox (Spain). The application of ultrasounds was carried out over a 5-min effective time, with pulses every 5 s (5 s on and 5 s off, 60 cycles; 30% amplitude, 500 W), to avoid overheating of the sample, using a high-intensity ultrasonic processor (Vibra-Cell VCX 500, Sonics & Materials Inc., USA) equipped with a 3 mm-diameter titanium alloy bicylindrical probe. The 1 cm skirt at the base of polystyrene tubes assisted homogeneous probe positioning in all samples. Throughout the ultrasonication process, the samples were immersed in an ice bath to prevent chemical degradation. Subsequently, the samples were centrifuged (Eppendorf 5804 centrifuge) in 15 cm^3 polystyrene centrifuge tubes for 45 min at 9000 rpm, in order to remove traces of metal that could be detached from the probe.

Solubilization experiments. Niosome solubilization experiments were carried out in 10 cm^3 blisters by contacting 5 cm^3 of the niosome suspension with different volumes of a 100 mol/m^3 SDS aqueous solution. The composition of samples is shown in Table 8.1 Samples were maintained in an incubator shaker (Model G25, New Brunswick Scientific Co) at 150 rpm and 25 °C during predetermined periods of time, after which they were analyzed by the undermentioned techniques.

Table 8.1. Composition of samples.

Sample name*	Concentration of Span 80		Concentration of SDS
	in niosomes (mol/m ³)	in the sample (mol/m ³)	
C1S0 / C2S0 / C10S0 / C20S0	1 / 2 / 10 / 20	0	
C1S2 / C2S2 / C10S2 / C20S2	1 / 2 / 10 / 20	2	
C1S4 / C2S4 / C10S4 / C20S4	1 / 2 / 10 / 20	4	
C1S6 / C2S6 / C10S6 / C20S6	1 / 2 / 10 / 20	6	
C1S8 / C2S8 / C10S8 / C20S8	1 / 2 / 10 / 20	8	
C1S10 / C2S10 / C10S10 / C20S10	1 / 2 / 10 / 20	10	
C1S12 / C2S12 / C10S12 / C20S12	1 / 2 / 10 / 20	12	
C1S14 / C2S14 / C10S14 / C20S14	1 / 2 / 10 / 20	14	
C1S16 / C2S16 / C10S16 / C20S16	1 / 2 / 10 / 20	16	
C1S18 / C2S18 / C10S18 / C20S18	1 / 2 / 10 / 20	18	
C1S20 / C2S20 / C10S20 / C20S20	1 / 2 / 10 / 20	20	
C1S22 / C2S22 / C10S22 / C20S22	1 / 2 / 10 / 20	22	
C1S24 / C2S24 / C10S24 / C20S24	1 / 2 / 10 / 20	24	

* Identified as CxSy where x and y represent the Span 80 and SDS individual sample concentrations, respectively.

Analytical methods. Turbidity of each sample was measured at different contact times after addition of SDS. A total sample volume of 1.2 cm³ was placed in a quartz cuvette (10 x 10 mm) and its optical density (O.D.) was measured at a 350 nm wavelength using a double beam UV-vis spectrophotometer (Hitachi U-2000). Milli-Q water was used as blank. Previously, it was checked that the optical density at 350 nm wavelength provided a good sensitivity to the turbidity caused by the presence of niosomes, whose size is well above than that of smaller size micelles. The same wavelength was used by Deo and Somasundaran in their study on liposome solubilization by SDS [18].

SDS monomer concentration was determined by spectrophotometry at a 615 nm wavelength (Hitachi U-2000 spectrophotometer), according to the ethyl violet method [23].

The samples were measured in triplicate in the case of SDS standards (0–12 mg/L), and twice in the case of experimental samples. For this, aliquots of Span 80 niosomes and SDS samples shown in Table 8.1, after 1 h of interaction, were ultrafiltered using Millipore Amicon Ultra-4 units with 3 kDa cut-off regenerated cellulose membranes and centrifuged (Eppendorf 5804 centrifuge) at 9000 rpm for 10 min. Permeates, free of niosomes and micelles, were suitably diluted before being analyzed.

The particle size distribution, the mean hydrodynamic diameter and the polydispersity index (PDI) of the samples were measured by dynamic light scattering (DLS) using a Zetasizer Nano ZS apparatus (Malvern Instruments Ltd., UK). The apparatus was equipped with a He-Ne laser emitting at 633 nm and with a 4.0 mW power source. It was set for backscattering detection at a scattering angle of 173°. Samples were diluted 1:100 to avoid multiple scattering effects and filtered with 0.45 µm Minisart RC 15 filters. Measurements were performed in DTS0012 square disposable polystyrene cells at 20 °C. Three replicates, each of 20 runs, were performed for each sample. The values shown in the tables and figures are the average value of the 3 replicates with the relative measurement error. The PDI is a dimensionless measure of the width of the size distribution ranging from 0 to 1, a higher value being indicative of a broader distribution of particle size [24,25].

The ζ -potential measurements were conducted with the aforementioned Zetasizer Nano ZS apparatus, using the Laser Doppler Velocimetry technique. They were performed on the same sample previously prepared to measure the particle size, but using the appropriate DTS1061 disposable folded capillary cell equipped with electrodes to allow the passage of electric current and the movement of the particles according to their charge. The ζ -potential is calculated using Henry's equation and the Smoluchowski approximation, which considers that the double layer thickness is much smaller than the particle size [26]. Six replicates of 11 measurements were performed for each sample at 20 °C. Figures and tables show average values of the 6 runs with the relative measurement error.

The pH was measured at 20 °C using a Crison GLP 22 pH-meter fitted with a Crison 52-02 glass pH electrode, with an error of ± 0.01 pH units.

Morphological analysis of niosomes was performed by negative staining transmission electron microscopy (NS-TEM), using a JEOL-2000 EX-II TEM operating at 160–180 kV, with an image resolution of 1 nm, located at the University of Oviedo (Spain). A drop of the selected niosome formulation was placed on a carbon-coated copper grid, and the sample excess was removed using a piece of filter paper.

Then, a drop of phosphotungstic acid solution (2% w/v) was applied to the carbon grid and left for 2 min. Once the excess of staining agent was removed by absorbing with the filter paper, the sample was air-dried and the thin film of stained niosomes was observed by TEM.

8.3. Results and discussion

Turbidity Variation throughout the Solubilization Process. The optical density variation of 1, 2, 10, and 20 mol/m³ Span 80 niosomes caused by the SDS surfactant presence at different contact times was measured. Fig. 8.1 shows results after 1 and 24 h contact times. A turbidity decrease due to the niosome solubilization by the addition of increasing SDS concentrations can be observed in all Span 80 formulations. Solubilization curves practically overlap, indicating that contact time does not significantly affect the determination of the critical points. Solubilization curves for contact times between 1 and 24 h were also measured (Fig. S1, Supporting Information).

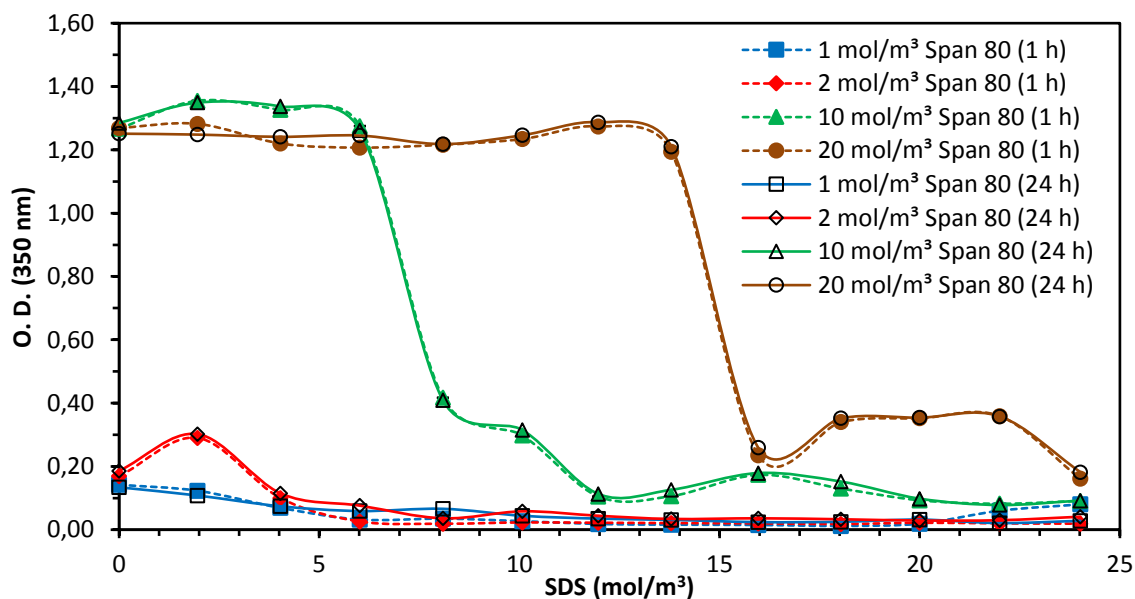


Figure 8.1. Solubilization curves of 1, 2, 10, and 20 mol/m³ Span 80 niosomes by SDS after 1 and 24 h contact times.

In SDS absence, optical density increases from 0.14 for 1 mol/m³ Span 80 niosomes to 1.27 for 10 and 20 mol/m³ Span 80 niosomes, as a result of both the higher concentration and the larger size of niosomes (as discussed later in connection with Table S1, Supporting Information).

In the solubilization curves the point of maximum optical density corresponds to saturation of niosomes by SDS. However, the minimum optical density corresponds to the complete solubilization of the niosome bilayer. Between the two points niosomes and mixed micelles coexist with SDS monomers in suspension. There is a continuous decrease of turbidity as the SDS concentration increases for 1 mol/m³ Span 80 niosomes, indicating that disruption of the bilayer takes place with the addition of very low SDS concentration and the saturation point is not observed for this formulation. The increase in the optical density observed for 2 mol/m³ Span 80 niosomes may be due to the increase in the size of the niosomes caused by the adsorption of SDS on their surface. Adsorption of SDS in 10 and 20 mol/m³ Span 80 niosomes hardly modifies the turbidity because niosomes are already large; however, saturation points are clearly identified in 6 and 12 mol/m³ of SDS, just before starting the sharp slope. The critical points of saturation and total solubilization of the niosomes are shifted to higher concentrations of SDS as the Span 80 concentration in niosomes increases, indicating that more SDS is required to disrupt the bilayers, which is in agreement with the literature on liposomes [18].

Critical points of saturation and total solubilization of niosomes by SDS are shown in Table 8.2. They correspond to the slope change in turbidity curves of Figs. 8.1 and S1 (Supporting Information). The total solubilization critical points will be confirmed later by measurement of monomeric SDS concentrations shown in Fig. 8.4.

Table 8.2. Critical points of saturation and total solubilization of 1, 2, 10, and 20 mol/m³ Span 80 niosomes by SDS.

Critical point of saturation		Critical point of total solubilization	
Span 80 (mol/m ³)	SDS (mol/m ³)	Span 80 (mol/m ³)	SDS (mol/m ³)
1	0	1	8
2	2	2	9
10	6	10	12
20	12	20	16

In the formulations with 1 and 2 mol/m³ Span 80 niosomes (Fig. S1a,b, Supporting Information) a slight increased turbidity with the SDS contact time is observed, that may be attributed to the association of the smaller mixed micelles in larger micelles due to its instability.

The influence of the contact time has been observed in several works on liposome solubilization by SDS using continuous analytical measurements [15,17,18,27,28]. Equilibrium time of 20 h was established for the stability of the mixed micelles of phosphatidylcholine and SDS by monitoring the variation in the static light scattered [27]. In this work, dispersion stability was measured by DLS and ζ -potential and it will be commented later. However, it was found that the composition of the critical points does not depend on contact time within the assay times tested (Figs. 8.1 and S1, Supporting Information).

Data of Table 8.2 are plotted in the pseudo-phase diagram shown in Fig. 8.2, where the bottom and upper lines correspond to the saturation and total solubilization lines, respectively. They fit a linear behavior with correlation coefficients close to 0.99. Similar pseudo-phase diagrams were obtained for the solubilization of triglycerides and egg phosphatidylcholine liposomes by the non-ionic surfactant Triton X-100 [29]. Below the saturation line, niosomes and SDS monomers coexist in equilibrium conditions. Due to the hydrophobic character of Span 80 (HLB = 4.3) [6], the presence of Span 80 monomers is highly improbable. Moreover, the presence of mixed micelles was observed in the niosome saturation domain, as we discuss later regarding Fig. 8.3. Above the total solubilization line, niosomes do not exist, and mixed micelles and SDS surfactant monomers coexist in equilibrium conditions. In the domain between both lines, niosomes, mixed micelles and SDS monomers are present in the suspension. This intermediate domain is characterized by the intensification of the bilayer solubilization and the mixed micelles formation. It is observed in Fig. 8.2 that the intermediate domain decreases with increasing Span 80 concentration, which reflects the existence of changes in the niosome bilayer structure. Size, PDI, and ζ -potential of 1, 2, 10, and 20 mol/m³ Span 80 niosomes without SDS were measured at different stabilization times after ultrasonication (Table S1, Supporting Information). Results for 1 and 2 mol/m³ Span 80 concentrations have large uncertainties due to their poor stabilities. Comparison of results after long time shows that the higher the Span 80 concentration, the larger the niosomes size and the lower its PDI. The ζ -potential measurements reveal negatively charged particles with higher absolute values, and hence more stable over time, for niosomes formulated with higher Span 80 concentration, for which size and ζ -potential remain largely unchanged in time. Several vesicles formulated with non-ionic surfactants without the inclusion of charged species in the bilayer possess negative ζ -potential attributed to the adsorption of hydroxyl ions [1,11–13].

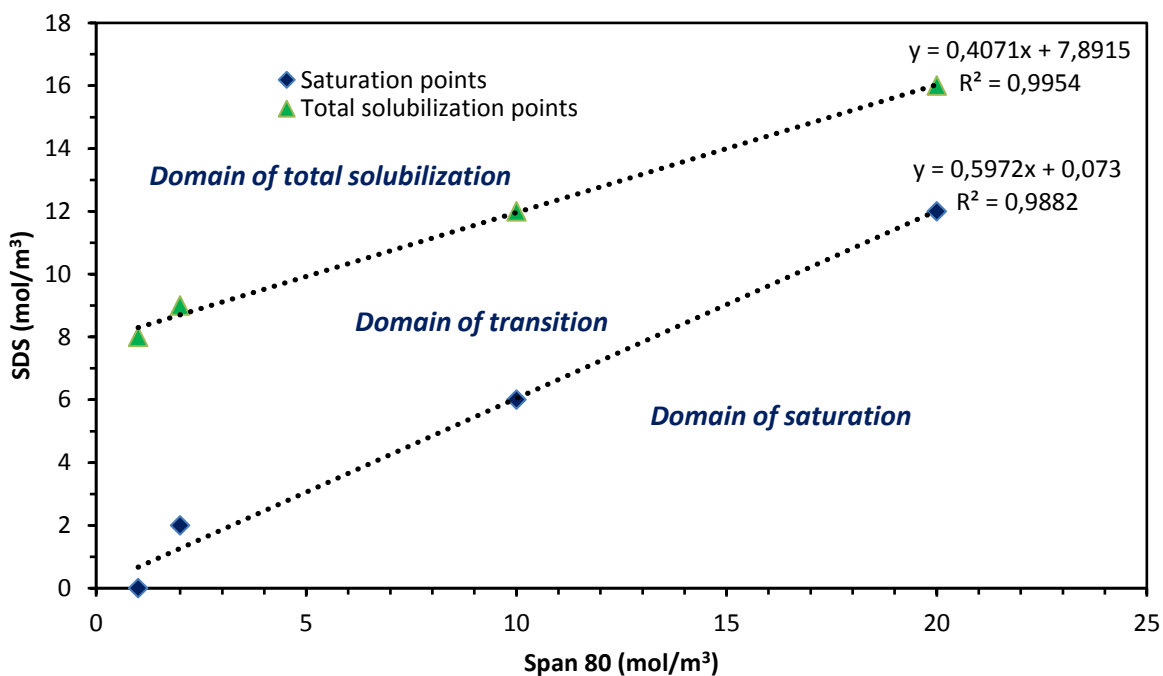


Figure 8.2. Pseudo-phase diagram of solubilization of Span 80 niosomes by SDS.

Size, PDI, and ζ -potential variation in the solubilization process. Size and PDI values after different intervals of contact time of niosomes with increasing amounts of SDS were measured (Fig. S2, Supporting Information). It is possible to discern a first zone for the lower SDS concentrations, where values of $\text{PDI} \leq 0.3$ indicate quite homogeneous particle size population, followed by a second zone with $\text{PDI} \geq 0.4$, with a more heterogeneous population in particle size. The boundary line between both zones corresponds to 0, 2, 6, and 10–12 mol/m³ SDS for the 1, 2, 10, and 20 mol/m³ Span 80 formulations, respectively, which are quite consistent with the saturation points shown in Table 8.2.

As expected, the higher the Span 80 concentration in niosomes, the larger its particle size at the saturation point. Sizes (<130, <147, <180 nm for 2, 10 and 20 mol/m³ Span 80 formulations, respectively) were lower than 200 nm, which is in agreement with the results from a previous work [13]. It must be noted that the sizes of niosomes at the saturation point with SDS were not larger than those without SDS. Such result was also obtained in previous works [12,13]. The increased size of liposomes due to the SDS adsorption on its surface has been shown in different works [18,30,31]. However, there are theoretical studies indicating a decrease in distance between lipid molecules in the presence of SDS [32], which may justify our results of niosome shrinkage by SDS intercalation.

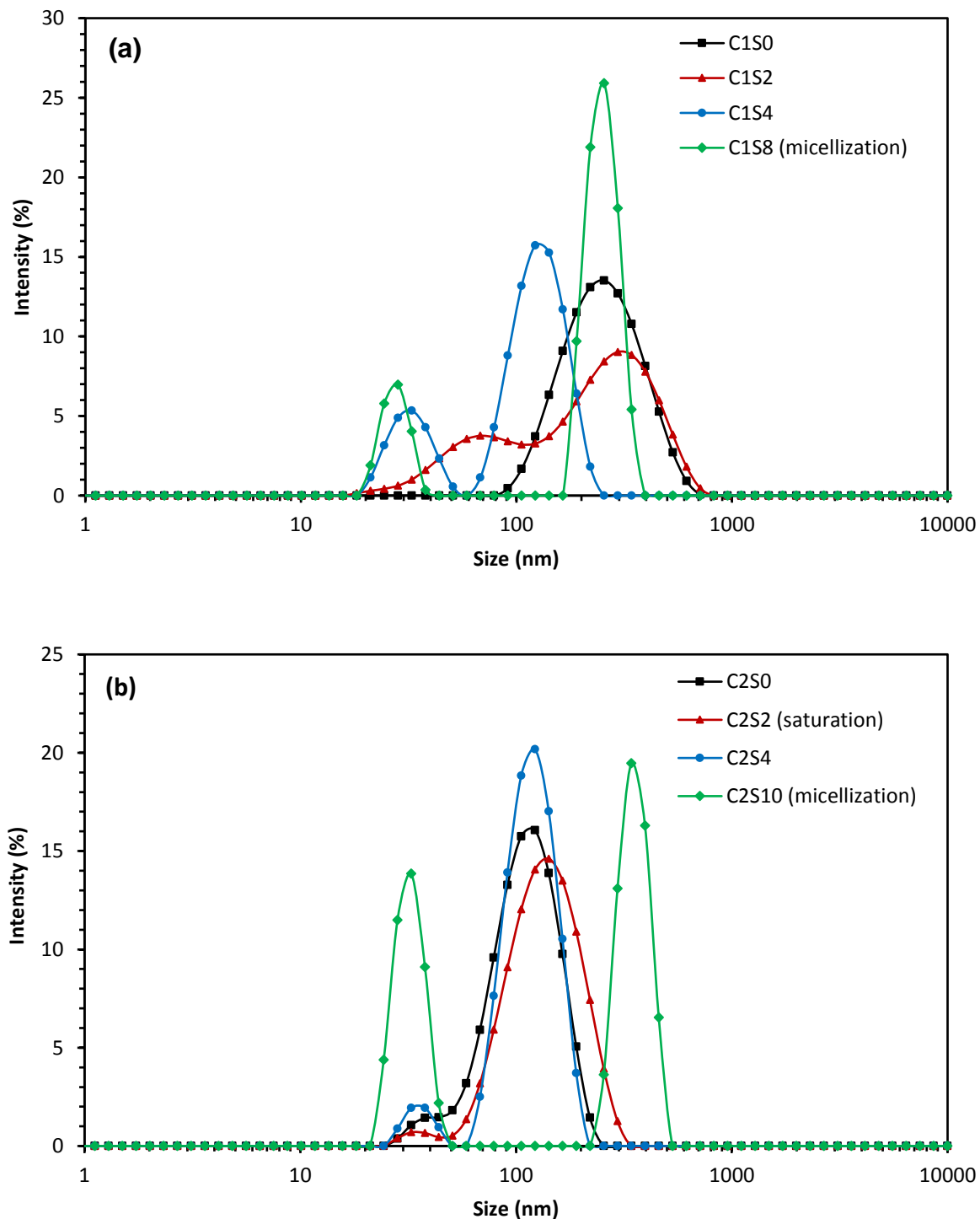
Solubilization of Span 80 niosomes by sodium dodecyl sulfate

The particle size decrease and PDI increase with the progress of the solubilization process can be more clearly seen in the 20 mol/m³ Span 80 formulation (Fig. S2d, Supporting Information), reaching the minimum size when total niosome solubilization is achieved. Average particle size of 70 nm for the mixed micelles at the critical point of total solubilization was obtained. However, it must be considered that values of PDI > 0.4 indicate heterogeneity in size and the average size is not a representative value for the sample.

The ζ -potential values in the saturation points ranged between -30 and -37, -45 and -50, and -50 and -60 mV for the 2, 10, and 20 mol/m³ Span 80 formulations, respectively, which are higher (in absolute value) than those of niosomes without SDS (Table S1, Supporting Information): this is an indicative of the SDS adsorption on the niosome surface due to hydrophobic and van der Waals forces [13,18]. ζ -potential absolute value decreased with the solubilization process until minimum values between -4 and -12 were reached, when solubilization of niosomes was completed. Values of pH were between 6.7–6.9 in all formulations.

Fig. 8.3 shows the particle size distribution during the niosome solubilization. The contact time of these samples was 1 h. They show a single peak when only niosomes are in the suspension, and a lower intensity second peak with the appearance of mixed micelles. Furthermore, it is observed that the small peak grows in intensity as the solubilization process elapses, while the initial large peak corresponding to niosomes decreases in intensity and becomes smaller. Formulations at the saturation critical points show two peaks; even the samples with SDS concentration below the saturation critical points also show two peaks indicating that SDS adsorption and mixed micelles desorption processes are simultaneous, so that the gaps left in the bilayer by the surfactant dissolved in mixed micelles are filled with new SDS at the same time. This result is consistent with those obtained for the solubilization of liposomes by SDS [15,17].

Fig. 8.3 also shows that the large peak corresponding to niosomes is still substantially large at the total micellization points. It should be noted that large particles scatter much more light than small ones because the intensity of scattering of a particle is proportional to the sixth power of its diameter. Therefore, the results of these samples indicate the presence of a few number of niosomes in formulations corresponding to critical points of total micellization, above which the complete solubilization of niosomes should occur. Regarding these inconclusive results, TEM measurements were conducted and shown at the end of this section.



Solubilization of Span 80 niosomes by sodium dodecyl sulfate

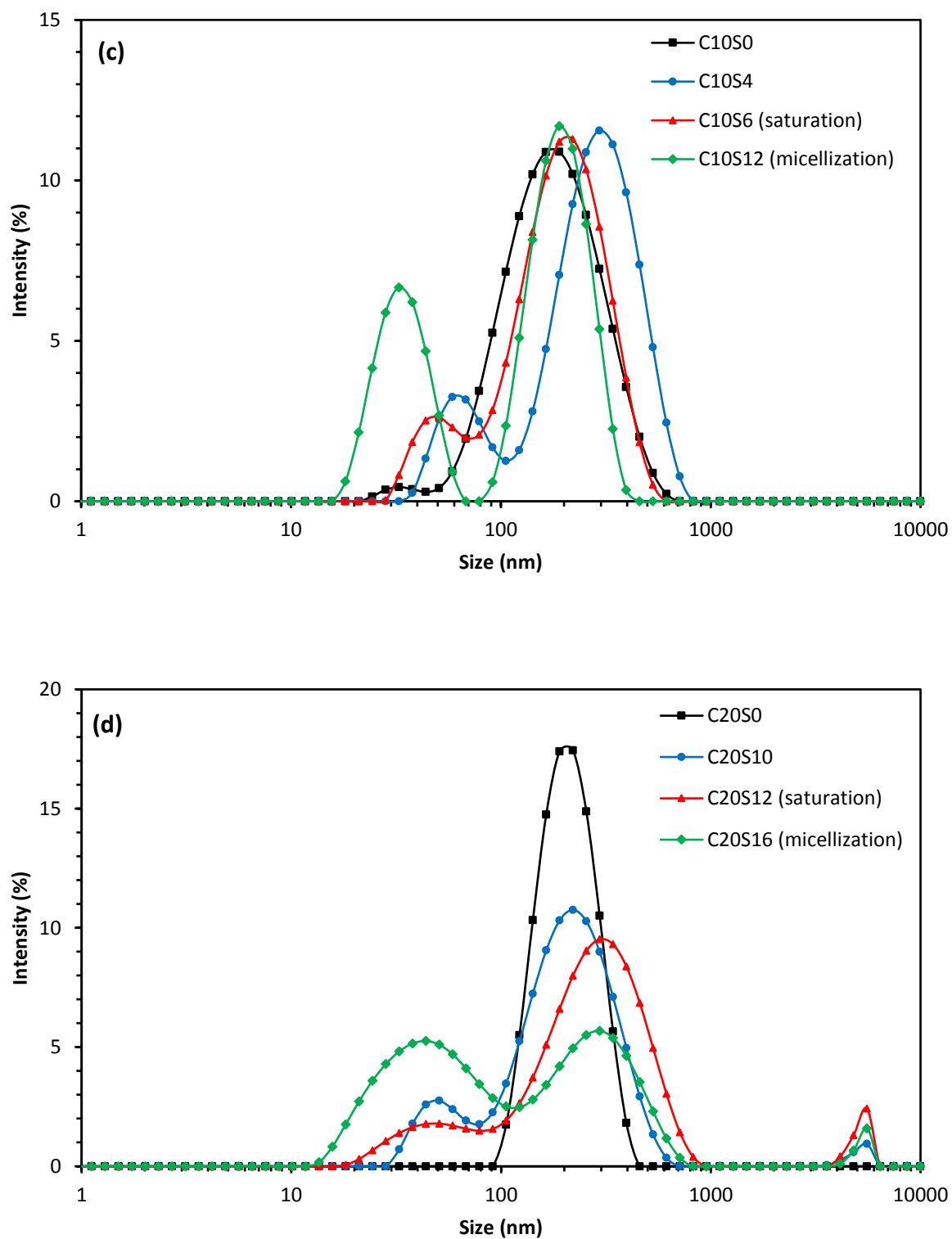


Figure 8.3. Particle size distribution of several samples during the solubilization of Span 80 niosomes by SDS: (a) $1 \text{ mol}/\text{m}^3$, (b) $2 \text{ mol}/\text{m}^3$, (c) $10 \text{ mol}/\text{m}^3$, (d) $20 \text{ mol}/\text{m}^3$ Span 80 formulations.

Variation of SDS monomer concentration in the solubilization process. SDS monomer concentration was analyzed for 1, 2, 10, and 20 mol/m³ Span 80 formulations after 1 h contact time with SDS. Results are shown in Fig. 8.4, where Fig. 8.4b is a magnified view of the micellization curves for 1 and 2 mol/m³ Span 80 formulations. The four curves represent similar behavior resulting in increased concentration of SDS monomers during the solubilization process until reaching a constant value. The value of SDS concentration added at the inflection point represents the CMC of total micellization of niosomes, above which the new SDS amount added is incorporated as mixed micelles in suspension, while the equilibrium concentration of SDS monomers remains constant. CMC values of total micellization shown in Fig. 8.4 are 8, 9, 12, and 16 mol/m³ of SDS for 1, 2, 10, and 20 mol/m³ Span 80 niosomes, respectively. These values match those previously shown in Table 8.2 from optical density measurements indicating that solubilization of Span 80 niosomes by SDS is a micellization process. Regarding the 10 and 20 mol/m³ Span 80 niosome solubilization curves, the SDS monomer concentration present in the suspension before the total micellization is relatively higher for the lower niosome concentration system (10 mol/m³ Span 80) than that for the higher niosome concentration system (20 mol/m³ Span 80). This behavior is in agreement with the solubilization of phospholipid bilayers by SDS described by Deo and Somasundaran [18], which is related to the larger surface available for the SDS incorporation in the bilayer as the lipid concentration increases. Oppositely, comparison of systems with 1 and 2 mol/m³ Span 80 niosomes shown in Fig. 8.4b reveals that the SDS monomer concentration is higher for the higher niosome concentration system (2 mol/m³ Span 80). This behavior can be attributed to the high permeability of the 1 mol/m³ Span 80 niosome bilayer, shown in Fig. 8.5, which could facilitate the rapid formation of mixed micelles, decreasing the concentration of SDS monomers. ATR-FTIR spectroscopy was used by Chen et al. [17] to conclude that the uptake of SDS in dipalmitoylphosphatidylcholine follows two routes: the adsorption of SDS on the outer liposome surface, and the intercalation of SDS into the outer monolayer followed by the transbilayer migration of the SDS into the inner layer of the liposomes. The intensity of each path depends on the lipid concentration thus, in the case of 1 mol/m³ Span 80 niosomes, it can be deduced that SDS intercalation by hydrophobic forces is dominant in comparison to surface adsorption, and SDS rapid migration through the niosome bilayer also occurs due to its high porosity.

Solubilization of Span 80 niosomes by sodium dodecyl sulfate

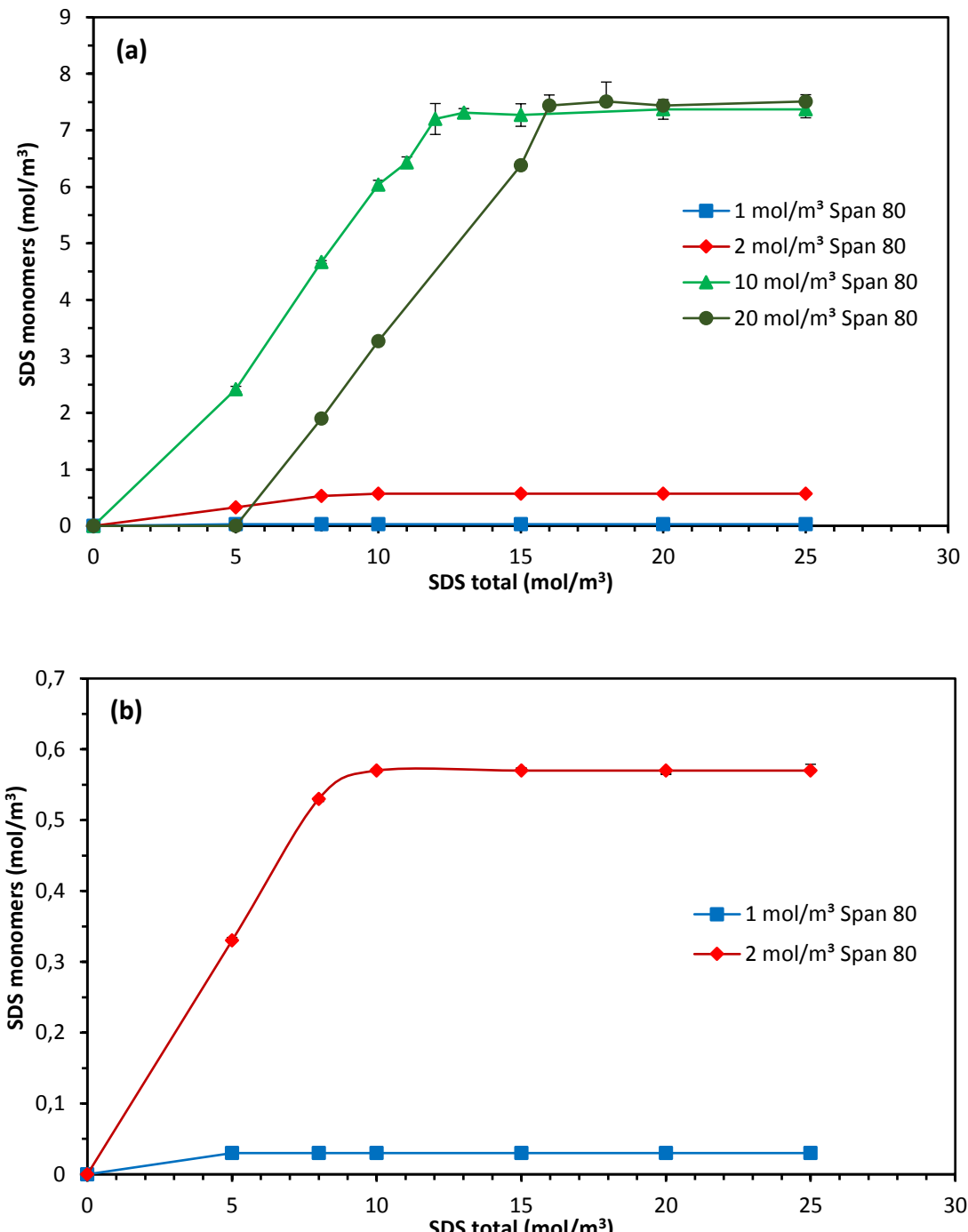
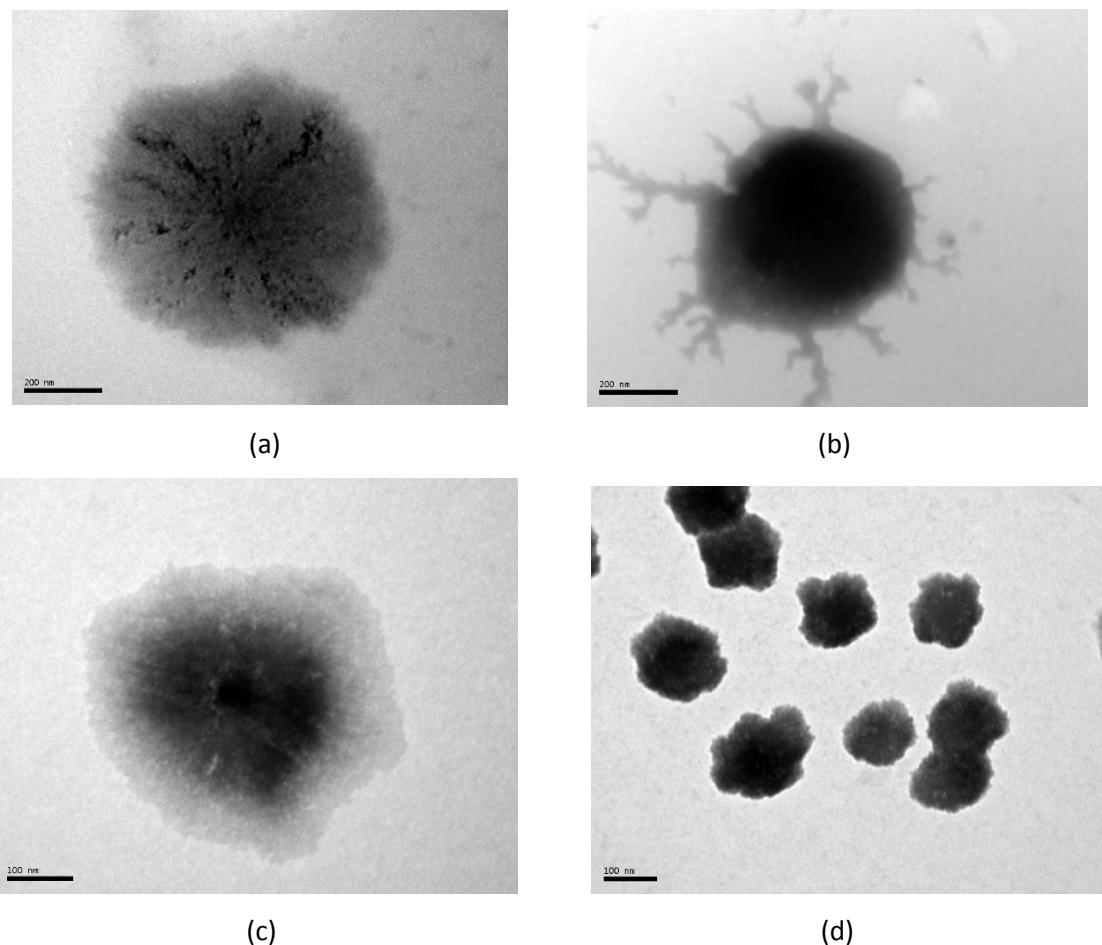


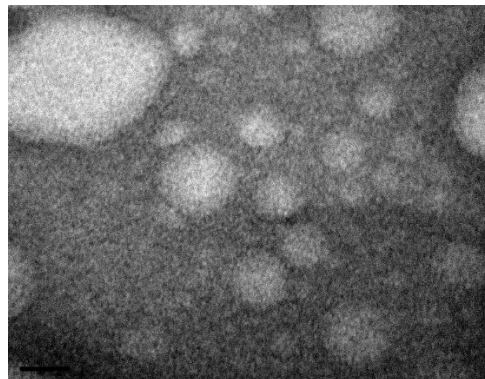
Figure 8.4. (a) Micellization curves of 1, 2, 10, and 20 mol/m^3 Span 80 niosomes by SDS, (b) amplified scale for the 1 and 2 mol/m^3 Span 80 formulations.

Niosome solubilization by SDS was confirmed by TEM measurements. Fig. 8.5 show negative stain micrographs of 1 and 20 mol/m^3 Span 80 niosomes in presence of different SDS concentrations after 24 h contact time. Dark structures shown in these micrographs correspond to spherical niosomes whose sizes agree with those measured by DLS and shown in Fig. 8.3.

Fig. 8.5a shows roughly spherical niosomes of 1 mol/m^3 of Span 80 without SDS, in which porosity of external surface can be observed.

The disruption of the bilayer process in presence of 6 mol/m^3 of SDS can be clearly observed in Fig. 8.5b. Fig. 8.5 also shows micrographs of samples containing 20 mol/m^3 Span 80 niosomes and different SDS concentrations, before saturation (Fig. 8.5c), before total solubilization (Fig. 8.5d) and after total solubilization (Fig. 8.5e). Adsorption of SDS at the niosome surface is observed in Fig. 8.5c for the sample C20S10, while partial solubilization of niosomes and their aggregation is observed for the sample C20S15 in Fig. 8.5d. Total solubilization can be seen in Fig. 8.5e for the sample C20S20, in which the absence of niosomes is confirmed and white air bubbles with surfactant adsorbed at the interface are also observed.





(e)

Figure 8.5. TEM micrographs of Span 80 niosomes in the presence of different SDS concentrations after 24 h contact time: (a) 1 mol/m³ Span 80 niosomes without SDS, sample C1S0; (b) 1 mol/m³ Span 80 niosomes with 6 mol/m³ SDS, sample C1S6; (c) 20 mol/m³ Span 80 niosomes with 10 mol/m³ SDS, sample C20S10; (d) 20 mol/m³ Span 80 niosomes with 15 mol/m³ SDS, sample C20S15; (e) 20 mol/m³ Span 80 niosomes with 20 mol/m³ SDS, sample C20S20. Scale bars: 200 nm (a, b), 100 nm (c, d), and 50 nm (e).

8.4. Conclusions

Simple experiments of contacting Span 80 niosomes (1, 2, 10 and 20 mol/m³), prepared by ultrasonication, with different SDS concentrations (between 0 and 24 mol/m³), together with the analytical techniques used (optical density, particle size, ζ -potential, and ethyl violet method for the determination of monomeric SDS) have allowed to do an original study, do not previously reported, on the niosome solubilization process by micellization.

The niosome solubilization is performed by a three-stage process comprising SDS adsorption until saturation, intensification of the bilayer solubilization, and total solubilization of the niosomes. The presence of mixed micelles was observed before reaching the saturation point, indicating that SDS adsorption and mixed micelles desorption in the bilayer take place simultaneously. Besides, the presence of a few number of niosomes at the total solubilization points was detected by DLS measurements. The absence of niosomes in formulations with SDS concentration above the total solubilization points was confirmed by TEM micrographs. Saturation and total solubilization represent critical points where suspension properties suffer sharp changes. SDS concentrations of 0, 2, 6 and 12 mol/m³ for the saturation critical points, and 8, 9, 12, and 16 mol/m³ for the total solubilization critical points were identified during the solubilization process of 1, 2, 10, and 20 mol/m³ Span 80 niosomes, respectively. Saturation and total solubilization of niosomes follow linear behavior in the pseudo-phase diagram.

The concentration of SDS monomers remaining free in the suspension increases with the addition of SDS, until a constant value is reached. This result indicates that above a certain value of SDS added to the suspension (CMC of total solubilization of niosomes) the SDS monomer concentration remains constant, while the concentration of mixed micelles increases. This result confirms that the solubilization process of Span 80 niosomes by SDS is produced by a micellization process.

The results of this study could be useful in many chemical and engineering applications that use surfactants and niosomes, particularly in the growing field of sustainable processes with biodegradable surfactants.

Supporting information

Size, PDI, and ζ -potential of Span 80 niosomes without SDS at several times after ultrasonication process, turbidity variation of Span 80 niosomes as a function of SDS concentration, and size and PDI values after different intervals of contact time with increasing amounts of SDS in niosome formulations.

Acknowledgments

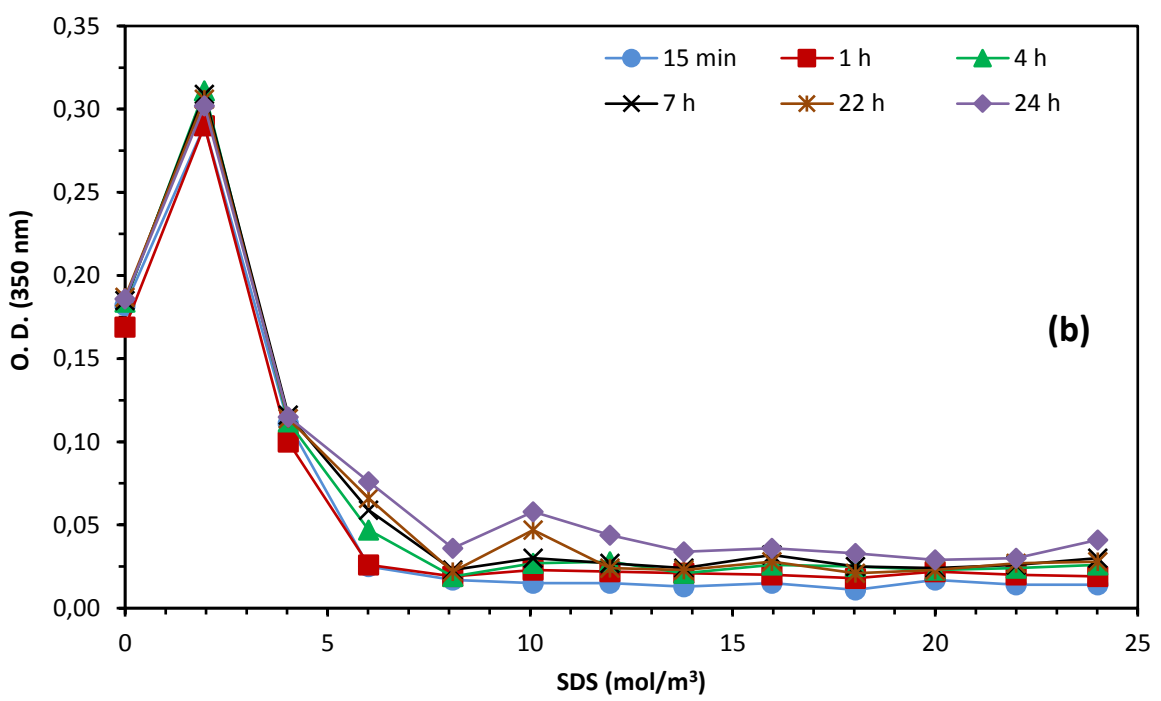
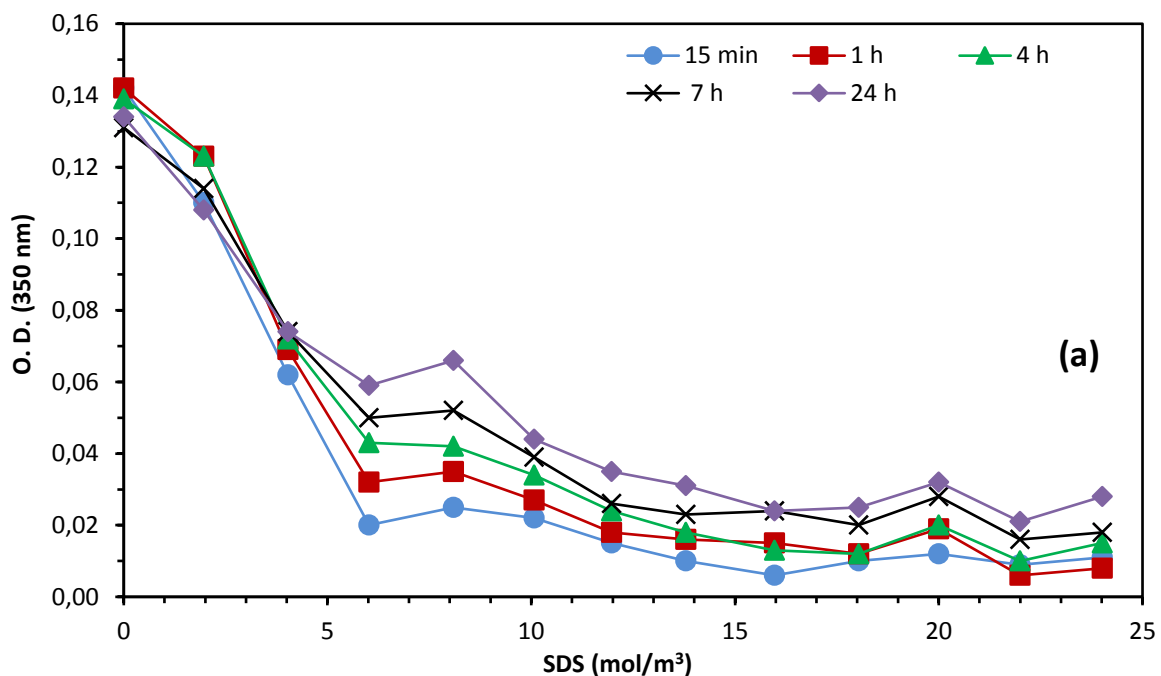
Financial support from the Ministerio de Economía y Competitividad (MINECO, Spain) through project CTQ2011-25239 is gratefully acknowledged. The authors would like to thank Dr. Carlos Álvarez (Scientific Technical Services, University of Oviedo, Spain) for his valuable help and assistance with TEM measurements.

8.5. References

- [1] I.F. Uchegbu, A.T. Florence, Non-ionic surfactant vesicles (niosomes): physical and pharmaceutical chemistry, *Adv. Colloid Interface Sci.* 58 (1995) 1–55.
- [2] I.F. Uchegbu, S.P. Vyas, Non-ionic surfactant based vesicles (niosomes) in drug delivery, *Int. J. Pharm.* 172 (1998) 33–70.
- [3] M.J. Choi, H.I. Maibach, Liposomes and niosomes as topical drug delivery systems, *Skin Pharmacol. Physiol.* 18 (2005) 209–219.
- [4] C. Marianetti, L. Di Marzio, F. Rinaldi, C. Celia, D. Paolino, F. Alhaique, S. Esposito, M. Carafa, Niosomes from 80s to present: the state of the art, *Adv. Colloid Interface Sci.* 205 (2014) 187–206.
- [5] Z. Sezgin-Bayindir, N. Yuksel, Investigation of formulation variables and excipient interaction on the production of niosomes, *AAPS Pharm. Sci. Tech.* 13 (2012) 826–835.
- [6] A.Y. Waddad, S. Abbad, F. Yu, W.L.L. Munyendo, J. Wang, H. Lv, J. Zhou, Formulation, characterization and pharmacokinetics of Morin hydrate niosomes prepared from various non-ionic surfactants, *Int. J. Pharm.* 456 (2013) 446–458.
- [7] E. Acosta, Bioavailability of nanoparticles in nutrient and nutraceutical delivery, *Curr. Op. Colloid Interface Sci.* 14 (2009) 3–15.
- [8] S. Gouin, Microencapsulation: industrial appraisal of existing technologies and trends, *Trends Food Sci. Technol.* 15 (2004) 330–347.
- [9] D.J. McClements, E.A. Decker, Y. Park, J. Weiss, Structural design principles for delivery of bioactive components in nutraceuticals and functional foods, *Crit. Rev. Food Sci. Nutr.* 49 (2009) 577–606.
- [10] Y.-M. Hao, K. Li, Entrapment and release difference resulting from hydrogen bonding interactions in niosome, *Int. J. Pharm.* 403 (2011) 245–253.
- [11] I. Escudero, R.M. Geanta, M.O. Ruiz, J.M. Benito, Formulation and characterization of Tween 80/cholesterol niosomes modified with tri-n-octylmethylammonium chloride (TOMAC) for carboxylic acids entrapment, *Colloid Surf. A-Physicochem. Eng. Asp.* 461 (2014) 167–177.
- [12] R. Fraile, R.M. Geanta, I. Escudero, J.M. Benito, M.O. Ruiz, Formulation of Span 80 niosomes modified with SDS for lactic acid entrapment, *Desalin. Water Treat.* 56 (2015) 3463–3475.
- [13] L. Roque, I. Escudero, J.M. Benito, Lactic acid recovery by microfiltration using niosomes as extraction agents, *Sep. Purif. Technol.* 151 (2015) 1–13.

- [14] D. Lichtenberg, R.J. Robson, E.A. Dennis, Solubilization of phospholipids by detergents. Structural and kinetic aspects, *Biochim. Biophys. Acta* 737 (1983) 285–304.
- [15] M. Cócera, O. López, R. Pons, H. Amenitsch, A. de la Maza, Effect of the electrostatic charge on the mechanism inducing liposome solubilization: a kinetic study by synchrotron radiation SAXS, *Langmuir* 20 (2004) 3074–3079.
- [16] D. Velluto, C. Gasbarri, G. Angelini, A. Fontana, Use of simple kinetic and reaction-order measurements for the evaluation of the mechanism of surfactant-liposome interactions, *J. Phys. Chem. B* 115 (2011) 8130–8137.
- [17] C. Chen, C. Jiang, C.P. Tripp, Molecular dynamics of the interaction of anionic surfactants with liposomes, *Colloid Surf. B-Biointerfaces* 105 (2013) 173–179.
- [18] N. Deo, P. Somasundaran, Effects of sodium dodecyl sulfate on mixed liposome solubilization, *Langmuir* 19 (2003) 7271–7275.
- [19] C.H. Tan, Z.J. Huang, X.G. Huang, Rapid determination of surfactant critical micelle concentration in aqueous solutions using fiber-optic refractive index sensing, *Anal. Biochem.* 401 (2010) 144–147.
- [20] A. Chatopadhyay, E. London, Fluorimetric determination of critical micelle concentration avoiding interference from detergent charge, *Anal. Biochem.* 139 (1984) 408–412.
- [21] M.O. Ruiz, J.M. Benito, B. Barriuso, J.L. Cabezas, I. Escudero, Equilibrium distribution model of betaine between surfactant micelles and water: application to a micellar-enhanced ultrafiltration process, *Ind. Eng. Chem. Res.* 49 (2010) 6578–6586.
- [22] R.M. Geanta, M.O. Ruiz, I. Escudero, Micellar-enhanced ultrafiltration for the recovery of lactic acid and citric acid from beet molasses with sodium dodecyl sulphate, *J. Membr. Sci.* 430 (2013) 11–23.
- [23] B.A. Uzoukwu, L.M.L. Nollet, Analysis of surfactants. In: L.M.L. Nollet (Ed.), *Handbook of Water Analysis*, Marcel Dekker, New York (2000), pp. 767–784.
- [24] V. Valiño, M.F. San Román, R. Ibáñez, J.M. Benito, I. Escudero, I. Ortiz, Accurate determination of key surface properties that determine the efficient separation of bovine milk BSA and LF proteins, *Sep. Purif. Technol.* 135 (2014) 145–157.
- [25] S. Rebollo, M.T. Sanz, J.M. Benito, S. Beltrán, I. Escudero, M.L. González San-José, Formulation and characterisation of wheat bran oil-in-water nanoemulsions, *Food Chem.* 167 (2015) 16–23.
- [26] M. Kaszuba, J. Corbett, F.M. Watson, A. Jones, High-concentration zeta potential measurements using light-scattering techniques, *Philos. Trans. R. Soc. A-Math. Phys. Eng. Sci.* 368 (2010) 4439–4451.

- [27] O. López, M. Cócera, E. Wehrli, J.L. Parra, A. de la Maza, Solubilization of liposomes by sodium dodecyl sulfate: new mechanism based on the direct formation of mixed micelles, *Arch. Biochem. Biophys.* 367 (1999) 153–160.
- [28] O. López, M. Cócera, R. Pons, H. Amenitsch, J. Caelles, J.L. Parra, L. Coderch, A. de la Maza, Use of synchrotron radiation SAXS to study the first steps of the interaction between sodium dodecyl sulfate and charged liposomes, *Spectroscopy* 16 (2002) 343–350.
- [29] M. Dahim, J. Gustafsson, F. Puisieux, M. Ollivon, Solubilization of phospholipid/triacylglycerol aggregates by non-ionic surfactants, *Chem. Phys. Lipids* 97 (1998) 1–14.
- [30] N. Deo, P. Somasundaran, Mechanism of mixed liposome solubilization in the presence of sodium dodecyl sulfate, *Colloid Surf. A-Physicochem. Eng. Asp.* 186 (2001) 33–41.
- [31] O. López, M. Cócera, R. Pons, N. Azemar, A. de la Maza, Kinetic study of liposome solubilization by sodium dodecyl sulfate based on a dynamic scattering technique, *Langmuir* 14 (1998) 4671–4674.
- [32] S. Bandyopadhyay, J.C. Shelley, M.L. Klein, Molecular dynamics study of the effect of surfactant on a biomembrane, *J. Phys. Chem. B* 105 (2001) 5979–5986.

Supporting Information

Solubilization of Span 80 niosomes by sodium dodecyl sulfate

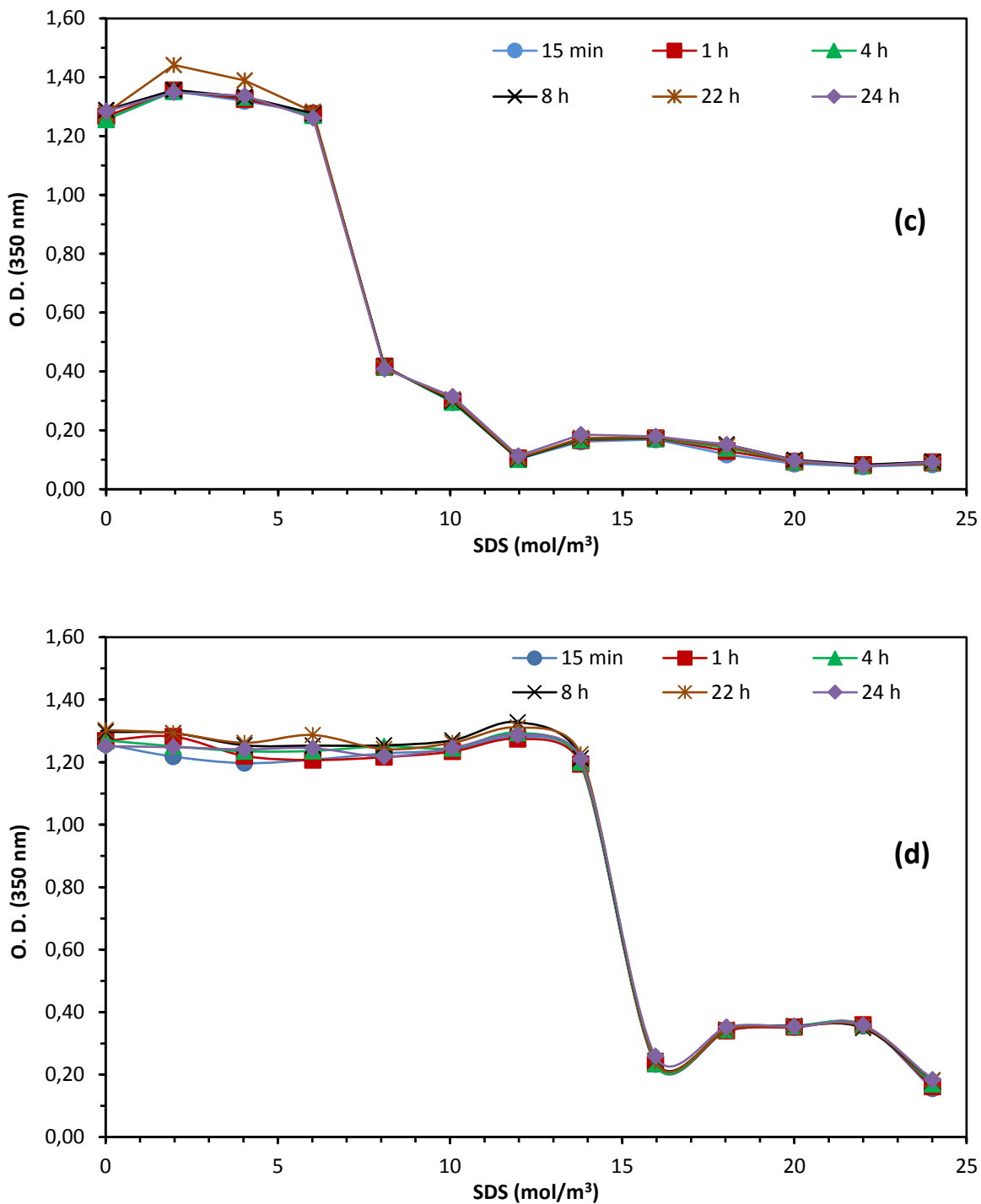
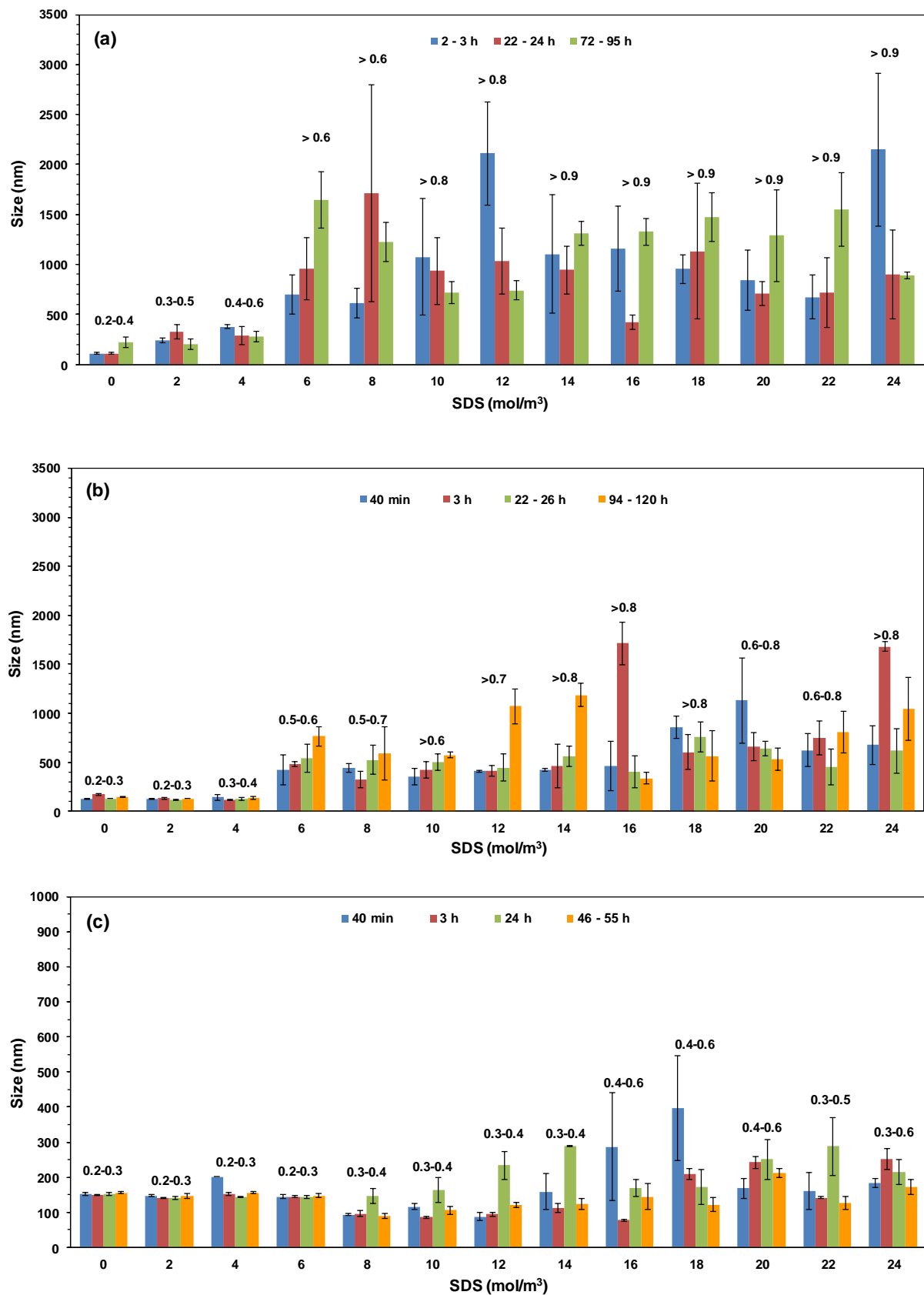


Figure S1. Turbidity variation of Span 80 niosomes as a function of SDS concentration at different contact times. Niosome formulations: (a) 1 mol/m³ Span 80, (b) 2 mol/m³ Span 80, (c) 10 mol/m³ Span 80, and (d) 20 mol/m³ Span 80.



Solubilization of Span 80 niosomes by sodium dodecyl sulfate

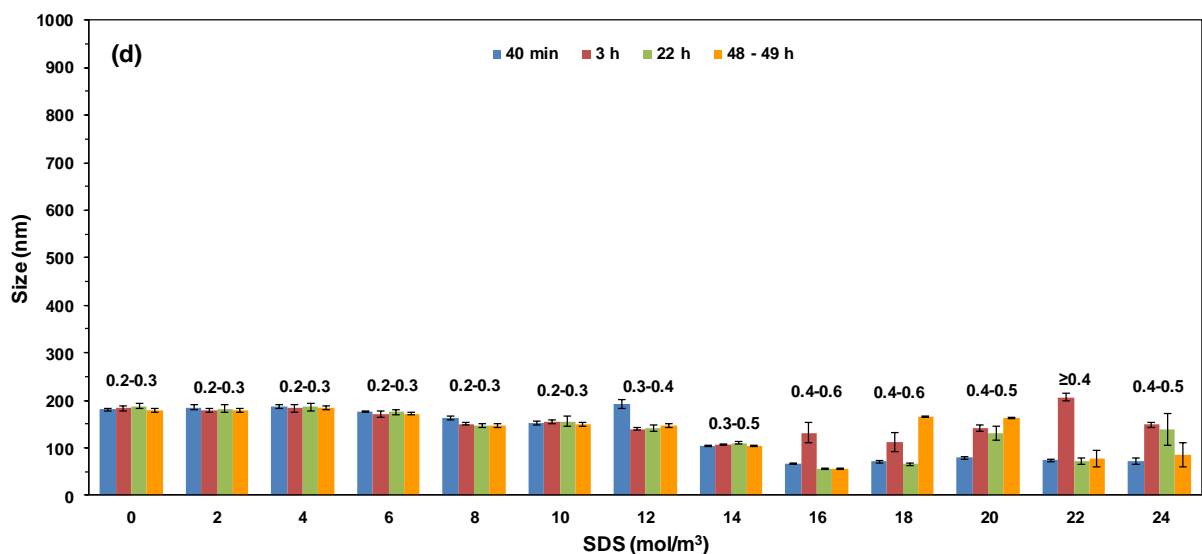
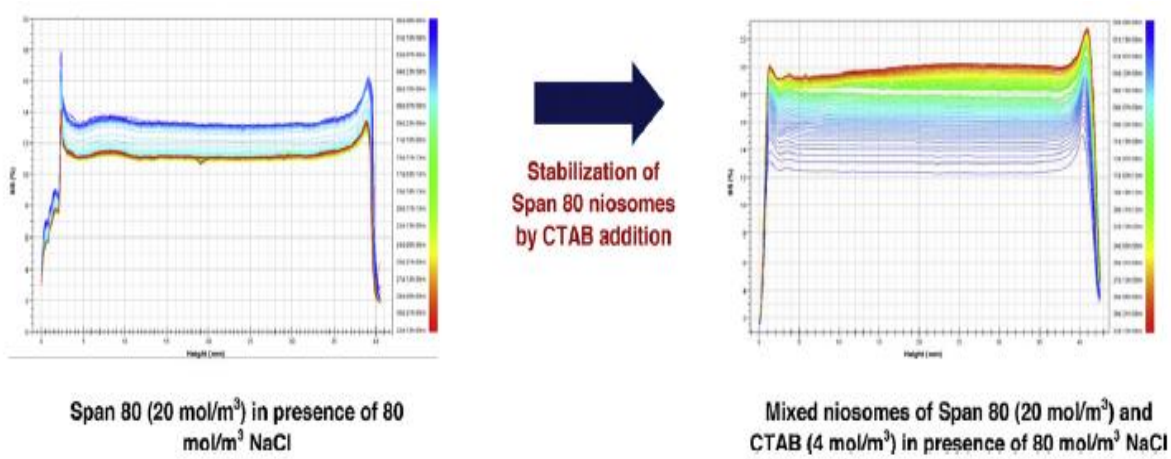


Figure S2. Size and PDI values (on bars) after different intervals of contact time with increasing amounts of SDS in niosome formulations of: (a) 1 mol/m³ Span 80, (b) 2 mol/m³ Span 80, (c) 10 mol/m³ Span 80 and (d) 20 mol/m³ Span 80.

Table S1. Size, PDI, and zeta potential of 1, 2, 10, and 20 mol/m³ Span 80 niosomes without SDS at several times after ultrasonication process.

Sample	Time (h)	Size (nm)	PDI	Zeta potential (mV)
1 mol/m³ Span 80 niosomes				
C1S0	0.5	245.7 ± 15.2	0.170 ± 0.042	-3.5 ± 0.6
	24	109.1 ± 29.1	0.384 ± 0.082	-15.0 ± 2.2
	48	149.7 ± 42.0	0.414 ± 0.088	-18.6 ± 3.3
	72	221.1 ± 51.1	0.465 ± 0.092	-20.9 ± 5.0
	174	183.2 ± 44.2	0.321 ± 0.039	-24.1 ± 4.7
	192	191.7 ± 39.8	0.372 ± 0.034	-28.6 ± 3.5
	222	222.3 ± 5.9	0.358 ± 0.018	-31.4 ± 3.4
2 mol/m³ Span 80 niosomes				
C2S0	0.66	123.2 ± 3.3	0.348 ± 0.089	-12.0 ± 2.0
	3	170.3 ± 11.1	0.465 ± 0.118	-18.7 ± 4.6
	26	129.0 ± 2.0	0.260 ± 0.017	-13.6 ± 0.7
	46	163.9 ± 73.6	0.380 ± 0.038	-19.3 ± 1.5
	122	145.1 ± 8.6	0.358 ± 0.037	-22.8 ± 2.4
	150	125.7 ± 4.4	0.372 ± 0.027	-25.3 ± 6.7
	168	154.5 ± 1.7	0.367 ± 0.011	-28.5 ± 2.0
	194	144.5 ± 6.2	0.275 ± 0.045	-28.8 ± 4.2
10 mol/m³ Span 80 niosomes				
C10S0	0.5	151.2 ± 4.4	0.229 ± 0.007	-27.1 ± 1.5
	3	149.6 ± 2.3	0.240 ± 0.004	-34.8 ± 0.9
	24	151.7 ± 3.7	0.244 ± 0.009	-35.7 ± 1.5
	55	155.2 ± 2.9	0.267 ± 0.030	-37.2 ± 1.4
	74	155.6 ± 4.6	0.241 ± 0.006	-33.8 ± 1.0
	98	154.8 ± 4.8	0.235 ± 0.013	-34.3 ± 0.8
	20 mol/m³ Span 80 niosomes			
C20S0	0.66	180.1 ± 3.2	0.270 ± 0.017	-37.0 ± 1.3
	3	183.4 ± 4.9	0.280 ± 0.024	-38.5 ± 1.5
	22	187.7 ± 6.3	0.250 ± 0.002	-34.5 ± 0.5
	48	179.1 ± 4.8	0.257 ± 0.011	-33.7 ± 1.1
	74	184.8 ± 6.2	0.263 ± 0.010	-42.6 ± 1.6
	94	182.2 ± 2.3	0.265 ± 0.008	-38.3 ± 1.1
	167	185.4 ± 2.6	0.214 ± 0.033	-39.6 ± 3.8



9. Stability and characterization studies of Span 80 niosomes modified with CTAB in the presence of NaCl

En este capítulo se estudia la estabilidad y la caracterización de niosomas formulados con el tensioactivo no iónico monooleato de sorbitán (Span 80) modificados con el tensioactivo catiónico bromuro de cetiltrimetilamonio (CTAB) en medio acuoso y en presencia de sal.

El objetivo de este trabajo fue obtener formulaciones estables de niosomas mixtos de Span 80 y CTAB utilizando la mínima concentración de tensioactivos. Además, los resultados facilitan el uso de CTAB, de gran interés en múltiples aplicaciones por sus propiedades antisépticas y antibacterianas, ya que al estar adsorbido en la bicapa niosomal se solventan las limitaciones impuestas por su elevada temperatura de Krafft.

Esta investigación se desarrolla en dos partes. En la primera se determinan los puntos críticos de adsorción máxima y solubilización de los niosomas de Span 80 en presencia de CTAB, al objeto de determinar el diagrama de pseudo-fases. En la segunda parte se analizan determinadas propiedades de superficie y de agregación. En concreto se examinan la tensión superficial, la distribución del tamaño de partícula, el potencial zeta, la estabilidad en el tiempo y la morfología. Los resultados fueron analizados y comparados con los de los tensioactivos individuales.

La adición de sal provoca una disminución de la concentración micelar crítica (CMC) y de la tensión superficial de las dispersiones de los tensioactivos.

La presencia de moléculas de CTAB en la bicapa de los niosomas mixtos produce una disminución del tamaño de partícula y un aumento de su estabilidad, en comparación con las formulaciones solamente de Span 80. Se verificó la existencia de sinergia en la formación de niosomas mixtos en agua y en presencia de 20 y 50 mol/m³ de sal, mientras que con 80 mol/m³ de NaCl se obtuvo un comportamiento antagónico entre los dos tensioactivos.

Este trabajo ha sido publicado en la revista *Colloids and Surfaces A: Physicochemical and Engineering Aspects* 601 (2020) 124999. <https://doi.org/10.1016/j.colsurfa.2020.124999>

9.1. Introduction

Niosomes are vesicles formed by self-assembly of non-ionic surfactants in aqueous media that results in closed bilayer structures. Their use has increased considerably in recent years due to their practical applications in many fields, such as medicine, cosmetics, food and pharmaceuticals, mainly due to their ability to microencapsulate compounds of different nature. They can be an alternative to liposomes due to their biological compatibility, high purity, greater chemical stability, low toxicity, low cost and better handling and storage [1–4]. Also, the use of niosomes as extraction agents of solutes present at very low concentration in aqueous solutions is a new application in the field of sustainable processes that has been explored in previous works [5–7].

The formation of stable niosomes is a non-spontaneous process that needs some energy input, so different techniques have been used to form these vesicles [8–10]. Sonication was used in this work, since it is an easy and fast technique, and does not involve the use of organic solvents.

There are a large number of non-ionic surfactants available, which are non-toxic and relatively low-cost materials for niosome design, greatly increasing the attractiveness of these vesicles for industrial production [3,11]. In general, vesicle formation without additives occurs for surfactants with a very low hydrophilic-lipophilic balance (HLB) at a relatively high surfactant concentration [12,13]. Sorbitan monooleate (Span 80) is an attractive surfactant because it is generally recognized as safe (GRAS) by FDA, biodegradable, biocompatible and non-toxic, features that make it ideal for use in pharmaceutical, cosmetic and food industry. It has a HLB value of 4.3 and can form stable niosomes with addition of small quantities of additives as ionic surfactants [7] or cholesterol, widely used in formulations to increase the membrane rigidity [14]. However, the study on its surface and bulk behavior has hardly been investigated.

Cetyltrimethylammonium bromide (CTAB) is a cationic surfactant with effective antiseptic properties against bacteria and fungi, which is used in pharmaceutical, cosmetic and food industries [15]. Micelles are formed above a certain surfactant concentration named critical micelle concentration (CMC). Above the CMC, the surfactants form micelles which favors their practical use as encapsulation agents [16,17], drug deliver [18,19] or toxic waste removal systems [20].

The adding of additives into associate structure of surfactants will change their physicochemical characteristic, for instance, the degree of ionization, reaction rates clouding or phase separation [21–23]. It is well known that CMC of surfactants depend on the electrolyte presence and temperature because they affect micellization and surface properties. Electrolytes affect the adsorption of surfactant monomers at the air-water interface because of the decrease of electrostatic repulsions and consequently the surface tension [19]. Many works [24–26] show the CMC decreasing of CTAB with salt addition, particularly Roy et al. [25] prove that CMC decreases from 0.98 mol/m³ in pure water to 0.47 mol/m³ in 10 mol/m³ NaCl solution, both at 25 °C.

Moreover, ionic surfactants work effectively only above a critical temperature called Krafft temperature (T_k). The T_k is generally conceived as the melting temperature of a hydrated solid surfactant [3]. Addition of inorganic electrolytes usually lowers the CMC of surfactants and the surface activity; however, its effect on T_k is not clear and depends on the ion common presence. Roy et al. [25] showed that the T_k of CTAB gradually decreases and increases from 24.8 °C in pure water with increasing the concentration of Cl⁻ and Br⁻, respectively. This fact shows that NaCl addition in CTAB formulations definitely favors their practical use.

The decrease of CMC and T_k and the simultaneous increase of stability of formulations is the subject of active research, as both industries and consumers demand to minimize the amount of surfactant used in the different formulations for health, economic and environment reasons [27]. In addition to electrolytes [28–30], the use of other additives such as alcohols, sugars, or mixed surfactant systems are also widely investigated due to their possible synergistic behavior that improves their properties and promotes new applications [31–33].

The present work focuses on the mixed niosomes of the cationic surfactant CTAB and the non-ionic surfactant Span 80. Mixed niosomes were formed by sonication of the 20 mol/m³ Span 80 and 4 mol/m³ CTAB formulations, which are below the saturation line in the pseudo-phase equilibrium diagram of solubilization of Span 80 niosomes by CTAB. The mixtures in pure water and NaCl solutions were analyzed by several techniques in order to evaluate their aggregation and surface properties in comparison with those of the single surfactants. This work can be of considerable interest from practical and fundamental points of view regarding the formulations of these mixed systems with respect to their possible use in multiple applications.

9.2. Materials and methods

9.2.1. Chemicals

The non-ionic surfactant sorbitan monooleate ($C_{24}H_{44}O_6$, Span 80, Sigma-Aldrich), the cationic surfactant cetyltrimethylammonium bromide ($C_{19}H_{42}NBr$, CTAB, 98%, Sigma-Aldrich) and sodium hydroxide (analysis grade, Scharlau) were used as supplied in the formulations. Ultrapure deionized Milli-Q water (Millipore, USA), with a conductivity of 0.1 $\mu\text{S}/\text{cm}$, was used for the preparation of all solutions.

9.2.2. Solubilization experiments of Span 80 niosomes by CTAB

Aqueous solutions of single surfactants (Span 80 and CTAB) were prepared 24 h before use, in order to hydrate and relax the carbonated chains of their molecular structures, weighing out the exact amounts of each surfactant on an analytical balance (Sartorius, accurate to ± 0.0001 g), and water addition up to a final volume of 100 cm^3 .

Span 80 niosomes were prepared by direct ultrasonication of 10 cm^3 aqueous solutions of Span 80 (5, 10, 15 and 20 mol/m^3). The application of ultrasounds was carried out over a 10 min effective time, with pulses every 5 s (5 s on and 5 s off, 60 cycles; 30% amplitude, 500 W), to avoid overheating of the sample, using a high-intensity ultrasonic processor (Vibra-Cell VCX 500, Sonics & Materials Inc., USA) equipped with a 3 mm-diameter titanium alloy bicylindrical probe. Subsequently, the samples were centrifuged (Eppendorf 5804 centrifuge) in 15 cm^3 polystyrene centrifuge tubes for 45 min at 9000 rpm, in order to remove traces of metal detached from the probe.

Niosome solubilization experiments were carried out in 20 cm^3 blisters by contacting 10 cm^3 of each niosome suspension (5, 10, 15 and 20 mol/m^3 of Span 80 in water) with different volumes of 25 or 50 mol/m^3 CTAB aqueous solutions. The composition of CTAB in samples was between 0–24 mol/m^3 . Samples were maintained in an incubator shaker (Model G25, New Brunswick Scientific Co.) at 150 rpm and 25 °C during predetermined periods of time (24–72 h), after which they were analyzed by the under mentioned techniques.

9.2.3. *Mixed niosomes formulation*

Mixed niosomes of Span 80 (20 mol/m^3) and CTAB (4 mol/m^3) were formulated by mixing appropriate volumes of the single surfactant solutions, previously prepared in water or in sodium chloride aqueous solutions ($20, 50$ and 80 mol/m^3 of NaCl), applying ultrasounds for 10 min and centrifugation, as described above. This formulation was chosen in light of the solubilization results of niosomes with CTAB, as will be explained below. Furthermore, for comparative purposes, the formulations of the individual surfactants (Span 80 niosomes or CTAB micelles suspensions) were also analyzed without salt and in the presence of the same salt concentrations as mentioned above.

9.2.4. *Analytical Techniques*

9.2.4.1. Optical density

A total sample volume of 1.2 cm^3 was placed in a quartz cuvette ($10 \times 10 \text{ mm}$) and its optical density (OD) was measured at a 350 nm wavelength using a double beam UV-vis spectrophotometer (Hitachi U-2000). Milli-Q water was used as blank. Previously, it was checked that the optical density at 350 nm wavelength provided a good sensitivity to the turbidity caused by the presence of niosomes, whose size is well above than that of smaller size micelles. The same wavelength was used in previous work on Span 80 niosomes solubilization by SDS [34].

9.2.4.2. Particle size distribution

The mean hydrodynamic diameter (Z-average) and the polydispersity index (PDI) of the samples were measured by dynamic light scattering (DLS) using a Zetasizer Nano ZS apparatus (Malvern Instruments Ltd., UK).

9.2.4.3. ζ -Potential

Measurements were conducted with the aforementioned Zetasizer Nano ZS apparatus, using the Laser Doppler Velocimetry technique. They were performed on the same sample previously prepared to measure the particle size, but using the appropriate cell equipped with electrodes to allow the passage of electric current.

9.2.4.4. Morphological analysis

It was performed by negative staining transmission electron microscopy (NS-TEM), using a JEOL-2000 EX-II TEM operating at 160-180 kV, with an image resolution of 1 nm.

The detailed description of the above mentioned techniques can be found in a previous work [34].

9.2.4.5. Surface tension

It was measured using an optical tensiometer (Attension Theta 200 Basic Model, Biolin Scientific Ltd.) by the drop shape analysis method at 20 °C. The apparatus is controlled by a computer equipped with pendant drop shape image analysis software. Each sample was analyzed over time. The time needed to achieve equilibrium was between 5 and 30 min depending to the surfactant concentration in the sample. The instrument was calibrated every day using a 4 mm diameter tungsten ball and checking the surface tension of distilled water ($\gamma = 72 \text{ mN/m}$). Dispersions containing CTAB (10 mol/m³) micelles, Span 80 (20 mol/m³) niosomes, or mixed niosomes of Span 80 (20 mol/m³) and CTAB (4 mol/m³), in water or sodium chloride solutions were diluted with the same solvent and maintained in an incubator shaker at 150 rpm and 25 °C for 24 h. Surface tension measurements were repeated at least twice to check the reproducibility. Surface tension data vs. time were used for the dynamic analysis of the surface tension in order to verify the existence of barrier effects to the surfactant adsorption at the interface. Equilibrium surface tension data vs. logarithm of surfactant concentration were used to determine the CMC of each formulation.

9.2.4.6. Stability measurement

Formulation stability was determined with a Turbiscan Lab Expert (Formulaction Co., France) by static multiple light scattering (S-MLS). The samples (20 mL) were placed without dilution in cylindrical glass cells where a near infrared light of 880 nm wavelength passes through them in an upward way at pre-set time intervals. Backscattered (BS) light was monitored as a function of sample height in the measurement cell (about 40 mm) at 25 °C every 5 h for 7 days, and later every 24 h for 34 days. BS value depends on the wavelength of the incident light. BS intensity increases with the concentration and the particle size for particles smaller than the incident wavelength. However, when the particles are larger than the incident wavelength (> 0.8 μm), the BS will decrease as the particle size increases [35–37].

9.3. Results and discussion

9.3.1. Solubilization of Span 80 niosomes by CTAB

Fig. 9.1 shows optical density (OD) at 350 nm wavelength of samples containing 20 mol/m³ Span 80 niosomes after prefixed contact times (24, 48 and 72 h) with different amount of CTAB (0–24 mol/m³). Solubilization curves by CTAB of 5, 10 and 15 mol/m³ Span 80 niosomes are available in Fig. S1 (Supplementary data).

It is observed in all Span 80 formulations (Figs. 9.1 and S1) that the OD curves measured at different contact time (24–72 h) are coincident, which reveals fast solubilization processes. In the niosome solubilization curves, the point of maximum OD corresponds to the saturation of the niosomes with CTAB; however, the minimum OD corresponds to the complete solubilization, where there is no presence of niosomes. Between the two points both niosomes and mixed micelles, together with the monomers of surfactants, coexist in the equilibrium dispersions. Critical saturation and complete solubilization points of niosomes move towards higher concentrations of CTAB as the concentration of Span 80 increases. The composition of the saturation critical points is confirmed by analysis of the particle size distribution shown in Figs. 9.2 and S2. In these figures, it is possible to discern a first zone at the lower CTAB concentrations, where values of PDI ≤ 0.3 indicate fairly homogeneous population in particle size, followed by a second zone with PDI ≥ 0.4 indicating heterogeneous population in particle size due to mixed micelles formation. The boundary line between both zones corresponds to 0, 2, 4, and 6 mol/m³ of CTAB for the 5, 10, 15, and 20 mol/m³ Span 80 formulations, respectively, which are consistent with the saturation points observed from OD data.

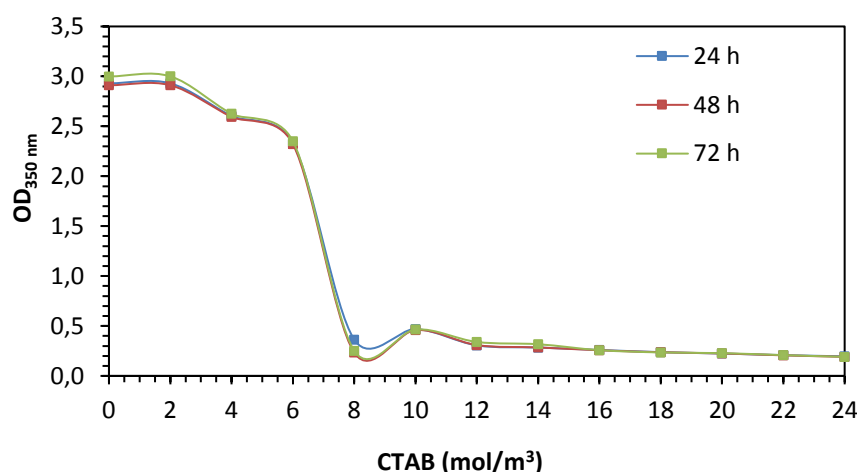


Figure 9.1. Optical density values of 20 mol/m³ Span 80 niosomes in water in presence of CTAB.

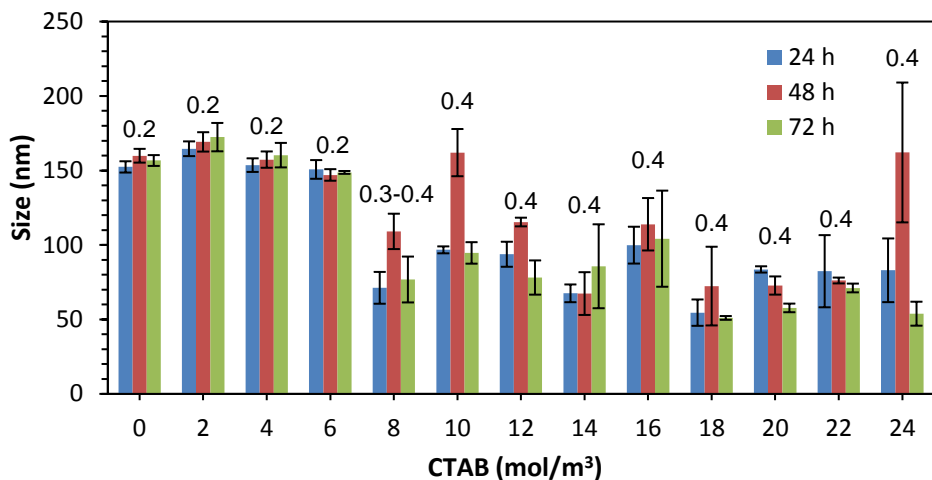


Figure 9.2. Mean hydrodynamic diameter (Z-average) and PDI (data over columns) of 20 mol/m³ Span 80 niosomes in water in presence of CTAB.

The points of saturation and total micellization are depicted in the pseudo-phase equilibrium diagram shown in Fig. 9.3. The union of the critical points of saturation and solubilization follow straight lines, according to the behavior observed in the bibliography [34,38,39]. These lines separate zones with different structures, mixed niosomes in zone below the saturation line, coexistence of niosomes and micelles in zone between both lines, and mixed micelles above the solubilization line. Some authors [40,41] have verified the formation of mixed micelles during the adsorption stage.

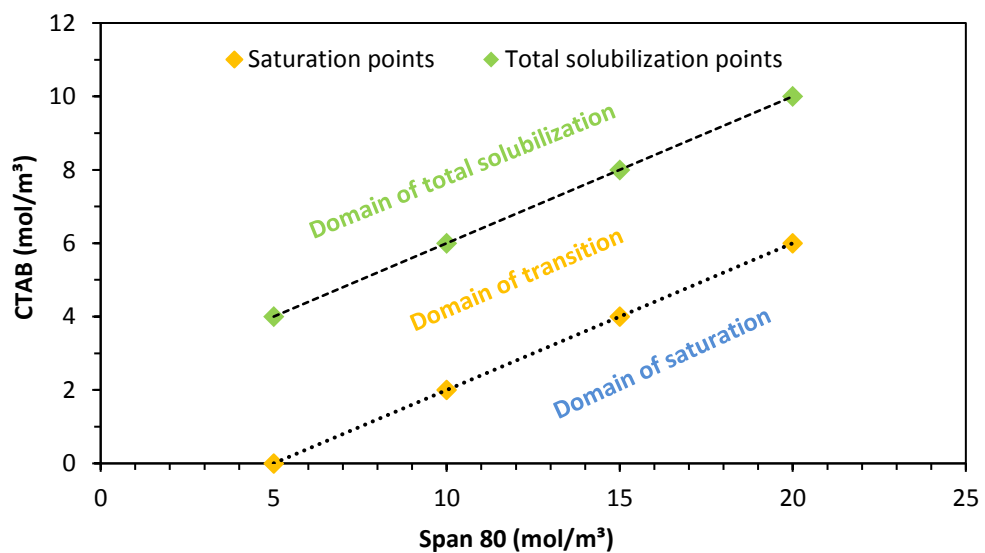


Figure 9.3. Pseudo-phase equilibrium diagram of CTAB – Span 80 niosomes in water.

9.3.2. Effect of NaCl on aggregation and surface properties

In view of the pseudo-phase diagram shown in Fig. 9.3, the formulation of Span 80 (20 mol/m^3) and CTAB (4 mol/m^3), just below the saturation line, was selected for stable mixed niosomes formation and to determine their aggregation and surface properties. The presence of different NaCl concentrations in the formulations is also studied due to its great interest in several food and biotechnological applications.

Figs. 9.4–9.6 depict the surface tension curves of individual and mixed surfactants (in a 4/20 molar ratio of CTAB/Span 80), respectively. The surface tension curves were used to calculate the points of inflection which correspond to the critical micelle concentration (CMC) and the surface tension at the CMC (γ_{CMC}).

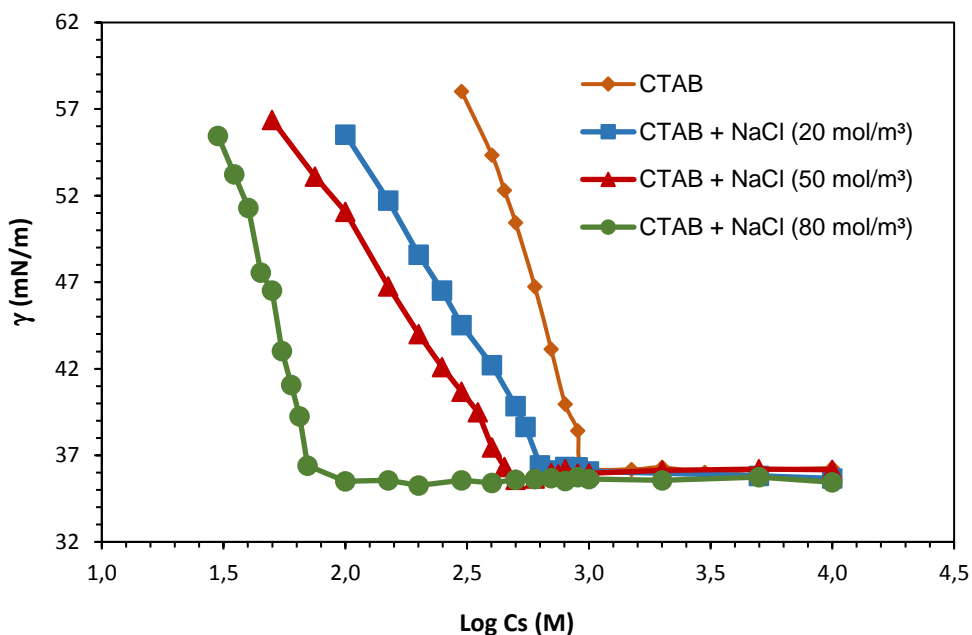


Figure 9.4. Surface tension vs. logarithmic concentration of CTAB in pure water and NaCl solutions (20, 50 and 80 mol/m³) at 25 °C.

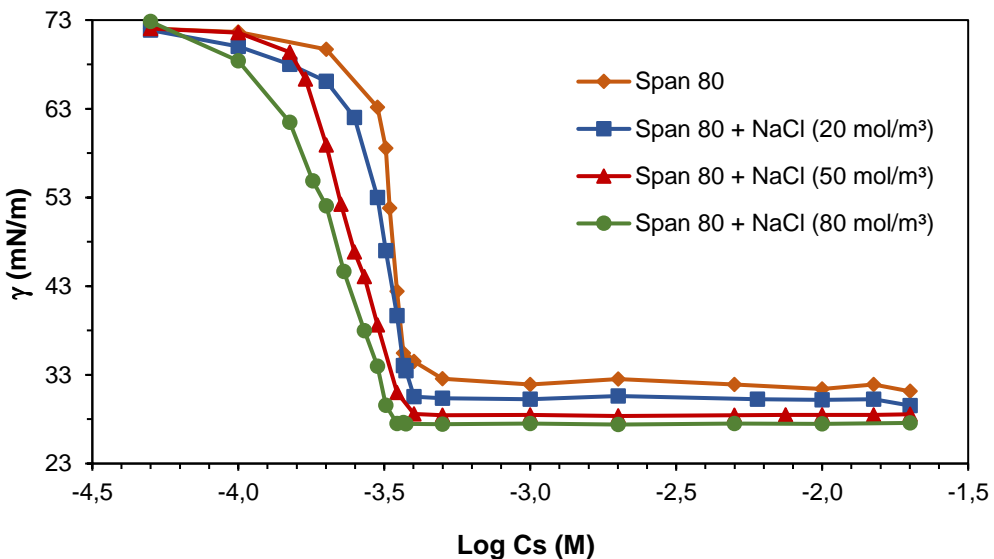


Figure 9.5. Surface tension vs. logarithmic concentration of Span 80 in pure water and NaCl solutions (20, 50 and 80 mol/m³) at 25 °C.

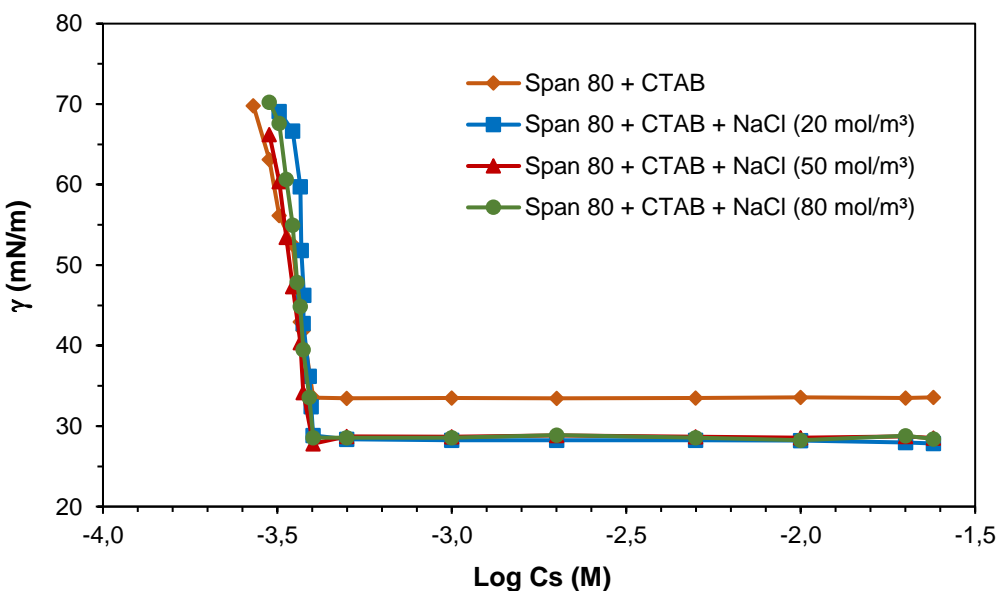


Figure 9.6. Surface tension vs. logarithm of the total concentration of surfactants, for mixed formulations of Span 80 and CTAB (in a 4/20 CTAB/Span 80 molar ratio) in pure water and NaCl solutions (20, 50 and 80 mol/m³) at 25 °C.

Additional parameters were studied to evaluate the effect of NaCl on formulations. The surface tension reduction effectiveness (π_{CMC}), the adsorption efficiency (pC_{20}), the maximum surface excess concentration in the air-water interface (Γ_{max}), the minimum area per molecule in the adsorption layer (A_{min}), the standard Gibbs free energy change of micellization (ΔG^0_m), the standard Gibbs free energy change of adsorption (ΔG^0_{ads}) were calculated using the following equations [41–43]:

$$\Pi_{CMC} = \gamma_0 - \gamma_{CMC} \quad (1)$$

$$pC_{20} = (\pi_{CMC} - 20) / (2.303nRT\Gamma_{max} - \log CMC) \quad (2)$$

$$\Gamma_{max} = -(1/(2.303nRT))(\partial\gamma/\partial\log C) \quad (3)$$

$$A_{min} = 10^{20} / N_A \Gamma_{max} \quad (4)$$

$$\Delta G^0_m = (2-\alpha)RT\ln X_{CMC} \quad (5)$$

$$\Delta G^0_{ads} = \Delta G^0_m - (\pi_{CMC}/\Gamma_{max}) \quad (6)$$

where γ_0 is the surface tension of water (72 mN/m), $R = 8.314 \text{ N m}/(\text{mol K})$ is the ideal gas constant, $N_A = 6.023 \times 10^{23}$ molecules/mol is the Avogadro's constant, $T = 298.15 \text{ K}$ the temperature, X_{CMC} is the mole fraction of the surfactant at the CMC ($X_{CMC} = \text{CMC}/55.55$, with CMC expressed in molar concentration), and $\partial\gamma/\partial\log C$ is the slope below the CMC in the surface tension plots. The parameter "n" in Eqs. (2) and (3) depends on the number of species constituting the adsorption layer. For nonionic surfactants, $n=1$. For 1:1 ionic surfactants, $n=2$ considering full ionization and absence of electrolytes; however, in presence of high concentration of electrolytes, $n=1$ [44]. In this work, the following values of n were used: for CTAB in water, the degree of counterion dissociation (α) was taken equal to 0.26 [45], and n was $2-0.26 = 1.74$. For CTAB in presence of NaCl, $n = 1$. For the mixed system CTAB/Span 80 (4/20 M ratio) n was estimated with those values used for the single surfactants multiplied by their mole fractions in the formulation, that is: $\alpha = 0.17 \times 0.26 = 0.04$ and $n = 0.17 \times 1.74 + 0.83 = 1.12$ for the mixed system in pure water, and $\alpha = 0$ and $n = 1$ in the mixed systems with salt. Results are shown in Table 9.1.

Table 9.1. Surface activity parameters of CTAB, Span 80 and CTAB + Span 80 (4/20 M ratio) in the presence and absence of NaCl at 298 K.

NaCl (mol/m ³)	CMC × 10 ³ (mol/dm ³)	γ _{CMC} × 10 ³ (N/m)	π _{CMC} × 10 ³ (N/m)	pC ₂₀	CMC/C ₂₀	Γ _{max} (mol/m ²)	A _{min} (Å ² /molec)	-ΔG ⁰ _m (kJ/mol)	-ΔG ⁰ _{ads} (kJ/mol)
CTAB									
0	0.978	36.19	35.81	2.78	0.59	3.78E-06	43.94	27.14	36.62
20	0.698	36.07	36.2	3.83	4.67	4.17E-06	39.82	27.97	36.59
50	0.496	35.85	35.82	3.9	3.97	4.73E-06	35.12	28.82	36.47
80	0.072	35.56	36.73	4.69	3.53	5.26E-06	31.58	33.59	40.52
Span 80									
0	0.392	31.9	40.1	3.46	1.13	6.45E-05	2.97	58.81	59.58.
20	0.391	30.24	41.76	3.51	1.26	6.14E-05	2.7	58.73	59.52
50	0.375	28.48	43.52	3.62	1.54	7.92E-05	2.1	59.04	61.04
80	0.347	27.5	44.5	3.61	1.43	6.36E-05	2.61	59.41	61.02
Span 80 + CTAB									
0	0.407	33.51	38.49	3.46	1.18	4.07E-05	4.08	57.45	58.39
20	0.401	28.24	43.76	3.47	1.19	5.57E-05	2.98	58.7	59.49
50	0.395	28.68	43.32	3.48	1.18	5.59E-05	2.97	58.77	59.54
80	0.401	28.58	43.42	3.47	1.18	5.69E-05	2.92	58.69	59.46

The existence of barrier effects to the adsorption at the air-liquid interface was verified by means of analysis of the variation of surface tension over time. The equilibrium times were comparatively shorter as the salt content in the formulations increased. Adsorption dynamic curves were analyzed by the Wars-Torday model based on diffusion controlled adsorption mechanism (Eq. (7)), and particularly by their analytical solutions at short time ($t \rightarrow 0$) and long time ($t \rightarrow \infty$) expressed by Eqs. (8) and (9), respectively [45].

$$\Gamma(t) = 2\sqrt{\frac{D}{\pi}} \left[C_0 t^{1/2} - \int_0^{\sqrt{t}} C_s d\sqrt{t-\tau} \right] \quad (7)$$

$$\gamma_{(t) t \rightarrow 0} = \gamma_0 - 2nRT C_0 \sqrt{\frac{D_s t}{\pi}} \quad (8)$$

$$\gamma_{(t) t \rightarrow \infty} = \gamma_{eq} + \frac{nRT \Gamma_{max}^2}{C_0} \sqrt{\frac{\pi}{4D_{ef}t}} \quad (9)$$

where $\gamma_{(t) t \rightarrow 0}$ and $\gamma_{(t) t \rightarrow \infty}$ are surface tensions at short time and long time, respectively, D_s and D_{ef} are the monomer diffusion and back-diffusion coefficients, γ_0 and γ_{eq} are the equilibrium surface tension of water and the formulation, C_0 is the bulk surfactant concentration and C_s and τ in Eq. (7) are the concentration in the subsurface and a dummy variable of integration, respectively.

Eqs. (8) and (9) represent a linear behavior of $\gamma(t)_{t \rightarrow 0}$ and $\gamma(t)_{t \rightarrow \infty}$ data as a function of $t^{1/2}$ and $t^{-1/2}$, respectively. D_s and D_{ef} were calculated through the gradients of the fitted lines obtained from these plots by using the following equations:

$$D_s = \left[\frac{grad_1 \pi^{1/2}}{2 n R T C_0} \right]^2 \quad (10)$$

$$D_{ef} = \left[\frac{n R T \Gamma_{max}^2 \pi^{1/2}}{2 C_0 grad_2} \right]^2 \quad (11)$$

Table 9.2. Average values of diffusion coefficients D_s and D_{ef} calculated by Eqs. (10) and (11) for the different CTAB, Span 80 and CTAB + Span 80 formulations in the absence and presence of salt.

Surfactant	NaCl (mol/m ³)	D_s (m ² /min)	D_{ef} (m ² /min)	D_{ef}/D_s	C_0 (mol/m ³)
CTAB	0	1.10E-11	2.18E-12	0.20	0.5
	20	3.65E-11	2.88E-12	0.08	0.5
	50	5.20E-11	2.24E-12	0.04	0.5
	80	1.28E-11	4.53E-11	3.55	0.5
Span 80	0	2.42E-10	7.48E-10	3.10	0.3
	20	2.03E-10	1.05E-09	5.19	0.3
	50	4.00E-10	1.47E-09	3.68	0.3
	80	7.83E-10	1.27E-09	1.62	0.3
Span 80 + CTAB	0	7.66E-10	1.03E-09	1.35	0.3
	20	3.02E-10	1.48E-09	4.89	0.3
	50	2.59E-10	1.81E-09	6.98	0.3
	80	7.97E-10	2.89E-10	2.76	0.3

Results of D_s and D_{ef} are shown in Table 9.2. Values of D_{ef}/D_s ratio close to 1 mean that adsorption of surfactant monomers at the air-liquid interface is controlled by diffusion of surfactant monomers, without the existence of barrier effects to adsorption. However, values of D_{ef} lower than D_s mean that diffusion to the air-liquid interface from an imaginary subsurface very close to the interface, slows down as the interface becomes more crowded.

9.3.2.1. Effect of NaCl on CTAB micelles

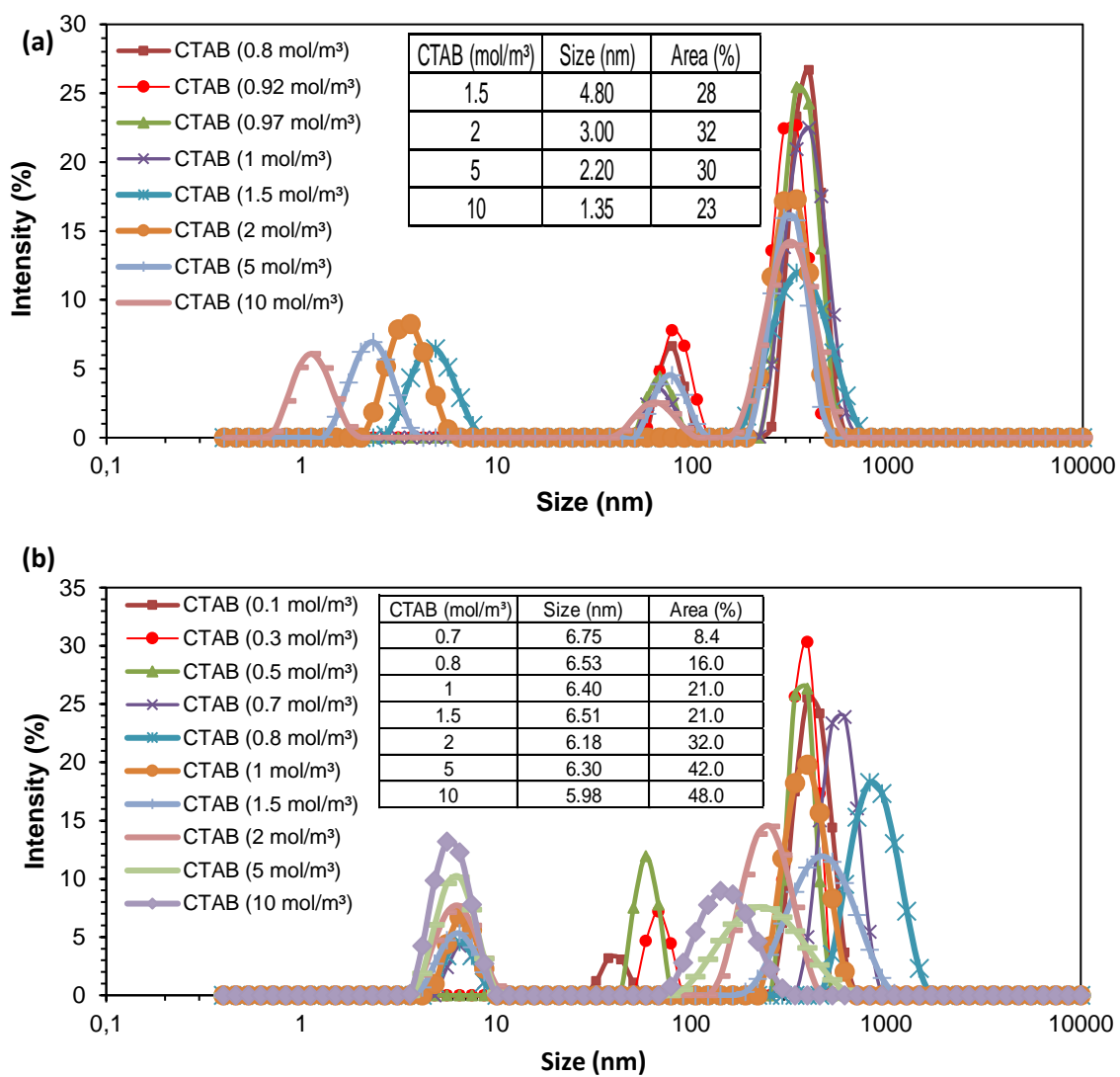
Data in Table 9.1 for CTAB in pure water agree with those published in several works [44,46,47]. It is also observed in Table 9.1 that the CMC of the CTAB surfactant decreases as the salt concentration increases, indicating a decrease in the concentration of monomers in solution, which may be due to the screening between the polar heads of the CTAB monomers produced by the Cl^- ions, lowering their stability in solution and promoting micellization. The screening effect that provides the presence of salt also occurs in the layer adsorbed in the air-liquid interface, which causes an increase in the number of monomers adsorbed providing a decrease in surface tension. Results are close to those published by Zhang et al. [44].

It is well-known that the Br^- ion remains more tightly bound to the polar head of the surfactant and is less hydrated than the Cl^- ion, so the former neutralizes more the positive charge of the CTAB head groups. Our hypothesis is that in formulations with 20 and 50 mol/m³ of salt, part of the Br^- ions remains still associated with the head group attenuating the repulsions between the polar heads of the monomers adsorbed at the interface, so the presence of salt does not have the expected effect on the decrease in surface tension. In the formulation with 80 mol/m³ of salt, practically all the Br^- ions have been replaced by the Cl^- ions which are more dissociated, so that the screening effect provided by the presence of Cl^- ions is more effective, facilitating the compaction of the adsorbed layer (increase of Γ_{\max} and reduction of the A_{\min}) and the decrease in surface tension. As a result, both effectiveness (π_{CMC}) and efficiency (pC_{20}) increase significantly in the formulation with the highest salt content. Negative values of ΔG_m^0 and ΔG_{ads}^0 indicate that micellization and adsorption are spontaneous processes with higher trend to adsorption than micellization, according with CMC/C₂₀ values higher than one.

Data of D_{ef} and D_s for CTAB surface adsorption shown in Table 9.2 are similar to those published by Zhang et al. [44]. It is observed that D_{ef}/D_s rates are lower than 1 in formulations with pure water and 20 and 50 mol/m³ NaCl; however, it is close to 1 in the 80 mol/m³ NaCl formulation. This fact suggests that the barrier effects to adsorption are fundamentally of electrostatic character as it decreases in the presence of high salt content.

The NaCl presence affects the CTAB aggregation properties. Fig. 9.7 shows DLS results of the CTAB dispersions in pure water and with 20 mol/m³ NaCl, after 24 h from its preparation. The absence of micelles can be observed in samples with CTAB concentrations lower than CMC, although large pre-micellar aggregates are observed. Furthermore, in the salt-free formulation (Fig. 9.7a) a decrease in micelle size is clearly observed when CTAB concentration increases. In the formulations with 20 mol/m³ of NaCl (Fig. 9.7b) micelles are quite larger than in pure water. It is also observed that the increase in CTAB concentration induces a slight decrease in the size of the micelles and a significant increase in the intensity of the diffracted light. It should be noted that large particles scatter much more light than small ones because the intensity of scattering of a particle is proportional to the sixth power of its diameter. These facts show that in presence of 20 mol/m³ NaCl the increase in CTAB concentration mainly yields the increase in the number of micelles at the expense of the most unstable pre-micellar aggregates, which demonstrates that the presence of salt favors micellization. Fig. 9.7c shows a larger micelle size with an increasing NaCl concentration due to the increase in its aggregation number. ζ -potential of these CTAB dispersions (10 mol/m³ CTAB) in the absence and presence of NaCl, measured after 24 h from their preparation, were 55, 39, 28 and 18 mV, which shows the increasing instability of

these dispersions by increasing the salt content. Backscattered light (BS) of these formulations throughout 32 days are depicted in Fig. S3. They show BS fluctuations in all formulations that indicate lack of homogeneity. The same samples analyzed by BS were then analyzed by DLS and ζ -potential. The average sizes were between 225 and 420 nm with very high PDI values (between 0.5 and 0.7), which indicates a high polydispersion in sizes for all formulations after 32 days from their preparation. ζ -potential of these dispersions was between 4 and 5 mV, confirming their loss of stability over time.



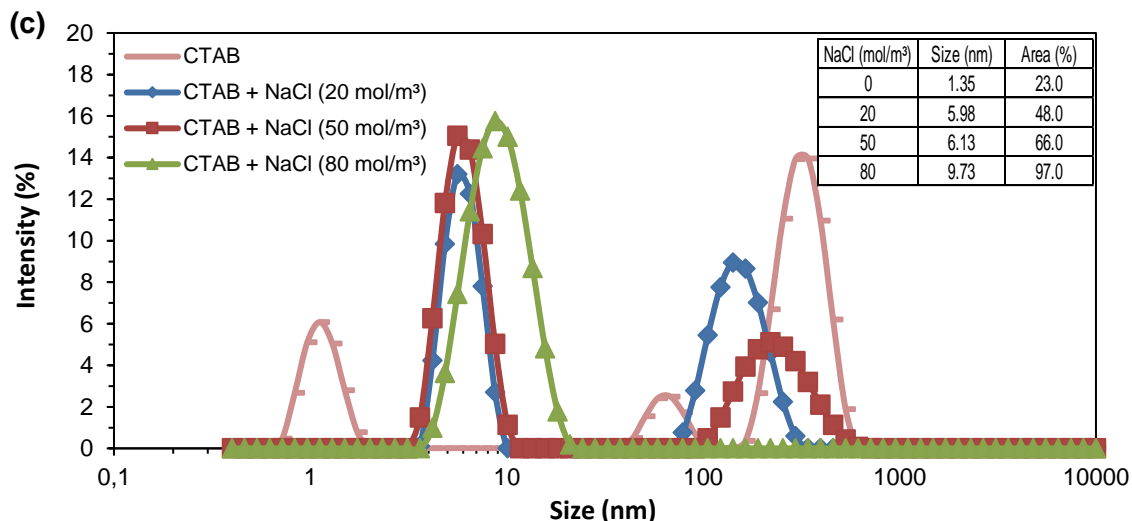


Figure 9.7. DLS results of CTAB dispersions in pure water and in presence of NaCl measured 24 h after formulation. a) CTAB in pure water. b) CTAB in 20 mol/m³ NaCl solutions. c) Formulations of 10 mol/m³ CTAB in pure water and 20, 50 and 80 mol/m³ NaCl solutions. Data in the inserted tables correspond to the small micelles.

9.3.2.2. Effect of NaCl on 20 mol/m³ Span 80 niosomes

A decrease in CMC and the γ_{CMC} for the Span 80 surfactant was observed in Table 9.1 with increasing NaCl concentration. This behavior leads to increasing values of effectiveness (π_{CMC}) and efficiency (pC_{20}), whereas increasing Γ_{max} and decreasing A_{min} values are also observed in Table 9.1 as the salt concentration increases, according to the decrease of γ_{CMC} . The values of ΔG_m^0 and ΔG_{ads}^0 are very close, indicating that micellization and surface adsorption are spontaneous processes with a similar tendency, regardless of salt concentration, in coherence with the values just higher than the unit of the CMC/C₂₀ ratios.

D_s values shown in Table 9.2 are one order of magnitude less than D_{ef}, both in the presence and absence of salt, leading D_{ef}/D_s ratios lower than 10 in all cases. These results reveal the absence of barrier effects to the adsorption at the air-liquid interface, being diffusion the mechanism that controls the interfacial adsorption. However, the fact that D_{ef} > D_s indicates the existence of unstable aggregates in the region near the interface (subsurface) that release monomers, which increasing the driving force for the diffusion of the monomers towards the interface.

Table 9.3 shows the mean values of the particle diameter, PDI and ζ -potential of the different formulations of Span 80 surfactant after 32 days from their preparation. In the formulations without salt and with 20 mol/m³ of NaCl, low values of PDI and high absolute values of ζ -

potential indicate that dispersions, formed by negatively charged niosomes with a size around 200 nm, are stable. Formulations with a high NaCl concentration contain much larger particles ($> 0.8 \mu\text{m}$) and much more unstable. It must be pointed out that although Span 80 is a non-ionic surfactant, Span 80 niosomes have negative charge (ζ -potential = -42 mV) due to the tendency of hydroxyl groups to adsorb on their surface. Na^+ ion has high hydration capacity, so its presence in the formulation medium increases hydrophobic interactions and decreases CMC. The Na^+ ions have a stabilizing effect of the niosomal bilayer at low concentration, reducing the volume of the aggregates. However, the presence of a large amount of Na^+ ions in the formulations with 50 and 80 mol/m³ of NaCl causes a strong screening effect that weakens the electrostatic repulsions between the negatively charged niosomes and increases their instability in suspension, facilitating the formation of large aggregates.

Table 9.3. Results of DLS and ζ -potential of 20 mol/m³ Span 80 niosomes measured 32 days after preparation.

Formulation	Size (nm)	PDI	ζ -potential (mV)
Span 80 without NaCl	205	0.289	-41.9
Span 80 with 20 mol/m ³ NaCl	179	0.151	-52.4
Span 80 with 50 mol/m ³ NaCl	803	0.550	-17.2
Span 80 with 80 mol/m ³ NaCl	1158	0.405	-12.4

DLS curves of Span 80 suspensions (20 mol/m³) without and with NaCl after 7 days from their preparation are depicted comparatively in Fig. 9.8. The presence of 200-300 nm diameter niosomes in the formulations without and with 20 mol/m³ of NaCl is observed. The formulation of Span 80 surfactant with 50 mol/m³ NaCl shows particles around 800 nm in size that can be produced by association of niosomes in a medium strongly screened by the presence of salt. In the formulation with 80 mol/m³ of NaCl, the particles show an average size of 300 nm, which indicates much smaller aggregates than those shown in Table 9.3 for this same formulation.

The explanation for this result is probably due to the fact that these aggregates have been formed by the association of Span 80 micelles from the previously breaking of the niosomes in the presence of 80 mol/m³ of NaCl. This hypothesis is based on the S-MLS results shown in Fig. 9.9, as discussed below

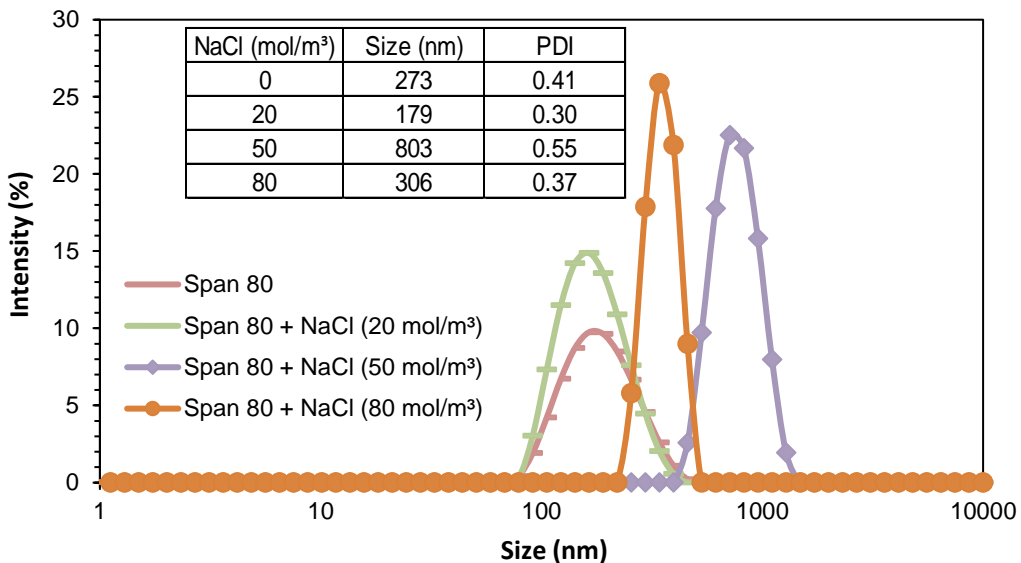


Figure 9.8. DLS results of 20 mol/m³ Span 80 niosomes without and with NaCl (20, 50 and 80 mol/m³) measured 7 days after preparation.

Fig. 9.9 depicts BS results of Span 80 formulations recorded for 7 days (Figs. 9.9a1, 9.9b1, 9.9c1 and 9.9d1) and 32 days (Figs. 9.9a2, 9.9b2, 9.9c2 and 9.9d2) immediately after their preparation. It is observed that the dispersion without salt is stable for 32 days, with a slight decrease in the height of the foam at the top of the flask. The presence of 20 mol/m³ of NaCl hardly affects BS profiles during the first 7 days (Fig. 9.9b1), however for longer times an increase in BS from 20% to 27% is observed (Fig. 9.9b2) which can be due to the increase in the number of particles in suspension. In formulations with 50 and 80 mol/m³ of NaCl, the BS decreases from 13% to 5% (Fig. 9.9c2) and from 13% to 11% (Fig. 9.9d2), respectively, after 32 days from the sample preparation. As stated before, BS is related to the concentration and size of the particles. The BS increases with increasing particle concentration and the size of the aggregates, if they are smaller than the wavelength of the incident light ($\lambda = 0.8 \mu\text{m}$). However, the BS decreases when the size of the aggregates is greater than the mentioned wavelength [34]. Therefore, the decrease in BS indicates the presence of large particles ($> 0.8 \mu\text{m}$), together with a smaller amount of particles in suspension. This fact is significant in Fig. 9.9d2 where accumulation of particles at the bottom of the flask is observed.

The small number of particles in the suspension justifies the smaller decrease of BS observed in Fig. 9.9d2 compared to Fig. 9.9c2. The instability of these formulations is due to the presence of a large quantity of Na^+ ions that screen the electrostatic repulsions between negatively charged niosomes, making them unstable in solution. Figs. 9.9c1 and 9.9d1 correspond to the BS profiles

recorded during the first 7 days. They show the BS decrease (from 12 to 5%) and the increase (from 4 to 15%) in the formulations with 50 and 80 mol/m³ of NaCl, respectively. This behavior indicates, as already mentioned, the presence of particles larger than 0.8 μm in the formulation with 50 mol/m³ of salt. However, the BS increase in Fig. 9.9d1 indicates the breaking of the niosomes and the proliferation of large number of small Span 80 micelles which, in turn, are unstable and aggregate in larger formations, but smaller than 0.8 microns (as observed in Fig. 9.8), significantly increasing the BS to values around 15% in Fig. 9.9d1. This phenomenon shown in Fig. 9.9d1 is known as "Ostwald ripening" [43,44]. Results shown in Figs. 9.9d1 and 9.9d2 indicate that Span 80 niosomes break in 80 mol/m³ NaCl solutions and then form large aggregates (> 0.8 μm, see Table 3) that tend to precipitate.

Stability and characterization of Span 80 niosomes modified with CTAB in the presence of NaCl

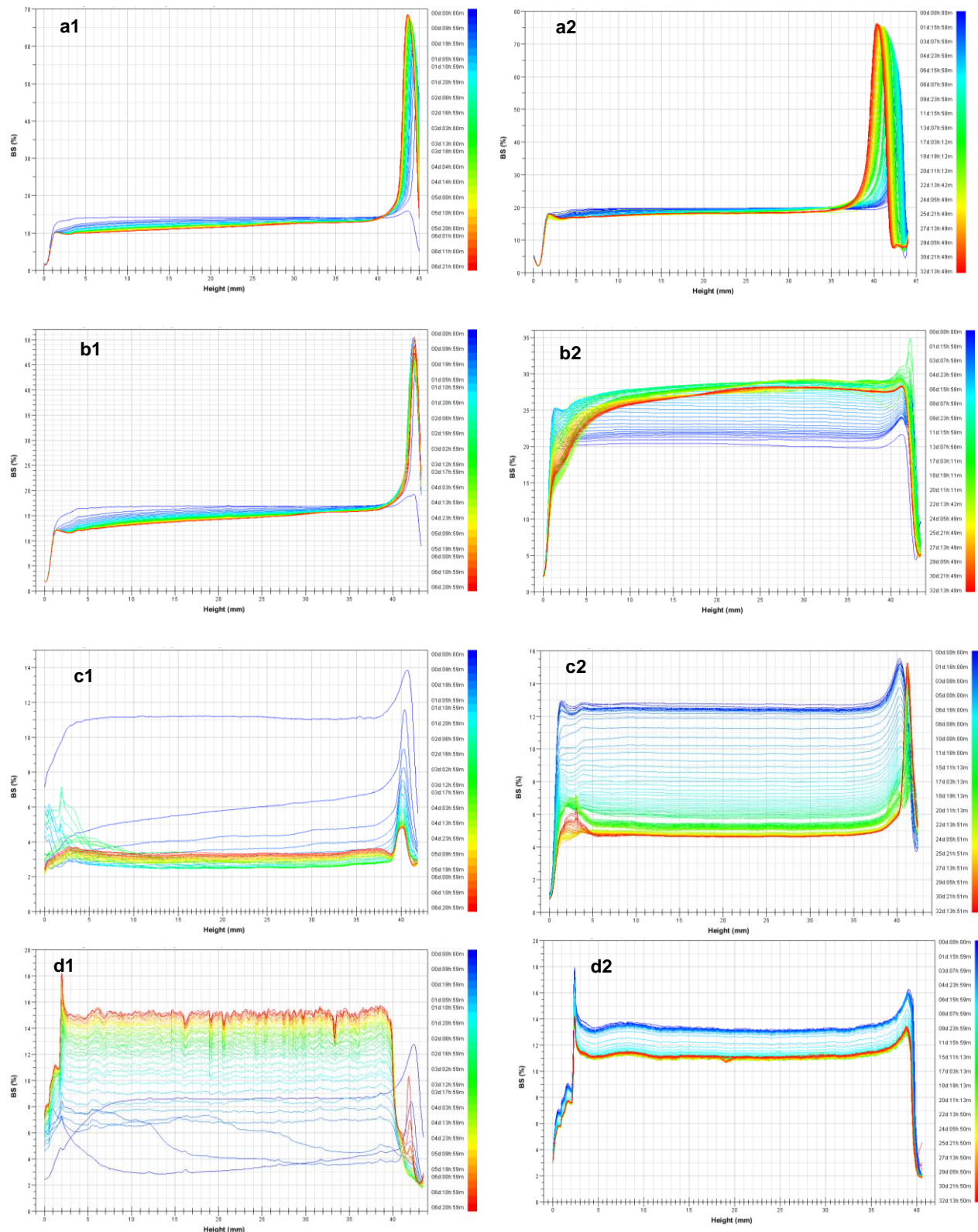


Figure 9.9. Evolution of BS profiles over time for 20 mol/m³ Span 80 niosomes in pure water (a1 and a2) and in 20 (b1 and b2), 50 (c1 and c2) and 80 mol/m³ (d1 and d2) NaCl solutions, measured for 7 days (a1, b1, c1 and d1) and 32 days (a2, b2, c2 and d2) after preparation.

TEM images confirm previous results. They show that in the absence and presence of 20 mol/m³ of NaCl (Figs. 9.10a and 9.10b), the niosomes remain independent and stable in solution, with sizes around 200 nm, in agreement with DLS measurements shown in Table 9.3. The small difference in size between both techniques is due to the fact that in TEM the vesicles adsorbed on the copper grid where the sample is deposited are reduced in size, resulting in slightly smaller aggregate sizes than by DLS [39]. Fig. 9.10c shows the rupture of the niosomal bilayer in the presence of 50 mol/m³ of NaCl. Fig. 9.10d shows large aggregates in the formulation with 80 mol/m³ of NaCl that come from associations of condensed phase after niosomes breakup and are coincident in size with those of Table 3. Moreover, the sample with higher NaCl content is very transparent, indicating the presence of very few particles in suspension due to precipitation of condensates, which justifies the smaller decrease of the BS observed in Fig. 9.9d2, as it was abovementioned.

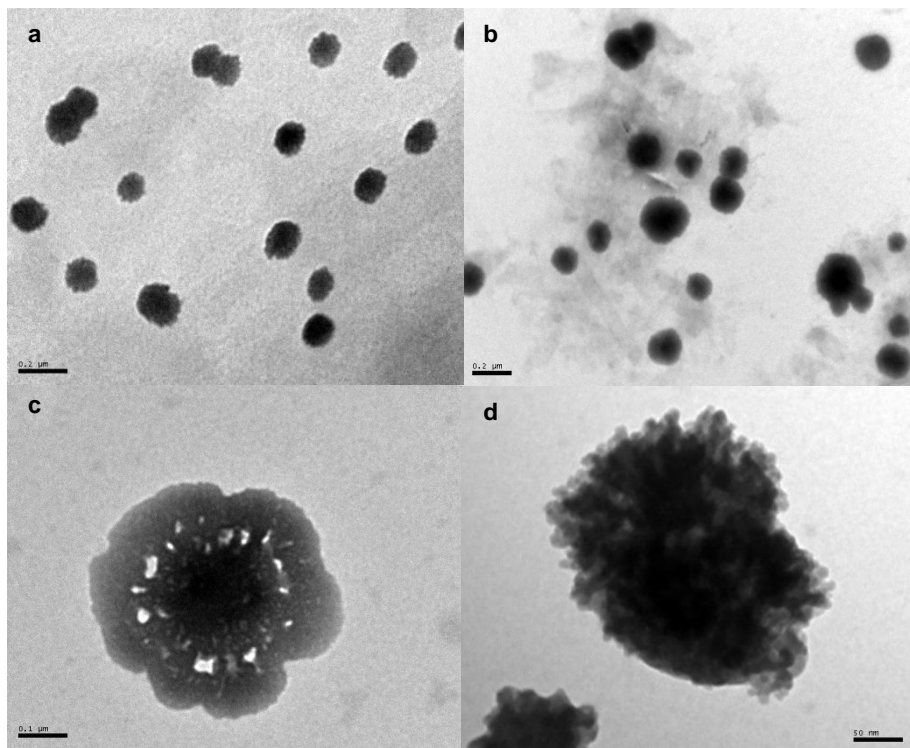


Figure 9.10. TEM images of 20 mol/m³ Span 80 dispersions in pure water (a) and in 20 mol/m³ (b), 50 mol/m³ (c) and 80 mol/m³ (d) NaCl solutions. Scale bars: 0.2 μm (a, b), 0.1 μm (c) and 50 nm (d).

9.3.2.3. Effect of NaCl on mixed niosomes of Span 80 (20 mol/m^3) and CTAB (4 mol/m^3)

Table 9.1 shows that the CMC and γ_{CMC} of the Span 80 and CTAB mixed niosomes have intermediate values between those of the pure surfactants. The addition of NaCl hardly changes the CMC value and nevertheless causes a significant decrease of γ_{CMC} with respect to the formulation without salt, with similar values in the three salt formulations tested. They show slight increase in the efficiency, π_{CMC} , and the maximum surface concentration, Γ_{max} , with respect to the salt-free formulation. Accordingly, a decrease in A_{\min} in the presence of electrolyte is observed. Free energy values indicate that both adsorption and micellization are spontaneous processes in all formulations tested, with similar values to those of Span 80 in the absence of CTAB. The CMC/C₂₀ ratios close to the unit indicates very similar trends for adsorption and micellization.

The diffusion coefficients, D_s and D_{ef}, for these mixed systems are shown in Table 9.2. As it can be seen, D_s and D_{ef} are practically of the same order of magnitude, which disregards the presence of barrier to adsorption at the liquid-air interface.

Table 9.4 reports the values of size, PDI and ζ -potential of the mixed niosomes after 35 days from their formation. Positive ζ -potentials reveal the adsorption of CTAB in the niosomal bilayer. The low PDI values indicate size homogeneity in all formulations, which are lower than formulations of single Span 80. Size increases in the presence of 50 and 80 mol/m³ of electrolyte, in accordance with TEM images and BS results, as discussed below.

Table 9.4. Size, PDI and ζ -potential for the different formulations of the mixed niosomes of Span 80 (20 mol/m^3) and CTAB (4 mol/m^3) 32 days after preparation.

Formulation	Size (nm)	PDI	ζ -potential (mV)
Span 80 + CTAB	90.16	0.276	51.0
Span 80 + CTAB + 20 mol/m ³ NaCl	120.6	0.252	74.8
Span 80 + CTAB + 50 mol/m ³ NaCl	224.6	0.293	67.7
Span 80 + CTAB + 80 mol/m ³ NaCl	211.1	0.262	52.3

The variation of BS for mixed niosomes in the absence and presence of NaCl is shown in Fig. 9.11. Stability in the salt-free formulation (Fig. 9.11a) and in the presence of 20 mol/m³ of NaCl (Fig. 9.11b) is observed during the 32 days of testing. The formulation with 50 mol/m³ of NaCl (Fig. 9.11c) shows slight increase of BS over time (from 16% to 20%) and decrease of particles number in the top of the sample. In the formulation with 80 mol/m³ of NaCl (Fig. 9.11d), the BS increase is even more marked (from 13% to 20%) and, like the previous formulation, is due to the increase in the particle size.

TEM images show spherical mixed niosomes in the salt-free formulation (Fig. 9.12a), smaller than those of Span 80 alone and stable in dispersion, with no aggregations, corroborating the BS and DLS results. In the presence of 20 mol/m³ of NaCl (Fig. 9.12b), the TEM image shows small size particles (120 nm) that remain stable in dispersion. In the formulations with 50 and 80 mol/m³ of NaCl (Figs. 9.12e–h) niosome associations of irregular form due to physical bonds between neighboring niosomes are observed; however, they are stable in dispersion, without presence of precipitates. Unlike the Span 80 formulation alone, the positive charge of the mixed niosomes, as indicated by the ζ -potential in Table 9.4, makes them remain stable in the bulk phase.

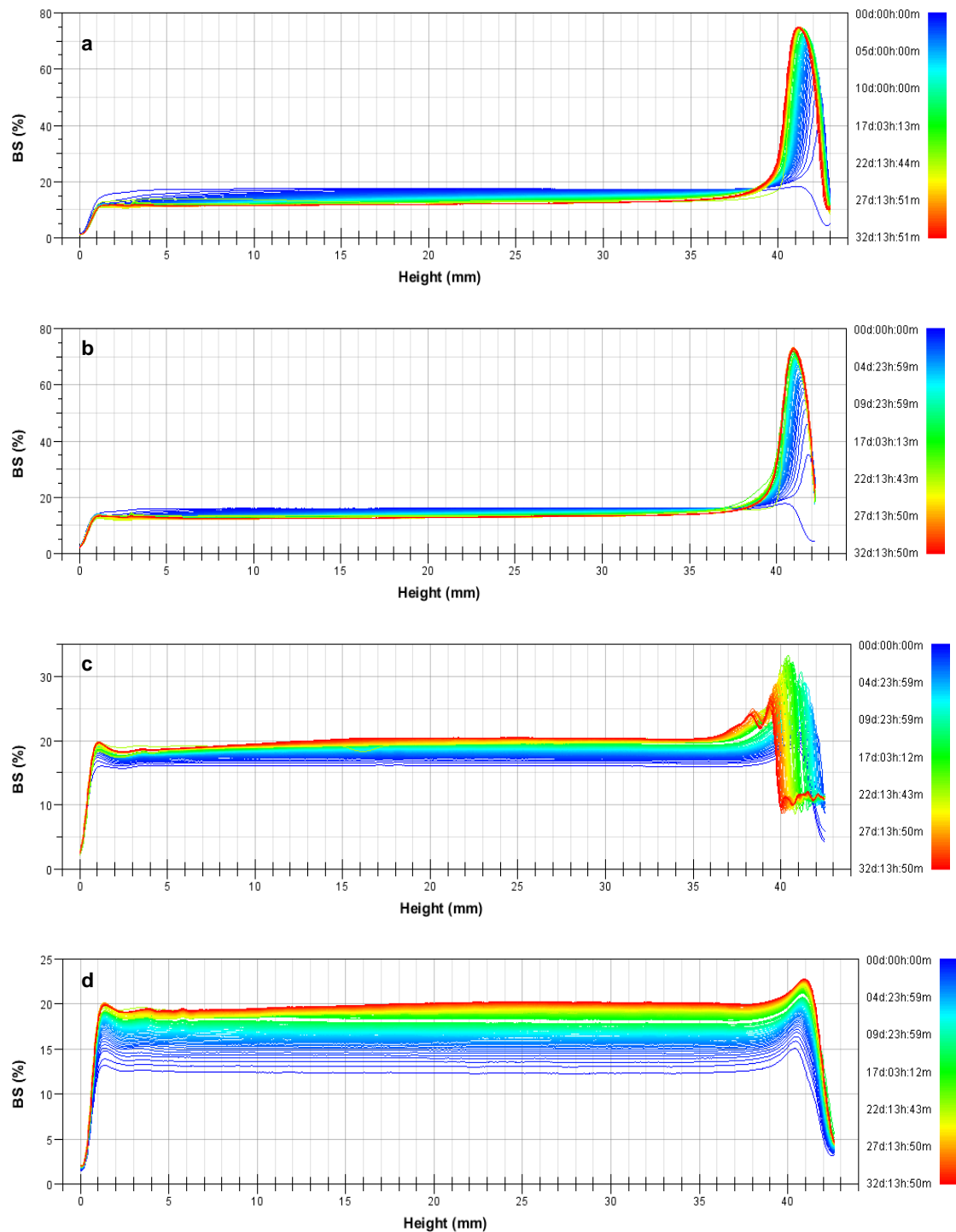


Figure 9.11. Evolution of BS profiles over time for Span 80 ($20 \text{ mol}/\text{m}^3$) and CTAB ($4 \text{ mol}/\text{m}^3$) mixed niosomes in pure water (a) and NaCl solutions: (b) $20 \text{ mol}/\text{m}^3$, (c) $50 \text{ mol}/\text{m}^3$, and (d) $80 \text{ mol}/\text{m}^3$, measured for 32 days after preparation.

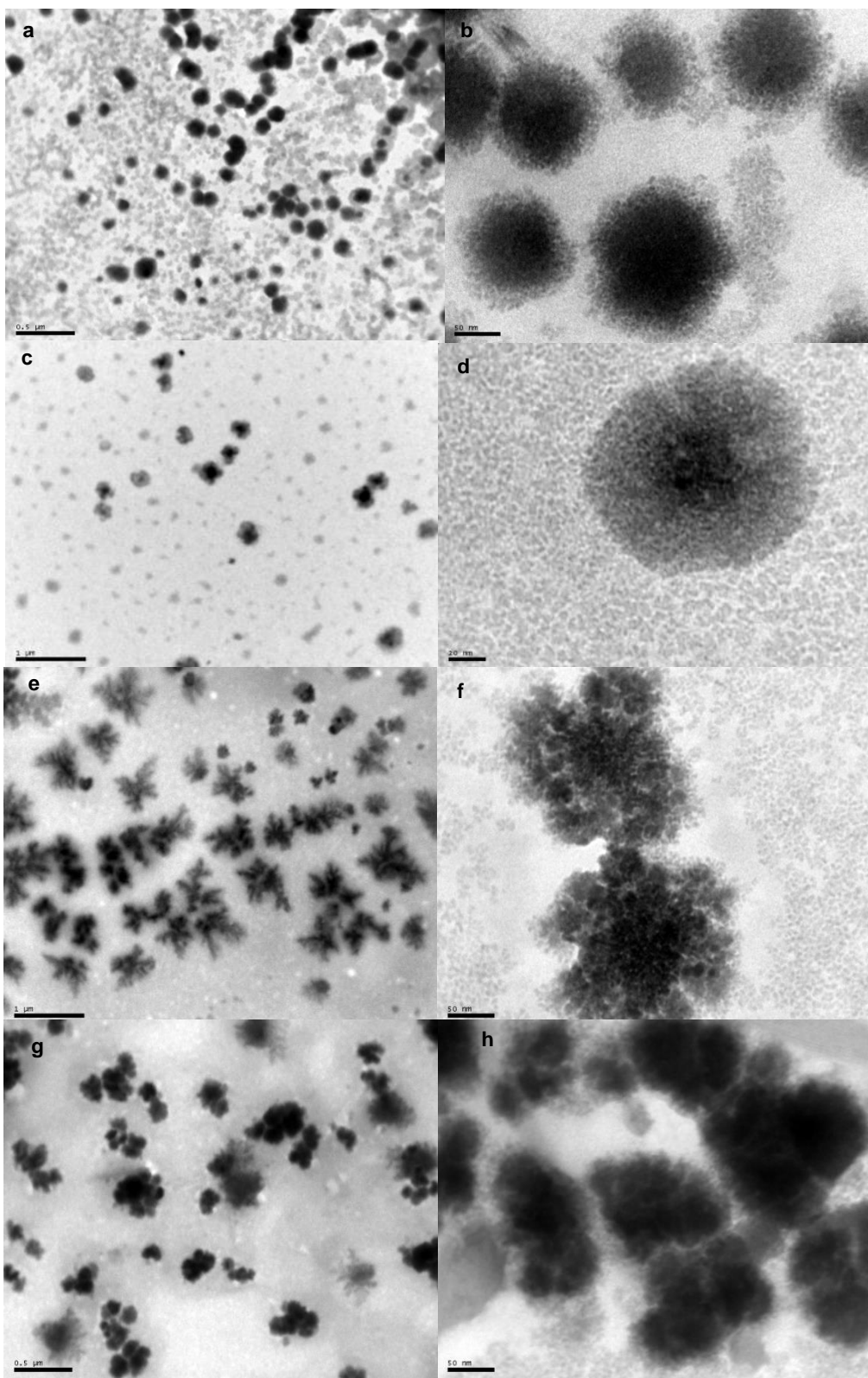


Figure 9.12. TEM images of mixed niosomes of Span 80 ($20 \text{ mol}/\text{m}^3$) and CTAB ($4 \text{ mol}/\text{m}^3$) in pure water (a, b) and in $20 \text{ mol}/\text{m}^3$ (c, d), $50 \text{ mol}/\text{m}^3$ (e, f) and $80 \text{ mol}/\text{m}^3$ (g, h) NaCl solutions.

Scale bars: 1 μm (c, e), 0.5 μm (a, g), 50 nm (b, f, h) and 20 nm (d).

The aggregation tendency of a mixture of surfactants can be very different from that of pure surfactants. There are different theories and models that describe molecular interaction. According to the theory of regular solutions formulated by Holland and Rubingh [50], the nature and strength of the interaction between two surfactants can be evaluated through the value of the interaction parameter in the formation of mixed aggregates in an aqueous medium (β^M). The molar fraction of component 1 in the mixed aggregate (x_1) and β^M can be calculated by solving the following equations:

$$x_1 = \frac{(x_1^M)^2 \ln\left(\frac{\alpha_1 C_{12}^M}{x_1^M C_1^M}\right)}{(1-x_1^M)^2 \ln\left(\frac{(1-\alpha_1) C_{12}^M}{(1-x_1^M) C_2^M}\right)} \quad (12)$$

$$\beta^M = \frac{\ln\left(\frac{\alpha_1 C_{12}^M}{x_1^M C_1^M}\right)}{(1-x_1^M)^2} \quad (13)$$

where C_1^M , C_2^M , and C_{12}^M are the CMC of single and mixed surfactants, respectively. In this work, 1 refers to CTAB, 2 to Span 80, and 12 refers to the 4/20 molar ratio mixture of both surfactants (molar fraction $\alpha_1 = 0.16$). The value of β^M can be negative, positive or zero, revealing synergism, antagonism or ideal mixing, respectively, of the surfactants in the formation of aggregates [31]. If the behavior is ideal, the CMC of the mixture (C_{12}^*) can be described by the following expression [51]:

$$\frac{1}{C_{12}^*} = \frac{\alpha_1}{C_1^M} + \frac{1-\alpha_1}{C_2^M} \quad (14)$$

In a mixture of surfactants, the mixture of hydrophobic chains can be considered as an ideal process in which the free energy of the system decreases when the chain of surfactant moves from a monomeric phase to the aggregates phase. However, interactions between head groups can be considered non-ideal. The difference between C_{12}^M and C_{12}^* is indicative of the non-ideal nature of the interaction [31,46,52]. The molar fraction in the ideal mixture aggregate can be calculated by the following relation:

$$x_1^* = \frac{\alpha_1 C_2^M}{\alpha_1 C_2^M + (1-\alpha_1) C_1^M} \quad (15)$$

The activity coefficients (f_1 and f_2) of the surfactants within the aggregates are related to the parameter β^M by the following expressions:

$$f_1 = \exp[\beta^M(1-x_1)^2] \quad (16)$$

$$f_2 = \exp[\beta^M(x_1)^2] \quad (17)$$

Values of f_1 and f_2 different from the unit indicate no ideality of the mixture in the aggregate. The activity coefficients can be used to calculate the excess free energy of the mixture (ΔG_{ex}), by Eq. (18). Negative values of ΔG_{ex} reveal that mixed aggregates are more stable than those formed by individual surfactants. Results are reported in Table 9.5.

$$\Delta G_{ex} = RT[x_1 \ln f_1 + (1-x_1) \ln f_2] \quad (18)$$

Table 9.5. Physicochemical parameters for Span 80 and CTAB mixed niosomes in pure water and in presence of NaCl, evaluated from surface tension measurements.

NaCl (mol/m ³)	Ln(C ₁ ^M /C ₂ ^M)	X ₁ [*]	C ₁₂ [*] (mol/m ³)	X ₁	β ^M	f ₁	f ₂	ΔG _{ex} (kJ/mol)
0	0.921	0.074	0.436	0.46	-6.512	0.150	0.252	-4.010
20	0.403	0.100	0.422	0.46	-4.890	0.223	0.371	-2.675
50	-1.492	0.131	0.391	0.44	-3.997	0.285	0.461	-2.441
80	-1.491	0.471	0.203	0.39	2.333	2.356	1.436	1.391

The fulfillment of the following two conditions indicates synergism in the formation of mixed aggregates: $\beta^M < 0$ and $|\beta^M| > |\ln(C_1^M/C_2^M)|$ [53]. This is the case for the salt-free and 20 and 50 mol/m³ NaCl formulations. It means that the attractive interactions between the two component molecules are stronger than the interactions between the same molecules. For these formulations, C_{12}^M is less than C_{12}^* (see Table 9.1), which means that formation of aggregates occurs at a lower concentration than the ideal mixing. However, in the formulation with 80 mol/m³ of NaCl, $\beta^M > 0$ and $|\beta^M| > |\ln(C_1^M/C_2^M)|$ indicate antagonism, which means that the repulsive forces between the different surfactant molecules are stronger than the repulsive forces between the same surfactant molecules. Furthermore, the X₁ values are greater than X₁^{*}

ones in all formulations, except for the formulation with 80 mol/m³ NaCl, indicating that the mixed aggregates are rich in CTAB, compared to the ideal state.

ΔG_{ex} is negative in all the formulations, except in the 80 mol/m³ NaCl formulation, and its magnitude decreases with the salt content. This suggests that the higher the salt concentration, the less stable aggregates are formed, which can be explained in terms of electrostatic repulsions between the polar heads of the surfactants in the bilayer, stronger at higher salt concentration.

9.4. Conclusions

Surface and aggregation properties of individual and mixed systems of the non-ionic surfactant Span 80 (20 mol/m³) and the cationic surfactant CTAB (4 mol/m³), in salt-free water and in the presence of NaCl (20, 50 and 80 mol/m³) have been studied in this work. The addition of NaCl favors the aggregation process of the CTAB surfactant in large but unstable micelles over time, decreasing the CMC with slight changes in surface tension, except in the presence of 80 mol/m³ of salt where the surface tension is significantly low. Although both the micellization and adsorption processes are spontaneous, the presence of NaCl reduces the barriers to adsorption and is thermodynamically more favored than micellization.

Span 80 niosomes are stable in salt-free formulation and in the presence of 20 mol/m³ of NaCl. Above this salt concentration large aggregates are formed, and in formulations with 80 mol/m³ of NaCl the breaking of niosomes and the formation of Span 80 precipitate occur.

The mixed niosomes of Span 80 (20 mol/m³) and CTAB (4 mol/m³) are positively charged structures. In the absence and presence of low salt concentration (20 mol/m³), the mixed niosomes are spherical, very stable in the bulk, and smaller in size than those of Span 80 alone. However, for high NaCl concentrations (50 and 80 mol/m³), mixed niosomes slightly increase in size due to associations between them, but they remained stable for 32 days in which neither rupture nor formation of precipitates occur. Synergism between surfactants is observed in salt-free water formulations and with 20 and 50 mol/m³ of NaCl, in which the formation of aggregates occurs at a concentration lower than the ideal. For these formulations, the niosomal bilayer is rich in CTAB, compared to the ideal state. Mixed niosomes formulated in presence of 80 mol/m³ of NaCl are unstable over time, and antagonism between surfactants was found in this formulation. These results shed light on the possibility of using CTAB adsorbed on mixed

niosomes, taking advantage of its antiseptic and antibacterial properties highly appreciated by the industry, and solving the limitation imposed by its high Krafft temperature.

Supplementary data

Turbidity variation at 350 nm wavelength of Span 80 niosomes (15, 10 and 5 mol/m³) in water as a function of CTAB concentration; size and PDI values after different intervals of contact time with increasing amounts of CTAB in niosome formulations; and evolution of BS profiles over time for CTAB (10 mol/m³) micelles in pure water and in NaCl solutions.

Acknowledgments

This work was supported by Junta de Castilla y León and the European Regional Development Fund (ERDF) through project BU301P18. The authors would like to thank Junta de Castilla y León and the European Social Fund (ESF) for the contract of Davinia Benito-Bedoya through the Youth Employment Initiative (YEI) program, and also to Dr. Carlos Álvarez (Scientific Technical Services, University of Oviedo, Spain) for his valuable help and assistance with TEM measurements.

9.5. References

- [1] E. Acosta, Bioavailability of nanoparticles in nutrient and nutraceutical delivery, *Curr. Opin. Colloid Interface Sci.* 14 (2009) 3–15.
- [2] C. Marianelli, L. Di Marzio, F. Rinaldi, C. Celia, D. Paolino, F. Alhaique, S. Esposito, M. Carafa, Niosomes from 80s to present: the state of the art, *Adv. Colloid Interface Sci.* 205 (2014) 187–206.
- [3] D.J. McClements, E.A. Decker, Y. Park, J. Weiss, Structural design principles for delivery of bioactive components in nutraceuticals and functional foods, *Crit. Rev. Food Sci. Nutr.* 49 (2009) 577–606.
- [4] M.J. Choi, H.I. Maibach, Liposomes and niosomes as topical drug delivery systems, *Skin Pharmacol. Physiol.* 18 (2005) 209–219.
- [5] L. Roque, I. Escudero, J.M. Benito, Lactic acid recovery by microfiltration using niosomes as extraction agents, *Sep. Purif. Technol.* 151 (2015) 1–13.

- [6] R. Fraile, R.M. Geanta, I. Escudero, J.M. Benito, M.O. Ruiz, Formulation of Span 80 niosomes modified with SDS for lactic acid entrapment, *Desalin. Water Treat.* 56 (2015) 3463–3475.
- [7] L. Roque, I. Escudero, J.M. Benito, Separation of sodium lactate from Span 80 and SDS surfactants by ultrafiltration, *Sep. Purif. Technol.* 180 (2017) 90–98.
- [8] G. Pando, G. Gutiérrez, J. Coca, C. Pazos, Preparation and characterization of niosomes containing resveratrol, *J. Food Eng.* 117 (2013) 227–234.
- [9] S. Chen, S. Hanning, J. Falconer, M. Lockem, J. Wen, Recent advances in non-ionic surfactant vesicles (niosomes): fabrication, characterization, pharmaceutical and cosmetic applications, *Eur. J. Pharm. Biopharm.* 144 (2019) 18–39.
- [10] S. Moghassemi, A. Hadjizadeh, Nano-niosomes as nanoscale drug delivery systems: An illustrated review, *J. Control. Release* 185 (2014) 22–36.
- [11] Z. Sezgin-Bayindir, N. Yuksel, Investigation of formulation variables and excipient interaction on the production of niosomes, *AAPS Pharm. Sci. Technol.* 13 (2012) 826–835.
- [12] I.F. Uchegbu, A.T. Florence, Non-ionic surfactant vesicles (niosomes): physical and pharmaceutical chemistry, *Adv. Colloid Interface Sci.* 58 (1995) 1–55.
- [13] B. Heurtault, P. Saulnier, B. Pech, J.-E. Proust, J.-P. Benoit, Physico-chemical stability of colloidal lipid particles, *Biomaterials* 24 (2003) 4283–4300.
- [14] S.K. Hait, S.P. Moulik, Determination of critical micelle concentration (CMC) of nonionic surfactants by donor-acceptor interaction with Iodine and correlation of CMC with hydrophile-lipophile balance and other parameters of the surfactant, *J. Surfactants Deterg.* 4 (2001) 303–309.
- [15] T. Geng, C. Zhang, Y. Jiang, H. Ju, Y. Wang, Synergistic effect of binarymixtures contained newly cationic surfactant: Interaction, aggregation behaviors and application properties, *J. Mol. Liq.* 232 (2017) 36–44.
- [16] A. Choucair, A. Eisenberg, Interfacial solubilization of model amphiphilic molecules in block copolymer micelles, *J. Am. Chem. Soc.* 125 (2003) 11993–12000.
- [17] M.F. Francis, M. Piredda, F.M. Winnik, Solubilization of poorly water soluble drugs in micelles of hydrophobically modified hydroxypropylcellulose copolymers, *J. Control. Release* 93 (2003) 59–68.
- [18] S. Paria, P.K. Yuet, Solubilization of naphthalene by pure and mixed surfactants, *Ind. Eng. Chem. Res.* 45 (2006) 3552–3558.
- [19] M.R. Behera, S.R. Varade, P. Ghosh, P. Paul, A.S. Negi, Foaming in micellar solutions: effects of surfactant, salt, and oil concentrations, *Ind. Eng. Chem. Res.* 53 (2014) 18497–18507.

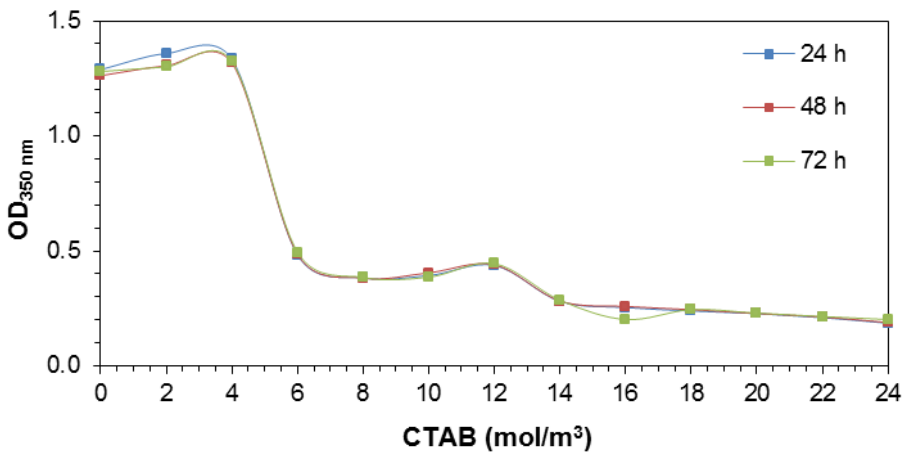
- [20] B. Naskar, A. Dey, S.P. Moulik, Counter-ion effect on micellization of ionic surfactants: A comprehensive understanding with two representatives, sodium dodecyl sulfate (SDS) and dodecytrimethylammonium bromide (DTAB), *J. Surfactants Deterg.* 16 (2013) 785–794.
- [21] D. Kumar, M.A. Rub, Role of cetyltrimethylammonium bromide (CTAB) surfactant micelles on kinetics of $[\text{Zn}(\text{II})\text{-Gly-Leu}]^+$ and ninhydrin, *J. Mol. Liq.* 274 (2019) 639–645.
- [22] S. Mahbub, M.A. Rub, Md.A. Hoque, M.A. Khan, Influence of NaCl/urea on the aggregation behavior of dodecytrimethylammonium chloride and sodium dodecyl sulfate at varying temperatures and compositions: experimental and theoretical approach, *J. Phys. Org. Chem.* 32 (2018) e3917.
- [23] M. Rahman, M.A. Khan, M.A. Rub, Md.A. Hoque, A.M. Asiri, Investigation of the effect of various additives on the clouding behavior and thermodynamics of polyoxyethylene (20) sorbitan monooleate in absence and presence of ceftriaxone sodium trihydrate drug, *J. Chem. Eng. Data* 62 (2017) 1464–1474.
- [24] G. Luo, X. Qi, C. Han, C. Liu, J. Gui, Salt effect on mixed micelle and interfacial properties of conventional cationic surfactants and the ionic liquid surfactant 1-tetradecyl-3-methylimidazolium bromide ($[\text{C}_{14}\text{mim}] \text{Br}$), *J. Surfactants Deterg.* 16 (2013) 531–538.
- [25] J.C. Roy, M. N. Islam, G. Aktaruzzaman, The effect of NaCl on the Krafft temperature and related behavior of cetyltrimethylammonium bromide in aqueous solution, *J. Surfactants Deterg.* 17 (2014) 231–242.
- [26] M.L. Corrin, W.D. Harkins, The effect of salts on the critical concentration for the formation of micelles in colloidal electrolytes, *J. Am. Chem. Soc.* 69 (1947) 683–688.
- [27] Q. Xu, M. Nakajima, S. Ichikawa, N. Nakamura, P. Roy, H. Okadome, T. Shiina, Effects of surfactant and electrolyte concentrations on bubble formation and stabilization, *J. Colloid Interface Sci.* 332 (2009) 208–214.
- [28] H. Ali, A. Niazi, M.K. Baloch, G.F. Durrani, A. Rauf, A. Khan, Effect of temperature, polymer, and salts on the interfacial and micellization behavior of 3-dodecyl-1-methyl-1h-imidazol-3-ium-bromide: a dispersion of a long-chain ionic liquid, *J. Dispersion Sci. Technol.* 36 (2015) 723–730.
- [29] Y. Jiang, T. Geng, Q. Li, G. Li, H. Ju, Influences of temperature, pH and salinity on the surface property and self-assembly of 1:1 salt-free catanionic surfactant, *J. Mol. Liq.* 199 (2014) 1–6.
- [30] K. Nyuta, T. Yoshimura, K. Esumi, Surface tension and micellization properties of heterogemini surfactants containing quaternary ammonium salt and sulfobetaine moiety, *J. Colloid Interface Sci.* 301 (2006) 267–273.

- [31] A. Trawińska, E. Hallmann, K. Mędrzycka, Synergistic effects in micellization and surface tension reduction in nonionic gemini S-10 and cationic RTAB surfactants mixtures, *Colloid Surf. A-Physicochem. Eng. Asp.* 488 (2016) 162–172.
- [32] K. Chen, T. Jiao, J. Li, D. Han, R. Wang, G. Tian, Q. Peng, Chiral nanostructured composite films via solvent-tuned self-assembly and their enantioselective performances, *Langmuir* 35 (2019) 3337–3345.
- [33] S.W. Huo, P.F. Duan, T.F. Jiao, Q.M. Peng, M.H. Liu, Self-assembled luminescent quantum dots to generate full-color and white circularly polarized light, *Angew. Chem. Int. Ed.* 56 (2017) 12174–12178.
- [34] L. Alonso, L. Roque, I. Escudero, J.M. Benito, M.T. Sanz, S. Beltrán, Solubilization of Span 80 niosomes by sodium dodecyl sulfate, *ACS Sustain. Chem. Eng.* 4 (2016) 1862–1869.
- [35] V.Y. Ixtaina, L.M. Julio, J.R. Wagner, S.M. Nolasco, M.C. Tomás, Physicochemical characterization and stability of chia oil microencapsulated with sodium caseinate and lactose by spray-drying, *Powder Technol.* 271 (2015) 26–34.
- [36] M.I. Capitani, S.M. Nolasco, M.C. Tomás, Stability of oil-in-water (O/W) emulsions with chia (*Salvia hispanica* L.) mucilage, *Food Hydrocolloids* 61 (2016) 537–546.
- [37] O. Mengual, G. Meunier, I. Cayré, K. Puech, P. Snabre, TURBISCAN MA 2000: multiple light scattering measurement for concentrated emulsion and suspension instability analysis, *Talanta* 50 (1999) 445–456.
- [38] D. Velluto, C. Gasbarri, G. Angelini, A. Fontana, Use of simple kinetic and reaction-order measurements for the evaluation of the mechanism of surfactant-liposome interactions, *J. Phys. Chem. B* 115 (2011) 8130–8137.
- [39] C. Chen, C. Jiang, C.P. Tripp, Molecular dynamics of the interaction of anionic surfactants with liposomes, *Colloid Surf. B-Biointerfaces* 105 (2013) 173–179.
- [40] M. Cócera, O. López, R. Pons, H. Amenitsch, A. de la Maza, Effect of the electrostatic charge on the mechanism inducing liposome solubilization: A kinetic study by synchrotron radiation SAXS, *Langmuir* 20 (2004) 3074–3079.
- [41] D.K. Chattoraj, K.S. Birdi, *Adsorption and the Gibbs Surface Excess*, Plenum, New York (1984).
- [42] M.J. Rosen, *Surfactants and Interfacial Phenomena*, third ed., Wiley-Interscience, New York (2004).
- [43] N. Azum, M.A. Rub, A.M. Asiri, W.A. Bawazeer, Micellar and interfacial properties of amphiphilic drug-non-ionic surfactants mixed systems: surface tension, fluorescence and UV-vis studies, *Colloid Surf. A-Physicochem. Eng. Asp.* 522 (2017) 183–192.

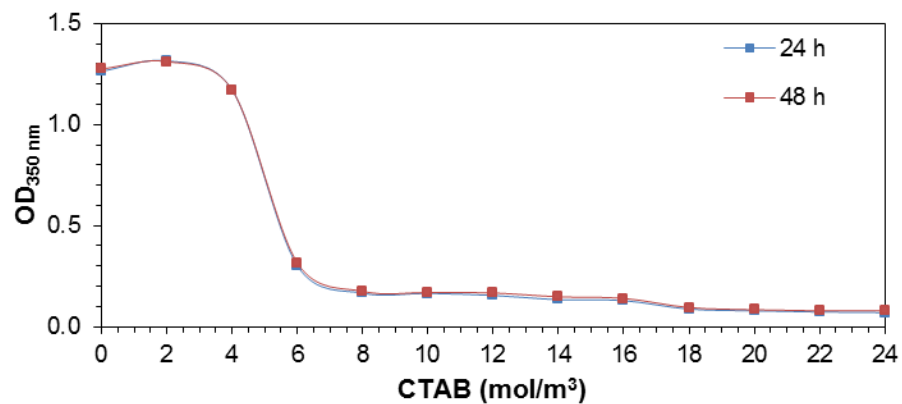
- [44] Ch. Zhang, T. Geng, Y. Jiang, L. Zhao, H. Ju, Y. Wang, Impact of NaCl concentration on equilibrium and dynamic surface adsorption of cationic surfactants in aqueous solution, *J. Mol. Liq.* 238 (2017) 423–429.
- [45] J. Eastoe, J.S. Dalton, Dynamic surface tension and adsorption mechanisms of surfactants at the air-water interface, *Adv. Colloid Interface Sci.* 85 (2000) 103–144.
- [46] N. Azum, A.Z. Naqvi, M. Akram, Kabir-ud-Din, Studies of mixed micelle formation between cationic gemini and cationic conventional surfactants, *J. Colloid Interface Sci.* 328 (2008) 429–435.
- [47] S. Mahbud, M.R. Molla, M. Saha, I. Shahriar, Md. A. Hoque, M.A. Halim, M.A. Rub, M.A. Khan, N. Azum, Conductometric and molecular dynamics studies of the aggregation behavior of sodium dodecyl sulfate (SDS) and cetyltrimethylammonium bromide (CTAB) in aqueous and electrolytes solution, *J. Mol. Liq.* 283 (2019) 263–275.
- [48] Z. Huang, M. Su, Q. Yang, Z. Li, S. Chen, Y. Li, X. Zhou, F. Li, Y. Song, A general patterning approach by manipulating the evolution of two-dimensional liquid foams, *Nat. Commun.* 8 (2017) 14110.
- [49] Z. Zhang, Z. Wang, S. He, C. Wang, M. Jin, Y. Yin, Redox reaction induced Ostwald ripening for size-and shape-focusing of palladium nanocrystals, *Chem. Sci.* 6 (2015) 5197–5203.
- [50] P.M. Holland, D.N. Rubingh, Mixed surfactant systems. An overview. In: P.M. Holland, D.N. Rubingh (Eds.), *Mixed Surfactant Systems*, ACS Symposium Series 501, American Chemical Society, Washington DC (1992), pp. 2–30.
- [51] J.H. Clint, Micellization of mixed nonionic surface active agents, *J. Chem. Soc. Faraday Trans.* 71 (1974) 1327–1334.
- [52] L. Liu, M.J. Rosen, The interaction of some novel diquaternary gemini surfactants with anionic surfactants, *J. Colloid Interface Sci.* 179 (1996) 454–459.
- [53] M.J. Rosen, X.Y. Hua, Dynamic surface tension of aqueous surfactant solutions: 2. Parameters at 1 s and at mesoequilibrium, *J. Colloid Interface Sci.* 139 (1990) 397–407.

Supplementary data

(a)



(b)



(c)

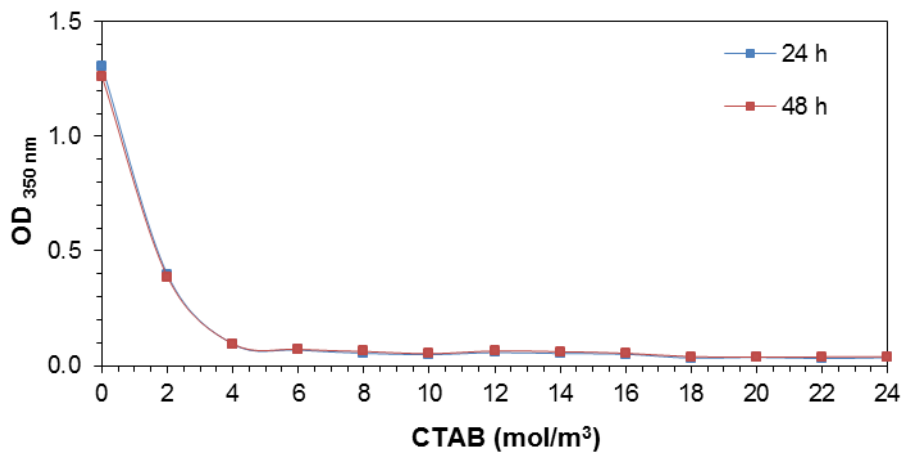
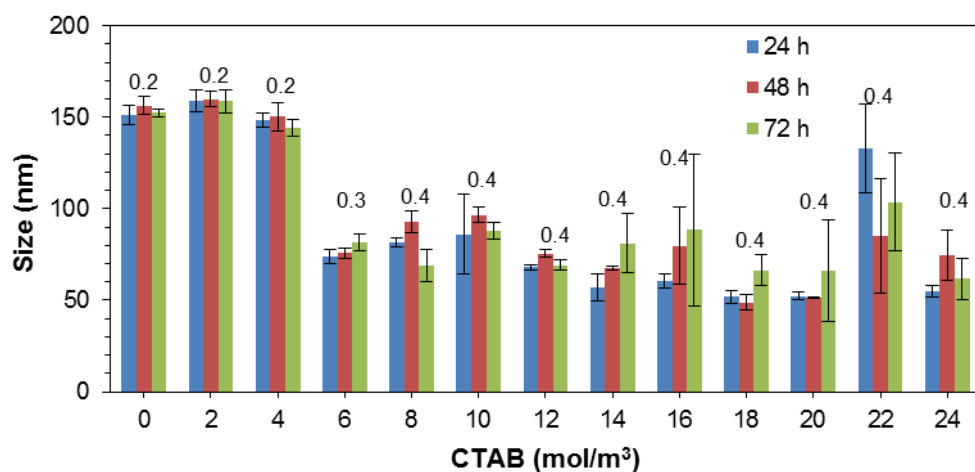
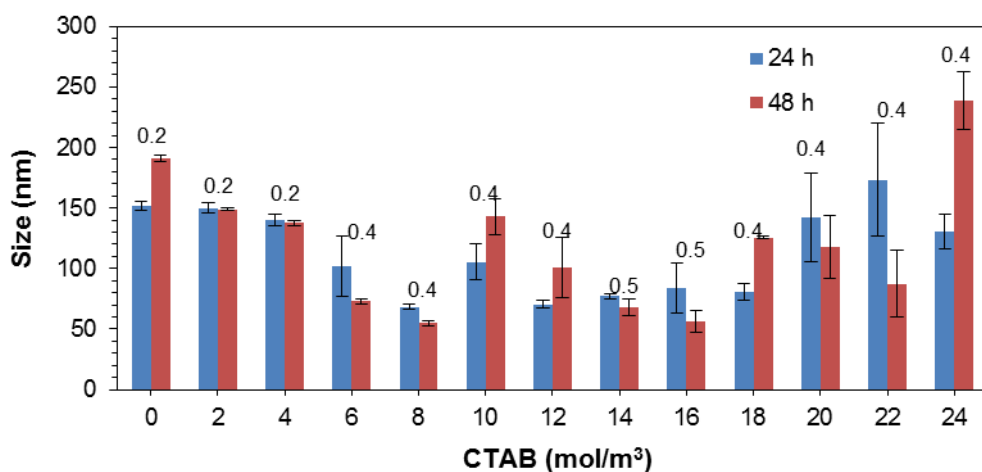


Figure S1. Solubilization curves of 15 mol/m³ (a), 10 mol/m³ (b) and 5 mol /m³ (c) Span 80 niosomes in water by CTAB at different contact times.

(a)



(b)



(c)

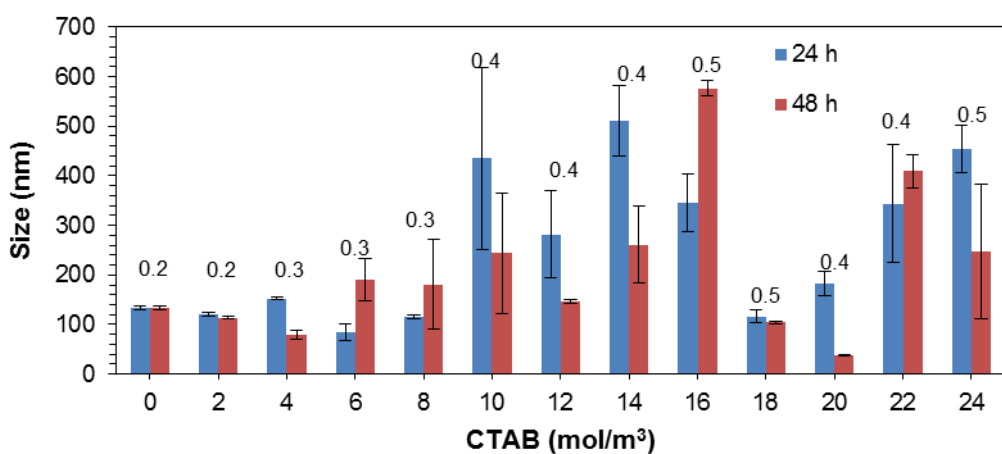


Figure S2. Mean hydrodynamic diameter (Z-average) and PDI (data over columns) of 15 mol/m³ (a), 10 mol/m³ (b) and 5 mol /m³ (c) Span 80 niosomes in water in presence of CTAB.

Stability and characterization of Span 80 niosomes modified with CTAB in the presence of NaCl

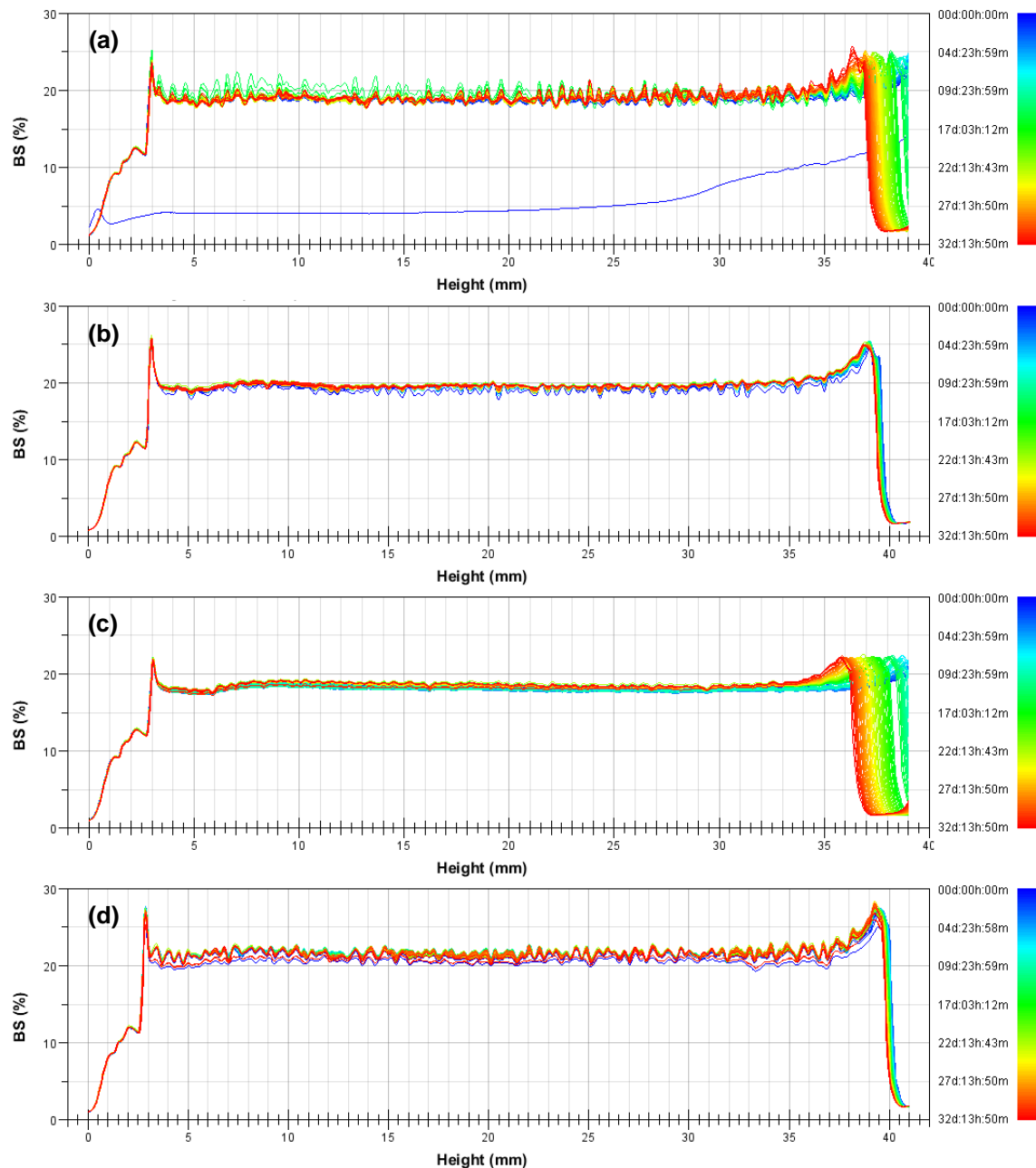


Figure S3. Evolution of BS profiles over time for CTAB ($10 \text{ mol}/\text{m}^3$) mixed micelles in pure water and in NaCl solutions: a) water, b) $20 \text{ mol}/\text{m}^3$ of NaCl, c) $50 \text{ mol}/\text{m}^3$ of NaCl, d) $80 \text{ mol}/\text{m}^3$ of NaCl.

10. Conclusiones generales

Las conclusiones generales de la investigación realizadas en esta Tesis Doctoral son las siguientes:

- Se ha verificado que los niosomas mixtos formulados con el tensioactivo no iónico Span 80 en una concentración de 20 mol/m^3 , modificados con pequeñas cantidades del tensioactivo aniónico dodecil sulfato sódico SDS (inferiores al punto crítico de saturación en la bicapa) y estabilizados mediante ultrasonidos, pueden ser utilizados como agentes de extracción del ácido láctico en medios acuosos diluidos.
- El grado de extracción del ácido láctico está afectado por la concentración de SDS utilizada en la formulación de los niosomas, el volumen de la fase dispersa añadida, el pH, y la concentración de ácido láctico en la alimentación; siendo éstos los parámetros de control para la optimización del proceso de extracción del ácido láctico.
- Se observó que, para una misma concentración de ácido láctico en la fase continua, el grado de extracción disminuía al aumentar el volumen de fase dispersa añadida, y además el grado de extracción fue máximo en las experiencias realizadas con valores intermedios de concentración de ácido láctico. Este resultado reveló la existencia de una relación molar óptima entre la concentración de SDS y la de ácido láctico.
- Los valores óptimos que proporcionan el mayor grado de extracción del ácido láctico fueron un pH alrededor de 2, una concentración de SDS en la formulación de niosomas de 4 mol/m^3 y una relación molar SDS/ácido láctico de 0,010, obteniendo con estas condiciones un grado de extracción máximo del 33%.
- Se observó que los niosomas tienen mayor afinidad (más del doble) por la especie no disociada del ácido láctico, lo que demuestra la optimización del proceso al trabajar a pH por debajo del pKa del ácido ($\text{pKa} = 3,86$). Al aumentar el pH del medio, el grado de extracción del ácido láctico disminuye hasta ser nulo a un $\text{pH} > 12$. Estas condiciones fueron las utilizadas para realizar la etapa de reextracción.
- El estudio de las cinéticas de extracción reveló tiempos de equilibrio en torno a 40 min, independientemente del pH de la dispersión.
- La etapa de concentración puede realizarse adecuadamente utilizando membranas planas de microfiltración de TiO_2 con un tamaño de poro de $0,20 \mu\text{m}$ y aplicando una presión de 0,3 bar. Se obtuvieron rechazos totales de los niosomas, con altas densidades de flujo de

Conclusiones generales

permeado ($J_p = 27 \text{ L/m}^2 \text{ h}$) que permanecieron constantes durante todo el proceso hasta un factor de concentración en volumen de 2,5.

- Para aumentar la eficacia, la extracción del ácido láctico puede realizarse mediante un proceso en múltiples etapas en el que el permeado obtenido tras la etapa de concentración mediante microfiltración (o ultrafiltración) debe someterse a una nueva etapa de extracción, con la adición de fase dispersa fresca (niosomas mixtos) en las condiciones óptimas anteriormente expuestas y durante un tiempo de 40 min para alcanzar el equilibrio, tras el cual puede ser concentrado de nuevo mediante membranas.
- El proceso de reextracción se realiza adecuadamente modificando las condiciones del medio por adición de NaOH hasta $\text{pH} > 12$. A este pH, se ha observado la ruptura de la bicapa niosomal y la liberación del ion lactato. Las cinéticas de reextracción arrojan valores de equilibrio en torno a 40 min.
- Las fracciones de retenido, obtenidas tras las etapas de concentración, pueden someterse a una etapa de reextracción a $\text{pH} > 12$ y, transcurrido el tiempo de equilibrio, las fases pueden ser separadas por ultrafiltración.
- Las membranas planas de ultrafiltración de ZrO_2 demostraron un gran potencial para emplearse en la etapa de reextracción a $\text{pH} > 12$, ya que mostraron mayores flujos de permeado que las de microfiltración y menor disminución del flujo de permeado respecto al agua pura, es decir, menor ensuciamiento.
- Se observó que existe un comportamiento antagónico entre el rechazo del SDS y el flujo de permeado. Bajo las condiciones de la etapa de reextracción, en presencia de elevadas concentraciones de NaOH, al aumentar el flujo de permeado, parte de las moléculas de SDS adsorvidas en la membrana o acumuladas en la capa de polarización atraviesan la membrana, disminuyendo el rechazo al SDS.
- La optimización del proceso de reextracción para la separación del lactato sódico de los tensioactivos se consiguió mediante el empleo de membranas de 15 kDa con una presión transmembranal de 2 bar. Se obtuvieron rechazos al ion lactato inferiores al 5%, y del 87,3% y 100% para los tensioactivos SDS y Span 80, respectivamente.

- A pH > 12 la retención por la membrana de ultrafiltración de los tensioactivos Span 80 y SDS está influenciada por tres efectos: el efecto de tamizado de la membrana sobre las micelas mixtas y grandes agregados de Span 80, la descompactación de la capa de polarización por el exceso de iones Na⁺ y el apantallamiento de la superficie de la membrana, que se encuentra cargada negativamente por ser el pH mayor que el punto isoeléctrico (PI = 4,1). Los dos últimos factores contribuyen a favorecer la permeación de monómeros de SDS al aumentar el flujo de permeado por incremento de la presión, ya que el flujo de permeado está controlado principalmente por convección.
- La formulación niosomal utilizada en estos trabajos, con los tensioactivos Span 80 y SDS, es atractiva debido a su bajo precio, su carácter biodegradable y por ser sustancias no tóxicas.
- La presencia de SDS en las formulaciones de niosomas de Span 80 tiene efectos diferentes en función de las concentraciones de ambos tensioactivos en la formulación. En general, la interacción se puede describir mediante un proceso en tres etapas que se producen de forma sucesiva al crecer la concentración de SDS: adsorción del SDS en la bicapa niosomal hasta alcanzar la saturación, a partir de ese punto comienza la solubilización de la bicapa niosomal, y finalmente se produce la solubilización total de los niosomas.
- Se ha comprobado que la adición de SDS por encima del valor crítico de solubilización total de los niosomas produce un aumento del número de micelas mixtas, mientras se mantiene constante el número de monómeros de SDS en disolución. Este hecho corrobora que el proceso de solubilización de los niosomas se produce por micelización.
- Se ha detectado la presencia de micelas mixtas en concentraciones de SDS inferiores al valor de saturación, indicando que la adsorción de monómeros de SDS y la desorción de monómeros de Span 80 de la bicapa niosomal se produce de forma simultánea para formar dichas micelas mixtas.
- Se determinaron las concentraciones de SDS y Span 80 en los puntos críticos de saturación y solubilización total. Las concentraciones de saturación son 0, 2, 6 y 12 mol/m³ de SDS y las de solubilización total 8, 9, 12 y 16 mol/m³ de SDS para formulaciones de 1, 2, 10 y 20 mol/m³ de Span 80, respectivamente, en agua. Estos valores configuran un comportamiento lineal en el diagrama de pseudo-fases en equilibrio.

- Se determinó el diagrama de equilibrio de pseudo-fases para el sistema Span 80 y el tensioactivo catiónico CTAB en agua. Los puntos críticos de saturación se corresponden con las concentraciones de 0, 2, 4 y 6 mol/m³ de CTAB y los de solubilización total con 4, 6, 8 y 10 mol/m³ de CTAB en formulaciones con 5, 10, 15 y 20 mol/m³ de Span 80, respectivamente.
- En formulaciones de CTAB solo, la presencia de NaCl favorece la adsorción superficial (reducción de la tensión superficial) y la formación de micelas. Los fenómenos de adsorción superficial están impedidos por fenómenos electrostáticos, los cuales disminuyen a medida que aumenta el contenido de sal. En presencia de 80 mol/m³ de NaCl desaparecen completamente las barreras a la adsorción superficial y el control es exclusivamente difusional. La presencia de NaCl reduce las barreras a la adsorción y la favorece termodinámicamente frente a la micelización.
- Los niosomas de Span 80 son estables en agua y en presencia de 20 mol/m³ de NaCl. Cantidad mayores de sal provocan inestabilidad y formación de grandes agregados. Incluso se ha observado la formación de precipitados en presencia de 80 mol/m³ de NaCl.
- Los niosomas mixtos de Span 80 (20 mol/m³) y CTAB (4 mol/m³) en agua y en presencia de una pequeña concentración de sal (20 mol/m³) son de menor tamaño y más estables que los de Span 80 solo. Mayores cantidades de sal provocan un fuerte aumento del tamaño de los agregados que, no obstante, se mantuvieron estables en el medio de dispersión durante más de 32 días de ensayo, sin observarse cambios en el tamaño ni formación de precipitados. Los estudios termodinámicos revelan sinergismos en la formación de agregados mixtos de Span 80 y CTAB en agua y en concentraciones de 20 y 50 mol/m³ de NaCl, mientras que existe antagonismo en presencia de 80 mol/m³ de sal.
- Los niosomas mixtos de Span 80 y CTAB tienen carga positiva, lo que indica adsorción de CTAB en la membrana niosomal. Este prometedor resultado abre la posibilidad de usar estas estructuras estables en diversas aplicaciones que utilizan CTAB por sus cualidades antibacterianas y antisépticas, solventándose así la necesidad de trabajar a temperatura superior a la temperatura de Krafft (24,8 °C en agua pura).